JAERI 1313

JAERI 1313

RESEARCH ON ONE-DIMENSIONAL TWO-PHASE FLOW

(Theory on Hydrodynamic Balance in Two-Fluid Model and Its Applications)

October 1988

日 本 原 子 力 研 究 所

Japan Atomic Energy Research Institute

JAERIレポートは，日本原子力研究所が研究成果編集委員会の審査を経て不定期に公刊している研究報告書です。

入手の問合わせは，日本原子力研究所技術情報部情報資料課（〒319-11茨城県那珂郡東海村）あて，お申しこしください。なお，このほかに財団法人原子力弘済会資料センター（〒319-11 茨城県那珂郡東海村日本原子力研究所内）で複写による実費頒布をおこなっております。

JAERI reports are reviewed by the Board of Editors and issued irregularly.

Inquiries about availability of the reports should be addressed to Information Division Department of Technical Information, Japan Atomic Energy Research Institute, Tokai-mura, Naka-gun, Ibaraki-ken 319-11, Japan.

編集兼発行　日本原子力研究所
印　　刷　いばらき印刷㈱

Research on One-Dimensional Two-Phase Flow (Theory on Hydrodynamic Balance in Two-Fluid Model and Its Application)

Hiromichi ADACHI

Department of Reactor Safety Research,
Tokai Research Establishment,
Japan Atomic Energy Research Institute
Tokai-mura, Naka-gun, Ibaraki-ken

(Received June 29, 1988)

In the Part I of this report, the author describes about the fundamental form of the hydrodynamic basic equations for a one-dimensional two-phase flow (two-fluid model). Most of the discussions are concentrated on the treatment of phase change inertial force terms in the equations of motion and the author's equations of motion which have a remarkable uniqueness on the following three points in comparison with conventional equations of motion.

(1) To express force balance of unit mass two-phase fluid instead of that of unit volume two-phase fluid.
(2) To pick up the unit existing mass and the unit flowing mass as the unit mass of two-phase fluid.
(3) To apply the kinetic energy principle instead of the momentum low in the evaluation of steady inertial force term.

In these three, the item (1) is for excluding a part of momentum change or kinetic energy change due to mass change of the examined part of fluid, which is independent of force. The item (2) is not to introduce a phenomenological physical model into the evaluation of phase change inertial force term. And the item (3) is for correctly applying the momentum law taking into account the difference of representative velocities between the main flow fluid (vapor phase or liquid phase) and the phase change part of fluid. These three items are for expressing the essence of force balance of two-phase flow most simply but they are not always necessary to establish equations of motion for two-phase flow. Therefore, two independent equations of motion based on these items can be transformed by mathematical treatment into various forms which are not restricted directly by these items.

In the Part II of this report, characteristics of various kinds of high speed two-phase flow are clarified theoretically by using the basic equations derived in the Part I. It is demonstrated that the steam-water two-phase critical flow with violent flashing and the air-water two-phase critical flow without phase change can be described with fundamentally the same basic equations. Furthermore, by comparing the experimental data from the two-phase critical discharge test and the author's theoretical prediction, the two-phase discharge coefficient, C_D, for large sharp-edged orifice is determined as the value which is not affected by the experimental facility characteristics, etc.

Keywords: One-Dimensional, Two-Phase Flow, Basic Equation, Momentum Equation, Slip, Phase Change, Critical Flow, Safety, LOCA, LWR

一次元二相流に関する研究

(二流体モデルの力学的平衡に関する理論とその応用)

日本原子力研究所東海研究所原子炉安全工学部

安達公道

(1988年6月29日受理)

要旨

本論文の第Ⅰ部では，一次元二相流(二流体モデル)の流体力学的な基礎方程式の基本形式について述べる．議論の中心は運動の式の相変化慣性力項の取扱いにあるが，従来の運動の式に較べて，以下の3点で著しい特徴を持つ．

(1) 単位体積あたりの力の平衡の代りに，単位質量あたりの力の平衡を取扱ったこと．

(2) 単位質量検査流体として，存在量基準および流量基準の2種類の二相流体を取上げたこと．

(3) 定常慣性力の評価に，運動量の法則の代りに運動エネルギの原理を適用したこと．

これらのうち，(1)は検査流体の質量変化に伴う外力と無関係な運動量ないし運動エネルギの変化を運動の式から排除するためである．(2)は相変化流体部分に作用する慣性力の評価に現象論的物理モデルを導入しないためである．また(3)は主流体(気相または液相)と相変化流体との速度の違いを運動量の法則の適用に正しく反映させるためである．これら3つの項目は，二相流の力の平衡の本質を最も簡潔に表現するために工夫されたものであるが，このように考えなければ二相流の運動の式が立たないという訳ではない．それ故，これらの工夫によって立てた2個の互いに独立な運動の式を数学的に変形することによって，二相流の力の平衡に関するこれら3項目によらない各種の表現上のヴァリエイションを導くことができる．

本論文の第Ⅱ部では，第Ⅰ部で導出した基礎方程式群を用いて，各種の高速二相流の特性を理論的に明らかにする．激しい減圧沸騰を伴う蒸気－水二相臨界流も，相変化がない空気－水二相臨界流も，基本的には全く同じ基礎方程式群で表現できることを示す．また，二相臨界流出実験を実施して，著者の理論と比較することにより，実験装置の特性等の影響を受けない大口径薄刃オリフィスの二相流出係数C_Dの値を明らかにする．

Contents

PREFACE 0

Part I HYDRODYNAMIC BASIC EQUATIONS FOR TWO-PHASE FLOW

1. Introduction 1
2. Number of Basic Equations and Selection of Examined Part of Fluid 11
   - 2.1 Number of Basic Equations 11
   - 2.2 Selection of Examined Part of Fluid 11
3. Equations of Continuity 13
   - 3.1 Equations of Continuity for Each Phase 13
   - 3.2 Mass Conservation Equation for Total Two-Phase Flow 13
   - 3.3 Equation of Phase Change (1) 13
   - 3.4 Independency of Equations of Continuity 14
   - 3.5 Equation of Phase Change (2) 14
4. Equations of Motion 16
   - 4.1 Steady Equations of Motion for Total Two-Phase Flow 16
     - 4.1.1 Equation based on "existing mass" 16
     - 4.1.2 Equation based on "flowing mass" 18
   - 4.2 Additional Explanations 19
     - 4.2.1 Starting from equations for total two-Phase flow 20
     - 4.2.2 Application of kinetic energy principle 20
     - 4.2.3 Coincidence between phase change part of fluid and main flow phases 24
     - 4.2.4 Mass change of examined part of fluid 27
   - 4.3 Transient Equations of Motion for Total Two-Phase Flow 28
     - 4.3.1 Equation based on "existing mass" 28
     - 4.3.2 Equation based on "flowing mass" 28
   - 4.4 Equations of Motion for Each Phase 29
   - 4.5 Momentum Equations 30
   - 4.6 Independency of Equations of Motion 32
   - 4.7 Comparison with Conventional Equations 32
     - 4.7.1 Mass change of examined part of fluid 32
     - 4.7.2 Steady phase change inertial force terms of momentum equations 34
     - 4.7.3 Relationship between inertial force and kinetic energy 36
5. Equations of Energy 38
   - 5.1 Balance Equations of Thermal Energy 38
   - 5.2 Balance Equations of Total Energy 39
   - 5.3 Equation of Total Energy Conservation 41
   - 5.4 Independency of Equations of Energy 43
6. Settled One-Dimensional Two-Phase Flow 44
   - 6.1 Definition of Frictional Forces 44
   - 6.2 Settlement of One-Dimensional Two-Phase Flow 44
   - 6.3 Characteristics of Perfectly Settled Two-Phase Flow 45
   - 6.4 Meaning of Settlement of Two-Phase Flow 46

7. Basic Equations for Three-Dimensional Two-Phase Flow 48
7.1 Time-Averaging of Variables 48
7.2 Equations of Continuity 48
7.3 Equations of Motion 49
7.3.1 Equations of motion for single-phase flow 49
7.3.2 Equations of motion for total two-phase flow 50
7.3.3 Equations of motion for each phase 52
7.4 Equations of Energy 53
7.5 Inherent Errors of One-Dimensional Approximation 56
8. Conclusion 57
9. Nomenclature 59
References 61
Appendix 1 Virtical Mass Force 62
Appendix 2 Kinetic Energy Type Expression of Inertial Force Term for Single-Phase Flow 63
Appendix 3 Definition of Frictional Force Terms 65

Part II RESEARCH ON HIGH-SPEED TWO-PHASE FLOW
1. Introduction 69
2. Saturated Two-Phase Critical Flow without Friction 71
2.1 Introduction 71
2.2 Basic Equations 71
2.2.1 Equations of motion 71
2.2.2 Equations of energy 73
2.2.3 Equations of continuity 74
2.2.4 Transformation of equation of motion based on flowing mass 76
2.3 Critical Discharge from High Pressure Reservoir 77
2.4 Calculation Results 80
2.5 Discussions 84
2.6 Conclusions 86
3. Saturated Two-Phase Critical Flow in a Constant-Flow-Area Channel 87
3.1 Introduction 87
3.2 Calculation Method 87
3.3 Flow Change with Respect to Pressure 88
3.4 Axial Change of Each Variable 93
3.5 Discussions 94
3.6 Conclusions 98
4. Two-Phase Critical Flow without Phase Change 100
4.1 Introduction 100
4.2 Calculation Method 100
4.3 Calculation Results and Discussions 101
4.4 Conclusions 107
5. Two-Phase Critical Discharge Experiment with a Converging-Diverging Nozzle 108
5.1 Introduction 108
5.2 Experimental Facility and Procedure 109
5.2.1 Experimental facility 109
5.2.2 Test nozzle 109
5.2.3 Experimental procedure 110

5.2.4 Calculation method of quality 111
5.3 Experimental Results 112
5.3.1 Discharge process 112
5.3.2 Distribution of static pressure 112
5.3.3 G–P curve and critical mass velocity 113
5.3.4 Distribution of fluid temperature 115
5.4 Discussions 117
5.5 Conclusions 120
6. Two-Phase Critical Discharge Experiment with a Large Sharp-Edged Orifice 122
6.1 Introduction 122
6.2 Test Facility 123
6.3 Analytical Method 124
6.4 Experimental Results and Discussions 124
6.4.1 Discharge process 124
6.4.2 Discharge coefficient of sharp-edged orifice 126
6.4.2.1 $x_0 \gg 0$ 126
6.4.2.2 $x_0 \approx 0$ 128
6.4.3 Comparison with RELAP code analysis 130
6.5 Conclusions 131
7. Frictional Energy Dissipation of Vertical Gas-Liquid Two-Phase Flow without Phase Change 132
7.1 Introduction 132
7.2 Theory 132
7.3 Application 133
7.4 Conclusions 136
8. Concluding Remarks 137
9. Nomenclature 138
References 140
Appendix 1 Local Condition for Single-Phase Critical Flow 141
Appendix 2 An Example of ζ_{xz} and Related Parameters 143
Concluding Remarks 147
Acknowledgement 147

目　　次

総　序 …… 0

第Ⅰ部　二相流の流体力学的基礎方程式
1. 緒　言 …… 1
2. 基礎方程式の個数と検査流体の選定 …… 11
2.1 基礎方程式の個数 …… 11
2.2 検査流体の選定 …… 11
3. 連続の式 …… 13
3.1 各相別の運動の式 …… 13
3.2 二相流全体の質量保存の式 …… 13
3.3 相変化の式（その１） …… 13
3.4 連続の式の独立性 …… 14
3.5 相変化の式（その２） …… 14
4. 運動の式 …… 16
4.1 二相流全体の定常運動の式 …… 16
4.1.1 存在量基準の式 …… 16
4.1.2 流量基準の式 …… 18
4.2 補足説明 …… 19
4.2.1 二相流全体の式より出発する理由 …… 20
4.2.2 運動エネルギの原理の適用 …… 20
4.2.3 相変化流体と主流体との対応関係 …… 24
4.2.4 検査流体の質量変化 …… 27
4.3 二相流全体の非定常運動の式 …… 28
4.3.1 存在量基準の式 …… 28
4.3.2 流量基準の式 …… 28
4.4 各相別の運動の式 …… 29
4.5 運動量の式 …… 30
4.6 運動の式の独立性 …… 32
4.7 従来の式との比較 …… 32
4.7.1 検査流体の質量変化 …… 32
4.7.2 運動量の式の定常相変化慣性力 …… 34
4.7.3 慣性力と運動エネルギの関係 …… 36
5. エネルギの式 …… 38
5.1 熱エネルギの収支式 …… 38
5.2 全エネルギの収支式 …… 39
5.3 二相流全体のエネルギ保存の式 …… 41
5.4 エネルギの式の独立性 …… 43
6. 整定された一次元二相流 …… 44
6.1 摩擦力の定義 …… 44
6.2 一次元二相流の整定 …… 44
6.3 完全に整定された二相流の性質 …… 45
6.4 二相流の整定の意味 …… 46
7. 三次元二相流の基礎方程式 …… 48
7.1 変数の時間平均化 …… 48

7.2 連続の式 …… 48
7.3 運動の式 …… 49
7.3.1 単相流の運動の式 …… 49
7.3.2 二相流全体の運動の式 …… 50
7.3.3 各相別の運動の式 …… 52
7.4 エネルギの式 …… 53
7.5 一次元的取扱いに起因する誤差 …… 56
8. 結 言 …… 57
9. 記 号 …… 59
文 献 …… 61
付録1 付加質量による力について …… 62
付録2 単相流の慣性力項の運動エネルギ型の表現 …… 63
付録3 摩擦力項の定義について …… 65

第Ⅱ部 高速二相流に関する研究
1. 緒 言 …… 69
2. 摩擦がない飽和二相臨界流 …… 71
2.1 はじめに …… 71
2.2 基礎方程式 …… 71
2.2.1 運動の式 …… 71
2.2.2 エネルギの式 …… 73
2.2.3 連続の式 …… 74
2.2.4 流量基準の運動の式の変形 …… 76
2.3 高圧貯槽からの臨界流出 …… 77
2.4 数値計算結果 …… 80
2.5 考 察 …… 84
2.6 本章の結論 …… 86
3. 等断面積流路の飽和二相臨界流 …… 87
3.1 はじめに …… 87
3.2 計算方法 …… 87
3.3 各変数の圧力に対する関係 …… 88
3.4 各変数の軸方向変化 …… 93
3.5 考 察 …… 94
3.6 本章の結論 …… 98
4. 相変化がない二相臨界流 …… 100
4.1 はじめに …… 100
4.2 計算方法 …… 100
4.3 数値計算結果および考察 …… 101
4.4 本章の結論 …… 107
5. 縮小拡大ノズルからの二相臨界流出実験 …… 108
5.1 はじめに …… 108
5.2 実験装置および方法 …… 109
5.2.1 実験装置 …… 109
5.2.2 テストノズル …… 109
5.2.3 実験方法 …… 110
5.2.4 クォリティの算出方法 …… 111

5.3 実験結果 …… 112
5.3.1 流出過程 …… 112
5.3.2 静圧分布 …… 112
5.3.3 G–P曲線と臨界質量速度 …… 113
5.3.4 流体温度分布 …… 115
5.4 考 察 …… 117
5.5 本章の結論 …… 120
6. 大口径薄刃オリフィスからの二相臨界流出実験 …… 122
6.1 はじめに …… 122
6.2 実験装置 …… 123
6.3 解析方法 …… 124
6.4 実験結果および考察 …… 124
6.4.1 流出過程 …… 124
6.4.2 薄刃オリフィスの流出係数 …… 126
6.4.2.1 $x_0 \gg 0$ の領域 …… 126
6.4.2.2 $x_0 \approx 0$ の領域 …… 128
6.4.3 RELAPコード解析との比較 …… 130
6.5 本章の結論 …… 131
7. 加速のない垂直気液二相流の摩擦エネルギ消散 …… 132
7.1 はじめに …… 132
7.2 理 論 …… 132
7.3 適用例 …… 133
7.4 本章の結論 …… 136
8. 結 言 …… 137
9. 記 号 …… 138
文 献 …… 140
付録1 単相臨界流の局所条件 …… 141
付録2 ζ_{x2} 等の変数の計算例 …… 143

結 言 …… 147
謝 辞 …… 147

List of Tables and Figures for Part I

Table 1 Comparison of basic equations for two-phase flow
Table 2 Combinations of two independent equations of continuity
Table 3 Combinations of two independent equations of motion
Table 4 Various expressions of phase change inertial force terms in momentum equations for total two-phase flow
Table 5 Combinations of two independent equations of energy

Fig. 1 Estimation of average velocity of phase change part of fluid based on mass displacement analysis
Fig. 2 One-dimensional two-fluid model
Fig. 3 Correspondence among main flow phases and phase change part of fluid in existing two-phase fluid
Fig. 4 Correspondence among main flow phases and phase change part of fluid in flowing two-phase fluid (1)
Fig. 5 Correspondence among main flow phases and phase change part of fluid in flowing two-phase fluid (2)
Fig. 6 Correspondence among main flow phases and phase change part of fluid in flowing two-phase fluid (3)
Fig. 7 Experiment in thought on gravitational water head in a vertical channel
Fig. A3-1 Definition of shear forces

List of Tables and Figures for Part II

Table 1 C_D-value determined with RELAP-3 code (ROSA–I)

Fig. 1 Change of two-phase flow in a converging-diverging channel
Fig. 2 Flow chart for calculation of two-phase critical discharge flow through a converging-diverging channel
Fig. 3 G–P curve for two-phase critical discharge flow
Fig. 4 Change of flow variables in two-phase critical discharge flow through a converging-diverging channel (1)
Fig. 5 Change of flow variables in two-phase critical discharge flow through a converging-diverging channel (2)
Fig. 6 Relationship between pressure and mass velocity changes in a converging-diverging channel
Fig. 7 Relationship among critical pressure, critical quality and critical mass velocity
Fig. 8 Relationship between reservoir conditions and critical mass velocity
Fig. 9 Relationship between pressure and slip ratio changes in a converging-diverging channel

Fig. 10 Comparison between analytical and experimental critical mass velocities
Fig. 11 Comparison among various theoretical critical slip ratios
Fig. 12 Two-phase critical discharge through a constant-flow-area channel
Fig. 13 Effect of ζ on G–P curve
Fig. 14 Characteristics of frictional pressure drop in a constant-flow-area channel
Fig. 15 Occurrence of critical flow at the exit of constant-flow-area channel
Fig. 16 Relationship between critical pressure and critical mass velocity for various reservoir conditions
Fig. 17 Change of flow variables in two-phase critical discharge flow through a constant-flow-area channel (1)
Fig. 18 Change of flow variables in two-phase critical discharge flow through a constant-flow-area channel (2)
Fig. 19 Example calculation of axial changes of flow variables for two-phase critical discharge through a constant-flow-area channel
Fig. 20 Comparison between analytical and experimental critical pressures for a constant-flow-area channel
Fig. 21 Comparison between analytical and experimental axial pressure changes for a constant-flow-area channel (1)
Fig. 22 Comparison between analytical and experimental axial pressure changes for a constant-flow-area channel (2)
Fig. 23 Estimated axial change of depressurization rates in a two-phase critical discharge experiment with constant-flow-area channel
Fig. 24 G–P curves in two-component two-phase critical discharge
Fig. 25 G–P curves in one-component two-phase critical discharge
Fig. 26 Comparison in critical pressure ratio between Akagawa's and the author's theories
Fig. 27 Axial change of test section flow area at the experiment by Smith, et al.
Fig. 28 Comparison between analytical and experimental mass velocities for two-component two-phase critical flow
Fig. 29 Measured axial pressure changes (Smith, et al.)[29]
Fig. 20 Comparison between analytical and experimental G–P curves for two-component two-phase critical flow
Fig. 31 Experimental facility
Fig. 32 Axial changes of diameter and flow area of the test nozzle
Fig. 33 Example changes of variables during discharge
Fig. 34 Examples of axial static pressure change in a converging-diverging nozzle
Fig. 35 Examples of G–P curve
Fig. 36 Comparison between analytical and experimental G–P curves (1)
Fig. 37 Comparison between analytical and experimental G–P curves (2)
Fig. 38 Comparison between analytical and experimental critical mass velocities
Fig. 39 Examples of axial fluid temperature change in a converging-diverging nozzle

Fig. 40 Relationship between pressure and fluid temperature changes in a converging-diverging nozzle
Fig. 41 Example of a temperature decreasing during depressurization in a converging-diverging nozzle
Fig. 42 Supposed temperature distribution near the steam-water interface
Fig. 43 Pressure vessel of ROSA−I test facility
Fig. 44 Test orifices for ROSA−I
Fig. 45 Examples of variable changes during bottom discharge
Fig. 46 Examples of variable changes during top discharge
Fig. 47 Two-phase discharge coefficient of sharp-edged orifice (1)
Fig. 48 Two-phase discharge coefficient of sharp-edged orifice (2)
Fig. 49 Summary of two-phase discharge coefficient of sharp-edged orifice
Fig. 50 Two-phase discharge coefficient of round-edged orifice
Fig. 51 Thermal non-equilibrium at just downstream of orifice
Fig. 52 Predicted two-phase discharge coefficient for the saturation water (non-equilibrium model)
Fig. 53 Relationship between superficial velocity and total frictional energy dissipation in a vertical circular pipe with water flow rate as parameter
Fig. 54 Relationship between wall and interfacial energy dissipations in a vertical circular pipe with water flow rate as parameter
Fig. 55 Energy dissipation characteristics in low air flow rate region for a vertical circular pipe
Fig. 56 Relationship between wall frictional energy dissipation and water linear velocity in a vertical circular pipe with water flow rate as parameter
Fig. A2-1 ζ_β and ζ_x at $P_0 = 1.0$ MPa, $x_0 = 0.05$
Fig. A2-2 η_g, η_l and η_{net} at $P_0 = 1.0$ MPa, $x_0 = 0.05$
Fig. A2-3 ζ_β and ζ_x at $P_0 = 1.0$ MPa, $x_0 = 0.30$
Fig. A2-4 η_g, η_l and η_{net} at $P_0 = 1.0$ MPa, $x_0 = 0.30$
Fig. A2-5 ζ_β and ζ_x at $P_0 = 1.0$ MPa, $x_0 = 0.70$
Fig. A2-6 η_g, η_l and η_{net} at $P_0 = 1.0$ MPa, $x_0 = 0.70$

PREFACE

Gas-liquid two-phase flow is handled in various industrial fields. In the field of nuclear power engineering, much effort has been made to study two-phase flow to meet the requirement from design of boiling water reactor (BWR). However, great attention was not paid to the general form of hydrodynamical basic equations for two-phase flow because the variety in studied two-phase flow conditions was usually limited for design purpose and, in addition, only steady or quasi-steady phenomena were studied in most cases.

In the resent twenty years, however, reliable and accurate analysis codes for a loss-of-coolant accident (LOCA) of a light water reactor (LWR) including a pressurized water reactor (PWR) became strongly needed. Consequently, the form of hydrodynamical basic equations for two-phase flow has attracted great attention of safety analysis people. As the result, various types of basic equation set were proposed and applied in each code.

In LOCA analysis, very wide range transient or quasi-steady changes of pressure, temperature, phase velocity, quality, etc. have to be treated consistently. Therefore, the basic equation set to be used should correctly describe the balance of mass, force (momentum) and energy. Of course, validity of a LOCA analysis code depends strongly not only on the validity of basic equations but also on the selection of constitutive equations and numerical method. Furthermore, deletion of some terms from basic equations could stabilize the calculation and shorten the computing time without large quality reduction of the calculation in a certain kinds of LOCA transient. However, importance of valid form of basic equation set to correctly describe the balance of mass, force and energy is never cancelled with importance of such practical approaches.

In Part I of the present report, general form of equations of continuity, equations of motion and equations of energy for a gas-liquid two-phase flow will be discussed from the view point of balance of mass, force (momentum) and energy, respectively. Any assumptions or physical insights from the view point other than balance of these quantities are excluded from the proposed basic equations.

Major discussions will be made, for simplicity, about one-dimensional separeted two-phase flow (two-fluid model), but the final form will be generalized into local, time-averaged, three-dimensional expression.

The investigation is strongly concentrated to the phase change intertial force terms of equations of motion. It will be pointed out that the corresponding terms of conventional equations of motion do not always represent the Newton's second law correctly. The conflict of Newton's second law is resulted from the conflict of Newton's third law between main gas or liquid phase and phase change part of fluid.

In Part II, on the other hand, analytical results on two-phase critical flow will be introduced as an application of the basic equation set established in Part I. Two-phase critical discharge flow has a steep pressure gradient along the flow axis. And a violent phase change due to this large pressure drop governs the characteristics of flow. Therefore, it is a suitable analytical object for verifying the validity of the author's basic equation set which has the remarkable features with the phase change inertial force terms. In the analyses introduced in this report, some additional assumptions corresponding to constitutive equations are introduced for simplicity and, therefore, they cannot always be considered to describe two-phase critical flow correctly. However, various unique characteristics of critical flow are

0-2

described almost perfectly. This fact demonstrates the validity and the resultant wide applicability of the author's basic equation set.

Some experimental analysis results on interfacial and wall frictional energy dissipations for a vertical gas-liquid two-phase flow without phase change are also introduced in the last chapter of Part II.

Major part of this report was transrated from Ref. (1) of Part I. Three-dimensional basic equations, however, will be described in much more detail. In addition, the author's opinion on virtual mass force due to relative acceleration between two phases also will be discussed briefly in this report.

1. Introduction

In a loss of coolant accident (LOCA) of a light water reactor (LWR), primary coolant pressure changes from about 16 MPa (in the case of pressurized water reactor) to near the atmospheric pressure. Temperature of the coolant in the primary system varies from higher than 600 K to lower than 400 K. Two-phase flow of much higher temperature than 600 K can be realized in the heated-up core as a droplet flow of superheated steam and the saturated water droplets. On the other hand, two-phase flow of steam and much colder subcooled water than 400 K also can appear, e.g., around the emergency core cooling (ECC) water injection ports. For fluid velocity, two-phase critical flow with very high linear velocities of some hundreds or more than one thousands m/s appears at the breaks, on the other hand, counter-current two-phase flow can be realized at the top of core and top of downcomer and even at hot leg piping. In the reflux cooling mode of small break LOCA, superficial velocity of the order of, in some cases, 0.01 m/s sould be treated.[2] Furthermore, for steam quality, every condition between 0 and 1 (thermodynamically from less than 0 to larger than 1) can be realized somewhere in the primary system.

Hydrodynamical basic equations for two-phase flow should, therefore, have very wide applicability for consistently analyzing complex transient or quasi-steady changes of two-phase flow eith such wide range changes of flow variables. However, two-phase basic equation sets currently used for safety analysis are different to each other in fundamental form[3]-[14] as shown in **Table 1**. As known from this table, one cannot find any established form of basic equation set. Form of equations of motion is on a specially imperfect stage.

Hydrodynamical basic equations describe the balance of mass, force (momentum) and energy and they should be easily established based on the mass conservation law, Newton's second law and the first low of thermodynamics, respectively. However, there are many disagreements even in the level of general form of basic equations as described above. The reason is that the spatial and time relationships between each component of two-phase fluid are very complex due to phase slip and, therefore, it is overlooked that some physical knowledges which are common senses in the single-phase hydrodynamics are not valid for two-phase flow.

In Part I of the present report, right form of the hydrodynamical basic equations will be discussed by picking up a one-dimensional separate two-phase flow (two-fluid model) as an example.

First, in Chapter 2, number of independent basic equations and selection of examined part of fluid are discussed. The latter is specially important because of the deep connection with the main theme of this report. Detailed discussion on this item will be made in Chapter 4, and only basic concept is given in Chapter 2.

In Chapter 3, equations of continuity are introduced with some variations in expression and, in addition, equivalent velocity of phase change part of fluid is discussed from the view point of mass displacement. The equivalent velocity of phase change part of fluid is the most important variable in this report and will be discussed in Chapter 4 from various points of view.

Chapter 4 describes equations of motion and is the central chapter of this report. First, the author establishes the equations of motion for steady two-phase flow and next he will extend them to transient two-phase flow. The reason is that the most important thing for

the readers is to get the image of the author's physical thought on hydrodynamical balance of two-phase flow, and for this purpose steady equations are more convenient.

Up to this stage, force balance is discussed for total two-phase flow. The author will, next, derive the equations of motion for each phase by purely mathematical transformation. Furthermore, various expressions of so-called momentum equations are also derived by mathematical treatment. Validity of the author's theory will be examined from various view angles through these discussions but more detailed discussions will be made on the differences between the author's and the typical conventional momentum equations in the last section of Chapter 4.

In Chapter 5, equations of energy are introduced with some variations in expression. In addition, total energy conservation equation for total two-phase flow will be derived based on the author's equations of motion and the first law of thermodynamics.

Chapter 6 discusses characteristics of interfacial frictional forces and wall frictional forces in relation with basic equations and definition of those frictional forces.

At last, in Chapter 7, local, time-averaged, three-dimensional basic equations will be introduced with more detailed explanations on each term of the equations.

Table 1 Comparison of basic equations for two-phase flow

code/researcher	balance equations	note	reference
TRAC – PD 2	equations of continuity $\frac{\partial \rho_m}{\partial t}+\frac{\partial(\rho_m u_m)}{\partial z}=0$ here, $\rho_m=\alpha\rho_g+(1-\alpha)\rho_l$, $u_m=\frac{\alpha\rho_g u_g+(1-\alpha)\rho_l u_l}{\rho_m}$ $\frac{\partial(\alpha\rho_g)}{\partial t}+\frac{\partial(\alpha\rho_g u_m)}{\partial z}+\frac{\partial}{\partial z}\left\{\frac{\alpha\rho_g(1-\alpha)\rho_l u_r}{\rho_m}\right\}=w$ here, $u_r=u_g-u_l$ equation of motion $\frac{\partial u_m}{\partial t}+u_m\frac{\partial u_m}{\partial z}+\frac{1}{C_m}\frac{\partial}{\partial z}\left\{\frac{\alpha\rho_g(1-\alpha)\rho_l u_r^2}{\rho_m}\right\}=-\frac{1}{\rho_m}\frac{\partial P}{\partial z}-Ku_m\lvert u_m\rvert+g$ g in coordinate direction is difined positive equations of energy $\frac{\partial}{\partial t}(\alpha\rho_g e_g)+\frac{\partial}{\partial z}(\alpha\rho_g u_m e_g)+\frac{\partial}{\partial z}\left\{\frac{\alpha\rho_g(1-\alpha)\rho_l u_r e_g}{\rho_m}\right\}+P\frac{\partial(\alpha u_m)}{\partial z}$ $+P\frac{\partial}{\partial z}\left\{\frac{\partial(1-\alpha)\rho_l u_r}{\rho_m}\right\}=Q_{GW}-Q_{IG}-P\frac{\partial\alpha}{\partial t}+wh_{gsat}$ $\frac{\partial}{\partial t}(\rho_m e_m)+\frac{\partial}{\partial z}(\rho_m e_m u_m)+\frac{\partial}{\partial z}\left\{\frac{(1-\alpha)\rho_l\alpha\rho_g(e_g-e_l)}{\rho_m}u_r\right\}+P\frac{\partial u_m}{\partial z}$ $+P\frac{\partial}{\partial z}\left\{\frac{\alpha(1-\alpha)(\rho_l-\rho_g)}{\rho_m}u_r\right\}=Q_{GW}+Q_{LW}$	1 D component	NUREG/CR – 2054 (April, 1981)
	equations of continuity $\frac{\partial \rho_m}{\partial t}+\nabla\cdot\{\alpha\rho_g\vec{u}_g+(1-\alpha)\rho_l\vec{u}_l\}=0$ $\frac{\partial(\alpha\rho_g)}{\partial t}+\nabla\cdot(\alpha\rho_g\vec{u}_g)=w$ equations of motion $\frac{\partial\vec{u}_g}{\partial t}+u_g\nabla\cdot\vec{u}_g=-\frac{C_i}{\alpha\rho_g}\vec{u}_r\lvert\vec{u}_r\rvert-\frac{1}{\rho_g}\nabla\cdot P-\frac{w}{\alpha\rho_g}(\vec{u}_g-\vec{u}_{ig})-\frac{C_{wg}}{\alpha\rho_g}\vec{u}_g\lvert\vec{u}_g\rvert+\vec{g}$ $\frac{\partial\vec{u}_l}{\partial t}+u_l\nabla\cdot\vec{u}_l=+\frac{C_i}{(1-\alpha)\rho_l}\vec{u}_r\lvert\vec{u}_r\rvert-\frac{1}{\rho_l}\nabla\cdot P+\frac{w}{(1-\alpha)\rho_l}(\vec{u}_l-\vec{u}_{il})-\frac{C_{wl}\vec{u}_l\lvert\vec{u}_l\rvert}{(1-\alpha)\rho_l}+\vec{g}$ equations of energy $\frac{\partial}{\partial t}\{(1-\alpha)\rho_l e_l+\alpha\rho_g e_g\}+\nabla\cdot\{(1-\alpha)\rho_l e_l\vec{u}_l+\alpha\rho_g e_g\vec{u}_g\}=-P\nabla\cdot\{(1-\alpha)\vec{u}_l+\alpha\vec{u}_g\}+Q_{LW}+Q_{GW}$ $\frac{\partial}{\partial t}(\alpha\rho_g e_g)+\nabla\cdot(\alpha\rho_g\vec{u}_g e_g)=-P\frac{\partial\alpha}{\partial t}-P\nabla\cdot(\alpha\vec{u}_g)+Q_{GW}-Q_{IG}+wh_{gsat}$	3 D component	

Table 1 (Continued)

code/researcher	balance equations	note	reference
TRAC − PF 1	equations of continuity		personal information
	$\frac{\partial(1-\alpha)\rho_l}{\partial t} + \nabla\cdot\{(1-\alpha)\rho_l\vec{u}_l\} = -w$	liquid	
	$\frac{\partial(\alpha\rho_g)}{\partial t} + \nabla\cdot(\alpha\rho_g\vec{u}_g) = w$	mixed gas	
	$\frac{\partial(\alpha\rho_a)}{\partial t} + \nabla\cdot(\alpha\rho_a\vec{u}_g) = 0$	non−condensible gas	
	$\frac{\partial(1-\alpha)m\rho_l}{\partial t} + \nabla\cdot\{(1-\alpha)m\rho_l u_l\} = s_c$	boron	
	equations of motion		
	$\frac{\partial\vec{u}_g}{\partial t} + \vec{u}_g\cdot\nabla\vec{u}_g = -\frac{1}{\rho_g}\nabla P - \frac{C_i}{\alpha\rho_g}(\vec{u}_g-\vec{u}_i)\lvert\vec{u}_g-\vec{u}_l\rvert - \frac{w^+}{\alpha\rho_g}(\vec{u}_g-\vec{u}_l) - \frac{C_{wg}}{\alpha\rho_g}\vec{u}_g\lvert\vec{u}_g\rvert + \vec{g}$	in evaporation $w^+=w,\ w^-=0$	
	$\frac{\partial\vec{u}_l}{\partial t} + \vec{u}_l\cdot\nabla\vec{u}_l = -\frac{1}{\rho_l}\nabla P + \frac{C_i}{(1-\alpha)\rho_l}(\vec{u}_g-\vec{u}_l)\lvert\vec{u}_g-\vec{u}_l\rvert - \frac{w^-}{(1-\alpha)\rho_l}(\vec{u}_g-\vec{u}_l) - \frac{C_{wl}}{(1-\alpha)\rho_l}\vec{u}_l\lvert\vec{u}_l\rvert + \vec{g}$	in condensation $w^+=0,\ w^-=w$	
	equations of energy		
	$\frac{\partial}{\partial t}(\alpha\rho_g e_g) + \nabla\cdot(\alpha\rho_g e_g\vec{u}_g) = -P\frac{\partial\alpha}{\partial t} - P\nabla\cdot(\alpha\vec{u}_g) + Q_{GW} - Q_{IG} + wh_{sg}$		
	$\frac{\partial}{\partial t}\{(1-\alpha)\rho_l e_l + \alpha\rho_g e_g\} + \nabla\cdot\{(1-\alpha)\rho_l e_l\vec{u}_l + \alpha\rho_g e_g\vec{u}_g\} = -P\nabla\cdot\{(1-\alpha)\vec{u}_l + \alpha\vec{u}_g\} + Q_{LW} + Q_{GW}$	$\rho_g = \rho_s + \rho_a$ $\rho_g e_g = \rho_s e_s + \rho_a e_a$ $P = P_s + P_a$	
TRAC − BD	equations of continuity		NUREG/CR − 2134 (1981)
	$\frac{\partial}{\partial t}(\alpha\rho_g) + \nabla\cdot(\alpha\rho_g\vec{u}_g) = w$		
	$\frac{\partial}{\partial t}\{(1-\alpha)\rho_l + \alpha\rho_g\} + \nabla\cdot\{(1-\alpha)\rho_l\vec{u}_l + \alpha\rho_g\vec{u}_g\} = 0$		
	equations of motion		
	$\frac{\partial}{\partial t}\vec{u}_g + \vec{u}_g\cdot\nabla\vec{u}_g + K\frac{\rho_c}{\alpha\rho_g}\left\{\frac{\partial}{\partial t}(\vec{u}_g-\vec{u}_l) + \vec{u}_{di}\cdot\nabla(\vec{u}_g-\vec{u}_l)\right\} + \frac{1}{\rho_g}\nabla P - \vec{g}$ $-\frac{f_{GL}}{\alpha\rho_g} - \frac{f_{GW}}{\alpha\rho_g} = 0$	ρ_c : density of continuous phase u_{di} : dispersed phase velocity	

Table 1 (Continued)

code/researcher	balance equations	note	reference
	$\frac{\partial}{\partial t}\vec{u}_l + \vec{u}_l \cdot \nabla \vec{u}_l - K \frac{\rho_c}{(1-\alpha)\rho_l}\left\{\frac{\partial}{\partial t}(\vec{u}_g - \vec{u}_l) + \vec{u}_{di} \cdot \nabla(\vec{u}_g - \vec{u}_l)\right\} + \frac{1}{\rho_l}\nabla P - \vec{g} - \frac{f_{LG}}{(1-\alpha)\rho_l} \frac{f_{LW}}{(1-\alpha)\rho_l} = 0$ equations of energy $\frac{\partial}{\partial t}(\alpha\rho_g e_g) + \nabla \cdot (\alpha\rho_g e_g \vec{u}_g) = -P\left\{\frac{\partial \alpha}{\partial t} + \nabla \cdot (\alpha \vec{u}_g)\right\} + Q_{GW} - Q_{IG} + w h_{sg}$ $\frac{\partial}{\partial t}\{(1-\alpha)\rho_l e_l + \alpha\rho_g e_g\} + \nabla \cdot \{(1-\alpha)\rho_l e_l \vec{u}_l + \alpha\rho_g \vec{u}_g\} = Q_{LW} + Q_{GW} - P\nabla \cdot \{(1-\alpha)\vec{u}_l + \alpha\vec{u}_g\}$	$f_{GL} + f_{LG} = 0$ e : specific internal energy h_{sg}: saturation enthalpy of steam	
RELAP 4	equation of continuity $A\frac{\partial \rho}{\partial t} = -\frac{\partial W}{\partial z}$ equation of motion $A\frac{\partial(\rho u)}{\partial t} + \frac{\partial(uW)}{\partial z} = -A\frac{\partial P}{\partial z} - \rho g A \cos\theta \frac{\partial F_k}{\partial z}$ equation of energy $A\frac{\partial(\rho e)}{\partial t} + \frac{\partial}{\partial z}\left\{W\left(h + \frac{u^2}{2} + gz\cos\theta\right)\right\} = AQ_e$	homogeneous, saturation, 1 D two-phase flow g in gravity direction is defined positive when accompanied with $\cos\theta$.	ANCR-1127 (1975)
RELAP 5	equations of continuity $\frac{\partial(\alpha\rho_g)}{\partial t} + \frac{1}{A}\frac{\partial}{\partial z}(\alpha\rho_g u_g A) = w$ $\frac{\partial\{(1-\alpha)\rho_l\}}{\partial t} + \frac{1}{A}\frac{\partial}{\partial z}\{(1-\alpha)\rho_l u_l A\} = -w$ equations of motion $\alpha\rho_g A\frac{\partial u_g}{\partial t} + \alpha\rho_g u_g A\frac{\partial u_g}{\partial z} = -\alpha A\frac{\partial P}{\partial z} - \alpha\rho_g A g\cos\theta - (\alpha\rho_g A)FWG(u_g)$ $+ wA(u_l - u_g) - (\alpha\rho_g A)FIG(u_g - u_l) - C\alpha(1-\alpha)\rho A\left\{\frac{\partial}{\partial t}(u_g - u_l) + u_l\frac{\partial u_g}{\partial z} - u_g\frac{\partial u_l}{\partial z}\right\}$ $(1-\alpha)\rho_l A\frac{\partial u_l}{\partial t} + (1-\alpha)\rho_l u_l A\frac{\partial u_l}{\partial z} = -(1-\alpha)A\frac{\partial P}{\partial z} - (1-\alpha)\rho_l A g\cos\theta - \{(1-\alpha)\rho_l A\}FWL(u_l)$ $- wA(u_l - u_l) - \{(1-\alpha)\rho_l A\}FIL(u_l - u_g) - C(1-\alpha)\alpha\rho A\left\{\frac{\partial}{\partial t}(u_l - u_g) + u_g\frac{\partial u_l}{\partial z} - u_l\frac{\partial u_g}{\partial z}\right\}$ equations of energy $\frac{\partial}{\partial t}\{\alpha\rho_g E_g + (1-\alpha)\rho_l E_l\} + \frac{1}{A}\frac{\partial}{\partial z}\{\alpha\rho_g u_g F_g A + (1-\alpha)\rho_l u_l E_l A\} + \frac{1}{A}\frac{\partial}{\partial z}\{\alpha u_g PA$ $+ (1-\alpha)u_l PA\} - \{\alpha\rho_g u_g + (1-\alpha)\rho_l u_l\}B_z - Q = 0$	6 th term of right side is virtual mass term FWG, FWL: wall friction FIG, FIL : interfacial friction $E = e + \frac{u^2}{2}$ e : internal energy B_z: body force	NUREG/CR-1826, Revisionl (1981)

Table 1 (Continued)

code/researcher	balance equations	note	reference
COBRA/TRAC	equations of continuity $\frac{\partial(\alpha_g\rho_g)}{\partial t}+\nabla\cdot(\alpha_g\rho_g\vec{u}_g)=-w'''$ $\frac{\partial(\alpha_l\rho_l)}{\partial t}+\nabla\cdot(\alpha_l\rho_l\vec{u}_l)=-w'''-s'''$ $\frac{\partial(\alpha_e\rho_l)}{\partial t}+\nabla\cdot(\rho_e\rho_l\vec{u}_e)=-w'''+s'''$ here, for phase change $w'''-w_l'''-w_e'''=0$ and $\alpha_g+\alpha_l+\alpha_e=1$ s''' represents entrainment rate. equations of motion $\frac{\partial(\alpha_g\rho_g\vec{u}_g)}{\partial t}+\nabla\cdot(\alpha_g\rho_g\vec{u}_g\vec{u}_g)=-\alpha_g\nabla\cdot P+\alpha_g\rho_g\vec{g}+\nabla\cdot\{\alpha_g(\sigma_g+I_g^T)\}+\tau_{GW}'''$ $-\tau_{l_{EG}}'''-\tau_{l_{EG}}'+(w'''\vec{u})$ $\frac{\partial(\alpha_l\rho_l\vec{u}_l)}{\partial t}+\nabla\cdot(\alpha_l\rho_l\vec{u}_l\vec{u}_l)=-\alpha_l\nabla\cdot P+\alpha_l\rho_l\vec{g}+\nabla\cdot\{\alpha_l(\sigma_l+T_l^T)\}+\tau_{lW}'''-\tau_{l_{LG}}'''+(w_l'''\vec{u})$ $(s'''\vec{u})$ $\frac{\partial(\alpha_e\rho_l\vec{u}_e)}{\partial t}+\nabla\cdot(\alpha_e\rho_l\vec{u}_e\vec{u}_e)=-\alpha_e\nabla\cdot P+\alpha_e\rho_l\vec{g}+\tau_{EG}'''+\tau_{l_{EG}}'''-(w_e'''\vec{u})-(s'''\vec{u})$ equations of energy $\frac{\partial(\alpha_g\rho_g h_g)}{\partial t}+\nabla\cdot(\alpha_g\rho_g h_g\vec{u}_g)=-\nabla\cdot\{\alpha_g(\vec{q}_g+\vec{q}_g^T)\}+w'''h_g+q_{l_G}'''+Q_{GW}'''+\alpha_g\frac{\partial P}{\partial t}$ $\frac{\partial}{\partial t}\{(\alpha_l+\alpha_e)\rho_l h_l\}+\nabla\cdot(\alpha_l\rho_l h_l\vec{u}_l)+\nabla\cdot(\alpha_e\rho_l h_l\vec{u}_e)=-\nabla\cdot\{\alpha_l(\vec{q}_l+\vec{q}_l^T)\}-w'''h_l+q_{l_L}'''+Q_{LG}'''$ $+(\alpha_l+\alpha_e)\frac{\partial P}{\partial t}$	COBRA/TRAC is a combined code of COBRA-TF and TRAC-PD2, COBRA-TF model is listed here, Sufix g, l, e represent gas, continuous liquid and droplet, respectively. Superscript ''' indicates volumetric value. Continuous liquid and droplets are not disting uished in equations of energy.	NUREG/CR-3046, vol. 1 (1983)
DRUFAN-01	equations of continuity $\frac{\partial(\alpha\rho_g)}{\partial t}+\nabla\cdot(\alpha\rho_g\vec{u})=w$	Homogeneous two-phase flow. Thermal non-equilibrium is considered by phase change rate.	GRS-A-846 (1983)

Table 1 (Continued)

code/researcher	balance equations	note	reference
	$\frac{\partial\{(1-\alpha)\rho_l\}}{\partial t}+\nabla\cdot\{(1-\alpha)\rho_l\vec{u}\}=-w$ equation of motion $\frac{\partial(\rho\vec{u})}{\partial t}+\nabla\cdot(\rho\vec{u}\vec{u})+\nabla\cdot P+\nabla\cdot\tau-\rho\vec{g}=0$ equation of energy $\frac{\partial}{\partial t}(\rho E)+\nabla\cdot(\rho E\vec{u})+\nabla\cdot\vec{q}+\nabla\cdot(P\vec{u})+\nabla\cdot(\vec{\tau}\vec{u})=0$	$E=e+\frac{u^2}{2}+\phi$ e : internal energy ϕ : potential energy	
CATHARE-1	equations of continuity $\frac{\partial}{\partial t}A<\alpha\rho_g>+\frac{\partial}{\partial z}A<\alpha\rho_g u_g>=-A_w$ $\frac{\partial}{\partial t}A<(1-\alpha)\rho_l>+\frac{\partial}{\partial z}A<(1-\alpha)\rho_l u_l>=-Aw$ equations of motion $\frac{\partial}{\partial t}A<\alpha\rho_g u_g>+\frac{\partial}{\partial z}A<\alpha\rho_g u_g^2>+\frac{\partial}{\partial z}A<\alpha P_g>=-Af_{GL}+Af_{GW}+A<\alpha\rho_g g>$ $\frac{\partial}{\partial t}A<(1-\alpha)\rho_l u_l>+\frac{\partial}{\partial z}A<(1-\alpha)\rho_l u_l^2>+\frac{\partial}{\partial z}A<(1-\alpha)P_l>=Af_{LG}+Af_{LW}+A<(1-\alpha)\rho_l g>$ equations of energy $\frac{\partial}{\partial t}A\left\langle\alpha\rho_g\left(h_g+\frac{\vec{u}_g^2}{2}\right)\right\rangle-\frac{\partial}{\partial t}A<\alpha P_g>+\frac{\partial}{\partial z}A\left\langle\alpha\rho_g u_g\left(h_g+\frac{\vec{u}_g^2}{2}\right)\right\rangle$ $=AQ_{IG}+AQ_{GW}+A<\alpha\rho_g\vec{u}_g\vec{g}>+Aq_{rpg}$ $\frac{\partial}{\partial t}A\left\langle(1-\alpha)\rho_l\left(h_l+\frac{\vec{u}_l^2}{2}\right)\right\rangle-\frac{\partial}{\partial t}A<(1-\alpha)P_l>+\frac{\partial}{\partial z}A\left\langle(1-\alpha)\rho_l u_l\left(h_l+\frac{\vec{u}_l^2}{2}\right)\right\rangle$ $=-AQ_{IL}+AQ_{LW}+A<(1-\alpha)\rho_l\vec{u}_l\vec{g}>+Aq_{rpl}$	1 D two-phase flow $<\ >$: area average $f_{GL}+f_{LG}=0$ q_{rp}: radiation heat transfer $Q_{IG}+Q_{IL}=0$	NOTE TT/EM/11, CEA-Grenoble (1984)
W.G. Mathers, et al.	equations of continuity $\frac{\partial}{\partial t}(\alpha\rho_g)+\frac{\partial}{\partial z}(\alpha\rho_g u_g)=w-\alpha\rho_g u_g\frac{1}{A}\frac{dA}{dz}$ $\frac{\partial}{\partial t}\{(1-\alpha)\rho_l\}+\frac{\partial}{\partial z}\{(1-\alpha)\rho_l u_l\}=-w-(1-\alpha)\rho_l u_l\frac{1}{A}\frac{dA}{dz}$	1 D two-phase flow	Proc. 2nd CSNI Spec. Mtg., vol. 1, pp.59 (1987)

Table 1 (Continued)

code/researcher	balance equations	note	reference
	equations of motion $\frac{\partial}{\partial t}(\alpha\rho_g u_g)+\frac{\partial}{\partial z}(\alpha\rho_g u_g^2)+\alpha\frac{\partial P_g}{\partial z}=mu_{g,i}+\tau_{g,i}-\alpha_g\rho_g g\cos\theta-\alpha\rho_g u_g^2\frac{1}{A}\frac{dA}{dz}$ $\frac{\partial}{\partial t}\{(1-\alpha)\rho_l u_l\}+\frac{\partial}{\partial z}\{(1-\alpha)\rho_l u_l^2\}+(1-\alpha)\frac{\partial P_l}{\partial z}=mu_{l,i}+\tau_{l,i}+\tau_{l,w}-(1-\alpha)\rho_l g\cos\theta$ $-(1-\alpha)\rho_l u_l^2\frac{1}{A}\frac{dA}{dz}$ equations of energy $\frac{\partial}{\partial t}\left\{\alpha\rho_g\left(h_g+\frac{u_g^2}{2}\right)\right\}+\frac{\partial}{\partial z}\left\{\alpha\rho_g u_g\left(h_g+\frac{u_g^2}{2}\right)\right\}-\alpha\frac{\partial P}{\partial t}=m\left(h_{g,i}+\frac{u_{g,i}^2}{2}\right)+\tau'_{g,i}u_{gi}-q_{g,i}$ $-q_{g,w}-\alpha\rho_g u_g g\cos\theta+\alpha\rho_g u_g g\cos\theta\cdot\frac{1}{A}\frac{dA}{dz}$ $\frac{\partial}{\partial t}\left\{(1-\alpha)\rho_l\left(h_l+\frac{u_l^2}{2}\right)\right\}+\frac{\partial}{\partial z}\left\{(1-\alpha)\rho_l u_l\left(h_l+\frac{u_l^2}{2}\right)\right\}-(1-\alpha)\frac{\partial P}{\partial t}=-m\left(h_{l,i}+\frac{u_{l,i}^2}{2}\right)$ $+\tau'_{l,i}u_{l,i}-q_{l,i}-q_{l,w}+(1-\alpha)\rho_l u_l g\cos\theta-(1-\alpha)\rho_l u_l\cos\theta\cdot\frac{1}{A}\frac{dA}{dz}$	m: evaporation rate per interfacial area i : interface	
HEXECO	equations of continuity $\frac{\partial}{\partial t}(A\alpha\rho_g)+\frac{\partial}{\partial z}(A\alpha\rho_g u_g)=Aw$ $\frac{\partial}{\partial t}\{A(1-\alpha)\rho_l\}+\frac{\partial}{\partial z}\{A(1-\alpha)\rho_l u_l\}=Aw$ equations of motion $\frac{\partial}{\partial t}(A\alpha\rho_g u_g)+\frac{\partial}{\partial z}(A\alpha\rho_g u_g^2)+A\alpha\frac{\partial P}{\partial z}=AI-A\tau_{gw}-A\alpha\rho_g g\cos\theta$ $\frac{\partial}{\partial t}\{A(1-\alpha)\rho_l u_l\}+\frac{\partial}{\partial z}\{A(1-\alpha)\rho_l u_l^2\}+A(1-\alpha)\frac{\partial P}{\partial z}=-AI-A\tau_{lw}$ $-A(1-\alpha)\rho_l g\cos\theta$ equations of energy $\frac{\partial}{\partial t}\left\{A\alpha\rho_g\left(h_g+\frac{u_g^2}{2}\right)\right\}+\frac{\partial}{\partial z}\left\{A\alpha\rho_g u_g\left(h_g+\frac{u_g^2}{2}\right)\right\}-A\alpha\frac{\partial P}{\partial t}=AQ+A\phi_{gw}+A\alpha\rho_g u_g g\cos\theta$ $\frac{\partial}{\partial t}\left\{A(1-\alpha)\rho_l\left(h_l+\frac{u_l^2}{2}\right)\right\}+\frac{\partial}{\partial z}\left\{A(1-\alpha)\rho_l u_l\left(h_l+\frac{u_l^2}{2}\right)\right\}-A(1-\alpha)\frac{\partial P}{\partial t}=-AQ+A\phi_{lw}$ $+A(1-\alpha)\rho_l u_l g\cos\theta$	1 D two-phase flow	Proc. 2ned CSNI Spec. Mtg., vol. 1, pp.99 (1978)

Table 1 (Continued)

code/researcher	balance equations	note	reference
M. Ishii	equations of continuity $\frac{\partial}{\partial t}(\alpha\rho_g)+\nabla\cdot(\alpha\rho_g\vec{u}_g)=w$ $\frac{\partial}{\partial t}\{(1-\alpha)\rho_l\}+\nabla\cdot\{(1-\alpha)\rho_l\vec{u}_l\}=-w$ equations of motion $\frac{\partial}{\partial t}(\alpha\rho_g\vec{u}_g)+\nabla\cdot(\alpha\rho_g\vec{u}_g\vec{u}_g)=-\alpha\nabla\cdot P_g+\nabla\cdot\alpha(\bar{\bar{\tau}}+\tau_g^t)+\alpha\rho_g\vec{g}+\vec{u}_{gi}w+M_{ig}-\nabla\alpha\cdot\tau_i$ $\frac{\partial}{\partial t}\{(1-\alpha)\rho_l\vec{u}_l\}+\nabla\cdot\{(1-\alpha)\rho_l\vec{u}_l\vec{u}_l\}=-(1-\alpha)\nabla\cdot P_l+\nabla\cdot(1-\alpha)(\bar{\bar{\tau}}+\tau_l^t)+(1-\alpha)\rho_l\vec{g}+\vec{u}_{li}w$ $-M_{il}-\nabla(1-\alpha)\cdot\tau_i$ equations of energy $\frac{\partial}{\partial t}(\alpha\rho_g h_g)+\nabla\cdot(\alpha\rho_g h_g\vec{u}_g)=-\nabla\cdot\alpha_g(\bar{\bar{q}}_g+q_g^t)+\alpha\frac{D_g}{Dt}P_g+h_{gi}w+q_{gi}''/L_s+\Phi_g$ $\frac{\partial}{\partial t}\{(1-\alpha)\rho_l h_l\}+\nabla\cdot\{(1-\alpha)\rho_l h_l\vec{u}_l\}=-\nabla\cdot(1-\alpha)(\bar{\bar{q}}_l+q_l^t)+(1-\alpha)\frac{D_l}{Dt}P_l-h_{li}w+q_{li}''/L_s+\Phi_l$	3 D two-phase flow M interfacial drag $\bar{\bar{\tau}}$ average viscous stress τ^t turaulent stress τ_i interfacial shear stress $\bar{\bar{q}}$ conduction heat flux q^t turbulent heat flux q'' interfacial heat flux L_s representative length of interface Φ energy dissipation	"Thermo-fluid Dinamic Theory of Two-phase Flow", Eyrolles, Paris (1975)
M. Ishii	equations of continuity $\frac{\partial<\alpha>\rho_g}{\partial t}+\frac{\partial}{\partial z}<\alpha>\rho_g\ll u_g\gg=<w>$ $\frac{\partial<1-\alpha>}{\partial t}+\frac{\partial}{\partial z}<1-\alpha>\rho_l\ll u_l\gg=-<w>$ equations of motion $\frac{\partial}{\partial t}<\alpha>\rho_g\ll u_g\gg+\frac{\partial}{\partial z}C_{vg}<\alpha>\rho_g\ll u_g\gg^2=-<\alpha>\frac{\partial}{\partial z}\ll P_g\gg+\frac{\partial}{\partial z}<\alpha>\ll\tau_{gzl}+\tau_{gzl}^T\gg$ $\frac{4\alpha_w\tau_{gw}}{D}-<\alpha>\rho_g g\cos\theta+<w>\ll u_{gi}\gg+<M_g^d>$ $\frac{\partial}{\partial t}<1-\alpha>\rho_l\ll u_l\gg+\frac{\partial}{\partial z}C_{vl}<1-\alpha>\rho_l\ll u_l\gg^2=<1-\alpha>\frac{\partial}{\partial z}\ll P_g\gg$ $+\frac{\partial}{\partial z}<1-\alpha>\ll\tau_{lzl}+\tau_{lzl}^T\gg-\frac{4(1-\alpha_w)\tau_{lw}}{D}-<1-\alpha>\rho_l g\cos\theta-<w>\ll u_{li}\gg+<M_l^d>$	1 D two-phase flow $<\ >$: area average $\ll\ \gg$: weighted mean area average $<M^d>$: total interfacial shear force $<C_v>$: momentum flux distribution parameter $<C_h>$: enthalpy distribation parameter	Nucl. Fngg Desigm, 82, pp.107 (1984)

Table 1 (Continued)

code/researcher	balance equations	note	reference
	equations of energy $\frac{\partial}{\partial t}<\alpha>\rho_g\ll h_g\gg+\frac{\partial}{\partial z}C_{hg}<\alpha>\rho_g\ll h_g\gg\ll u_g\gg=\frac{\partial}{\partial z}<\alpha>\ll q_g+q_g^T\gg_t+<\alpha>\frac{D_g}{Dt}\ll P_g\gg$ $+\frac{\xi_h}{A}\alpha_{gw}q_{gw}^*+<w>\ll h_{gi}\gg+<q_{gi}^*/L_s>+<\phi_g>$ $\frac{\partial}{\partial t}<1-\alpha>\rho_l\ll h_l\gg+\frac{\partial}{\partial z}C_{hl}<1-\alpha>\rho_l\ll h_l\gg\ll u_l\gg=\frac{\partial}{\partial z}<1-\alpha>\ll q_l+q_l^T\gg_t$ $+<1-\alpha>\frac{D_l}{Dt}\ll P_l\gg+\frac{\xi_h}{A}\alpha_{lw}q_{lw}^*-<w>\ll h_{li}\gg+<q_{li}^*/L_s>+<\phi_l>$		

2. Number of Basic Equations and Selection of Examined Part of Fluid

2.1 Number of Basic Equations

Gas and liquid phases of examined part of two-phase fluid have, in a two-fluid model, respective values of mass, momentum and energy. Therefore, differential equations on balance of those quantities should hold good under proper boundary conditions at the gas-liquid interface and wall surface. That is, two equations of continuity, two equations of motion and two equations of energy can be established as independent hydrodynamical basic equations.

Total six independent differential equations describing directly or indirectly the balance of mass, force (momentum) and energy of gas and liquid phases are actually just equivalent both physically and mathematically with the above described most typical combination of basic equations for each phase. Therefore, form of the basic equation set is not unique. However, number of independent basic equations is always six.

2.2 Selection of Examined Part of Fluid

Balance of various physical quantities of a one-dimensional flow is usually described for a elementary part of fluid between two cross sections perpendicular to the flow axis. This method is quite convenient especially for describing balance of scalar quantities such as mass and energy. And, therefore, it is used in the present report as well as in the conventional theories in the literature.

This method, of course, can be used also for equation of motion but special care should be paid in the case of two-phase flow. Because, there is a momentum change due to time or spatial change of mass of the examined part of fluid which is independent of real acceleration of mass as discussed in detail in the subsections 4.2.4 and 4.7.1. This problem is seen also in single-phase flow but it does not cause any misevaluation of inertial force in relation with equation of continuity as described in the subsection 4.7.1.

In the present report, equations of motion are established first for unit mass of examined part of two-phase fluid. No change of total mass of examined part of fluid appears in this case even if mixing fraction of gas and liquid phases changes. Therefore, one can easily convert change of momentum or kinetic energy of examined part of fluid with this method into inertial force and equate it to the sum of all external forces.

On the other hand, one can pick up two kinds of unit mass two-phase fluid. One is based on two-phase fluid which instantaneously exists between two cross sections with small distance dz. Mass fraction of gas phase β in this case is given as:

$$\beta = \frac{A\alpha\rho_g dz}{A\alpha\rho_g dz + A(1-\alpha)\rho_l dz} = \frac{\alpha\rho_g}{\alpha\rho_g + (1-\alpha)\rho_l} \tag{1}$$

Here, A, α, ρ_g and ρ_l are the average values in distance dz. Unit mass two-phase fluid with gas mass fraction of β is called unit mass of "existing two-phase fluid".

The other kind of unit mass two-phase fluid is based on two-phase fluid which flows penetrating through a cross section in short time dt. Mass fraction of gas phase x in this case is represented as:

$$x=\frac{A\alpha\rho_g u_g dt}{A\alpha\rho_g u_g dt+A(1-\alpha)\rho_l u_l dt}=\frac{\alpha\rho_g u_g}{\alpha\rho_g u_g+(1-\alpha)\rho_l u_l} \tag{2}$$

Here, A, α, ρ_g, ρ_l, u_g and u_l are the average values in time dt. When both dz and dt become infinitigimal, each of these values becomes the local, instantaneous value and, therefore, they have the same values in Eqs. (1) and (2). Unit mass two-phase fluid with gas mass fraction of x is called unit mass of "flowing two-phase fluid".

Force balance equation for unit mass of existing two-phase fluid is named equation of motion "based on existing mass" and similarly, that for unit mass of flowing two-phase fluid as equation of motion "based on flowing mass".

β and x are independent to each other although they are connected together through slip ratio u_g/u_l. Therefore, equations of motion based on existing mass and based on flowing mass are independent to each other. So that, one can establish these two kinds of equation of motion instead of equations of motion for each phase. Of course, if the former two equations of motion are already established the latter two equations of motion should be derived by a purely mathematical transformation. This will be demonstrated later in Section 4.4.

3. Equations of Continuity

3.1 Equations of Continuity for Each Phase

Equations of continuity for each phase are the following two in the two-fluid model, i.e.,

$$A\frac{\partial}{\partial t}(\alpha\rho_g)+\frac{\partial}{\partial z}(A\alpha\rho_g u_g)=Aw \tag{3}$$

$$A\frac{\partial}{\partial t}\{(1-\alpha)\rho_l\}-\frac{\partial}{\partial z}\{A(1-\alpha)\rho_l u_l\}=-Aw \tag{4}$$

Here, flow area A is assumed constant with respect to time. If one does not assume this, A in the first terms should be included in the differentiated variables.

Changes of densities of each phase can be expressed with compressibilities $K_g=(d\rho_g/dP)/\rho_g$ and $K_l=(d\rho_l/dP)/\rho_l$ which are affected by temperature changes. Therefore, Eqs. (3) and (4) can be written as:

$$\frac{\partial u_g}{\partial z}+\frac{1}{\alpha}\left(\frac{\partial\alpha}{\partial t}+u_g\frac{\partial\alpha}{\partial z}\right)+K_g\left(\frac{\partial P}{\partial t}+u_g\frac{\partial P}{\partial z}\right)+\frac{u_g}{A}\frac{dA}{dz}-\frac{w}{\alpha\rho_g}=0 \tag{5}$$

$$\frac{\partial u_l}{\partial z}-\frac{1}{1-\alpha}\left(\frac{\partial\alpha}{\partial t}+u_l\frac{\partial\alpha}{\partial z}\right)-K_l\left(\frac{\partial P}{\partial t}+u_l\frac{\partial P}{\partial z}\right)+\frac{u_l}{A}\frac{dA}{dz}+\frac{w}{(1-\alpha)\rho_l}=0 \tag{6}$$

Equations (5) and (6) are more convinient than Eqs. (3) and (4) in some problems.

These equations of continuity include phase change rate w for unit volume of channel (w is positive when evaporation). w can be obtained by using the balance relationship of heat flow including latent heat at the interface between gas and liquid phases. That is, with representing the heat flow rates for unit volume of channel from insides of each phase to the interface with Q_{IG} and Q_{IL}, respectively, one can obtain

$$w=\frac{Q_{IG}-Q_{IL}}{h_g-h_l} \tag{7}$$

3.2 Mass Conservation Equation for Total Two-Phase Flow

By summing up Eqs. (3) and (4), the mass conservation equation for total two-phase flow can be obtained as:

$$A\frac{\partial}{\partial t}\{\alpha\rho_g+(1-\alpha)\rho_l\}+\frac{\partial}{\partial z}[A\{\alpha\rho_g u_g+(1-\alpha)\rho_l u_l\}]=0 \tag{8}$$

3.3 Equation of Phase Change (1)

By subtracting Eq. (4) from Eq. (3), equation of phase change rate w can be obtained as:

$$A\frac{\partial}{\partial t}\{\alpha\rho_g-(1-\alpha)\rho_l\}+\frac{\partial}{\partial z}[A\{\alpha\rho_g u_g-(1-\alpha)\rho_l u_l\}]=2Aw \tag{9}$$

3.4 Independency of Equations of Continuity

The author derived six equations, Eqs. (3), (4), (5), (6), (8) and (9), as equations of continuity for one-dimensional two-phase flow in the two-fluid model. As described in Section 2.1, however, number of independent equations of continuity is two. Therefore, if such two equations are given the rest equations of continuity should lose their independencies automatically. Such perfect combinations of two equations of continuity are shown with symbol "○" in **Table 2**.

Table 2 Combinations of two independent equations of continuity

	(3)	(4)	(5)	(6)	(8)	(9)
(3)		○	×	○	○	○
(4)	○		○	×	○	○
(5)	×	○		○	○	○
(6)	○	×	○		○	○
(8)	○	○	○	○		○
(9)	○	○	○	○	○	

3.5 Equation of Phase Change (2)

At last, a very important equation on phase change rate w shall be introduced although it is not an equation of continuity.

In **Fig. 1**, gas phase passed cross section ① at a moment arrives after short time dt at cross section 1'-2' which is $u_g dt$ distant from cross section ①. Similarly, liquid phase passed cross section ① at the same moment arrives after time dt at cross section 3'-4' which is $u_l dt$ distant from cross section ①. Phase change part of fluid which passed cross section ① as liquid phase and became gas phase during time dt arrives after time dt at some location on the line 2'-3' depending on phase change timing. For example, fluid particle evaporated at the beginning of time dt arrives at location 2' and fluid particle evaporated at the end of time dt arrives at location 3'. The average arrival location of phase change part of fluid is apparently given by cross section 2"-3", i.e., cross section ② which is distant from cross section ① by $(1/2)(u_g+u_l)dt$. Therefore, average velocity of phase change part of fluid u_{PC} is:

$$u_{PC}=\frac{1}{2}(u_g+u_l) \tag{10}$$

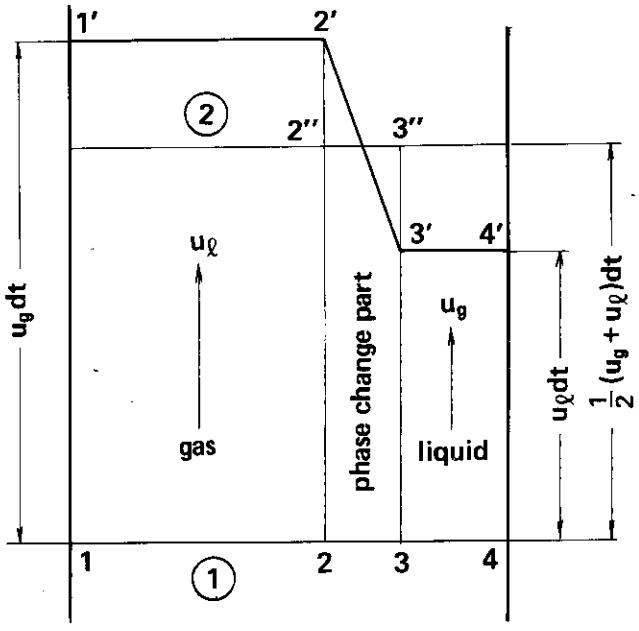

Fig. 1 Estimation of average velocity of phase change part of fluid based on mass displacement analysis.

It must be noted that u_{PC} is not the interfacial velocity between two phases but the average or representative velocity of phase change part of fluid. u_{PC} is one of the most important key variables in the author's theory.

Based on Eq. (10), phase change rate for unit length of channel Aw is expressed as:

$$Aw=W\left(\frac{\partial x}{\partial t}\frac{dz}{u_{PC}}+\frac{\partial x}{\partial z}dz\right)/dz=W\left(\frac{2}{u_g+u_l}\frac{\partial x}{\partial t}+\frac{\partial x}{\partial z}\right). \tag{11}$$

Equation (11) is a definition equation of phase change rate w as function of total mass flow rate W and change of quality x from the view point of mass displacement of phase change part of fluid itself. The equation does not include the variables such as α, ρ_g and ρ_l which express mass fraction of gas and liquid phases of the main flow. Although it includes u_g and u_l, they are not for evaluation of the main flow phase velocities but for evaluation of representative velocity of phase change part of fluid. These facts indicate that Eq. (11) is independent of mass balance of the main flow gas and liquid phases, i.e., Eq. (11) is not an equation of continuity for the main flow fluid.

However, Eq. (11) or essentially, Eq. (10) are very important because these equations clearly indicate the fact that phase change part of fluid has a unique representative velocity different from those for gas and liquid phases of the main flow. The importance of this fact will be made clear through the discussions of Chapter 4.

4. Equations of Motion

4.1 Steady Equations of Motion for Total Two-Phse Flow

4.1.1 Equation based on "existing mass"

Equation of motion based on existing mass is the equation on instantaneous force balance for unit mass of existing two-phase fluid. To describe the force balance, one must start from evaluation of various kinds of force acting on each component of unit mass of existing two-phase fluid.

At first, let us evaluate the inertial force terms. In the present report, inertial forces acting on each component of examined part of fluid are counted for the steady acceleration term by applying the kinetic energy principle instead of the momentum principle which is applied in the conventional theories. That is, inertial force acting on each component of examined part of fluid is calculated by dividing kinetic energy change of the component by traveled distance dz during the change. As kinetics for point of mass indicates, this is one of the general principles of kinetics which holds good regardless of elapsed time for traveling the distance dz. The momentum principle is never ignored by applying the kinetic energy principle but, on the contrary, is correctly applied as described later. Application of the kinetic energy principle, instead of the momentum principle, is one of the remarkable features of the author's theory together with picking up the two kinds of "unit mass" of examined part of fluid, i.e., one is "existing mass" and the other is "flowing mass".

In **Fig. 2**, each component of unit mass of existing two-phase fluid at cross section ① will arrive at cross section ② although the elapsed time is different among the components.

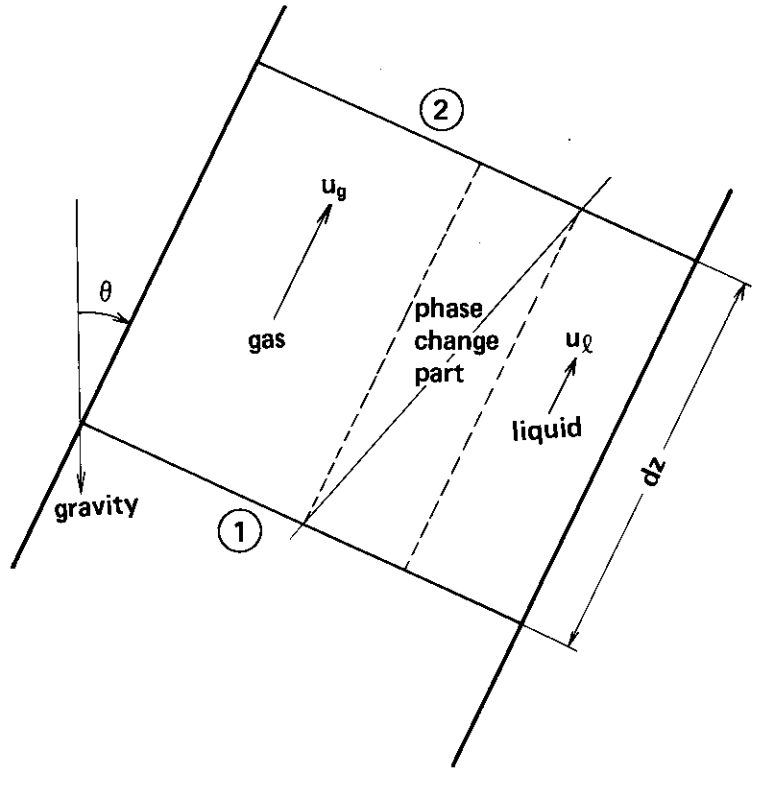

Fig. 2 One-dimensional two-fluid model.

In steady flow, flows at cross section ① and ② do not change with time, therefore, one can evaluate the average inertial forces acting on each component one by one by dividing the spatial changes of kinetic energy between cross sections ① and ② by distance dz. If dz becomes infinitegimal, the results give the local values of inertial forces for each component of unit mass of existing two-phase fluid. By this method, inertial force for gas phase is evaluated as:

$$\frac{1}{2}\beta\frac{d(u_g^2)}{dz}=\beta u_g\frac{du_g}{dz} \tag{12}$$

Similarly, for liquid phase:

$$\frac{1}{2}(1-\beta)\frac{d(u_l^2)}{dz}=(1-\beta)u_l\frac{du_l}{dz} \tag{13}$$

There is a change of β between cross sections ① and ② due to phase change, and inertial force acting on the phase change part of fluid is given similarly, as:

$$\frac{1}{2}(u_g^2-u_l^2)\frac{d\beta}{dz}=(u_g-u_l)u_{PC}\frac{d\beta}{dz} \tag{14}$$

Here, u_{PC} in Eq. (14) agrees with that in Eq. (10). More detailed discussion on Eq. (14) will be made in the subsection 4.2.2.

Sum of Eqs. (12) through (14) gives inertial force acts on unit mass of existing two-phase fluid.

Here, it is necessary to give some explanation on the effect of replacement of substances which compose the examined part of fluid. Due to phase slip, gas phase, liquid phase and phase change part of fluid which passed cross section ① simultaneously never arrive at cross section ② at the same time. This means substance of examined part of fluid is partially replaced between cross sections ① and ②. In the author's theory, since "unit mass" of existing two-phase fluid is selected as examined part of fluid, total mass of examined part of fluid never changes even if the substance is replaced. Replacement of substance without change of total mass does not cause any inertial force if the new substance has the same velocity as that of the old substance. Therefore, replacement of substance itself of examined part of fluid and the resultant change in the corresponding relationship among substances of each component of examined part of fluid do not affect the value of inertial force acting on the mass center of examined part of fluid.

External forces to be balanced with the inertial forces given by Eqs. (12) through (14) are pressure force, gravitational force, interfacial fractional force (drag force) and wall frictional force. And they can be written, respectively, for unit mass of existing two-phase fluid, as:

$$-\left(\frac{\beta}{\rho_g}+\frac{1-\beta}{\rho_l}\right)\frac{dP}{dz} \tag{15}$$

$$-g\cos\theta \tag{16}$$

$$\frac{\beta}{\rho_g}F_{GL}+\frac{1-\beta}{\rho_l}F_{LG} \tag{17}$$

$$\frac{\beta}{\rho_g}F_{GW}+\frac{1-\beta}{\rho_l}F_{LW} \tag{18}$$

Here, interfacial frictional forces are internal forces for the total two-phase fluid and by Newton's thrid law,

$$\frac{\beta}{\rho_g} F_{GL} - \frac{1-\beta}{\rho_l} F_{LG} = 0 \tag{19}$$

However, since the first and second terms of Eq. (17) are external forces for each phase, Eq. (17) shall be remaind for convenience in the later discussion.

In some conventional equations of motion, A and α or $1-\alpha$ are included in the differentiated variables of pressure force terms. However, the differentiated variable sould be only P because form of the terms is simply based on the Green's theorem.

Next, F_{GL} and F_{LG} consist of various terms. The regular drag force which is the sum of skin drag and form drag is assumed to be propertional to square of relative velocity between two phases and the drag coefficient is given with experimental basis. Basset force which represents the effect of relative acceleration between two phases on viscous drag and boundary layer development should be considered in some case. Furthermore, lift force due to rotation of dispersed phase (Magnus effect) and diffusion force due to concentration gradient of dispersed phase are known to act on two-phase fluid. However, these two forces are usually negligible.

Some convensional equations of motion for two-phase flow have so-called virtual mass force terms. However, it seems quite doubtful to introduce virtual mass force into equations of motion. Because, virtual mass force and its reaction force should be included potentially in inertial force terms and pressure force terms for each phase, respectively, as described in Appendix 1. Therefore, no virtual mass force terms shall be introduced in this report.

There is no external force which directly acts on phase change part of fluid although finite inertial force given by Eq. (14) acts on the part. The reason is that even if there is body force or surface force directly acts on the phase change part of fluid, since mass fraction of the part $d\beta$ to the total approaches to zero when dz approaches to zero, effect of such force also approaches to zero. Inertial force given by Eq. (14) due to phase change acceleration is actually balanced with a part of external forces given by Eqs. (15) through (18) through interaction with the gas or liquid phases of the main flow.

Because the sum of Eqs. (12) through (14) balances with the sum of Eqs. (15) through (18),

$$\beta u_g \frac{du_g}{dz} + (1-\beta) u_l \frac{du_l}{dz} + \frac{1}{2}(u_g^2 - u_l^2)\frac{d\beta}{dz} + \left(\frac{\beta}{\rho_g} + \frac{1-\beta}{\rho_l}\right)\frac{dP}{dz}$$
$$+ g\cos\theta - \left(\frac{\beta}{\rho_g} F_{GL} + \frac{1-\beta}{\rho_l} F_{LG}\right) - \left(\frac{\beta}{\rho_g} F_{GW} + \frac{1-\beta}{\rho_l} F_{LW}\right) = 0 \tag{20}$$

Here, the sixth term of Eq. (20) is zero because of Eq. (19).

4.1.2 Equation based on "flowing mass"

Equations of motion based on flowing mass is essentially the equation of instantaneous force balance for unit mass of flowing two-phase fluid. However, the formulation is based on the interaction among gas and liquid phases of the main flow and phase change part of fluid during common elapsed time. This will be explained in detail in the subsection 4.2.3.

In **Fig. 2**, each component of unit mass of flowing two-phase fluid at cross section ① will arrive at cross section ② although the elapsed time is different among the components. In steady flow, flows at cross sections ① and ② do not change with time, therefore, one can evaluate the average inertial forces acting on each component one by one by dividing

the spatial changes of kinetic energy between cross sections ① and ② by distance dz. If dz becomes infinitesimal, the results give the local values of inertial forces for each component of unit mass of flowing two-phase fluid. By this method, inertial force is evaluated for gas phase as:

$$\frac{1}{2}x\frac{d(u_g^2)}{dz}=xu_g\frac{du_g}{dz} \tag{21}$$

Similarly, for liquid phase:

$$\frac{1}{2}(1-x)\frac{d(u_l^2)}{dz}=(1-x)u_l\frac{du_l}{dz} \tag{22}$$

There is a change of x between cross sections ① and ② due to phase change, and inertial force acting on the phase change part of fluid is given similarly, as:

$$\frac{1}{2}(u_g^2-u_l^2)\frac{dx}{dz}=(u_g-u_l)u_{PC}\frac{dx}{dz} \tag{23}$$

Here, u_{PC} in Eq. (23) also agrees with that in Eq. (10). More detailed discussion on Eq. (23) will be made in the subsection 4.2.2.

Sum of Eqs. (21) through (23) gives inertial force acts on unit mass of flowing two-phase fluid.

External forces to be balanced with the inertial forces given by Eqs. (21) through (23) are pressure force, gravitational force, interfacial frictional force (drag force) and wall frictional force. And they can be written, respectively, for unit mass of flowing two-phase fluid, as:

$$-\left(\frac{x}{\rho_g}+\frac{1-x}{\rho_l}\right)\frac{dP}{dz} \tag{24}$$

$$-g\cos\theta \tag{25}$$

$$\frac{x}{\rho_g}F_{GL}+\frac{1-x}{\rho_l}F_{LG} \tag{26}$$

$$\frac{x}{\rho_g}F_{GW}+\frac{1-x}{\rho_l}F_{LW} \tag{27}$$

Because the sum of Eqs. (21) through (23) balances with the sum of Eqs. (24) through (27), steady equation of motion for unit mass of flowing two-phase fluid is written as:

$$xu_g\frac{du_g}{dz}+(1-x)u_l\frac{du_l}{dz}+\frac{1}{2}(u_g^2-u_l^2)\frac{dx}{dz}+\left(\frac{x}{\rho_g}+\frac{1-x}{\rho_l}\right)\frac{dP}{dz}+g\cos\theta$$
$$-\left(\frac{x}{\rho_g}F_{GL}+\frac{1-x}{\rho_l}F_{LG}\right)-\left(\frac{x}{\rho_g}F_{GW}+\frac{1-x}{\rho_l}F_{LW}\right)=0 \tag{28}$$

Here, the sixth term of interfacial frictional force in Eq. (28) is not zero. This is a different point from the case of Eq. (20).

4.2 Additional Explanations

In Section 4.1, two equations of motion for steady one-dimensional two-phase flow were derived. One is Eq. (20) based on existing two-phase fluid and the other is Eq. (28) based on flowing two-phase fluid. There are physically no doubts in derivation process of

these equations but form of the equations is quite different from that of equations of motion in the literature (See **Table 1**.). Therefore, explanation of the unique features and physical meanings of the author's equations of motion is necessary for justifying the author's theory.

4.2.1 Starting from equations for total two-phase flow

As described previously, two independent equations of motion for total two-phase flow were established first, before the derivation of equations of motion for each phase, in the present report. Equations of motion for each phase will be derived in Section 4.4 based on the equations of motion for total two-phase flow.

The reason why such approach is possible is clearly that steam mass fraction β in unit mass of existing two-phase fluid is, as already described in Section 2.2, independent of steam mass fraction of x in unit mass of flowing two-phase fluid because of phase slip. Therefore, combination of equations of motion for existing two-phase fluid and for flowing two-phase fluid is equivalent both physically and mathematically with combination of equations of motion for each phase.

If one established equations of motion for each phase first, a difficulty arises in evaluation of inertial forces due to phase change acceleration and then some physical models (such as velocities at the interface) on mechanism of phase change acceleration have to be assumed. Because, equations of motion for each phase are essentially two equations of motion for single-phase flow and effect of phase change acceleration is additionally evaluated by introducing some special terms. However, since there are no restriction conditions from the view point of balance of physical values (momentum or kinetic energy) of total two-phase flow including other phase, one must introduce some models instead of the restriction conditions by physical insight (Actually speaking, mathematical expression of the restriction conditions is no other than the equation of motion.). Such equations of motion for each phase including special physical models on mechanism of phase change acceleration do not guarantee balance of the physical values and, therefore, they cannot be called "balance equations" in strict sense although they seem like balance equations.

In Eqs. (20) and (28), inertial force due to phase change acceleration is expressed very simply in the balance relationship in kinetic energy (also in momentum as described in the next subsection) of total two-phase flow. In addition, since two independent equations of motion for total two-phase flow were established already, equations of motion for each phase can be determined uniquely as described in Section 4.4. Therefore, there is no room to introduce physical models on the mechanism of phase change acceleration.

4.2.2 Application of kinetic energy principle

In derivation of Eqs. (20) and (28), relationship between spatial differentiation of kinetic energy and force was applied instead of relationship between time differentiation of momentum and force. This method might seem contrary to the common understanding in hydrodynamics for single-phase flow. However, this method is a direct application of definition of kinetic energy : (kinetic energy change) = (force) × (traveled distance). Generality of this relationship is equivalent to that of definition relationship of momentum : (momentum change) = (force) × (elapsed time).

For steady flow, changes of each variable necessary to evaluate inertial force are given for a short distance dz. In Euler type equation of motion for single-phase flow, steady inertial force term has velocity u to convert the spatial change of momentum, $\rho(du/dz)$, into time change of momentum, $\rho(du/dt)$. And the momentum principle can be applied correctly by this conversion, i.e.,

$$\rho u \frac{du}{dz} = \rho \underbrace{\frac{du}{dz}}_{(\frac{\cdot}{u})} = \rho \frac{du}{dt} \tag{29}$$

In two-phase flow, representative velocity is different among each component of the examined part of fluid. Therefore, elapsed time to travel the commonly given distance dz is also different one by one. Representative velocities for gas and liquid phases of main flow are evidently u_g and u_l, respectively, and one can easily evaluate the effect of different elapsed time of the main flow phases to travel the common distance dz by using the above described method. In fact, one can confirm the fact that the elapsed times for gas phase, dt_g, and for liquid phase, dt_l, are du/u_g and du/u_l, respectively, by applying similar rearrangement as Eq. (29) to the right hand sides of Eqs. (12) and (13) or (21) and (22).

However, representative velocity for phase change part of fluid is unknown because the part is essentially not perfectly gas phase and on the same time it is not perfectly liquid phase. Of course, average velocity u_{PC} of the part was already obtained as Eq. (10). Therefore, one can make similar handling as the above discussion by using the u_{PC} value. In fact, this approach gives correct result as known through the following discussion. However, Eq. (10) was derived by examination of mass displacement and is not based on Newton's second law. So that it is hesitated to take this approach without confirmation of internal consistency between mass displacement and force balance.

Essentially speaking, the reason why representative velocity of phase change part of fluid is necessary is to apply the momentum principle to evaluate the steady phase change intertial force which is caused by spatial change of flow. That is, to calculate inertial forces by using the momentum principle, elapsed time to travel the given distance dz should be correctly estimated for each part of fluid, and, therefore, the representative velocities of the parts should be known. If one applies the kinetic energy principle, he can calculate the inertial forces regardless of the difference in elapsed time to travel the given distance dz among the parts of fluid. In fact, in the case of single-phase flow, it is also possible to estimate the inertial force term based on the kinetic energy principle. That is,

$$\rho u \frac{du}{dz} = \frac{1}{2} \rho \frac{d(u)^2}{dz} \tag{30}$$

This idea can easily be generalized to the case of three-dimensional single-phase flow as described in Appendix 2.

Based on the above described consideration, the left hand sides of Eqs. (14) and (23) were made for steady phase change inertial force terms with the kinetic energy principle. And the results can be interpreted with the momentum principle as shown in the right hand sides of the equations, giving the same expression of representative velocity of the phase change part of fluid with Eq. (10).

Next, let us discuss microscopically the physical meaning of representative velocity of phase change part of fluid. For simplicity of discussion, phase change acceleration process shall be assumed as the finite acceleration from u_l to u_g of many small fluid particles with mass μ. Let us also assume that each fluid particle is accelerated in time τ with traveling distance δ. As described later, those simplifications never spoil the generality of the discussion. Then, time averaged force f_τ and spatially averaged force f_δ during phase change acceleration are written as:

$$f_\tau = \frac{\mu\int_0^\tau \frac{du}{dt}dt}{\int_0^\tau dt} = \frac{\mu\int_{u_l}^{u_g} du}{\int_0^\tau dt} = \frac{\mu(u_g-u_l)}{\tau} \tag{31}$$

$$f_\delta = \frac{\frac{1}{2}\mu\int_0^\delta \frac{d(u^2)}{dz}dz}{\int_0^\delta dz} = \frac{\frac{1}{2}\mu\int_{u_l{}^2}^{u_g{}^2} d(u^2)}{\int_0^\delta dz} = \frac{\mu(u_g{}^2-u_l{}^2)}{2\delta} \tag{32}$$

f_τ and f_δ are equal to each other when each fluid particle is accelerated by constant force. However, they are not equal to each other generally.

Phase change occurs at mass rate $d\beta/dt_{PC}$ per unit mass of existing two-phase fluid*. Number rate of fluid particles per unit mass of existing two-phase fluid is, therefore, $(d\beta/dt_{PC})/\mu$. Since each fluid particle is accelerated during time τ, number of fluid particles which are accelerated on the same time is $(d\beta/dt_{PC})\tau/\mu$. This number is generally so large that, probability distribution of acceleration stage is considered flat. Therefore, average force acting on each fluid particle is given by Eq. (31). Thus, total force acts on unit mass of existing two-phase fluid is:

$$F_{PC} = \frac{d\beta}{dt_{PC}}\cdot\frac{1}{\mu}\cdot\tau\cdot f_\tau = (u_g-u_l)\frac{d\beta}{dt_{PC}} \tag{33}$$

Next, let us discuss the same problem from spatial point of view. Spatial change of β appears* corresponding to phase change rate $d\beta/dt_{PC}$ in unit mass of existing two-phase fluid. Number of fluid particles existing in unit length of channel is $(dM/dz)(d\beta/dz)/\mu$. Here, $dM/dz(=A\{\alpha\rho_g+(1-\alpha)\rho_l\})$ is existing mass per unit length of channel. Since each fluid particle is accelerated within distance δ, number of spatial superposition of fluid particles under phase change acceleration is $(dM/dz)(d\beta/dz)\delta/\mu$. This number is generally so large that probability distribution of acceleration stage is considered flat. Therefore, average force acting on each fluid particle is given by Eq. (32). Thus, total force acting on unit mass of existing two-phase fluid is:

$$F_{PC} = \frac{dM}{dz}\cdot\frac{d\beta}{dz}\cdot\frac{1}{\mu}\cdot\delta\cdot f_\delta\cdot\frac{1}{(dM/dz)} = \frac{1}{2}(u_g{}^2-u_l{}^2)\frac{d\beta}{dz} \tag{34}$$

Since Eqs. (33) and (34) should be the same to each other,

$$u_{PC} \equiv \frac{dz}{dt_{PC}} = \frac{1}{2}(u_g+u_l) \tag{35}$$

Eq. (35) gives the representative velocity of phase change part of fluid which was derived with microscopic kinetic model of phase change acceleration. It is just the same as Eq. (10) which was derived based on the consideration on mass displacement of phase change part of fluid.

When $f_\tau=f_\delta$ in Eqs. (31) and (32), i.e., when each fluid particle is accelerated by constant force, u_{PC} can be defined as:

$$u_{PC} \equiv \frac{\delta}{\tau} = \frac{1}{2}(u_g+u_l) \tag{36}$$

That is, general representative velocity u_{PC} is equal to the average velocity of phase change

* In general case, $d\beta=(\partial\beta/\partial t)dt+(\partial\beta/\partial z)dz=\{(\partial\beta/\partial t)+u_{PC}(\partial\beta/\partial z)\}dt_{PC}=\{(\partial\beta/\partial t)/u_{PC}+(\partial\beta/\partial z)\}\cdot dz$. In the case of steady flow, $\partial\beta/\partial t=0$. Therefore, $d\beta/dt_{PC}=u_{PC}(d\beta/dz)$ or $d\beta/dz=(d\beta/dt_{PC})/u_{PC}$.

fluid particles which are assumed to be accelerated by constant force. This means that although each fluid particle is not always accelerated by constant force, the change of force during phase change acceleration does not affect the final value of phase change inertial force, because inertial forces acting on all the fluid particles are averaged and summed up.

For making the physical picture more clear, an additional explanation shall be provided. Representative velocity u_{PC} is considered to be equal to the average velocity of chained fluid particles of which one fluid particle which terminated the acceleration under constant force at some moment at some place is connected to another fluid particle which begins the acceleration at the same moment at the same place. It is like the velocity in a relay race instead of that in a personal race. This is physically very reasonable because phase change part of fluid is not the phase change part of fluid before initiation of phase change acceleration and also is not the phase change part of fluid after termination of phase change acceleration.

Finally, it must be noted that μ, τ and δ which represent the kinetic characteristics of acceleration of each fluid particle are not included in the final results of Eqs. (33) through (35), although they are included in Eqs. (31) and (32). This is because phase change inertial force and representative velocity of phase change part of fluid are determined only by phase change rate ($d\beta/dt_{PC}$ or $d\beta/dz$) and velocities before and after phase change (u_g and u_l), regardless of microscopic mechanism of phase change acceleration. The fact that μ, τ and δ are not included in Eqs. (33) through (35) also clearly indicates that the above discussion started from introduction of those microscopic parameters is not limited by the physical modeling.

Of course, the microscopic examination described above is only an additional explanation of validity of the author's equation of motion, Eq. (20). Validity of the equation is not guaranteed by the model investigation in this subsection but by the deriving procedure itself.

The above discussion can simply be applied to the equation of motion (28) for flowing two-phase fluid if only β is replaced with x. Difference from the case of existing two-phase fluid is that phase change part of fluid dx is accelerated not by the instantaneously interacted main flow phases but by the phases interacted during some elapsed time. This difference shall be discussed in detail in the next section.

Finally, one of the problems related to the application of the kinetic energy principle may be the energy dissipation. That is, there can generally be energy dissipation due to internal forces among multiple points of mass in addition to work done by external forces because of difference in velocity among the points of mass.[15]

In the case of the most simple two points of mass system moving on a straight line, mechanism of energy dissipation is as follows. When internal forces, f_{12} and $f_{21}(=-f_{12})$, act on each other between two points of mass, m_1 and m_2, and the velocities, u_1 and u_2, are different to each other, mechanical work per unit time $-f_{12}u_l$ which point of mass m_1 performs is different to mechanical work $f_{21}u_2$ which point of mass m_2 is performed. And the difference is dissipated. Therefore, energy dissipation rate is given by:

$$-(f_{12}u_1+f_{21}u_2)\neq 0 \tag{37}$$

As known from this examination, energy dissipation appears when mechanical works per "unit time" done by every point of mass are algebraically summed up. In the evaluation of steady inertial force terms in this report, mechanical works per "unit distance" done by each part of fluid are counted. In this case, energy dissipation is never calculated even if the mechanical works per unit distance are summed up. This fact is equivalent to the following relationship for the two points of mass problem:

$$-(f_{12}dz+f_{21}dz)=0 \tag{38}$$

Equation (38) holds good regardless of whether energy dissipation exists or not. Therefore, kinetic energy change per unit traveled distance can be equated to the sum of external forces without any considerations on internal forces.

Relationship between phase change acceleration and energy dissipation should be explained in more detail and it will be done in Chapter 5.

4.2.3 Coincidence between phase change part of fluid and main flow phases

In this subsection, let us examine the coincidental relationship between amount of phase change part of fluid and amounts of main flow gas and liquid phases. The reason why the coincidental relationship should be examined is as follows. All terms of Eq. (20) or (28) except the phase change inertial force term can easily be divided into forces which act on gas phase and, therefore, are proportional to the amount of gas phase and forces which act on liquid phases and, therefore, are proportional to the amount of liquid phase. Therefore, there are no doubts in quantitative coincidental relationship among those forces. However, for the phase change inertial force term, such coincidental relationship is unclear. Therefore, even if evaluation of phase change inertial force is valid itself, there are still some doubts whether one can validly equate the sum of all terms including phase change inertial force term to zero. In other words, if quantitative relationships between $d\beta$ and β or $1-\beta$ in Eq. (20) and between dx and x or $1-x$ in Eq. (28) are justified, validity of those equations will naturally be guaranteed. In addition, detailed examination of this relationships is expected to make clear the difference in physical meaning between equations of motion based on existing fluid and based on flowing fluid.

At first, let us discuss about Eq. (20) for unit mass of existing two-phase fluid. As known from the previous discussions in the subsections 4.1.1 and 4.2.2, phase change inertial force term of Eq. (20) represents inertial force acting on phase change part of unit mass two-phase fluid which instantly exists in distance dz. Amount of gas and liquid phases contributing to the acceleration of the phase change part of fluid are, as illustrated in **Fig. 3**, β and $1-\beta$, respectively. Because, the other part of fluid cannot interact with the phase change part of fluid at the moment.

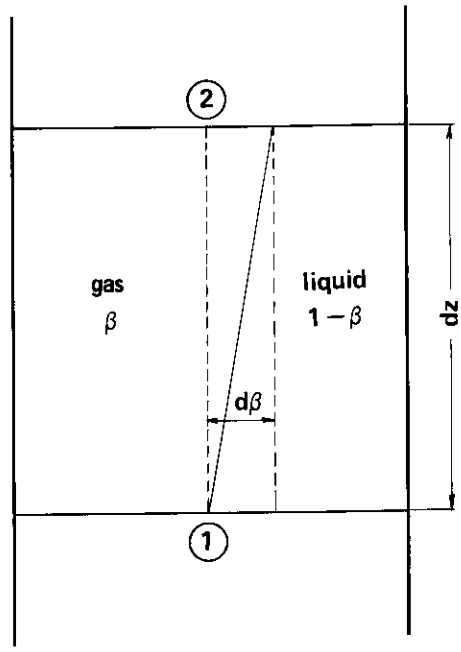

Fig. 3 Correspondence among main flow phases and phase change part of fluid in existing two-phase fluid.

However, situation of Eq. (28) for unit mass of flowing two-phase fluid is more complicated. dx in the equation stands for phase changed mass in the section dz per unit mass of flowing two-phase fluid. Phase change part of fluid travels distance dz, likely in a relay race, within time dt_{PC} $(=dz/u_{PC}=2dz/(u_g+u_l))$. This means that gas and liquid phases which interacted with phase change part of fluid in the section dz "during time dt_{PC}" contribute to the acceleration of the phase change part of fluid. In **Fig. 4**, gas phase which instantly existed between cross sections ① and ② with distance dz moves to between cross sections ③ and ④ during time dt_{PC}. Similarly, liquid phase which instantly existed between cross sections ① and ② moves to between cross sections ⑤ and ⑥. Therefore, gas phase between cross sections ① and ④ and liquid phase between cross sections ① and ⑥ contribute to the phase change acceleration between cross sections ① and ② during time dt_{PC}. However, some part of the main flow phases cannot contribute to the phase change acceleration perfectly but only partially, because it is in the outside of the section dz during so large portion of time dt_{PC}. Spatial contribution coefficients defined as the ratios of contributed distances to the total distance dz are given in **Fig. 4** with line 1-2-3-4 for gas phase and with line 5-6-7 for liquid phase. Here, length 1-2' and length 5-6' are 1.0. Since the area △1-2-3-4 is equal to the area □1-2'-3-4' and the area △5-6-7 is equal to the area □ 5-6'-6''-7', equivalent amount of gas phase between cross sections ① and ③ and equivalent amount of liquid phase between cross sections ① and ⑤ are considered to contribute to the phase change acceleration between cross sections ① and ② during time dt_{PC} at the spatial contribution coefficient of 1.0. That is, gas phase x and liquid phase $1-x$ of unit mass of flowing two-phase fluid contribute to the acceleration of phase change part of fluid dx.

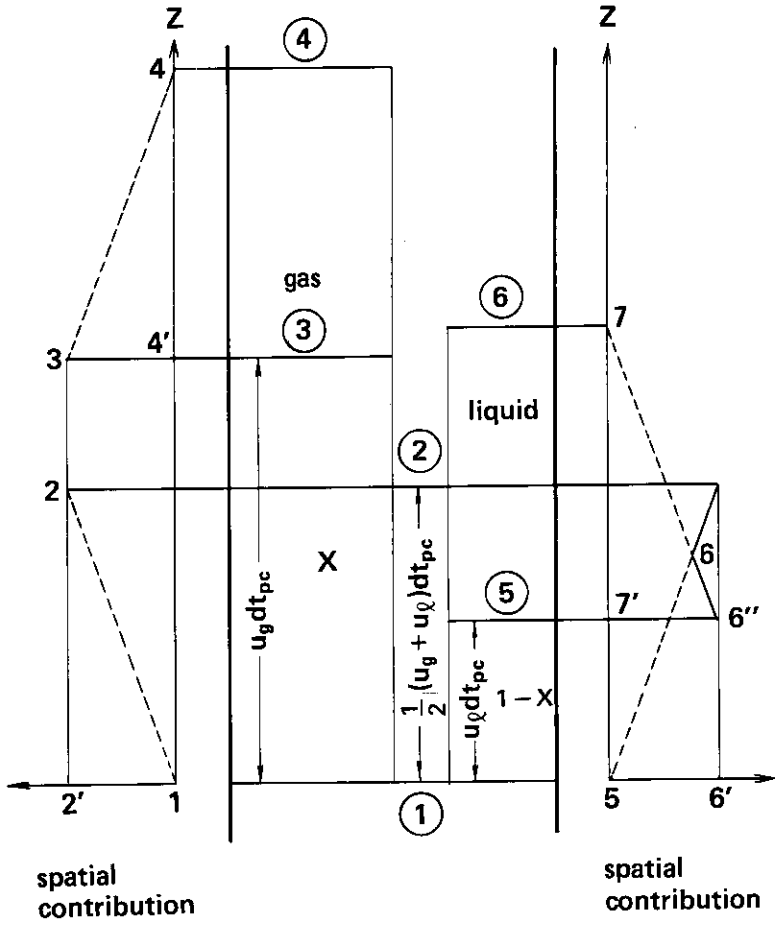

Fig. 4 Correspondence among main flow phases and phase change part of fluid in flowing two-phase fluid (1).

Here, the spatial contribution coefficient is defined from phase change part side of two-phase fluid. From the main flow side, different observation is possible on contribution fraction of each phase. For example, each part of gas phase contributes to the phase change accdleration between cross sections ① and ② only for the time $dt_g=dz/u_g$ out of the time $dt_{PC}=2dz/(u_g+u_l)$ and it contributes to the phase change acceleration outside of the region in the rest time. This means that when $u_g > u_l$ time contribution coefficient of gas phase defined as dt_g/dt_{PC} $(=(u_g+u_l)/2u_g)$ is less than 1.0, i.e., gas phase has a cutoff of contribution time. On the other hand, time contribution coefficient of liquid phase defined as dt_l/dt_{PC} $(=(u_g+u_l)/2u_l)$ is larger than 1.0, i.e., liquid phase has an extra contribution time.

Figure 5 illustrates the fact described above. In equation of motion based on flowing fluid, time contribution coefficient of gas phase (length 1-2) is smaller than 1.0 but amount of contributed gas phase (proportional to length 1-4) is larger than the amount of existing gas phase (proportional to length 1-4'). Resultantly, phase change part of fluid between cross sections ① and ② is accelerated by the main flow gas phase at the net contribution coefficient of 1.0. Note that the area □ 1-2-3-4 is equal to the area □ 1-2'-3'-4'. On the other hand, time contribution coefficient of liquid phase (proportional to length 5-6) is larger than 1.0 but amount of contributed liquid phase (proportional to length 5-8) is smaller than the amount of existing liquid phase (proportional to length 5-8'). Resultantly, phase change part of fluid between cross sections ① and ② is accelerated by the main flow liquid phase at the net contribution coefficient of 1.0. Again, note that the area □ 5-6-7-8 is equal to the area □ 5-6'-7'-8'. Total force accelerating the phase change part of fluid between cross sections ① and ② during time dt_{PC} is, of course, acted by the both gas and liquid phases of main flow and, therefore, the reaction force is distributed to the main flow gas and liquid phases.

Through the above discussions, it was clarified that amounts of gas and liquid phases contributing to the acceleration of phase change part dx of unit mass of flowing two-phase fluid in the section dz are x and $1-x$, respectively. For existing two-phase fluid, on the other hand, since time contribution coefficient is smaller than 1.0, existing amount of gas phase between cross sections ① and ② cannot cover the acceleration of the all phase change part

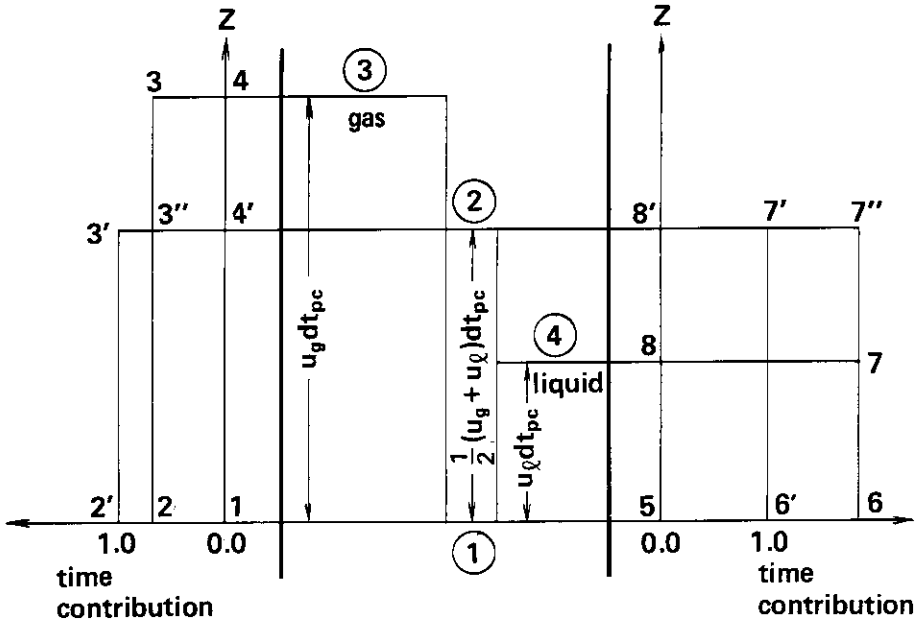

Fig. 5 Correspondence among main flow phases and phase change part of fluid in flowing two-phase fluid (2).

of fluid between the two cross sections (cutoff of contribution time). Similarly, since time contribution coefficient is larger than 1.0, existing amount of liquid phase between cross sections ① and ② accelerates more amount of phase change part of fluid than that between cross sections ① and ② (extra contribution time). Therefore, the amount of phase change part of fluid which acts the reaction forces on existing gas and liquid phases of the main flow is different from that for the case of flowing two-phase fluid. The value is no other then $d\beta$.

These facts will be explained in more detail in the subsection 4.7.2.

4.2.4 Mass change of examined part of fluid

In derivation of equations of motion in the present report, unit mass of two-phase fluid was selected as examined part of fluid instead of unit volume of two-phase fluid, regardless of whether it was of existing two-phase fluid or of flowing one. The reason is as follows.

If one selects the examined part of fluid as, e.g., two-phase fluid between two cross sections of which volume is constant, there is generally a change of mass of the examined part of fluid. The mass change results in change in momentum or kinetic energy of the examined part of fluid. However, such change in momentum or kinetic energy should not always be connected to inertial force acting on the examined part of fluid. Because, the mass change is only an artificial one depending on selection of examined part of fluid and, therefore, change in momentum or kinetic energy due to the mass change is not always the result of real acceleration of mass.

However, to ignore all the change in momentum or kinetic energy due to mass change is invalid, because there can be mass change with real acceleration of mass.

Then, how one should treat the effect of mass change? The answer is that the mass change which does not cause the change in momentum or kinetic energy per unit mass of examined part of fluid should be excluded from inertial force estimation because it is not accompanied by real acceleration of mass. Since any mass change can be considered to be the sum of mass change which does not cause change in momentum or kinetic energy per unit mass and pure change in momentum or kinetic energy without mass change, one can evaluate the inertial force due to real acceleration of mass by subtracting the former from the total change in momentum or kinetic energy. Let us discuss an example of two points of mass problem with continuous change of mass. Real inertial force acts on the mass center of the two points of mass is described based on the momentum principle or the kinetic energy principle as:

$$f=\frac{d(m_1u_1)}{dt}+\frac{d(m_2u_2)}{dt}-\frac{m_1u_1+m_2u_2}{m_1+m_2}\left(\frac{dm_1}{dt}+\frac{dm_2}{dt}\right) \tag{39}$$

$$f=\frac{1}{2}\cdot\frac{d(m_1u_1^2)}{dz}-\frac{1}{2}\cdot\frac{d(m_2u_2^2)}{dz}-\frac{1}{2}\cdot\frac{m_1u_1^2+m_2u_2^2}{m_1+m_2}\left(\frac{dm_1}{dz}+\frac{dm_2}{dz}\right) \tag{40}$$

Change of total mass is not discussed in usual multiple points of mass problem because of conflict with the mass conservation law. However, in the field of hydrodynamics, since there is mass in-flow or out-flow in examined part of fluid this should be carefully examined. Specially in the case of two-phase flow with both phase change and phase slip, this will be one of the key problems. More detailed discussions will be made in the subsection 4.7.1.

If there is no change of total mass,

$$\frac{dm_1}{dt}=-\frac{dm_2}{dt}=\frac{dm}{dt} \tag{41}$$

or

$$\frac{dm_1}{dz} = -\frac{dm_2}{dz} = \frac{dm}{dz} \tag{42}$$

holds good. Then, Eqs. (39) and (40) become

$$f = m_1 \frac{du_1}{dt} + m_2 \frac{du_2}{dt} + (u_1 - u_2)\frac{dm}{dt} \tag{43}$$

$$f = \frac{1}{2} m_1 \frac{d(u_1^2)}{dz} + \frac{1}{2} m_2 \frac{d(u_2^2)}{dz} + \frac{1}{2}(u_1^2 - u_2^2)\frac{dm}{dz} \tag{44}$$

The reason why such simple expressions are possible is that there is no total mass change. Unit mass of total two-phase fluid was picked up in the present report just for making similar simple expressions to Eqs. (43) and (44) possible. This can be easily understood from the form of the first through third terms of left hand side of Eqs. (20) and (28).

4.3 Transient Equations of Motion for Total Two-Phase Flow

4.3.1 Equations based on "existing mass"

In the subsection 4.1.1, steady equation of motion (20) for existing two-phase fluid was derived. Transient equation of motion can be obtained by adding transient inertial force terms to this equation. All informations related to the transient inertial forces are given for a common short time dt. Therefore, the inertial forces can be evaluated by applying the momentum principle, regardless of different traveled distances due to different representative velocities of each component of two-phase fluid. By this method, Eq. (20) can be extended to the transient two-phase flow situation as:

$$\left\{\beta\left(\frac{\partial u_g}{\partial t} + u_g \frac{\partial u_g}{\partial z}\right) + (1-\beta)\left(\frac{\partial u_l}{\partial t} + u_l \frac{\partial u_l}{\partial z}\right)\right\} + (u_g - u_l)\frac{\partial \beta}{\partial t} + \frac{1}{2}(u_g^2 - u_l^2)\frac{\partial \beta}{\partial z}$$
$$+ \left(\frac{\beta}{\rho_g} + \frac{1-\beta}{\rho_l}\right)\frac{\partial P}{\partial z} + g\cos\theta - \left(\frac{\beta}{\rho_g} F_{GL} + \frac{1-\beta}{\rho_l} F_{LG}\right) - \left(\frac{\beta}{\rho_g} F_{GW} + \frac{1-\beta}{\rho_l} F_{LW}\right) = 0 \tag{45}$$

Here, the sixth term of left hand side of this equation is zero because of the Newton's third law, Eq. (19).

4.3.2 Equation based on "flowing mass"

Steady equation of motion (28) for flowing two-phase fluid derived in the subsection 4.1.2 can be extended to transient two-phase flow situation by the similar method described above as:

$$\left\{x\left(\frac{\partial u_g}{\partial t} + u_g \frac{\partial u_g}{\partial z}\right) + (1-x)\left(\frac{\partial u_l}{\partial t} + u_l \frac{\partial u_l}{\partial z}\right)\right\} + (u_g - u_l)\frac{\partial x}{\partial t} + \frac{1}{2}(u_g^2 - u_l^2)\frac{\partial x}{\partial z}$$
$$+ \left(\frac{x}{\rho_g} + \frac{1-x}{\rho_l}\right)\frac{\partial P}{\partial z} + g\cos\theta - \left(\frac{x}{\rho_g} F_{GL} + \frac{1-x}{\rho_l} F_{LG}\right) - \left(\frac{x}{\rho_g} F_{GW} + \frac{1-x}{\rho_l} F_{LW}\right) = 0 \tag{46}$$

This is the transient equation of motion for unit flowing mass of total two-phase flow. The sixth term of left hand side is not zero in this equation.

4.4 Equations of Motion for Each Phase

In this section, equations of motion for each phase shall be derived based on those for existing and flowing total two-phase fluids which were introduced as Eqs. (45) and (46) in the previous section.

In both Eqs. (45) and (46), each term except phase change inertial force terms, the second and third terms, can be divided into two parts: one is for gas phase and the other is for liquid phase. However, the phase change part of fluid is included essentially in neither gas phase nor liquid phase. Therefore, there is no criterion to distribute the phase change inertial force terms to each phase. So, let us distribute them formally by introducing tentative distribution coefficients $\zeta_{\beta t}$, $\zeta_{\beta z}$, ζ_{xt} and ζ_{xz} for transient and steady terms of the equations of motion based on existing mass and flowing mass, respectively. Then, Eqs. (45) and (46) can be divided as:

$$\beta\left(\frac{\partial u_g}{\partial t}+u_g\frac{\partial u_g}{\partial z}\right)+\zeta_{\beta t}(u_g-u_l)\frac{\partial \beta}{\partial t}+\frac{\zeta_{\beta z}}{2}(u_g^2-u_l^2)\frac{\partial \beta}{\partial z}+\frac{\beta}{\rho_g}\frac{\partial P}{\partial z}+\beta g\cos\theta$$
$$-\frac{\beta}{\rho_g}F_{GL}-\frac{\beta}{\rho_g}F_{GW}=0 \tag{47}$$

$$(1-\beta)\left(\frac{\partial u_l}{\partial t}+u_l\frac{\partial u_l}{\partial z}\right)+(1-\zeta_{\beta t})(u_g-u_l)\frac{\partial \beta}{\partial t}+\frac{1-\zeta_{\beta z}}{2}(u_g^2-u_l^2)\frac{\partial \beta}{\partial z}$$
$$+\frac{1-\beta}{\rho_l}\frac{\partial P}{\partial z}+(1-\beta)g\cos\theta-\frac{1-\beta}{\rho_l}F_{LG}-\frac{1-\beta}{\rho_l}F_{LW}=0 \tag{48}$$

$$x\left(\frac{\partial u_g}{\partial t}+u_g\frac{\partial u_g}{\partial z}\right)+\zeta_{xt}(u_g-u_l)\frac{\partial x}{\partial t}+\frac{\zeta_{xz}}{2}(u_g^2-u_l^2)\frac{\partial x}{\partial z}+\frac{x}{\rho_g}\frac{\partial P}{\partial z}+xg\cos\theta$$
$$-\frac{x}{\rho_g}F_{GL}-\frac{x}{\rho_g}F_{GW}=0 \tag{49}$$

$$(1-x)\left(\frac{\partial u_l}{\partial t}+u_l\frac{\partial u_l}{\partial z}\right)+(1-\zeta_{xt})(u_g-u_l)\frac{\partial x}{\partial t}+\frac{1-\zeta_{xz}}{2}(u_g^2-u_l^2)\frac{\partial x}{\partial z}$$
$$+\frac{1-x}{\rho_l}\frac{\partial P}{\partial z}+(1-x)g\cos\theta-\frac{1-x}{\rho_l}F_{LG}-\frac{1-x}{\rho_l}F_{LW}=0 \tag{50}$$

Equation (47) divided by β and Eq. (49) divided by x should be identical because both equations are for unit mass of gas phase. Unit mass of existing gas should be identical with unit mass of flowing gas even if they are components of two-phase flow. Therefore, corresponding terms of those equations should be the same to each other. Similarly, in Eq. (48) divided by $1-\beta$ and Eq. (50) divided by $1-x$, corresponding terms should also be the same to each other. From these facts,

$$\frac{\zeta_{\beta t}}{\beta}\frac{\partial \beta}{\partial t}=\frac{\zeta_{xt}}{x}\frac{\partial x}{\partial t} \tag{51}$$

$$\frac{1-\zeta_{\beta t}}{1-\beta}\frac{\partial \beta}{\partial t}=\frac{1-\zeta_{xt}}{1-x}\frac{\partial x}{\partial t} \tag{52}$$

$$\frac{\zeta_{\beta z}}{\beta}\frac{\partial \beta}{\partial z}=\frac{\zeta_{xz}}{x}\frac{\partial x}{\partial z} \tag{53}$$

$$\frac{1-\zeta_{\beta z}}{1-\beta}\frac{\partial \beta}{\partial z}=\frac{1-\zeta_{xz}}{1-x}\frac{\partial x}{\partial z} \tag{54}$$

hold good.

From Eqs. (51) through (54),

$$\zeta_{\beta t}=\frac{\beta\left\{(1-\beta)-(1-x)\dfrac{\partial\beta/\partial t}{\partial x/\partial t}\right\}}{\{x(1-\beta)-\beta(1-x)\}\dfrac{\partial\beta/\partial t}{\partial x/\partial t}} \tag{55}$$

$$\zeta_{\beta z}=\frac{\beta\left\{(1-\beta)-(1-x)\dfrac{\partial\beta/\partial z}{\partial x/\partial z}\right\}}{\{x(1-\beta)-\beta(1-x)\}\dfrac{\partial\beta/\partial z}{\partial x/\partial z}} \tag{56}$$

$$\zeta_{xt}=\frac{x\left\{(1-\beta)-(1-x)\dfrac{\partial\beta/\partial t}{\partial x/\partial t}\right\}}{x(1-\beta)-\beta(1-x)} \tag{57}$$

$$\zeta_{xz}=\frac{x\left\{(1-\beta)-(1-x)\dfrac{\partial\beta/\partial z}{\partial x/\partial z}\right\}}{x(1-\beta)-\beta(1-x)} \tag{58}$$

are obtained. By substituting Eqs. (55) through (58), equations of motion, (47) through (50), for each phase are completed.

Here, it must be noted that $\zeta_{\beta t}$, $\zeta_{\beta z}$, ζ_{xt} and ζ_{xz} are not limited within the range of 0 to 1 because they are only the tentatively introduced distribution coefficients. Examples of these coefficients will be shown and discussed in Appendix 2 of Part II of this report.

It seems quite reasonable that phase change inertial force terms of equations of motion for each phase were derived without introduction of any physical models on phase change acceleration, based only on purely hydrodynamical balance consideration and mathematical treatment. To the contrary, equations of motion based on some physical models on mechanism of phase change acceleration generally have an imperfectness in expression of hydrodynamical balance relationship. This problem will be indicated in detail through the discussions in the subsections 4.7.2 and 4.7.3.

4.5 Momentum Equations

In the previous discussions, the author's physical understanding on force balance of two-phase flow was directly described and some variations in expression were introduced. In this section, the author's equations of motion will be transformed into the momentum equation form. The result is different from the conventional momentum equations for two-phase flow. Comparison between the author's momentum equations and conventional momentum equations and physical justification of the author's theory will be made in Section 4.7.

Equation that momentum production rate between two cross sections is equated to the sum of all external forces acting on the part of fluid is called momentum equation in the single-phase hydrodynamics. Momentum equation is essentially an equation for existing fluid (of constant volume). However, it is quite unique because the inertial force term is evaluated with the method for flowing fluid. From this fact, momentum equation is sometimes very useful for single-phase flow analysis in which unit existing mass and unit flowing mass are just identical to each other. However, it is quite dangerous for two-phase flow analysis because the two unit mass fluids are really independent in two-phase flow. Correct expression of momentum equations for two-phase flow can be obtained based on the equations of motion for each phase which were established in Section 4.4

By multiplying Eq. (49) by W/u_g and rearranging with $xW=A\alpha\rho_g u_g$ and Eq. (51),

$$A\alpha\rho_g\frac{\partial u_g}{\partial t}+xW\frac{\partial u_g}{\partial z}+A\{\alpha\rho_g+(1-\alpha)\rho_l\}(u_g-u_l)\zeta_{\beta t}\frac{\partial\beta}{\partial t}+W(u_g-u_l)\zeta_{xz}\frac{u_{PC}}{u_g}\frac{\partial x}{\partial z}$$
$$+A\alpha\frac{\partial P}{\partial z}+A\alpha\rho_g g\cos\theta-A\alpha F_{GL}-A\alpha F_{GW}=0 \qquad (59)$$

is obtained. Here, $u_{PC}=(u_g+u_l)/2$. Similarly, by multiplying Eq. (50) by W/u_l and rearranging with $(1-x)W=A(1-\alpha)\rho_l u_l$ and Eq. (52),

$$A(1-\alpha)\rho_l\frac{\partial u_l}{\partial t}+(1-x)W\frac{\partial u_l}{\partial z}+A\{\alpha\rho_g-(1-\alpha)\rho_l\}(u_g-u_l)(1-\zeta_{\beta t})\frac{\partial\beta}{\partial t}$$
$$+W(u_g-u_l)(1-\zeta_{xz})\frac{u_{PC}}{u_l}\frac{\partial x}{\partial z}+A(1-\alpha)\frac{\partial P}{\partial z}+A(1-\alpha)\rho_l g\cos\theta$$
$$-A(1-\alpha)F_{LG}-A(1-\alpha)F_{LW}=0 \qquad (60)$$

is obtained. Equations (59) and (60) are momentum equations for each phase.

By summing up Eqs. (59) and (60), momentum equation for total two-phase flow is derived as:

$$A\alpha\rho_g\frac{\partial u_g}{\partial t}+xW\frac{\partial u_g}{\partial z}+A(1-\alpha)\rho_l\frac{\partial u_l}{\partial t}+(1-x)W\frac{\partial u_l}{\partial z}+A\{\alpha\rho_g-(1-\alpha)\rho_l\}(u_g-u_l)\frac{\partial\beta}{\partial t}$$
$$+W(u_g-u_l)\left\{\zeta_{xz}\frac{u_{PC}}{u_g}+(1-\zeta_{xz})\frac{u_{PC}}{u_l}\right\}\frac{\partial x}{\partial z}+A\frac{\partial P}{\partial z}-A\{\alpha\rho_g+(1-\alpha)\rho_l\}g\cos\theta$$
$$-AF_W=0 \qquad (61)$$

Here, by using the Newton's third law:

$$\alpha F_{GL}+(1-\alpha)F_{LG}=0 \qquad (62)$$

and definition equation of total wall frictional force:

$$\alpha F_{GW}+(1-\alpha)F_{LW}\equiv F_W \qquad (63)$$

the expression of Eq. (61) was simplified.

The meaning of the sixth term of Eq. (61) will be discussed in the subsection 4.7.2 but the term includes correction coefficients of the effects of difference in representative velocity between phase change part of fluid and main flow phases. The reason why such correction coefficients appeared is that this term is evaluated with the method for flowing two-phase fluid. If the term is evaluated with the method for existing two-phase fluid, as well as the first, third, fifth and seventh through ninth terms, such kind correction coefficients naturally disappear. This can easily be demonstrated by rearranging Eq. (61) with Eqs. (53), (54) and (10), i.e.,

$$A\alpha\rho_g\frac{\partial u_g}{\partial t}+xW\frac{\partial u_g}{\partial z}-A(1-\alpha)\rho_l\frac{\partial u_l}{\partial t}+(1-x)W\frac{\partial u_l}{\partial z}+A\{\alpha\rho_g+(1-\alpha)\rho_l\}(u_g-u_l)\frac{\partial\beta}{\partial t}$$
$$+\frac{1}{2}A\{\alpha\rho_g+(1-\alpha)\rho_l\}(u_g^2-u_l^2)\frac{\partial\beta}{\partial z}+A\frac{\partial P}{\partial z}+A\{\alpha\rho_g+(1-\alpha)\rho_l\}g\cos\theta$$
$$-AF_W=0 \qquad (64)$$

The discussion in this section started from Eqs. (49) and (50). The same result can be obtained also from Eqs. (47) and (48) because these two couples of equations of motion are just equivalent to each other.

4.6 Independency of equations of motion

Ten differential equations, Eqs. (45), (46), (47), (48), (49), (50), (59), (60), (61) and (64), have been derived up to now as equations describing transient force balance of one-dimensional gas-liquid two-phase flow. As described in Section 2.1, however, number of independent equations of motion is only two. Therefore, if such two equations are given, the rest equations of motion should lose their independencies automatically. Such perfect combinations of two independent equations of motion are shown with the symbol "○" in **Table 3**.

Table 3 Combinations of two independent equations of motion

	(45)	(46)	(47)	(48)	(49)	(50)	(59)	(60)	(61)	(64)
(45)		○	○	○	○	○	○	○	×	×
(46)	○		○	○	○	○	○	○	○	○
(47)	○	○		○	×	○	×	○	○	○
(48)	○	○	○		○	×	○	×	○	○
(49)	○	○	×	○		○	×	○	○	○
(50)	○	○	○	×	○		○	×	○	○
(59)	○	○	×	○	×	○		○	○	○
(60)	○	○	○	×	○	×	○		○	○
(61)	×	○	○	○	○	○	○	○		×
(64)	×	○	○	○	○	○	○	○	×	

4.7 Comparison with Conventional Equations

In the present section, unique features of the author's equations of motion shall be explained by comparison with conventional equations of motion in two-fluid model.

4.7.1 Mass change of examined part of fluid

Most of conventional equations of motion for transient two-phase flow have the following form. $\hat{u}$ is, however, different one by one reflecting idea of each researcher.

$$\frac{\partial(A\alpha\rho_g u_g)}{\partial t}+\frac{\partial(A\alpha\rho_g u_g^2)}{\partial z}+A\alpha\frac{\partial P}{\partial z}+A\alpha\rho_g g\cos\theta-A\alpha F_{GL}-A\alpha F_{GW}$$
$$-Aw\hat{u}=0 \qquad \text{—C—}\ (65)$$

$$\frac{\partial\{A(1-\alpha)\rho_l u_l\}}{\partial t}+\frac{\partial\{A(1-\alpha)\rho_l u_l^2\}}{\partial z}+A(1-\alpha)\frac{\partial P}{\partial z}+A(1-\alpha)\rho_l g\cos\theta$$
$$-A(1-\alpha)F_{LG}-A(1-\alpha)F_{LW}+Aw\hat{u}=0 \qquad \text{—C—}\ (66)$$

Here, "—C—" before the equation number indicates that the equation is conventional one.

These equations are force balance equations for a constant volume of two-phase fluid

between two cross sections which are unit length distant each other. In such equations, as described in the subsection 4.2.4, an invalidity will appear in force balance because of change in momentum or kinetic energy due to mass change of the examined part of fluid which is independent of real acceleration of mass. It will be shown below that Eqs. (65) and (66) actually include such invalidity.

By summing up Eqs. (65) and (66) and rearranging with Eqs. (62) and (63), the following equation is obtained.

$$\frac{\partial\{A\alpha\rho_g u_g+A(1-\alpha)\rho_l u_l\}}{\partial t}+\frac{\partial\{A\alpha\rho_g u_g^2+A(1-\alpha)\rho_l u_l^2\}}{\partial z}+A\frac{\partial P}{\partial z}$$
$$+A\{\alpha\rho_g+(1-\alpha)\rho_l\}g\cos\theta-AF_w=0 \qquad \text{—C— (67)}$$

Rearrange Eq. (67) by using $xW=A\alpha\rho_g u_g$, $(1-x)W=A(1-\alpha)\rho_l u_l$, $\beta\{\alpha\rho_g+(1-\alpha)\rho_l\}=\alpha\rho_g$, and $(1-\beta)\{\alpha\rho_g+(1-\alpha)\rho_l\}=(1-\alpha)\rho_l$, then,

$$A\alpha\rho_g\frac{\partial u_g}{\partial t}+xW\frac{\partial u_g}{\partial z}+A(1-\alpha)\rho_l\frac{\partial u_l}{\partial t}+(1-x)W\frac{\partial u_l}{\partial z}+A\{\alpha\rho_g+(1-\alpha)\rho_l\}(u_g-u_l)\frac{\partial\beta}{\partial t}$$
$$+\{\beta u_g+(1-\beta)u_l\}\frac{\partial[A\{\alpha\rho_g+(1-\alpha)\rho_l\}]}{\partial t}+W(u_g-u_l)\frac{\partial x}{\partial z}$$
$$+\{xu_g+(1-x)u_l\}\frac{\partial W}{\partial z}+A\frac{\partial P}{\partial z}+A\{\alpha\rho_g+(1-\alpha)\rho_l\}g\cos\theta$$
$$-AF_w=0 \qquad \text{—C— (68)}$$

The sixth and eighth terms of Eq. (68) do not exist in the author's momentum equation (61). Form of these terms is similar to that of the third term of Eq. (39), indicating that these terms are corresponding to momentum change due to mass change which is independent of real acceleration of mass. Therefore, these terms should be excluded from force balance equations.

Actually speaking, similar confusion can be seen even in momentum equation for single-phase flow. However, it never causes any problems in evaluation of inertial force, in relation with the equation of continuity. To point out this fact is very useful to clarify the uniqueness of two-phase flow. In single-phase flow, equation of motion can be written in the form of:

$$\rho\left(\frac{\partial u}{\partial t}+u\frac{\partial u}{\partial z}\right)=F \qquad (69)$$

The momentum equation corresponding to Eq. (67) is:

$$\frac{\partial(A\rho u)}{\partial t}+\frac{\partial(A\rho u^2)}{\partial z}=AF \qquad (70)$$

Equation (70) can be written as:

$$A\rho\frac{\partial u}{\partial t}+u\frac{\partial(A\rho)}{\partial t}+A\rho u\frac{\partial u}{\partial z}+u\frac{\partial(A\rho u)}{\partial z}=AF \qquad (71)$$

Equation (71) corresponds to Eq. (68). The second and fourth terms of Eq. (71) are not included in Eq. (69). However, since there is equation of continuity, i.e.,

$$\frac{\partial(A\rho)}{\partial t}+\frac{\partial(A\rho u)}{\partial z}=0 \qquad (72)$$

the sum of these terms is always zero although the each term has some value. Therefore, one

can use Eq. (70) instead of Eq. (69). That is, Eq. (70) is valid in relation with equation of continuity (72).

The reason why the momentum change independent of real acceleration of mass does not cause any problems in single-phase flow is that the coefficients of the second and fourth terms of Eq. (71) are both u. That is, unit existing mass and unit flowing mass have the common momentum of u. On the other hand, in two-phase flow,

$$\beta u_g+(1-\beta)u_l \neq x u_g+(1-x)u_l \tag{73}$$

holds generally because of phase slip. Therefore, even if equation of continuity (8) is applied, the sum of sixth and eighth terms of Eq. (68) is not zero generally, That is, the mistake which is allowed in single-phase flow is not allowed in two-phase flow. The reason is the most important feature of two-phase flow, i.e., unit existing two-phase fluid with gas mass fraction of β and unit flowing two-phase fluid with gas mass fraction of x are completely independent of each other and, therefore, they have different momentum values, respectively.

4.7.2 Steady phase change inertial force terms of momentum equations

Even if the sixth and eighth terms are deleted from Eq. (68) because they are independent of real acceleration of mass, Eq. (68) still does not agree with the author's momentum equation (61). That is, Eq. (68) without the sixth and eighth terms is

$$A\alpha\rho_g\frac{\partial u_g}{\partial t}+xW\frac{\partial u_g}{\partial z}+A(1-\alpha)\rho_l\frac{\partial u_l}{\partial t}+(1-x)W\frac{\partial u_l}{\partial z}+A\{\alpha\rho_g+(1-\alpha)\rho_l\}(u_g-u_l)\frac{\partial \beta}{\partial t}$$

$$+W(u_g-u_l)\frac{\partial x}{\partial z}+A\frac{\partial P}{\partial z}+A\{\alpha\rho_g+(1-\alpha)\rho_l\}g\cos\theta-AF_W=0 \qquad \text{–C–} \tag{74}$$

and the sixth term of this equation is different from the corresponding term of Eq. (61).

The coefficient $\zeta_{xz}(u_{PC}/u_g)+(1-\zeta_{xz})(u_{PC}/u_l)$ in the sixth term of Eq. (61) converts the phase change inertial force evaluated with the method based on flowing mass into the value for the existing mass between two cross sections. As shown in **Fig. 6**, let us divide formally the momentum production of $W(u_g-u_l)(\partial x/\partial z)$ due to steady phase change per

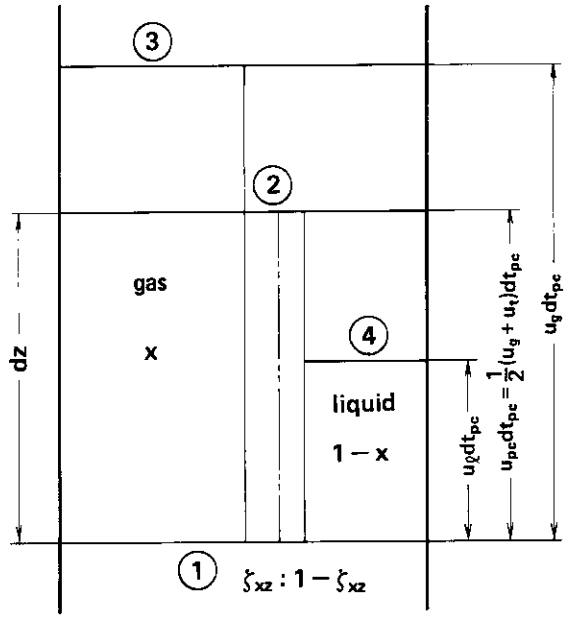

Fig. 6 Correspondence among main flow phases and phase change part of fluid in flowing two-phase fluid (3).

unit time per unit channel length into two parts: one part with fraction ζ_{xz} to the total is caused by the main flow gas phase and the rest part with fraction $1-\zeta_{xz}$ is caused by the main flow liquid phase. The reaction forces, of course, act on the gas and liquid phases, respectively. Since gas velocity u_g and liquid velocity u_l are different from representative velocity u_{PC} of phase change part of fluid, these reaction forces act on gas phase between cross sections ① and ③ and liquid phase between cross sections ① and ④ as described in the subsection 4.2.3. In the case of existing two-phase fluid, only the amount of phase change inertial force to be added to the instantly contacting gas and liquid phases between cross sections ① and ② should be counted. If all of $W(u_g-u_l)(\partial x/\partial z)$ is counted without any corrections, balance of forces (Newton's third law) is evidently ignored. That is, one should evaluate the phase change inertial forces taking into account the time contribution coefficients described in the subsection 4.2.3. Multiplying phase change inertial force $\zeta_{xz}W(u_g-u_l)(\partial x/\partial z)$ due to gas phase by time contribution coefficient $dt_g/dt_{PC}(=u_{PC}/u_g)$ and phase change inertial force $(1-\zeta_{xz})W(u_g-u_l)(\partial x/\partial z)$ due to liquid phase by time contribution coefficient $dt_l/dt_{PC}(=u_{PC}/u_l)$ and summing up the results, one can obtain $\{\zeta_{xz}(u_{PC}/u_g)+(1-\zeta_{xz})(u_{PC}/u_l)\}W(u_g-u_l)(\partial x/\partial z)$. This is no other than the sixth term of Eq. (61). Since the sixth term of Eq. (74) does not have the conversion coefficient including the time contribution coefficients, force balance is not described correcly with this equation. This wrong formulation of Eq. (74) was resulted from the mixing mode of existing fluid and flowing fluid in one equation, i.e., the treatment without distinction between unit mass of existing two-phase fluid and unit mass of flowing two-phase fluid broke the force balance relationship.

The fifth term of Eq. (61), transient phase change inertial force term, does not include the similar time contribution coefficients although differences in representative velocity between phase change part of fluid and main flow phases still exist as well as in steady phase change inertial force term. The reason is that the term is constituted based on existing mass. As seen in Eq. (64), even in steady phase change inertial force term, such conversion coefficient disappears naturally if one evaluates the term based on existing mass. Various expressions of transient and steady phase change inertial force terms are summarized in **Table 4**.

Table 4 Various expressions of phase change inertial force terms in momentum equations for total two-phase flow

$u_{pc}=\frac{1}{2}(u_g+u_l)$

		transient term	steady term
existing mass	momentum type	$A\{\alpha\rho_g+(1-\alpha)\rho_l\}(u_g-u_l)\frac{\partial\beta}{\partial t}$	$A\{\alpha\rho_g-(1-\alpha)\rho_l\}(u_g-u_l)u_{pc}\frac{\partial\beta}{\partial z}$
	kinetic energy type	$\frac{1}{2}\frac{A\{\alpha\rho_g-(1-\alpha)\rho_l\}}{u_{pc}}(u_g^2-u_l^2)\frac{\partial\beta}{\partial t}$	$\frac{1}{2}A\{\alpha\rho_g+(1-\alpha)\rho_l\}(u_g^2-u_l^2)\frac{\partial\beta}{\partial z}$
flowing mass	momentum type	$W(u_g-u_l)\left(\frac{\zeta_{xt}}{u_g}+\frac{1-\zeta_{xt}}{u_l}\right)\frac{\partial x}{\partial t}$	$W(u_g-u_l)\left\{\zeta_{xz}\frac{u_{pc}}{u_g}+(1-\zeta_{xz})\frac{u_{pc}}{u_l}\right\}\frac{\partial x}{\partial z}$
	kinetic energy type	$\frac{1}{2}\frac{W}{u_{pc}}(u_g^2-u_l^2)\left(\frac{\zeta_{xt}}{u_g}+\frac{1-\zeta_{xt}}{u_l}\right)\frac{\partial x}{\partial t}$	$\frac{1}{2}W(u_g^2-u_l^2)\left(\frac{\zeta_{xz}}{u_g}+\frac{1-\zeta_{xz}}{u_l}\right)\frac{\partial x}{\partial z}$

4.7.3 Relationship between inertial force and kinetic energy

Inertial force (to be balanced with sum of all external forces) acting on each component of examined part of fluid multiplied by traveled distance gives kinetic energy change of the part. This is the kinetic energy principle which holds good regardless of whether energy dissipation exists or not as described in the subsection 4.2.2.

On the other hand, sum of kinetic energy changes occurring in every component of fluid should be equal to the kinetic energy change of the total two-phase fluid. This is only the logical truth, i.e., sum of parts is equal to the total.

Let us examine Eqs. (65) and (66) from the view point of these two principles. However, if one trys to investigate this problem generally, he will experience a difficulty in analysis of the transient terms because representative velocity of phase change part of fluid is unclear for Eqs. (65) and (66). Therefore, let us limit the discussion for steady flow problem.

Equation (65) expresses force balance of gas phase with mass of $A\alpha\rho_g$. In steady flow, the first term of Eq. (65) disappears and the seventh term becomes $-\hat{u}W(dx/dz)$. The seventh term represents the additional inertial force to the gas phase due to phase change. Therefore, total inertial force acting on the gas phase is the sum of second and seventh terms. By multiplying the terms by traveled distance dz and dividing by $A\alpha\rho_g$, kinetic energy change across section dz in unit mass of gas phase is obtained. By multiplying the result by x, one can get kinetic energy change across section dz in the gas phase of unit mass of flowing two-phase fluid. That is,

$$\frac{x\cdot dz}{A\alpha\rho_g}\frac{d(A\alpha\rho_g u_g^2)}{dz}-\frac{x\cdot dz}{A\alpha\rho_g}\hat{u}W\frac{dx}{dz}$$

$$=\frac{u_g}{W}\frac{d(A\alpha\rho_g u_g^2)}{dz}dz-\frac{u_g}{W}\hat{u}W\frac{dx}{dz}dz$$

$$=\frac{u_g}{W}d(xWu_g)-u_g\hat{u}dx$$

$$=xu_g du_g+u_g^2dx-u_g\hat{u}dx$$

$$=\frac{1}{2}xd(u_g^2)+u_g(u_g-\hat{u})dx \qquad \text{–C– (75)}$$

Here, steady flow condition $dW=0$ was applied when the second expression of right hand side was transformed into the third expression.

Similarly, kinetic energy change across section dz in the liquid phase of unit mass of flowing two-phase fluid is:

$$\frac{1}{2}(1-x)d(u_l^2)+u_l(\hat{u}-u_l)dx \qquad \text{–C– (76)}$$

By summing up Eqs. (75) and (76), kinetic energy change across section dz in unit mass of flowing two-phase fluid is obtained as:

$$\frac{1}{2}xd(u_g^2)+u_g(u_g-\hat{u})dx+\frac{1}{2}(1-x)d(u_l^2)+u_l(\hat{u}-u_l)dx$$

$$=\frac{1}{2}d\{xu_g^2+(1-x)u_l^2\}+\frac{1}{2}\{u_g^2-2(u_g-u_l)\hat{u}-u_l^2\}dx \qquad \text{–C– (77)}$$

Kinetic energy change across section dz of unit mass of flowing two-phase fluid should essentially be the first term of Eq. (77) only and the second term is an excess.

$\hat{u}$ in the second term of Eq. (77) is usually given by some physical model or insight on phase change acceleration. However, no physical model can make the second term always zero. That is, simple formal logic that sum of parts is equal to the total does not hold good on kinetic energy change of flowing two-phase fluid.

For being the second term of Eq. (77) always zero,

$$\hat{u}=\frac{u_g+u_l}{2} \tag{78}$$

should hold. That is, $\hat{u}$ should agree with u_{PC} which the author showed as representative velocity of phase change part of fluid. Thus, kinetic energy change of unit mass of flowing two-phase fluid can be correctly described* only when u_{PC} is used as $\hat{u}$.

From the author's equations of motion (59) and (60),

$$\frac{1}{2}\left\{\frac{x}{u_g}\frac{\partial(u_g{}^2)}{\partial t}+\frac{1-x}{u_l}\frac{\partial(u_l{}^2)}{\partial t}-\frac{1}{u_{PC}}(u_g{}^2-u_l{}^2)\frac{\partial x}{\partial t}\right\}$$

$$+\frac{1}{2}\frac{\partial\{xu_g{}^2-(1-x)u_l{}^2\}}{\partial z} \tag{79}$$

is obtained as kinetic energy change of unit mass of flowing two-phase fluid per unit channel length for general transient two-phase flow. The second term of Eq. (79) is steady term. The term multiplied by dz corresponds to Eq. (77) but does not include excess term like the second term of right hand side of Eq. (77). In Eq. (79), representative velocities of each component of two-phase fluid are included in denominators of each coefficient of the transient terms (in the first term). The reason is that the equation represents the spatial change in kinetic energy. That is, difference in representative velocity should be taken into account in estimation of the transient terms for each component with different traveling distance in common short time dt. This fact is considered quite reasonable. From these examinations, Eq. (79) is recognized to validly describe the spatial change of kinetic energy of unit mass of flowing two-phase fluid.

* This does not means that Eqs. (65) and (66) are correct when Eq. (78) is used. Because, total phase change inertial force acting on unit mass of flowing two-phase fluid is correctly expressed but the correct distribution to each phase is not guaranteed.

5. Equations of Energy

5.1 Balance Equations of Thermal Energy

Balance of mechanical energy is described by equations of motion integrated with respect to traveled distance, i.e., Bernoulli's equation in a wide sense. Therefore, it has been essentially established already because equations of motion were already established in the previous chapter. However, changes of states of gas and liquid phases and phase change rate are not be able to be described unless balance of thermal energy is formulated. That is, purpose of equations of energy is to describe changes of states of each phase and phase change rate.

Balance of thermal energy is expressed by the first law of thermodynamics. By applying the low to gas and liquid phases of unit mass of existing two-phase fluid, the following equations are obtained:

$$-\alpha\rho_g\frac{Dq_g}{Dt}-[\zeta_I\{\alpha u_g F_{GL}+(1-\alpha)u_l F_{LG}\}-\alpha u_g F_{GW}]+\zeta_e Q_e-Q_{IG}=0 \tag{80}$$

$$-(1-\alpha)\rho_l\frac{Dq_l}{Dt}[(1-\zeta_I)\{\alpha u_g F_{GL}+(1-\alpha)u_l F_{LG}\}+(1-\alpha)u_l F_{LW}]$$
$$+(1-\zeta_e)Q_e-Q_{IL}=0 \tag{81}$$

where,

$$\frac{Dq_g}{Dt}=\left(\frac{dh_g}{dP}-\frac{1}{\rho_g}\right)\left(\frac{\partial P}{\partial t}+u_g\frac{\partial P}{\partial z}\right) \tag{82}$$

$$\frac{Dq_l}{Dt}=\left(\frac{dh_l}{dP}-\frac{1}{\rho_l}\right)\left(\frac{\partial P}{\partial t}+u_l\frac{\partial P}{\partial z}\right) \tag{83}$$

Here, dh_g/dP and dh_l/dP are enthalpy changes per unit pressure change including effect of temperature change for gas and liquid phases, respectively. Equations (80) and (81) are an example couple of two independent equations of energy.

There are two different procedures to use these equations of energy. First is to calculate Q_{IG} and Q_{IL} with Eqs. (80) and (81) based on given dh_g/dP and dh_l/dP and then determine w by using Eq. (7). This procedure is very convenient for saturated two-phase flow (two-phase flow where thermodynamical non-equilibrium is sufficiently small) analysis. Constitutive equations are, in this case, necessary to give F_{GL}, F_{LG}, ζ_I, F_{GW}, F_{LW}, Q_e and ζ_e. Since Q_{IG} and Q_{IL} are usually not necessary to know but only w is necessary, it is convenient to sum up Eqs. (80) and (81) at first and then apply Eq. (7). In such case, constitutive equations on ζ_I and ζ_e are not necessary.

The second procedure is to calculate dh_g/dP and dh_l/dP based on given Q_{IG} and Q_{IL} and simulaneously determine w with Eq. (7). This procedure is used usually in two-temperature model analysis. In this case, two constitutive equations on interfacial heat transfer are still necessary to give Q_{IG} and Q_{IL}*. Furthermore, since dh_g/dP and dh_l/dP cannot be determined without ζ_I and ζ_e and resultantly state variables such as ρ_g and ρ_l also cannot be calculated, constitutive equations are required also for ζ_I and ζ_e.

* Three constitutive equations are required actually for interfacial heat transfer coefficients of gas phase side and liquid phase side and interfacial area. In such case, number of constitutive equations and number of parameters are both increased to simplify the estimation. However, a general expression that two constitutive equations are necessary to determine two unknown parameters shall be taken in this report.

In the second procedure, constitutive equations for Q_{IG} and Q_{IL} are used instead of, e.g., the saturation relationships

$$T_g = T_{sat}(P) \tag{84}$$

$$T_l = T_{sat}(P) \tag{85}$$

in the first procedure (for the case of Q_{IG} and Q_{IL} are required). But necessary number of constitutive equations are the same.

Furthermore, for saturation two-phase flow, Eqs. (84) and (85) can be considered to be the equations of energy because the purpose of equations of energy is to describe the change of states of each phase. On such stand point, Eqs. (80) and (81) become constitutive equations to calculate phase change rete w.

One must be very careful to judge the acts of each basic equation and constitutive equation in a equation set for two-phase flow analysis.

5.2 Balance Equations for Total Energy

The sum of mechanical energy and thermal energy is called total energy. Mechanical energy balance equation for gas phase of unit mass of existing two-phase fluid can be obtained by multiplying equation of motion (47) for gas phase based on existing mass by gas velocity u_g, i.e.,

$$\beta u_g\left(\frac{\partial u_g}{\partial t}+u_g\frac{\partial u_g}{\partial z}\right)+\zeta_{\beta t}u_g(u_g-u_l)\frac{\partial \beta}{\partial t}+\frac{1}{2}\zeta_{\beta z}u_g(u_g^2-u_l^2)\frac{\partial \beta}{\partial z}+\frac{\beta}{\rho_g}u_g\frac{\partial P}{\partial z}$$

$$+\beta u_g g\cos\theta-\frac{\beta}{\rho_g}u_g F_{GL}-\frac{\beta}{\rho_g}u_g F_{GW}=0 \tag{86}$$

By dividing Eq. (86) by $\beta u_g+(1-\beta)u_l$ and rearranging with $x=\beta u_g/\{\beta u_g+(1-\beta)u_l\}$ and Eqs. (51) and (53), Eq. (49) can be derived.

Similarly, mechanical energy balance equation for liquid phase is obtained by multiplying equation of motion (48) for liquid phase based on existing mass by liquid velocity u_l, as:

$$(1-\beta)u_l\left(\frac{\partial u_l}{\partial t}+u_l\frac{\partial u_l}{\partial z}\right)+(1-\zeta_{\beta t})u_l(u_g-u_l)\frac{\partial \beta}{\partial t}+\frac{1}{2}(1-\zeta_{\beta z})u_l(u_g^2-u_l^2)\frac{\partial \beta}{\partial z}$$

$$+\frac{1-\beta}{\rho_l}u_l\frac{\partial P}{\partial z}+(1-\beta)u_l g\cos\theta-\frac{1-\beta}{\rho_l}u_l F_{LG}-\frac{1-\beta}{\rho_l}u_l F_{LW}=0 \tag{87}$$

Equation (87) can be transformed into Eq. (50) by dividing by $\beta u_g+(1-\beta)u_l$ and using $1-x=(1-\beta)u_l/\{\beta u_g+(1-\beta)u_l\}$ and Eqs. (52) and (54).

From these facts, another meaning of equations of motion (49) and (50) based on flowing mass is made clear. That is, since essence of a equation is not changed by dividing by some term, equations of motion (49) and (50) for flowing two-phase fluid can be said as the mechanical energy balance equations based on unit mass of existing two-phase fluid. This looks a little bit strange but is actually quite reasonable. Because, velocities which represent traveled distances per unit time of each phase in mechanical energy balance equations express, in the case of equations of motion, the quantitative coincidental relationships among each component of unit mass of flowing two-phase fluid which act forces to each other.

As described above, equation of motion (49) for gas phase based on flowing mass is the mechanical energy balance equation for gas phase of unit mass of existing two-phase fluid divided by $\beta u_g+(1-\beta)u_l$. By multiplying this equation by total mass flow rate W and rearranging with the relationship of $W/\{\beta u_g+(1-\beta)u_l\}=A\{\alpha\rho_g+(1-\alpha)\rho_l\}$, mechanical energy

balance equation for existing gas phase in unit channel length can be obtained. On the other hand, thermal energy balance equation (80) for gas phase of unit volume of existing two-phase fluid multiplied by flow area A gives thermal energy balance equation for existing gas phase in unit channel length. By algebraically summing up these two equations, total energy balance equation for gas phase of existing two-phase fluid in unit channel length can be obtained, i.e., after several transformations:

$$\frac{1}{2}A\alpha\rho_g\left\{\frac{\partial(u_g^2)}{\partial t}+u_g\frac{\partial(u_g^2)}{\partial z}\right\}+\frac{\zeta_{xt}}{2}(u_g^2-u_l^2)\frac{1}{u_{PC}}W\frac{\partial x}{\partial t}+\frac{\zeta_{xz}}{2}(u_g^2-u_l^2)W\frac{\partial x}{\partial z}$$
$$+A\alpha u_g\frac{\partial P}{\partial z}+xWg\cos\theta-A\alpha u_gF_{GL}-A\alpha u_gF_{GW}+A\alpha\rho_g\frac{\partial h_g}{\partial t}+A\alpha\rho_gu_g\frac{\partial h_g}{\partial z}-A\alpha\frac{\partial P}{\partial t}$$
$$-A\alpha u_g\frac{\partial P}{\partial z}+A[\zeta_I\{\alpha u_gF_{GL}+(1-\alpha)u_lF_{LG}\}+\alpha u_gF_{GW}]-A(\zeta_eQ_e-Q_{IG})$$
$$=\frac{1}{2}A\alpha\rho_g\left\{\frac{\partial(u_g^2)}{\partial t}+u_g\frac{\partial(u_g^2)}{\partial z}\right\}+\frac{\zeta_{xt}}{2}(u_g^2-u_l^2)\frac{1}{u_{PC}}W\frac{\partial x}{\partial t}-\frac{\zeta_{xz}}{2}(u_g^2-u_l^2)W\cdot\frac{\partial x}{\partial z}$$
$$+xWg\cos\theta-A[\alpha u_gF_{GL}-\zeta_I\{\alpha u_gF_{GL}+(1-\alpha)u_lF_{LG}\}]+A\alpha\rho_g\frac{\partial h_g}{dt}$$
$$+A\alpha\rho_gu_g\frac{\partial h_g}{\partial z}-A\alpha\frac{\partial P}{\partial t}-A(\zeta_eQ_e-Q_{IG})=0 \qquad (88)$$

Similarly, by algebraically summing up Eq. (50) multiplied by W and Eq. (81) multiplied by A, total energy balance equation for liquid phase of existing two-phase fluid in unit channel length can be obtained as:

$$\frac{1}{2}A(1-\alpha)\rho_l\left\{\frac{\partial(u_l^2)}{\partial t}+u_l\frac{\partial(u_l^2)}{\partial z}\right\}+\frac{1-\zeta_{xt}}{2}(u_g^2-u_l^2)\frac{1}{u_{PC}}W\frac{\partial x}{\partial t}+\frac{1-\zeta_{xz}}{2}(u_g^2$$
$$-u_l^2)W\frac{\partial x}{\partial z}+(1-x)Wg\cos\theta-A[(1-\alpha)u_lF_{LG}-(1-\zeta_I)\{\alpha u_gF_{GL}-(1-\alpha)\cdot$$
$$u_lF_{LG}\}]+A(1-\alpha)\rho_l\frac{\partial h_l}{\partial t}+A(1-\alpha)\rho_lu_l\frac{\partial h_l}{\partial z}-A(1-\alpha)\frac{\partial P}{\partial t}-A\{(1-\zeta_e)Q_e$$
$$-Q_{IL}\}=0 \qquad (89)$$

Equations (88) and (89) are balance equations of total energy for each phase.

In these equations, the first terms give kinetic energy changes of main flow gas and liquid phases. The second and third terms describe the transient and steady kinetic energy changes due to phase change, respectively. These terms can also be said as works done by the main flow phases overcoming inertial force of phase change part of fluid. The fourth terms define potential energy changes of the main flow phases. Potential energy terms for phase change part of fluid do not exist because mass fraction of phase change part to the total approaches to zero when dt or dz approaches to zero. The fifth terms represent the part of works done by the main flow phases overcoming interfacial frictional forces, which are transfered to the other phases as effective mechanical works. Sum of these terms is zero because they are not the dissipation terms. Since all of works done to overcome wall frictional forces are completely dissipated, the wall frictional terms corresponding to the fifth terms of Eqs. (88) and (89) cannot be seen. The sums of sixth and eighth terms give the transient changes of sensible heat and the seventh terms the steady changes of enthalpy. The dissipated energies due to interfacial and wall frictional forces are included in these terms. The last terms are the external heatings and interfacial heat removals, which are heat exchanges of each phase with the outside. These expressions of each component of energy change are quite reasonable.

5.3 Equation of Total Energy Conservation

By summing up Eqs. (88) and (89), equation of conservation relationship of total energy can be obtained for total two-phase flow, after rearranging with Eqs. (3), (4), (10) and (11), as:

$$\frac{1}{2}A\left\{\alpha\rho_g\frac{\partial(u_g^2)}{\partial t}+(1-\alpha)\rho_l\frac{\partial(u_l^2)}{\partial t}\right\}+\frac{1}{2}A\left\{\alpha\rho_g u_g\frac{\partial(u_g^2)}{\partial z}+(1-\alpha)\rho_l u_l\frac{\partial(u_l^2)}{\partial z}\right\}$$
$$+\frac{1}{2}(u_g^2-u_l^2)W\left(\frac{2}{u_g+u_l}\frac{\partial x}{\partial t}+\frac{\partial x}{\partial z}\right)+Wg\cos\theta-A\left\{\alpha\rho_g\frac{\partial h_g}{\partial t}+(1-\alpha)\rho_l\frac{\partial h_l}{\partial t}\right.$$
$$\left.-\frac{\partial P}{\partial t}\right\}+A\left\{\alpha\rho_g u_g\frac{\partial h_g}{\partial z}+(1-\alpha)\rho_l u_l\frac{\partial h_l}{\partial z}\right\}-AQ_e+A(Q_{IG}+Q_{IL})$$
$$=\frac{1}{2}A\left\{\alpha\rho_g\frac{\partial(u_g^2)}{\partial t}+(1-\alpha)\rho_l\frac{\partial(u_l^2)}{\partial t}\right\}+\frac{1}{2}A\left\{\alpha\rho_g u_g\frac{\partial(u_g^2)}{\partial z}+(1-\alpha)\rho_l u_l\cdot\right.$$
$$\left.\frac{\partial(u_l^2)}{\partial z}\right\}+\frac{1}{2}u_g^2Aw-\frac{1}{2}u_l^2Aw+Wg\cos\theta+A\left\{\alpha\rho_g\frac{\partial h_g}{\partial t}+(1-\alpha)\rho_l\frac{\partial h_l}{\partial t}-\frac{\partial P}{\partial t}\right\}$$
$$+A\left\{\alpha\rho_g u_g\frac{\partial h_g}{\partial z}+(1-\alpha)\rho_l u_l\frac{\partial h_l}{\partial z}\right\}-AQ_e+A(Q_{IG}+Q_{IL})$$
$$=\frac{1}{2}A\left\{\alpha\rho_g\frac{\partial(u_g^2)}{\partial t}+(1-\alpha)\rho_l\frac{\partial(u_l^2)}{\partial t}\right\}+\frac{1}{2}A\left\{\alpha\rho_g u_g\frac{\partial(u_g^2)}{\partial z}+(1-\alpha)\rho_l u_l\frac{\partial(u_l^2)}{\partial z}\right\}$$
$$+\frac{1}{2}u_g^2\left\{A\frac{\partial}{\partial t}(\alpha\rho_g)+\frac{\partial}{\partial z}(A\alpha\rho_g u_g)\right\}+\frac{1}{2}u_l^2\left[A\frac{\partial}{\partial t}\{(1-\alpha)\rho_l\}+\frac{\partial}{\partial z}\{A(1-\alpha)\cdot\right.$$
$$\left.\rho_l u_l\}\right]+Wg\cos\theta+A\left\{\alpha\rho_g\frac{\partial h_g}{\partial t}+(1-\alpha)\rho_l\frac{\partial h_l}{\partial t}-\frac{\partial P}{\partial t}\right\}+A\left\{\alpha\rho_g u_g\frac{\partial h_g}{\partial z}+(1-\alpha)\cdot\right.$$
$$\left.\rho_l u_l\frac{\partial h_l}{\partial z}\right\}-AQ_e+A(Q_{IG}+Q_{IL})$$
$$=A\frac{\partial}{\partial t}\left(\frac{1}{2}\alpha\rho_g u_g^2\right)+A\frac{\partial}{\partial t}\left\{\frac{1}{2}(1-\alpha)\rho_l u_l^2\right\}+\frac{\partial}{\partial z}\left(\frac{1}{2}A\alpha\rho_g u_g u_g^2\right)+\frac{\partial}{\partial z}\left\{\frac{1}{2}A(1-\alpha)\cdot\right.$$
$$\left.\rho_l u_l u_l^2\right\}+Wg\cos\theta+A\left\{\alpha\rho_g\frac{\partial h_g}{\partial t}+(1-\alpha)\rho_l\frac{\partial h_l}{\partial t}-\frac{\partial P}{\partial t}\right\}+A\left\{\alpha\rho_g u_g\frac{\partial h_g}{\partial z}+(1-\alpha)\right.$$
$$\left.\rho_l u_l\frac{\partial h_l}{\partial z}\right\}-AQ_e+A(Q_{IG}+Q_{IL})=0 \tag{90}$$

From Eqs. (3), (4) and (7),

$$A(Q_{IG}+Q_{IL})=A(h_g-h_l)w$$
$$=h_g\left\{A\frac{\partial}{\partial t}(\alpha\rho_g)+\frac{\partial}{\partial z}(A\alpha\rho_g u_g)\right\}+h_l\left[A\frac{\partial}{\partial t}\{(1-\alpha)\rho_l\}\right.$$
$$\left.+\frac{\partial}{\partial z}\{A(1-\alpha)\rho_l u_l\}\right] \tag{91}$$

So, Eq. (90) can be rewritten as:

$$A\frac{\partial}{\partial t}\left\{\alpha\rho_g\left(\frac{1}{2}u_g^2+h_g\right)+(1-\alpha)\rho_l\left(\frac{1}{2}u_l^2+h_l\right)-P\right\}+\frac{\partial}{\partial z}\left[A\left\{\alpha\rho_g u_g\left(\frac{1}{2}u_g^2+h_g\right)\right.\right.$$
$$\left.\left.+(1-\alpha)\rho_l u_l\left(\frac{1}{2}u_l^2+h_l\right)\right\}\right]+Wg\cos\theta-AQ_e=0 \tag{92}$$

This equation is the total energy conservation equation for total two-phase flow. Only the potential energy term is, however, treated in different way in this equation. Therefore, let us try to include the potential energy term into the first and second terms for equal expression. For this purpose, let us pick up the following quantity.

$$A\frac{\partial}{\partial t}(\alpha\rho_g gz\cos\theta)+\frac{\partial}{\partial z}(A\alpha\rho_g u_g gz\cos\theta)+A\frac{\partial}{\partial t}\{(1-\alpha)\rho_l gz\cos\theta\}$$
$$+\frac{\partial}{\partial z}\{A(1-\alpha)\rho_l u_l gz\cos\theta\}$$
$$=gz\cos\theta\cdot A\frac{\partial}{\partial t}(\alpha\rho_g)+g\cos\theta\cdot A\alpha\rho_g\frac{\partial z}{\partial t}+gz\cos\theta\cdot\frac{\partial}{\partial z}(A\alpha\rho_g u_g)$$
$$+g\cos\theta\cdot A\alpha\rho_g u_g\frac{\partial z}{\partial z}+gz\cos\theta\cdot A\frac{\partial}{\partial t}\{(1-\alpha)\rho_l\}+g\cos\theta\cdot A(1-\alpha)\rho_l\frac{\partial z}{\partial t}$$
$$+gz\cos\theta\cdot\frac{\partial}{\partial z}\{A(1-\alpha)\rho_l u_l\}+g\cos\theta\cdot A(1-\alpha)\rho_l u_l\frac{\partial z}{\partial z} \tag{93}$$

The sum of the first, third, fifth and seventh terms of Eq. (93) is zero because of mass conservation equation (8). $\partial z/\partial t$ in the second and sixth terms is zero because the coordinate axis is fixed. Therefore, only the fourth and eighth terms remain. And $\partial z/\partial z$ in these two terms is, of course, one. So that,

$$A\frac{\partial}{\partial t}(\alpha\rho_g gz\cos\theta)+\frac{\partial}{\partial z}(A\alpha\rho_g u_g gz\cos\theta)+A\frac{\partial}{\partial t}\{(1-\alpha)\rho_l gz\cos\theta\}$$
$$+\frac{\partial}{\partial z}\{A(1-\alpha)\rho_l u_l gz\cos\theta\}$$
$$=A\alpha\rho_g u_g g\cos\theta+A(1-\alpha)\rho_l u_l g\cos\theta$$
$$=Wg\cos\theta \tag{94}$$

The last expression of Eq. (94) is no other than the third term of Eq. (92). Therefore, Eq. (92) can be rewritten as:

$$A\frac{\partial}{\partial t}\left\{\alpha\rho_g\left(\frac{1}{2}u_g{}^2+gz\cos\theta+h_g\right)+(1-\alpha)\rho_l\left(\frac{1}{2}u_l{}^2+gz\cos\theta+h_l\right)-P\right\}$$
$$+\frac{\partial}{\partial z}\left[A\left\{\alpha\rho_g u_g\left(\frac{1}{2}u_g{}^2+gz\cos\theta+h_g\right)+(1-\alpha)\rho_l u_l\left(\frac{1}{2}u_l{}^2+gz\cos\theta\right.\right.\right.$$
$$\left.\left.\left.+h_l\right)\right\}\right]-AQ_e=0 \tag{95}$$

Equation (95) expresses most simply the conservation relationship of the sum of mechanical energy (kinetic energy + potential energy) and thermal energy.

In this chapter, total energy conservation equation for total two-phase flow was derived from the first low of thermodynamics on thermal energy balance and equations of motion for each phase. Such derivation is of common sense in single-phase flow. However, significance of the fact that similar fundamental consistency among the first law of thermodynamics, equations of motion (Newton's second law) and total energy conservation law was actually demonstrated for two-phase flow should be quite large. Because, it strongly indicates the validity of the author's basic equation set for two-phase flow, especially of the equations of motion.

5.4 Independency of Equations of Energy

The author derived five equations, (80), (81), (88), (89) and (95), as equations of energy for one-dimensional transient two-phase flow. In this case, as well as in equations of continuity and equations of motion, number of independent equations is two. Therefore, if such two equations are given the rest equations of energy should lose their independencies automatically. Such perfect combinations of two equations of energy are shown with symbol "○" in **Table 5**.

In the case of two-phase flow, basic equation set is sometimes composed confusedly. For example, excess equation of energy often cancels lack of equations of motion. And such handling is not always wrong. Therefore, one should carefully judge how each balance equation acts in the basic equation set in relation with the other balance equations, constitutive equations and analytical assumptions.

Table 5 Combinations of two independent equations of energy

	(80)	(81)	(88)	(89)	(95)
(80)		○	×	○	○
(81)	○		○	×	○
(88)	×	○		○	○
(89)	○	×	○		○
(95)	○	○	○	○	

(Note) Equations of motion and equations of continuity are assumed to have been provided.

6. Settled One-Dimensional Two-Phase Flow

Discussions on hydrodynamic basic equations themselves for one-dimensional two-phase flow have already been finished in the previous chapters. Since understanding on force balance between each component of two-phase fluid was made clear, characteristics of interfacial and wall frictional forces became able to discuss. Let us examine on this item in this chapter.

6.1 Definition of Frictional Forces

To define interfacial and wall frictional forces as the actual drag forces or shear forces acting on the interface and on the wall is quite natural from the view point of physical mechanism of the frictional forces and then is usually quite practical. According to such definition, wall frictional force acts on gas phase is zero in, e.g., bubble flow or annular flow.

As discussed in detail in Appendix 3, however, a part of interfacial frictional force acts on gas phase can be considered to be a part of wall frictional forces transmitted through liquid phase even in the above mentioned flow regimes. In the most simple example case of horizontal annular flow, the wall frictional force acts on the liquid film on the channel wall. The resultant radial velocity gradient in the liquid film gives a velocity gradient and a shear stress at the interface between liquid film and gas core. This interfacial shear stress has no difference from that of usual single-phase shear stress due to wall friction. From liquid phase side, the sum of interfacial shear force and wall shear force acts on it as the net wall frictional force. And from gas phase side, a part of wall frictional force acts on it as interfacial shear force which is transmitted through liquid phase, i.e., interfacial shear force in this case can be said to be a kind of wall frictional force. In a general two-phase flow, the other interfacial shear force (drag) acts on the interface in addition to such wall-friction-transmitted shear force as described in the next section. Therefore, if one define wall frictional force as the net wall frictional force described above instead of frictional force really acts on the wall surface, interfacial frictional force should be defined as the additional interfacial shear force without the wall-friction-transmitted shear force instead of real shear force acts on the interface. Since Eqs. (62) and (63) hold good also under the new definition of interfacial and wall frictional forces, all of the discussions on hydrodynamic balance equations in the present report hold good regardless of difference in definition of frictional forces.

Such new definition of interfacial and wall frictional forces enable us to simply express the corresponding relationships of those terms with the other terms of basic equations. In this chapter, therefore, the new definition shall be used for discussing the corresponding relationships.

6.2 Settlement of One-Dimensional Two-Phase Flow

As known from, e.g., Eqs. (47) and (48), inertial force acting on each phase balances with pressure force, gravitational force, interfacial frictional force and wall frictional force. Inertial force acting on phase change part of fluid balances with the parts of pressure force, etc., as additional term to inertial force term for the main flow phase.

In the above various kinds of forces, pressure force is given for unit volume of fluid as $-(\partial P/\partial z)$. Because pressure distribution in any cross section is assumed uniform in one-

dimensional two-phase flow, pressure gradient is common for each phase. Therefore, the same pressure forces act on gas and liquid phases if only the volumes are the same. Let us call the fact as that pressure force is volume-proportional type.

Next, let us pick up the sum of gravitational force, interfacial frictional force and wall frictional force for each phase, i.e.,

$$-\rho_g g \cos\theta + F_{GL} + F_{GW} \tag{96}$$

$$-\rho_l g \cos\theta + F_{LG} + F_{LW} \tag{97}$$

The forces represented by Eqs. (96) and (97) are generally not volume-proportional type but are supposed to have a tendency to approach to be volume-proportional type. Because, since the sum of pressure force and the force (96) or (97) is balanced with inertial force acts on each phase and pressure force is volume-proportional type, if the forces (96) and (97) are not volume-proportional type inertial forces for each phase should also not be volume-proportional type. That is, when the force (96) or (97) is algebraically too large in a phase the acceleration will be too large and it will be too small in the opposite case. Such unbalanced accelerations of two phases will cause different situation of u_g, u_l and α in the downstream and will result in different values of F_{GL}, F_{LG}, F_{GW} and F_{LW}. Consequently, the forces (96) and (97) will approach to volume-proportional type. Such sequential facts may easily be understood if one imagines axial change of steady two-pyase flow without phase change where gas and liquid velocities approach to the respective terminal value from any given upstream velocities. This axial flow change process will be discussed in more detail in Section 6.4. If redistribution of flow described above is completed perfectly, the forces (96) and (97) become volume-proportional type. Then,

$$-\rho_g g \cos\theta - F_{GL} + F_{GW} = -\rho_l g \cos\theta + F_{LG} + F_{LW} \tag{98}$$

When Eq. (98) holds good, inertial forces which act on each phase become volume-proportional type. Therefore, from Eqs. (47) and (48),

$$\rho_g\left(\frac{\partial u_g}{\partial t} + u_g \frac{\partial u_g}{\partial z}\right) + \frac{\zeta_{\beta t}}{\beta}\rho_g(u_g - u_l)\frac{\partial \beta}{\partial t} + \frac{\zeta_{\beta z}}{2\beta}\rho_g(u_g^2 - u_l^2)\frac{\partial \beta}{\partial z}$$
$$= \rho_l\left(\frac{\partial u_l}{\partial t} - u_l \frac{\partial u_l}{\partial z}\right) + \frac{1-\zeta_{\beta t}}{1-\beta}\rho_l(u_g - u_l)\frac{\partial \beta}{\partial t} + \frac{1-\zeta_{\beta z}}{2(1-\beta)}\rho_l(u_g^2 - u_l^2)\frac{\partial \beta}{\partial z} \tag{99}$$

And from Eqs. (49) and (50),

$$\rho_g\left(\frac{\partial u_g}{\partial t} + u_g \frac{\partial u_g}{\partial z}\right) + \frac{\zeta_{xt}}{x}\rho_g(u_g - u_l)\frac{\partial x}{\partial t} + \frac{\zeta_{xz}}{2x}\rho_g(u_g^2 - u_l^2)\frac{\partial x}{\partial z}$$
$$= \rho_l\left(\frac{\partial u_l}{\partial t} + u_l \frac{\partial u_l}{\partial z}\right) + \frac{1-\zeta_{xt}}{1-x}\rho_l(u_g - u_l)\frac{\partial x}{\partial t} + \frac{1-\zeta_{xz}}{2(1-x)}\rho_l(u_g^2 - u_l^2)\frac{\partial x}{\partial z} \tag{100}$$

Of course, Eqs. (99) and (100) are the same to each other.

One-dimensional two-phase flow where Eqs. (98) through (100) hold good is named as perfectly settled one-dimensional two-phase flow. On the other hand, if these equations do not hold good, the flow is imperfectly settled one-dimensional two-phase flow.

6.3 Characteristics of Perfectly Settled Two-Phase Flow

F_{GL}, F_{LG}, F_{GW} and F_{LW} which are defined with the previously described new method are different from actually acting frictional forces f_{GL}, f_{LG}, f_{GW} and f_{LW}, respectively. However,

$$F_{GL} + F_{GW} = f_{GL} + f_{GW} \tag{101}$$

$$F_{LG}+F_{LW}=f_{LG}+f_{LW} \tag{102}$$

$$\alpha F_{GL}+(1-\alpha)F_{LG}=\alpha f_{GL}+(1-\alpha)f_{LG}(=0) \tag{103}$$

$$\alpha F_{GW}+(1-\alpha)F_{LW}=\alpha f_{GW}+(1-\alpha)f_{LW} \tag{104}$$

hold good. Therefore, in the basic equation set, any set of F_{GL}, F_{LG}, F_{GW} and F_{LW} is equivalent to the set of f_{GL}, f_{LG}, f_{GW} and f_{LW}.

Since Eq. (104) is not independent* from the set of Eqs. (101), (102) and (103), degree of restriction is only three for the four parameters, F_{GL}, F_{LG}, F_{GW} and F_{LW}. This means that one can introduce one more restriction condition. Therefore, let us assume that wall frictional forces F_{GW} and F_{LW} are volume-proportional type. Then,

$$F_{GW}=F_{LW}\equiv F_W \tag{105}$$

From Eqs. (98) and (105),

$$-\rho_g g\cos\theta+F_{GL}=-\rho_l g\cos\theta+F_{LG} \tag{106}$$

is obtained. That is, the sum of gravitational force and interfacial frictional force is considered to be volume-proportional type. Then, from Eqs. (103) and (106),

$$F_{GL}=-(1-\alpha)(\rho_l-\rho_g)g\cos\theta \tag{107}$$

$$F_{LG}=\alpha(\rho_l-\rho_g)g\cos\theta \tag{108}$$

Furthermore, Eq. (106) can be rewritten by using these equations as:

$$\begin{aligned}-\rho_g g\cos\theta+F_{GL}&=-\rho_l g\cos\theta+F_{LG}\\&=-\{\alpha\rho_g+(1-\alpha)\rho_l\}g\cos\theta\end{aligned} \tag{109}$$

That is, the sum of gravitational force and interfacial frictional force gives gravitational head of two-phase flow.

Pressure drop of two-phase flow is generally considered as the sum of gravitational head, wall frictional pressure loss and accelerational pressure drop. However, each term becomes volume-proportional type as pressure force only when the two-phase flow is perfectly settled one.

6.4 Meaning of Settlement of Two-Phase Flow

In Section 6.2, perfectly settled one-dimensional two-phase flow was defined with a general way. The physical meaning will be explained more clearly in this section by applying an experiment in thought.[16]

Let us consider, for simplicity, gas phase is distributed as bubbles in a continuous liquid phase which is at rest in a vertical channel. The bubbles are assumed to be fixed with the channel wall, as illustrated in **Fig. 7**, by wires without diameter and weight. Buoyancy force and gravitational force acting on bubbles are transmitted to the wall through the elastic stress of the wires. In this case, gravitational head is given by $\rho_l g$ as well known as namely the communicating-vessel problem.

* By summing up Eq. (101) multiplied by α and Eq. (102) multiplied by 1 α, and using Eq. (103), Eq. (104) can be derived.

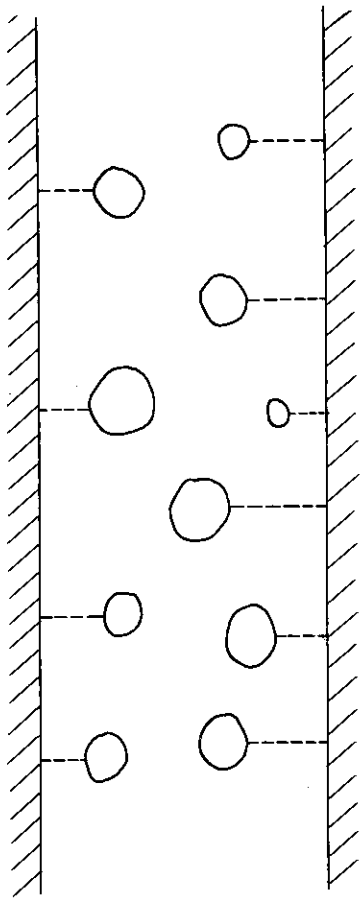

Fig. 7 Experiment in thought on gravitational water head in a vertical channel.

Next, let us cut the wires fixing the bubbles. Since the bubbles become unsupported by the wires, they begine to rise due to the buoyancy force. The relative velocity between gas and liquid phases increases untill the buoyancy force, drag force and gravitational force acting on the bubbles balance together. The drag force partially transmits the gravitational force acting on liquid phase to the bubbles. Consequently, gravitational head per unit vertical length becomes the well known void-averaged value $\{\alpha\rho_g+(1-\alpha)\rho_l\}g$. Since buoyancy force is integrated pressure force with respect to the whole surface of bubbles, change of buoyancy force, i.e., change of pressure gradient caused by cutting the wires is no other than the drag force acts on continuous liquid phase due to phase slip. That is,

$$F_{LG}=\rho_l g-\{\alpha\rho_g+(1-\alpha)\rho_l\}g=\alpha(\rho_l-\rho_g)g \tag{110}$$

Equation (110) is just the same as Eq. (108) for a vertical channel ($\theta=0$).

By applying the Newton's third law to Eq. (110),

$$F_{GL}=-(1-\alpha)(\rho_l-\rho_g)g \tag{111}$$

is obtained. This equation is the same as Eq. (107) for $\theta=0$.

As clearly known through the above discussion, Eqs. (110) and (111) hold good only after bubble rising velocity became the terminal velocity. When bubble rising velocity is not the terminal velocity, the flow is not perfectly settled yet and Eqs. (110) and (111) do not hold good. That is, the sum of gravitational force and drag force, in this case, does not balanced with gravitational head term for the two-phase flow.

7. Basic Equations for Three-Dimensional Two-Phase Flow

In this chapter, basic equations for three-dimensional two-phase flow shall be discussed. For equations of motion, specially detailed explanation will be made. Since each variable on two-phase flow has large time fluctuation, balance equations for time-averaged variables are necessary to be established for practical purpose based on the local, instantaneous balance relationships. This process produces several terms related to the fluctuational components which cannot be seen in the local, instantaneous expressions. And variation rate of transient to be described is limited by this time-averaging process.

Inherent error of two-fluid model for one-dimensional two-phase flow will be discussed in the last section of this chapter.

7.1 Time-Averaging of Variables

Since each variable on two-phase flow has large time fluctuation, balance equations for time-averaged variables are required for practical purpose. Fluctuational components are handled as follows.

$$\bar{X}=\overline{\bar{X}+X'}=\bar{\bar{X}}+\overline{X'}=\bar{X} \tag{112}$$

$$\overline{XY}=\overline{(\bar{X}+X')(\bar{Y}+Y')}=\overline{\bar{X}\bar{Y}}+\overline{\bar{X}Y'}+\overline{X'\bar{Y}}+\overline{X'Y'}=\bar{X}\bar{Y}+\overline{X'Y'} \tag{113}$$

$$\begin{aligned}\overline{XYZ}&=\overline{(\bar{X}+X')(\bar{Y}+Y')(\bar{Z}+Z')}=\overline{\bar{X}\bar{Y}\bar{Z}}+\overline{\bar{X}\bar{Y}Z'}+\overline{\bar{Y}\bar{Z}X'}+\overline{\bar{Z}\bar{X}Y'}+\overline{\bar{X}Y'Z'}+\overline{\bar{Y}Z'X'}\\&\quad+\overline{\bar{Z}X'Y'}+\overline{Z'Y'Z'}\\&=\bar{X}\bar{Y}\bar{Z}+\bar{X}\overline{Y'Z'}+\bar{Y}\overline{Z'X'}+\bar{Z}\overline{X'Y'}+\overline{X'Y'Z'}\end{aligned} \tag{114}$$

Here, "——" indicates time-averaged value and "," indicates fluctuational component. Time-average of the product of two or more time fluctuational components is generally not zero.

Averaging time should be chosen so as to get the averaged results which are independent of the averaging time. Therefore, averaging time should be sufficiently longer than fluctuation period. This fact means that phenomena with comparable or higher frequency of transient than the fluctuational components cannot be described with such method.

7.2 Equations of Continuity

Local, instantaneous equations of continuity for three-dimensional two-phase flow are given for gas and liquid phases, respectively, as:

$$\frac{\partial}{\partial t}(\alpha\rho_g)+\sum_{i=1}^{3}\frac{\partial}{\partial z_i}(\alpha\rho_g u_{gi})=w \tag{115}$$

$$\frac{\partial}{\partial t}\{(1-\alpha)\rho_l\}+\sum_{i=1}^{3}\frac{\partial}{\partial z_i}\{(1-\alpha)\rho_l u_{li}\}=-w \tag{116}$$

Here,

$$w=\frac{Q_{IG}+Q_{IL}}{h_g-h_l} \tag{117}$$

For time-averaged variables, Eqs. (115) and (116) can be written as:

$$\frac{\partial}{\partial t}(\bar{\alpha}\bar{\rho}_g)+\sum_{i=1}^{3}\frac{\partial}{\partial z_i}(\bar{\alpha}\bar{\rho}_g\bar{u}_{gi})+\frac{\partial}{\partial t}(\overline{\alpha'\rho_g'})+\sum_{i=1}^{3}\frac{\partial}{\partial z_i}(\bar{\alpha}\overline{\rho_g'u_{gi}'}+\bar{\rho}_g\overline{\alpha'u_{gi}'}+\bar{u}_{gi}\overline{\alpha'\rho_g'}+\overline{\alpha'\rho_g'u_{gi}'})=\bar{w} \tag{118}$$

$$\frac{\partial}{\partial t}\{(1-\bar{\alpha})\bar{\rho}_l\}+\sum_{i=1}^{3}\frac{\partial}{\partial z_i}\{(1-\bar{\alpha})\bar{\rho}_l\bar{u}_{li}\}-\frac{\partial}{\partial t}(\overline{\alpha'\rho_l'})+\sum_{i=1}^{3}\frac{\partial}{\partial z_i}\{(1-\bar{\alpha})\overline{\rho_l'u_{li}'}-\bar{\rho}_l\overline{\alpha'u_{li}'}-\bar{u}_{li}\overline{\alpha'\rho_l'}-\overline{\alpha'\rho_l'u_{li}'}\}=-\bar{w} \tag{119}$$

The third and fourth terms of Eqs. (118) and (119) are the fluctuational terms. If fluctuational flow is incompressible, the third terms and the first and third terms of the fourth terms of Eqs. (118) and (119) become zero.

Representing the fluctuational terms by $\dot{M}_g$ for gas phase and $\dot{M}_l$ for liquid phase respectively, and eliminating the averaging symbol "——" for simplicity, one can derive the following expressions.

$$\frac{\partial}{\partial t}(\alpha\rho_g)+\sum_{i=1}^{3}\frac{\partial}{\partial z_i}(\alpha\rho_g u_{gi})+\dot{M}_g=w \tag{120}$$

$$\frac{\partial}{\partial t}\{(1-\alpha)\rho_l\}+\sum_{i=1}^{3}\frac{\partial}{\partial z_i}\{(1-\alpha)\rho_l u_{li}\}+\dot{M}_l=-w \tag{121}$$

7.3 Equations of Motion

7.3.1 Equation of motion for single-phase flow

Let us start from the discussion on single-phase flow.

Instantaneous force balance on unit volume of single-phase fluid can be described by the following equation[17]:

$$\rho\frac{du_i}{\partial t}+\rho\sum_{j=1}^{3}u_j\frac{\partial u_i}{\partial z_j}+\frac{\partial p}{\partial z_i}-F_{Bi}+\frac{2}{3}\frac{\partial}{\partial z_i}\left(\mu\sum_{j=1}^{3}\frac{\partial u_j}{\partial z_j}\right)-\sum_{j=1}^{3}\frac{\partial}{\partial z_j}\left(\mu\frac{\partial u_i}{\partial z_j}\right)-\sum_{j=1}^{3}\frac{\partial}{\partial z_j}\left(\mu\frac{\partial u_j}{\partial z_i}\right)=0, \qquad i=1,\ 2,\ 3 \tag{122}$$

Here, the fifth through seventh terms are viscous stress terms.

By applying Eqs. (112) through (114), Eq. (122) can be transformed as:

$$\begin{aligned}&\bar{\rho}\frac{d\bar{u}_i}{dt}+\bar{\rho}\sum_{j=1}^{3}\bar{u}_j\frac{\partial\bar{u}_i}{\partial z_j}+\frac{\partial\bar{P}}{\partial z_i}-\overline{F_{Bi}}+\frac{2}{3}\frac{\partial}{\partial z_i}\left(\bar{\mu}\sum_{j=1}^{3}\frac{\partial\bar{u}_j}{\partial z_j}\right)-\sum_{j=1}^{3}\frac{\partial}{\partial z_j}\left(\bar{\mu}\frac{\partial\bar{u}_i}{\partial z_j}\right)\\&-\sum_{j=1}^{3}\frac{\partial}{\partial z_j}\left(\bar{\mu}\frac{\partial\bar{u}_j}{\partial z_i}\right)+\overline{\rho'\frac{du_i'}{dt}}+\bar{\rho}\sum_{j=1}^{3}\overline{u_j'\frac{\partial u_i'}{\partial z_j}}+\sum_{j=1}^{3}\bar{u}_j\overline{\rho'\frac{\partial u_i'}{\partial z_j}}+\sum_{j=1}^{3}\frac{\partial\bar{u}_i}{\partial z}\overline{\rho'u_j'}\\&+\sum_{j=1}^{3}\overline{\rho'u_j'\frac{\partial u_i'}{\partial z_j}}+\frac{2}{3}\frac{\partial}{\partial z_i}\left(\overline{\mu'\sum_{j=1}^{3}\frac{\partial u_j'}{\partial z_j}}\right)-\sum_{j=1}^{3}\frac{\partial}{\partial z_j}\left(\overline{\mu'\frac{\partial u_i'}{\partial z_j}}\right)\\&-\sum_{j=1}^{3}\frac{\partial}{\partial z_j}\left(\overline{\mu'\frac{\partial u_j'}{\partial z_i}}\right)=0, \qquad i=1,\ 2,\ 3\end{aligned} \tag{123}$$

Here, the fifth through seventh terms are shear force terms due to average flow and the eighth through fifteenth terms are those due to fluctuational components of flow. The thirteenth through fifteenth terms become zero when μ is constant. Furthermore, the eighth

and the tenth through twelfth terms become zero when ρ is constant. This situation gives the Navier-Stokes' equation.

Let us express the sum of the fifth through fifteenth terms of Eq. (123) with $-F_{Si}$ and eliminate the averaging symbol "——" for simplicity, then,

$$\rho \frac{du_i}{dt} + \rho \sum_{j=1}^{3} u_i \frac{\partial u_i}{\partial z_j} + \frac{\partial P}{\partial z_i} - F_{Bi} - F_{Si} = 0, \qquad i=1, 2, 3 \qquad (124)$$

Equation (124) can easily be transformed into the expression for unit mass of fluid as:

$$\frac{du_i}{dt} + \sum_{j=1}^{3} u_i \frac{\partial u_i}{\partial z_j} + \frac{1}{\rho} \frac{\partial P}{\partial z_i} - f_{Bi} - \frac{F_{Si}}{\rho} = 0, \qquad i=1, 2, 3 \qquad (125)$$

Here, f_{Bi} is body force acting on unit mass of fluid.

The second term of Eq. (125) can be transformed into kinetic energy type expression, i.e.,

$$\frac{\partial u_i}{\partial t} + \frac{1}{2} \frac{\mathfrak{H}(u_i^2)}{\mathfrak{H} z_i} + \frac{1}{\rho} \frac{\partial P}{\partial z_i} - f_{Bi} - \frac{F_{Si}}{\rho} = 0, \qquad i=1, 2, 3 \qquad (126)$$

Here, differentiation operator $\mathfrak{H}/\mathfrak{H} z_i$ expresses steady change of a variable during unit displacement in z_i-axis direction, i.e.,

$$\frac{\mathfrak{H}}{\mathfrak{H} z_i} = \sum_{j=1}^{3} \left(\frac{u_j}{u_i}\right) \frac{\partial}{\partial z_j} \qquad (127)$$

Equation (126) also can be written as:

$$\frac{1}{2} \frac{1}{u_i} \frac{\partial (u_i^2)}{\partial t} + \frac{1}{2} \frac{\mathfrak{H}(u_i^2)}{\mathfrak{H} z_i} + \frac{1}{\rho} \frac{\partial P}{\partial z_i} - f_{Bi} - \frac{F_{Si}}{\rho} = 0, \qquad i=1, 2, 3 \qquad (128)$$

This expression is of perfect kinetic energy type.

7.3.2 Equations of motion for total two-phase flow

Even in the case of two-phase flow, inside of each phase is a single-phase fluid. Therefore, Eq.(126) should hold good for each phase when phase change does not occur, i.e.,

$$\frac{\partial u_{gi}}{\partial t} + \frac{1}{2} \frac{\mathfrak{H}(u_{gi}^2)}{\mathfrak{H} z_i} + \frac{1}{\rho_g} \frac{\partial P}{\partial z_i} - f_{Bgi} - \frac{F_{GLi}}{\rho_g} - \frac{F_{GSi}}{\rho_g} = 0, \qquad i=1, 2, 3 \quad (129)$$

$$\frac{\partial u_{li}}{\partial t} + \frac{1}{2} \frac{\mathfrak{H}(u_{li}^2)}{\mathfrak{H} z_i} + \frac{1}{\rho_l} \frac{\partial P}{\partial z_i} - f_{Bli} - \frac{F_{LGi}}{\rho_l} - \frac{F_{LSi}}{\rho_l} = 0, \qquad i=1, 2, 3 \quad (130)$$

Here, F_{GLi}, F_{GSi}, and F_{LGi}, F_{LSi} are frictional forces acted by the other phase in the examined part of fluid and by the outside of the examined part of fluid for gas and liquid phases, respectively. And these frictional forces are the parts of total frictional forces F_{Sgi} and F_{Sli} for gas and liquid phases, corresponding to the fifth term of Eq. (126). And the following equations hold good.

$$F_{GLi} + F_{GSi} = F_{Sgi}, \qquad i=1, 2, 3 \qquad (131)$$

$$F_{LGi} + F_{LSi} = F_{Sli}, \qquad i=1, 2, 3 \qquad (132)$$

$$\alpha F_{GLi} - (1-\alpha) F_{LGi} = 0, \qquad i=1, 2, 3 \qquad (133)$$

$$\alpha F_{GSi} + (1-\alpha) F_{LSi} = \alpha F_{Sgi} + (1-\alpha) F_{Sli}, \qquad i=1, 2, 3 \qquad (134)$$

For unit mass of existing two-phase fluid without change of β, force balance can be written by using time-averaged β, as follows:

$$\beta\frac{\partial u_{gi}}{\partial t}+\frac{1}{2}\beta\frac{\mathfrak{H}(u_{gi}^2)}{\mathfrak{H}z_i}+(1-\beta)\frac{\partial u_{li}}{\partial t}+\frac{1}{2}(1-\beta)\frac{\mathfrak{H}(u_{li}^2)}{\mathfrak{H}z_i}+\left(\frac{\beta}{\rho_g}+\frac{1-\beta}{\rho_l}\right)\frac{\partial P}{\partial z_i}$$
$$-\{\beta f_{Bgi}+(1-\beta)f_{Bli}\}-\left(\frac{\beta}{\rho_g}F_{GLi}+\frac{1-\beta}{\rho_l}F_{LGi}\right)-\left(\frac{\beta}{\rho_l}F_{GSi}+\frac{1-\beta}{\rho_l}F_{LSi}\right)$$
$$=0, \qquad i=1,\ 2,\ 3 \tag{135}$$

Here, the seventh term of Eq. (135) is zero because of Eq. (133).

It must be noted that since each term of Eqs. (129) and (130) are time-averaged value, the expression with time-averaged β in Eq. (135) becomes possible.

On the other hand, the problem is not so simple when phase change occurs. Phase change part of fluid penetrates through the velocity boundary layers in both sides of the interface and is accelerated significantly. Inertial force due to this phase change acceleration is not included in Eq. (135) because differentiation terms of β do not exist in this equation.

Phase change inertial force can be written in the local, instantaneous expression, as follows:

$$(u_{gi}-u_{li})\frac{\partial\beta}{\partial t}+\frac{1}{2}(u_{gi}^2-u_{li}^2)\frac{\mathfrak{H}\beta}{\mathfrak{H}z_i}, \qquad i=1,\ 2,\ 3 \tag{136}$$

Here,

$$\frac{\mathfrak{H}\beta}{\mathfrak{H}z_i}=\sum_{j=1}^{3}\frac{(u_{gj}+u_{lj})/2}{(u_{gi}+u_{li})/2}\frac{\partial\beta}{\partial z_i}, \qquad i=1,\ 2,\ 3 \tag{137}$$

Time-average of Eq. (136) is given by

$$\overline{(u_{gi}-u_{li})\frac{\partial\beta}{\partial t}}+\frac{1}{2}\overline{(u_{gi}^2-u_{li}^2)\frac{\mathfrak{H}\beta}{\mathfrak{H}z_i}}$$
$$=(\overline{u_{gi}}-\overline{u_{li}})\frac{\partial\bar{\beta}}{\partial t}+\frac{1}{2}(\overline{u_{gi}}^2-\overline{u_{li}}^2)\frac{\mathfrak{H}\bar{\beta}}{\mathfrak{H}z_i}+\overline{(u_{gi}'-u_{li}')\frac{\partial\beta'}{\partial t}}+\frac{1}{2}(\overline{u_{gi}'^2})\frac{\mathfrak{H}\bar{\beta}}{\mathfrak{H}z_i}$$
$$-\frac{1}{2}(\overline{u_{li}'^2})\frac{\mathfrak{H}\bar{\beta}}{\mathfrak{H}z_i}+\overline{u}_{gi}\overline{u_{gi}'\frac{\mathfrak{H}\beta'}{\mathfrak{H}z_i}}-\overline{u}_{li}\overline{u_{li}'\frac{\mathfrak{H}\beta'}{\mathfrak{H}z_i}}+\frac{1}{2}\overline{(u_{gi}')^2\frac{\mathfrak{H}\beta'}{\mathfrak{H}z_i}}$$
$$-\frac{1}{2}\overline{(u_{li}')^2\frac{\mathfrak{H}\beta'}{\mathfrak{H}z_i}}, \qquad i=1,\ 2,\ 3 \tag{138}$$

Here,

$$\frac{\mathfrak{H}\beta}{\mathfrak{H}z_i}=\sum_{j=1}^{3}\frac{\overline{u_{gj}}+\overline{u_{lj}}}{\overline{u_{gi}}+\overline{u_{li}}}\frac{\partial\bar{\beta}}{\partial z_i}, \qquad i=1,\ 2,\ 3 \tag{139}$$

$$\frac{\mathfrak{H}\beta'}{\mathfrak{H}z_i}=\sum_{j=1}^{3}\frac{\overline{u_{gj}}+\overline{u_{lj}}}{\overline{u_{gi}}+\overline{u_{li}}}\frac{\partial\beta'}{\partial z_j}+\sum_{j=1}^{3}\left\{\frac{(u_{gj}'+u_{lj}')}{(\overline{u_{gi}}+\overline{u_{li}})+(u_{gi}'+u_{li}')}\frac{\partial(\bar{\beta}+\beta')}{\partial z_j}\right\}$$
$$-\sum_{j=1}^{3}\left[\frac{(\overline{u_{gj}}-\overline{u_{lj}})(u_{gi}'+u_{li}')}{(\overline{u_{gi}}+\overline{u_{li}})\{(\overline{u_{gi}}+\overline{u_{li}})-(u_{gi}'+u_{li}')\}}\frac{\partial(\bar{\beta}+\beta')}{\partial z_i}\right],$$
$$i=1,\ 2,\ 3 \tag{140}$$

The third through ninth terms of Eq. (138) are inertial force due to fluctuation of phase change. By adding Eq. (138) to Eq. (135), equation of motion for unit mass of existing two-

phase fluid with phase change is obtained as:

$$\beta\frac{\partial u_{gi}}{\partial t}+\frac{1}{2}\beta\frac{\partial(u_{gi}^2)}{\partial z_i}+(1-\beta)\frac{\partial u_{li}}{\partial t}+\frac{1}{2}(1-\beta)\frac{\partial(u_{li}^2)}{\partial z_i}+(u_{gi}-u_{li})\frac{\partial\beta}{\partial t}$$
$$+\frac{1}{2}(u_{gi}^2-u_{li}^2)\frac{\partial\beta}{\partial z_i}+\left(\frac{\beta}{\rho_g}+\frac{1-\beta}{\rho_l}\right)\frac{\partial P}{\partial z_i}-\{\beta f_{Bgi}+(1-\beta)f_{Bli}\}-\left(\frac{\beta}{\rho_g}F_{GLi}$$
$$+\frac{1-\beta}{\rho_l}F_{LGi}\right)-\left(\frac{\beta}{\rho_g}F_{GSi}+\frac{1-\beta}{\rho_l}F_{LSi}\right)=0,\qquad i=1,\ 2,\ 3 \tag{141}$$

Here, each parameter is time-averaged value although the averaging symbols "——" are eliminated.

F_{GLi}, F_{LGi}, F_{GSi} and F_{LSi} in Eq. (141) are determined from F_{sgi} and F_{sli} including the third through ninth terms of Eq. (138) so as to satisfy Eqs. (131) through (134). The ninth term of Eq. (141) is zero again because of Eq. (133).

For unit mass of flowing two-phase fluid with phase change, similar equation of motion can be obtained, by exchanging β by x, as:

$$x_i\frac{\partial u_{gi}}{\partial t}+\frac{1}{2}x_i\frac{\partial(u_{gi}^2)}{\partial z_i}+(1-x_i)\frac{\partial u_{li}}{\partial t}+\frac{1}{2}(1-x_i)\frac{\partial(u_{li}^2)}{\partial z_i}+(u_{gi}-u_{li})\frac{\partial x_i}{\partial t}$$
$$+\frac{1}{2}(u_{gi}^2-u_{li}^2)\frac{\partial x_i}{\partial z_i}+\left(\frac{x_i}{\rho_g}+\frac{1-x_i}{\rho_l}\right)\frac{\partial P}{\partial z_i}-\{x_i f_{Bgi}+(1-x_i)f_{Bli}\}$$
$$-\left(\frac{x_i}{\rho_g}F_{GLi}+\frac{1-x_i}{\rho_l}F_{LGi}\right)-\left(\frac{x_i}{\rho_g}F_{GSi}+\frac{1-x_i}{\rho_l}F_{LSi}\right)=0,\qquad i=1,\ 2,\ 3 \tag{142}$$

Here, the ninth term is not zero.

And x_i is defined by

$$x_i=\frac{\alpha\rho_g u_{gi}}{\alpha\rho_g u_{gi}+(1-\alpha)\rho_l u_{li}},\qquad i=1,\ 2,\ 3 \tag{143}$$

F_{GLi}, F_{LGi}, F_{GSi} and F_{LSi} are common between Eqs. (141) and (142), respectively, because each phase is originally single-phase fluid and, therefore, there is no difference between unit existing mass and unit flowing mass. Difference between unit mass of existing two-phase fluid and unit mass of flowing two-phase fluid comes from the difference in mixing fraction of gas and liquid phases.

7.3.3 Equations of motion for each phase

By formally dividing Eqs. (141) and (142) into two parts for gas and liquid phases, respectively, one can obtain the following four equations:

$$\beta\frac{\partial u_{gi}}{\partial t}+\frac{1}{2}\beta\frac{\partial(u_{gi}^2)}{\partial z_i}+\zeta_{\beta ti}(u_{gi}-u_{li})\frac{\partial\beta}{\partial t}+\zeta_{\beta zi}\frac{1}{2}(u_{gi}^2-u_{li}^2)\frac{\partial\beta}{\partial z_i}$$
$$+\frac{\beta}{\rho_g}\frac{\partial P}{\partial z_i}-\beta f_{Bgi}-\frac{\beta}{\rho_g}F_{GLi}-\frac{\beta}{\rho_g}F_{GSi}=0,\qquad i=1,\ 2,\ 3 \tag{144}$$

$$(1-\beta)\frac{\partial u_{li}}{\partial t}+\frac{1}{2}(1-\beta)\frac{\partial(u_{li}^2)}{\partial z_i}+(1-\zeta_{\beta ti})(u_{gi}-u_{li})\frac{\partial\beta}{\partial t}$$
$$+(1-\zeta_{\beta zi})\frac{1}{2}(u_{gi}^2-u_{li}^2)\frac{\partial\beta}{\partial z_i}+\frac{1-\beta}{\rho_l}\frac{\partial P}{\partial z_i}-(1-\beta)f_{Bli}-\frac{1-\beta}{\rho_l}F_{LGi}$$
$$-\frac{1-\beta}{\rho_l}F_{LSi}=0,\qquad i=1,\ 2,\ 3 \tag{145}$$

$$x_i \frac{\partial u_{gi}}{\partial t} + \frac{1}{2} x_i \frac{\partial (u_{gi}^2)}{\partial z_i} - \zeta_{xti}(u_{gi} - u_{li}) \frac{\partial x_i}{\partial t} + \zeta_{xzi} \frac{1}{2} (u_{gi}^2 - u_{li}^2) \frac{\partial x_i}{\partial z_i}$$
$$+ \frac{x_i}{\rho_g} \frac{\partial P}{\partial z_i} - x_i f_{Bgi} - \frac{x_i}{\rho_g} F_{GLi} - \frac{x_i}{\rho_g} F_{GSi} = 0, \qquad i = 1, 2, 3 \tag{146}$$

$$(1 - x_i) \frac{\partial u_{li}}{\partial t} + \frac{1}{2} (1 - x_i) \frac{\partial (u_{li}^2)}{\partial z_i} + (1 - \zeta_{xti})(u_{gi} - u_{li}) \frac{\partial x_i}{\partial t}$$
$$+ (1 - \zeta_{xzi}) \frac{1}{2} (u_{gi}^2 - u_{li}^2) \frac{\partial x_i}{\partial z_i} + \frac{1 - x_i}{\rho_l} \frac{\partial P}{\partial z_i} - (1 - x_i) f_{Bli} - \frac{1 - x_i}{\rho_l} F_{LGi}$$
$$- \frac{1 - x_i}{\rho_l} F_{LSi} = 0, \qquad i = 1, 2, 3 \tag{147}$$

Since Eq. (144) divided by β and Eq. (146) divided by x_i should be identical to each other and Eq. (145) divided by $1-\beta$ and Eq. (147) divided by $1 - x_i$ should be identical to each other, $\zeta_{\beta ti}$, $\zeta_{\beta zi}$, ζ_{xti} and ζ_{xzi} are determined, similarly to the one-dimensional case, as follows:

$$\zeta_{\beta ti} = \frac{\beta \left\{ (1-\beta) - (1 - x_i) \dfrac{\partial \beta / \partial t}{\partial x_i / \partial t} \right\}}{\{x_i (1-\beta) - \beta (1 - x_i)\} \dfrac{\partial \beta / \partial t}{\partial x_i / \partial t}}, \qquad i = 1, 2, 3 \tag{148}$$

$$\zeta_{\beta zi} = \frac{\beta \left\{ (1-\beta) - (1 - x_i) \dfrac{\partial \beta / \partial z_i}{\partial x_i / \partial z_i} \right\}}{\{x_i (1-\beta) - \beta (1 - x_i)\} \dfrac{\partial \beta / \partial z_i}{\partial x_i / \partial z_i}}, \qquad i = 1, 2, 3 \tag{149}$$

$$\zeta_{xti} = \frac{x_i \left\{ (1-\beta) - (1 - x_i) \dfrac{\partial \beta / \partial t}{\partial x_i / \partial t} \right\}}{x_i (1-\beta) - \beta (1 - x_i)}, \qquad i = 1, 2, 3 \tag{150}$$

$$\zeta_{xzi} = \frac{x_i \left\{ (1-\beta) - (1 - x_i) \dfrac{\partial \beta / \partial z_i}{\partial x_i / \partial z_i} \right\}}{x_i (1-\beta) - \beta (1 - x_i)}, \qquad i = 1, 2, 3 \tag{151}$$

Equations (144) through (147) substituted Eqs. (148) through (151) are equations of motion for each phase based on existing mass and based on flowing mass.

7.4 Equations of Energy

Local, instantaneous equations of energy for three-dimensional two-phase flow are given for gas and liquid phases, respectively, as:

$$-\alpha \rho_g \frac{Dq_g}{Dt} - \zeta_I \{ \alpha \sum_{i=1}^{3} u_{gi} F_{GLi} + (1-\alpha) \sum_{i=1}^{3} u_{li} F_{LGi} \} - \alpha \sum_{i=1}^{3} u_{gi} F_{GSi} - \zeta_e Q_e$$
$$- Q_{IG} = 0 \tag{152}$$

$$-(1-\alpha) \rho_l \frac{Dq_l}{Dt} - (1-\zeta_I) \{ \alpha \sum_{i=1}^{3} u_{gi} F_{GLi} + (1-\alpha) \sum_{i=1}^{3} u_{li} F_{LGi} \}$$
$$- (1-\alpha) \sum_{i=1}^{3} u_{li} F_{LSi} + (1-\zeta_e) Q_e - Q_{IL} = 0 \tag{153}$$

Here,

$$\frac{Dq_g}{Dt}=\left(\frac{dh_g}{dP}-\frac{1}{\rho_g}\right)\left(\frac{\partial P}{\partial t}+\sum_{i=1}^{3}u_{gi}\frac{\partial P}{\partial z_i}\right) \tag{154}$$

$$\frac{Dq_l}{Dt}=\left(\frac{dh_l}{dP}-\frac{1}{\rho_l}\right)\left(\frac{\partial P}{\partial t}+\sum_{i=1}^{3}u_{li}\frac{\partial P}{\partial z_i}\right) \tag{155}$$

Expressions with time-averaged variables are derived from Eqs. (152) and (153) as follows:

$$\begin{aligned}
&-\bar{\alpha}\bar{\rho}_g\frac{D\bar{q}_g}{Dt}-\bar{\zeta}_I\{\bar{\alpha}\sum_{i=1}^{3}\bar{u}_{gi}\bar{F}_{GLi}+(1-\bar{\alpha})\sum_{i=1}^{3}\overline{u_{li}F_{LGi}}\}-\bar{\alpha}\sum_{i=1}^{3}\bar{u}_{gi}\bar{F}_{GSi}+\bar{\zeta}_e\bar{Q}_e\\
&-\overline{Q_{IG}}-\overline{\bar{\alpha}\rho_g'\frac{Dq_g'}{Dt}}-\bar{\rho}_g\overline{\alpha'\frac{Dq_g'}{Dt}}-\frac{D\bar{q}_g}{Dt}\overline{\alpha'\rho_g'}-\overline{\alpha'\rho_g'\frac{Dq'}{Dt}}-\bar{\zeta}_I\bar{\alpha}\sum_{i=1}^{3}\overline{u_{gi}'F_{GLi}'}\\
&-\bar{\zeta}_I\sum_{i=1}^{3}\bar{u}_{gi}\overline{\alpha'F_{GLi}'}-\bar{\zeta}_I\sum_{i=1}^{3}\bar{F}_{GLi}\overline{\alpha'u_{gi}'}-\bar{\alpha}\sum_{i=1}^{3}\bar{u}_{gi}\overline{\zeta_I'F_{GLi}'}\\
&-\bar{\alpha}\sum_{i=1}^{3}\bar{F}_{GLi}\overline{\zeta_I'u_{gi}'}-\sum_{i=1}^{3}\bar{u}_{gi}\bar{F}_{GLi}\overline{\zeta_i'\alpha'}-\bar{\zeta}_I\sum_{i=1}^{3}\overline{\alpha'u_{gi}'F_{GLi}'}\\
&-\bar{\alpha}\sum_{i=1}^{3}\overline{\zeta_I'u_{gi}'F_{GLi}'}-\sum_{i=1}^{3}\bar{u}_{gi}\overline{\zeta_I'\alpha'F_{GLi}'}-\sum_{i=1}^{3}\bar{F}_{GLi}\overline{\zeta_I'\alpha'u_{gi}'}\\
&-\sum_{i=1}^{3}\overline{\zeta_I'\alpha'u_{gi}'F_{GLi}'}-\bar{\zeta}_I(1-\bar{\alpha})\sum_{i=1}^{3}\overline{u_{li}'F_{LGi}'}+\bar{\zeta}_I\sum_{i=1}^{3}\bar{u}_{li}\overline{\alpha'F_{LGi}'}\\
&+\bar{\zeta}_I\sum_{i=1}^{3}\bar{F}_{LGi}\overline{\alpha'u_{li}'}-(1-\bar{\alpha})\sum_{i=1}^{3}\bar{u}_{li}\overline{\zeta_I'F_{LGi}'}-(1-\bar{\alpha})\sum_{i=1}^{3}\bar{F}_{LGi}\overline{\zeta_I'u_{li}'}\\
&+\sum_{i=1}^{3}\bar{u}_{li}\bar{F}_{LGi}\overline{\zeta_I'\alpha'}+\bar{\zeta}_I\sum_{i=1}^{3}\overline{\alpha'u_{li}'F_{LGi}'}-(1-\bar{\alpha})\sum_{i=1}^{3}\overline{\zeta_I'u_{li}'F_{LGi}'}\\
&+\sum_{i=1}^{3}\bar{u}_{gi}\overline{\zeta_I'\alpha'F_{LGi}'}+\sum_{i=1}^{3}\bar{F}_{LGi}\overline{\zeta_I'\alpha'u_{li}'}+\sum_{i=1}^{3}\overline{\zeta_I'\alpha'u_{li}'F_{LGi}'}\\
&-\bar{\alpha}\sum_{i=1}^{3}\overline{u_{gi}'F_{GSi}'}-\sum_{i=1}^{3}\bar{u}_{gi}\overline{\alpha'F_{GSi}'}-\sum_{i=1}^{3}\bar{F}_{GSi}\overline{\alpha'u_{gi}'}\\
&-\sum_{i=1}^{3}\overline{\alpha'u_{gi}'F_{GSi}'}+\overline{\zeta_e'Q_e'}=0
\end{aligned} \tag{156}$$

$$\begin{aligned}
&-(1-\bar{\alpha})\bar{\rho}_l\frac{D\bar{q}_l}{Dt}-(1-\bar{\zeta}_I)\{\alpha\sum_{i=1}^{3}\bar{u}_{gi}\bar{F}_{GLi}+(1-\bar{\alpha})\sum_{i=1}^{3}\overline{u_{li}F_{LGi}}\}\\
&-(1-\bar{\alpha})\sum_{i=1}^{3}\overline{u_{li}F_{LSi}}+(1-\bar{\zeta}_e)\bar{Q}_e-\overline{Q_{IL}}-(1-\bar{\alpha})\overline{\rho_l'\frac{Dq_l'}{Dt}}+\bar{\rho}_l\overline{\alpha'\frac{Dq_l'}{Dt}}\\
&+\frac{D\bar{q}_l}{Dt}\overline{\alpha'\rho_l'}+\overline{\alpha'\rho_l'\frac{Dq_l'}{Dt}}-(1-\bar{\zeta}_I)\bar{\alpha}\sum_{i=1}^{3}\overline{u_{gi}'F_{GLi}'}\\
&-(1-\bar{\zeta}_I)\sum_{i=1}^{3}\bar{u}_{gi}\overline{\alpha'F_{GLi}'}-(1-\bar{\zeta}_I)\sum_{i=1}^{3}\bar{F}_{GLi}\overline{\alpha'u_{gi}'}+\bar{\alpha}\sum_{i=1}^{3}\bar{u}_{gi}\overline{\zeta_I'F_{GLi}'}\\
&+\bar{\alpha}\sum_{i=1}^{3}\bar{F}_{GLi}\overline{\zeta_I'u_{gi}'}+\sum_{i=1}^{3}\bar{u}_{gi}\bar{F}_{GLi}\overline{\zeta_I'\alpha'}-(1-\bar{\zeta}_I)\sum_{i=1}^{3}\overline{\alpha'u_{gi}'F_{GLi}'}\\
&+\bar{\alpha}\sum_{i=1}^{3}\overline{\zeta_I'u_{gi}'F_{GLi}'}+\sum_{i=1}^{3}\bar{u}_{gi}\overline{\zeta_I'\alpha'F_{GLi}'}+\sum_{i=1}^{3}\bar{F}_{GLi}\overline{\zeta_I'\alpha'u_{gi}'}\\
&+\sum_{i=1}^{3}\overline{\zeta_I'\alpha'u_{gi}'F_{GLi}'}-(1-\bar{\zeta}_I)(1-\bar{\alpha})\sum_{i=1}^{3}\overline{u_{li}'F_{LGi}'}
\end{aligned}$$

$$+(1-\bar{\zeta}_l)\sum_{i=1}^{3}\overline{u_{li}\,\alpha'\,F_{LGi}'}+(1-\bar{\zeta}_l)\sum_{i=1}^{3}\overline{F_{LGi}\,\alpha'\,u_{li}'}$$

$$+(1-\bar{\alpha})\sum_{i=1}^{3}\overline{u_{li}\,\zeta_l'\,F_{LGi}'}+(1-\bar{\alpha})\sum_{i=1}^{3}\overline{F_{LGi}\,\zeta_l'\,u_{li}'}-\sum_{i=1}^{3}\overline{u_{li}}\,\overline{F_{LGi}}\,\overline{\zeta_l'\,\alpha'}$$

$$+(1-\bar{\zeta}_l)\sum_{i=1}^{3}\overline{\alpha'\,u_{li}'\,F_{LGi}'}+(1-\bar{\alpha})\sum_{i=1}^{3}\overline{\zeta_l'\,u_{li}'\,F_{LGi}'}$$

$$-\sum_{i=1}^{3}\overline{u_{gi}}\,\overline{\zeta_l'\,\alpha'\,F_{LGi}'}-\sum_{i=1}^{3}\overline{F_{LGi}}\,\overline{\zeta_l'\,\alpha'\,u_{li}'}-\sum_{i=1}^{3}\overline{\zeta_l'\,\alpha'\,u_{li}'\,F_{LGi}'}$$

$$-(1-\bar{\alpha})\sum_{i=1}^{3}\overline{u_{li}'\,F_{LSi}'}+\sum_{i=1}^{3}\overline{u_{li}}\,\overline{\alpha'\,F_{LSi}'}+\sum_{i=1}^{3}\overline{F_{LSi}}\,\overline{\alpha'\,u_{li}'}$$

$$+\sum_{i=1}^{3}\overline{\alpha'\,u_{li}'\,F_{LSi}'}-\overline{\zeta_e'\,Q_e'}=0 \tag{157}$$

Here,

$$\frac{D\bar{q}_g}{Dt}=\left(\frac{d\bar{h}_g}{dP}-\frac{1}{\bar{\rho}_g}\right)\left(\frac{\partial\bar{P}}{\partial t}+\sum_{i=1}^{3}\overline{u_{gi}}\,\frac{\partial\bar{P}}{\partial z_i}\right) \tag{158}$$

$$\frac{Dq_g'}{Dt}=\left(\frac{d\bar{h}_g}{dP}-\frac{1}{\bar{\rho}_g}\right)\left(\frac{\partial P'}{\partial t}+\sum_{i=1}^{3}\frac{\partial\bar{P}}{\partial z_i}u_{gi}'+\sum_{i=1}^{3}\overline{u_{gi}}\,\frac{\partial P'}{\partial z_i}+\sum_{i=1}^{3}u_{gi}'\,\frac{\partial P'}{\partial z_i}\right)$$
$$+\left\{\frac{dh_g}{dP}+\frac{\rho_g'}{\bar{\rho}_g(\bar{\rho}_g+\rho_g')}\right\}\left(\frac{\partial\bar{P}}{\partial t}+\sum_{i=1}^{3}\overline{u_{gi}}\,\frac{\partial\bar{P}}{\partial z_i}+\frac{\partial P'}{\partial t}+\sum_{i=1}^{3}\frac{\partial\bar{P}}{\partial z_i}u_{gi}'\right.$$
$$\left.+\sum_{i=1}^{3}\overline{u_{gi}}\,\frac{\partial P'}{\partial z_i}+\sum_{i=1}^{3}u_{gi}'\,\frac{dP'}{\partial z_i}\right) \tag{159}$$

$$\frac{D\bar{q}_l}{Dt}=\left(\frac{d\bar{h}_l}{dP}-\frac{1}{\bar{\rho}_l}\right)\left(\frac{\partial\bar{P}}{\partial t}+\sum_{i=1}^{3}\overline{u_{li}}\,\frac{\partial\bar{P}}{\partial z_i}\right) \tag{160}$$

$$\frac{Dq_l'}{Dt}=\left(\frac{d\bar{h}_l}{dP}-\frac{1}{\bar{\rho}_l}\right)\left(\frac{\partial P'}{\partial t}+\sum_{i=1}^{3}\frac{\partial\bar{P}}{\partial z_i}u_{li}'+\sum_{i=1}^{3}\overline{u_{li}}\,\frac{\partial P'}{\partial z_i}+\sum_{i=1}^{3}u_{li}'\,\frac{\partial P'}{\partial z_i}\right)$$
$$+\left\{\frac{dh_l'}{dP}+\frac{\rho_l'}{\bar{\rho}_l(\bar{\rho}_l+\rho_l')}\right\}\left(\frac{\partial\bar{P}}{\partial t}+\sum_{i=1}^{3}\overline{u_{li}}\,\frac{\partial\bar{P}}{\partial z_i}+\frac{\partial P'}{\partial t}+\sum_{i=1}^{3}\frac{\partial\bar{P}}{\partial z_i}u_{li}'\right.$$
$$\left.+\sum_{i=1}^{3}\overline{u_{li}}\,\frac{\partial P'}{\partial z_i}+\sum_{i=1}^{3}u_{li}'\,\frac{\partial P'}{\partial z_i}\right) \tag{161}$$

With representing the fluctuation-induced terms by $\dot{E}_g$ for gas phase and $\dot{E}_l$ for liquid phase, respectively, and eliminating the averaging symbols "——" for simplicity, one can obtain the following equations from Eqs. (156) and (157).

$$-\alpha\rho_g\frac{Dq_g}{Dt}-\zeta_I\{\alpha\sum_{i=1}^{3}u_{gi}F_{GLi}+(1-\alpha)\sum_{i=1}^{3}u_{li}F_{LGi}\}-\alpha\sum_{i=1}^{3}u_{gi}F_{GSi}+\zeta_eQ_e$$
$$-Q_{IG}+\dot{E}_g=0 \tag{162}$$

$$-(1-\alpha)\rho_l\frac{Dq_l}{Dt}-(1-\zeta_I)\{\alpha\sum_{i=1}^{3}u_{gi}F_{GLi}+(1-\alpha)\sum_{i=1}^{3}u_{li}F_{LGi}\}$$
$$-(1-\alpha)\sum_{i=1}^{3}u_{li}F_{LSi}+(1-\zeta_e)Q_e-Q_{IL}+\dot{E}_l=0 \tag{163}$$

7.5 Inherent Errors of One-Dimensional Approximation

One-dimensional basic equations described in Chapters 3 throuth 5 have inherent errors although they are practically very useful. The errors come from two different causes. One is neglection of fluctuational terms. That is, equations of continuity (3) and (4) do not have fluctuational terms corresponding to $\dot{M}_g$ in Eq. (120) and $\dot{M}_l$ in Eq. (121). Also, equations of energy (80) and (81) do not have the terms corresponding to $\dot{E}_g$ in Eq. (162) and $\dot{E}_l$ in Eq. (163). Furthermore, F_{GL}, F_{LG}, F_{GW} and F_{LW} in equations of motion introduced in Chapter 4 are not including fluctuation-induced forces which are included in F_{GLi}, F_{LGi}, F_{GSi} and F_{LSi} in Eqs. (141), (142) and (144) through (147) in Chapter 7. Such approximations in one-dimensional basic equations in this report will give some inherent errors of two-phase flow analysis.

Another cause of inherent errors of one-dimensional basic equations is distribution of variables in channel cross section. When the author derived one-dimensional equations of motion (45) and (46), u_g, u_l and P were assumed to be common between unit mass of existing two-phase fluid and unit mass of flowing two-phase fluid. However, if one derives these equations based on Eqs. (140) and (141), these variables should be averaged with respect to the existing two-phase mass and flowing two-phase mass, respectively, and the two kinds of averaged values are generally different to each other. Especially, in u_g and u_l the difference is considered relatively large.

However, if the errors are sufficiently small for practical purpose, one-dimensional approximation of basic equations in this report is still useful. Usefulness of the one-dimensional basic equations should, of course, be judged through applications to various two-phase flow problems.

On the other hand, strict three-dimensional basic equations are not always suitable because of the complication and lack of enough experimental information on detailed structure of two-phase flow. Computing time required is also big problem. Therefore, selection of basic equations should be carefully made.

8. Conclusion

In the present report, the author examined equations of continuity, equations of motion and equations of energy for one-dimensional two-phase flow (two-fluid model) from the view point of describing balance of each physical quantity as strictly as possible, and derived various types of those balance equations. The main discussion item is how to treate the inertial force terms of equations of motion due to phase change acceleration. Invalidity of conventional treatment of the terms was pointed out, which was simple extension of the single-phase hydrodynamics. The conventional treatment cannot describe force balance correctly because of conflict of Newton's second law.

Discussion on this item in the present report is summarized as follows:

(1) Phase change part of fluid has a representative velocity of $(u_g+u_l)/2$ during phase change acceleration, which is different from both gas phase velocity u_g and liquid phase velocity u_l of the main flow. This fact was discussed with the following three independent procedures.
   i. Evaluation of the average displacement velocity of phase change part of fluid (Section 3.5)
   ii. Application of the kinetic energy principle to the total two-phase flow and transformation into the momentum principle type expression (Section 4.1, Subsection 4.2.2)
   iii. Microscopic examination on phase change acceleration process (Subsection 4.2.2)

(2) Difference in representative velocity between the main flow phases and phase change part of fluid was automatically taken into account and, therefore, time and spatial corresponding relationships among each part of fluid were handled correctly (Subsection 4.2.3) by applying the kinetic energy principle to the steady inertial force terms (Sections 4.1, 4.3). In other words, Newton's third law was strictly applied. It was demonstrated that correct application of Newton's third law is indispensable for correct application of Newton's second law.

(3) Two independent equations of motion were established (Sections 4.1, 4.3) for total two-phase flow based on the independency between unit mass of existing two-phase fluid and unit mass of flowing two-phase fluid (Section 2.2) because of phase slip. From those two equations, equations of motion for each phase were derived by only a purely mathematical treatment without introduction of any physical models on the mechanism of phase change acceleration (Section 4.4).

(4) Momentum change or kinetic energy change due to mass change of examined part of fluid was pointed out, which was independent of real acceleration of mass and, therefore, had no relation with inertial force (Subsection 4.2.4). Equations of motion were established for "unit mass" of two-phase fluid for preventing from this problem (Sections 4.1, 4.3).

(5) Equations of motion established were transformed purely mathematically into usual momentum equation type expressions (Section 4.5). By comparing the results with typical conventional momentum equations, kinetic contradictions in the conventional expressions were indicated (Section 4.7).

(6) As the result of these considerations, the kinetic treatment became very strict and the inconsistency between inertial force terms of equations of motion and kinetic energy terms of equations of energy was eliminated although it is often seen in conventional

basic equation sets (Subsection 4.7.3). Also, conservation equation of total energy was derived based on the equations of motion and the first law of thermodynamics, indicating the validity of the author's basic equations especially of the equations of motion (Section 5.3).

Each problem described above is considered physically very simple and valid itself but usually appears in a combined manner. In addition, not only when one treates a single-phase flow or non-slip two-phase flow with only one representative velocity but also even when he treates two-phase flow with phase slip these problems are never realized if there is no phase change. This fact seems to make it so difficult to find out these problems.

Major advantages to use the author's basic equation set are considered to be:

(1) Highly accurate two-phase flow analysis is possible since balance of mass, force and energy are correctly described.

(2) Calculational instability due to incorrect balances of mass, force and energy can be avoided.

(3) Correct basic equations help us to find how to solve two-phase flow problem.

Out of these three, item (1) will be impotant especially when contribution of phase change inertial force is large. In Part II of this report, two-phase critical flow shall be discussed as an example of such cases.

Next, for item (2), not only the total value of phase change inertial force but also the distribution to each phase is correctly evaluated in the author's equations of motion, based on Newton's second and third laws. That is, the distribution fractions are automatically controled by Eqs. (55) through (58). This means that the feed-back characteristics through the phase change inertial force is quite different from conventional equations of motion. A part of calculational instability is expected to be reduced by this. This is one of the most important examination items in the future.

Next, Chapter 6 of Part I is considered to be an example of item (3). More examples will be introduced in Part II.

Finally, three-dimensional basec equation set was introduced in Chapter 7. Such general expressions are not always practical at present because of lack of enough experimental information on detailed structure of two-phase flow. However, basic understanding on two-phase flow phenomena is deepened through such examinations.

9. Nomenclature

Simbols used in Part I of the present report are listed below. The same simbols are commonly used also in Appendices 1 through 3.

A = flow area
E = energy diffusion due to fluctuation
e = energy per unit mass (Appendix 2)
F = force per unit volume of fluid
f = force; force acted by interface or wall per unit volume of fluid ; force acts on unit mass of fluid
g = gravitational acceleration
h = specific enthalpy
K = compressibility
M = mass diffusion due to fluctuation
m = mass
P = pressure
Q = heat transfer rate per unit volume of channel
q = sensible heat per unit mass of fluid
r = displacement (Appendix 2)
S = interfacial area per unit volume of channel
T = temperature
t = time
u = velocity
W = mass flow rate
w = phase change rate per unit volume of channel
x = gas mass flow rate fraction (quality)
z = position
α = gas volume fraction (void fraction)
β = gas mass fraction
δ = displacement during phase change acceleration
ζ = distribution fraction to gas phase
μ = mass of phase change particle
θ = inclination of channel from vertical upward direction
ρ = density
τ = time for phase change acceleration

Subscripts:

g : gas phase
l : liquid phase
PC : phase change part of fluid
GL : to gas phase from liquid phase
LG : to liquid phase from gas phase
GW : to gas phase from wall
LW : to liquid phase from wall
W : wall
IG : to interface from gas phase

IL : to interface from liquid phase
I : interface
GS : to gas phase from surface of examined part of fluid
LS : to liquid phase from surface of examined part of fluid
S : contact area per unit volume of channel (Appendix 3)
B : body force
K : kinetic energy (Appendix 2)
VM : virtual mass effect (Appendix 1)
e : external
xt : time variation of x
xz : spatial variation of x
βt : time variation of β
βz : spatial variation of β
sat : saturation
τ : time average during time τ
δ : spatial average in distance δ
i, j : axis number of coordinate ($i, j = 1, 2, 3$)

References

(1) H. Adachi, "Research on One-Dimensional Two-Phase Flow (Theory and application on hydrodynamic balances in two-fluid model)", Dissertation, Tokyo Univ. 1987).

(2) P.A. Weiss and R.J. Hertlein, "UPTF Test Results - First 3 Separate Effect Tests", presented at the 14th water Reactor Safety Information Meeting (October 27-31, 1986).

(3) D. Liles, et al., "TRAC–PD2 An Advanced Best Estimate Computer Program for Pressurized Water Reactor Thermal-Hydraulic Analysis", NUREG/CR-2054 (April, 1981).

(4) D. Liles, et al., "TRAC–PF1/MOD1 An Advanced Best Estimate Computer Program for Pressurized Water Reactor Thermal-Hydraulic Analysis", Private Communication.

(5) J.G.M. Anderson and K.H. Chu, "BWR Refill-Reflood Program Task 4.7-Constitutive Correlations for Shear and Heat Transfer for the BWR Version of TRAC", NUREG/CR-2134 (November, 1982).

(6) K.V. Moor and W.H. Rettig, "RELAP4-A Computer Program for Transient Thermal-Hydraulic Analysis", ANCR-1127 (March, 1975).

(7) "RELAP5/MOD1 Code Manual, Volume 1 : System Models and Numerical Methods", NUREG/CR-1826, Revision 1 (March, 1981).

(8) M.J. Thurgood, J.M. Kelly, T.E. Guidotti, R.J. Kohrt and K.R. Crowell, "COBRA/TRAC–A Thermal-Hydraulics Code for Transient Analysis of Nuclear Reactor Vessels and Primary Coolant Systems", NUREG/CR-3046, Vol.1 (March, 1983).

(9) M.J. Burwell, et al., "DRUFAN-01/MOD2, Vol.III-Model Description", GRS–A-845 (July, 1983).

(10) "CATHARE-Model D'ecoulement Diphasique Monodimensionnel en Regime Transitoire", NOTETT/11, Centre D'etndes Nucleaires de Grenoble (January, 1984).

(11) W.G. Mathers, R.L. Ferch, W.T. Hancox and B.H. Donald, "Equations for Transient Flow-Boiling in a Duct", Proc. 2nd CSNI Specialists Mtg., pp.59 (June 12-14, 1978 at Paris).

(12) G. Hondayer, B. Pinet and J. Vigneron, "HEXECO Code-A Six Equation Model", Proc. 2nd CSNI Specialists Mtg., pp.99 (June 12-14, 1978 at Paris).

(13) M. Ishii, "Thermo-Fluid Dynamic Theory of Two-Phase Flow", Eyrolles, Paris (1975).

(14) M. Ishii, "Two-Fluid Model and Hydrodynamic Constitutive Relations", Nucl. Engg. Design, Vol.82, pp.107 (1984).

(15) T. Yamanouchi, "General Kinetics" (Japanese), Iwanami (1951).

(16) H. Adachi and M. Okazaki, "Frictional Energy Dissipation in Two-Phase Flow", J. Nucl. Energy Soc. Japan, Vol.18, No.12, pp.786 (1976).

(17) J.G. Knudsen and D.L. Katz, "Fluid Dynamics and Heat Transfer", McGRAW–HILL (1958).

Appendix 1 Virtical Mass Force

When an object moves in a continuous fluid with a relative acceleration, a certain reaction force called virtual mass force (VMF) acts on the object. VMF is essentially the inertial force acts on the surrounding fluid which is accelerated by the object. That is, the external should act force on the object not only for accelerating the object itself but also for accelerating the surrounding fluid. VMF is transmitted to the object through the pressure distribution on the surface of the object.

Since VMF is an inertial force, all work done by the external overcoming VMF is converted to kinetic energy of the surrounding fluid, i.e., no energy dissipation occurs due to VMF. Therefore, even the perfect fluid without viscosity can realize VMF.

People often say the continuous phase of a two-phase flow acts VMF on the dispersed phase when there is a relative acceleration between two phases. In fact, flow of the continuous phase around the dispersed phase is supposed quite similar to the flow of the surrounding fluid in a usual VMF problem. However, VMF should not be introduced in equations of motion for two-phase flow. The reason is as follows.

In a usual VMF problem, VMF is balanced with a part of force acted by the external which is different from both the object and the surrounding fluid. From the view point of energy flow, kinetic energy increase of the surrounding fluid due to VMF acceleration should be given by the external. On the other hand, in the case of two-phase flow, the dispersed phase is accelerated by the surrounding continuous phase through pressure force. Although additional force to accelerate the continuous phase is necessary to relatively accelerate the dispersed phase, the force is given also by the continuous phase as a part of pressure force. Therefore, VMF effect should be already included in the usual relationship between pressure force and inertial force. From the view point of energy flow, kinetic energy increase of the continuous phase due to VMF effect is provided by spending pressure energy of the continuous phase itself. By this reason, VMF causes no energy dissipation.

If one introduces additional terms due to VMF into equations of motion for two-phase flow, invalid energy dissipation should appear as described below.

Let us represent VMF's per unit volume of gas and liquid phases with $F_{VM,g}$ and $F_{VM,l}$, respectively. Then, from Newton's third law,

$$\alpha F_{VM,g}+(1-\alpha)F_{VM,l}=0 \tag{A1-1}$$

Sum of the work which the gas phase does per unit volume of channel per unit time overcoming VMF and the work which the liquid phase is done by VMF effect per unit volume of channel per unit time is given by

$$\Delta E=\alpha u_g F_{VM,g}+(1-\alpha)u_l F_{VM,l} \tag{A1-2}$$

When $u_g \neq u_l$, ΔE of Eq. (A1-2) is never equal to zero because of Eq. (A1-1). That is, energy dissipation exists. This fact is inconsistent with the essence of VMF.

As well known through the above discussions, if one introduces additional terms due to VMF into equations of motion for two-phase flow, the VMF effect is taken into account duplicatedly and an invalid energy dissipation appears.

Appendix 2 Kinetic Energy Type Expression of Inertial Force Term for Single-Phase Flow

Transient and steady inertial force terms in equation of motion for single-phase flow are usually explained based on the momentum principle : (force) = (momentum change)/(elapsed time). However, this explanation can be translated into the explanation due to the kinetic energy principle : (force) = (kinetic energy change)/(traveled distance).

General expression of equation of motion for single-phase flow is written for z_1, z_2 and z_3 axis directions as follows:

$$\Sigma F_1=\rho\left(\frac{\partial u_1}{\partial t}+u_1\frac{\partial u_1}{\partial z_1}+u_2\frac{\partial u_1}{\partial z_2}+u_3\frac{\partial u_1}{\partial z_3}\right) \tag{A2-1}$$

$$\Sigma F_2=\rho\left(\frac{\partial u_2}{\partial t}+u_1\frac{\partial u_2}{\partial z_1}+u_2\frac{\partial u_2}{\partial z_2}+u_3\frac{\partial u_2}{\partial z_3}\right) \tag{A2-2}$$

$$\Sigma F_3=\rho\left(\frac{\partial u_3}{\partial t}+u_1\frac{\partial u_3}{\partial z_1}+u_2\frac{\partial u_3}{\partial z_2}+u_3\frac{\partial u_3}{\partial z_3}\right) \tag{A2-3}$$

Equation (A2-1) can be rearranged into form of kinetic energy change per unit volume of fluid during unit displacement in z_1 axis direction, i.e.,

$$\Sigma F_1=\frac{1}{2}\rho\frac{\partial(u_1^2)}{\partial t}\frac{1}{u_1}+\frac{1}{2}\rho\frac{\partial(u_1^2)}{\partial z_1}+\frac{1}{2}\rho\frac{\partial(u_1^2)}{\partial z_2}\frac{u_2}{u_1}+\frac{1}{2}\rho\frac{\partial(u_1^2)}{\partial z_3}\frac{u_3}{u_1} \tag{A2-4}$$

In this equation, coefficient $1/u_1$ in the first term converts the unsteady change of $\rho u_1^2/2$, which is a component of kinetic energy per unit volume of fluid with respect to z_1 axis, into the change per unit displacement in z_1 axis direction. Similarly, coefficients u_2/u_1 in the third term and u_3/u_1 in the fourth term convert the steady changes of $\rho u_1^2/2$ in z_2 or z_3 axis direction into the changes per unit displacement in z_1 axis direction, respectively. Therefore, total change of $\rho u_1^2/2$ during displacement dz_1 in z_1 axis direction is written as:

$$\frac{1}{2}\rho d(u_1^2)=\frac{1}{2}\rho\frac{\partial(u_1^2)}{\partial t}\frac{1}{u_1}dz_1+\frac{1}{2}\rho\frac{\partial(u_1^2)}{\partial z_1}dz_1+\frac{1}{2}\rho\frac{\partial(u_1^2)}{\partial z_2}\frac{u_2}{u_1}dz_1+\frac{1}{2}\rho\frac{\partial(u_1^2)}{\partial z_3}\frac{u_3}{u_1}dz_1 \tag{A2-5}$$

Therefore, Eq. (A2-4) can be written for displacement dz_1 in z_1 axis direction as:

$$\Sigma F_1 dz_1=\frac{1}{2}\rho d(u_1^2) \tag{A2-6}$$

Similarly, from Eqs. (A2-2) and (A2-3),

$$\Sigma F_2 dz_2=\frac{1}{2}\rho d(u_2^2) \tag{A2-7}$$

$$\Sigma F_3 dz_3=\frac{1}{2}\rho d(u_3^2) \tag{A2-8}$$

Since kinetic energy per unit mass of fluid is

$$e_K=\frac{1}{2}(u_1^2+u_2^2+u_3^2) \tag{A2-9}$$

summation of Eqs. (A2-6) through (A2-8) can be written as:

$$\Sigma(F_1dz_1+F_2dz_2+F_3dz_3)=\Sigma(\vec{F}\,\vec{dr}) \\ =\rho de_K \tag{A2-10}$$

Equation (A2-10) is no other than the expression with the kinetic energy principle : (force) × (traveled distance) = (kinetic energy change). That is, equations of motion for single-phase flow, Eqs. (A2-1) through (A2-3) for each direction, also can be said to be based on the kinetic energy principle.

The author's theory on two-phase flow based on the kinetic energy principle is, thus, not a heretic one but is established on the same basis of point-of-mass kinetics as in the theory of usual single-phase hydrodynamics.

Appendix 3 Definition of Frictional Force Terms

Interfacial frictional forces f_{GL} and f_{LG} which really act at the interface between two phases and wall frictional forces f_{GW} and f_{LW} which really act at the wall surface are given for unit volumes of gas and liquid phases, respectively, by using the average shear stress components in the flow direction $\tau_{GL}=-\tau_{LG}$, τ_{GW} and τ_{LW} and the average contact areas per unit volume of channel $S_{GL}=S_{LG}$, S_{GW} and S_{LW}, as follows:

$$f_{GL}=\frac{1}{\alpha}\tau_{GL}S_{GL} \tag{A3-1}$$

$$f_{LG}=\frac{1}{1-\alpha}\tau_{LG}S_{LG} \tag{A3-2}$$

$$f_{GW}=\frac{1}{\alpha}\tau_{GW}S_{GW} \tag{A3-3}$$

$$f_{LW}=\frac{1}{1-\alpha}\tau_{LW}S_{LW} \tag{A3-4}$$

The notation is illustrated in **Fig. A3-1**. Such definition of interfacial and wall frictional forces shall be called as "Definition I" in this report. The following two equations hold good generally.

$$\alpha f_{GL}+(1-\alpha)f_{LG}=\tau_{GL}S_{GL}+\tau_{LG}S_{LG}=0 \tag{A3-5}$$

$$\alpha f_{GW}+(1-\alpha)f_{LW}=\tau_{GW}S_{GW}+\tau_{LW}S_{LW}=f_W \tag{A3-6}$$

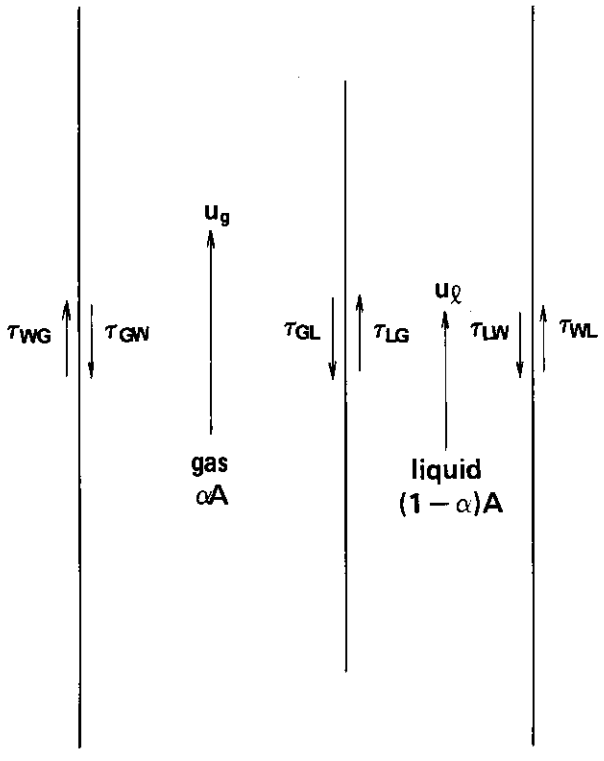

Fig. A3-1 Definition of shear forces.

Here, Eq. (A3-5) expresses Newton's third law and Eq. (A3-6) is definition equation of wall frictional force f_W. According to this definition, f_{GW} for annular two-phase flow should be zero because of $S_{GW}=0$.

Let us examine, e.g., annular two-phase flow in a horizontal pipe. Since velocity of the central gas core is higher than velocity of the peripheral liquid film, interfacial frictional forces f_{GL} and f_{LG} due to phase slip exist. However, the phase slip in this case is just in equivalent sense to velocity distribution in a cross section of single-phase flow. That is, f_{GL} and f_{LG} are no other than wall shear forces transmitted through the liquid film to the interface. Therefore, net frictional forces due to existence of wall should be:

$$F_{GW}=f_{GL} \tag{A3-7}$$

$$F_{LW}=f_{LW}+f_{LG} \tag{A3-8}$$

On the other hand, net interfacial frictional forces are:

$$F_{GL}=f_{GL}-f_{GL}=0 \tag{A3-9}$$

$$F_{LG}=f_{LG}-f_{LG}=0 \tag{A3-10}$$

because f_{GL} and f_{LG} have already been included in wall frictional forces F_{GW} and F_{LW}.

This is only the result for annular two-phase flow (or similar flow regime with wetted wall) in a horizontal pipe. In more general case, wall frictional forces transmitted to the interface, f_{GL}' and f_{LG}', are not the whole of f_{GL} and f_{LG}. Therefore,

$$F_{GW}=f_{GW}+f_{GL}' \tag{A3-11}$$

$$F_{GL}=f_{GL}-f_{GL}' \tag{A3-12}$$

$$F_{LW}=f_{LW}+f_{LG}' \tag{A3-13}$$

$$F_{LG}=f_{LG}-f_{LG}' \tag{A3-14}$$

Here, f_{GL}' and f_{LG}' are a couple of shear forces, therefore, by Newton's third law,

$$\alpha f_{GL}'+(1-\alpha)f_{LG}'=0 \tag{A3-15}$$

should hold good. Definition of interfacial and wall frictional forces expressed by Eqs. (A3-11) through (A3-14) shall be called as "Definition II" in this report.

By applying Eqs. (A3-5), (A3-6) and (A3-15) to Eqs. (A3-11) through (A3-14),

$$\alpha F_{GL}+(1-\alpha)F_{LG}=0 \tag{A3-16}$$

$$\alpha F_{GW}+(1-\alpha)F_{LW}\equiv F_W=f_W \tag{A3-17}$$

are obtained for Definition II. These equations are of the same form to Eqs. (A3-5) and (A3-6).

On the other hand, from Eqs. (A3-11) through (A3-14),

$$F_{GL}+F_{GW}=f_{GL}+f_{GW} \tag{A3-18}$$

$$F_{LG}+F_{LW}=f_{LG}+f_{LW} \tag{A3-19}$$

hold good. Since F_{GL}, F_{LG}, F_{GW} and F_{LW} appears in the basic equation set always in form of Eqs. (A3-16) through (A3-19), Definitions I and II are just equivalent to each other.

Relationship between Definitions I and II is, from the view point of basic equation set, not unique because Eq. (A3-17) can be derived from Eqs. (A3-16), (A3-18) and (A3-19). That is, since there are only three restriction conditions for determining four parameters of F_{GL} etc. from four parameters of f_{GL}, etc., there is one excess degree of freedom. This fact is easily understood in the case of equations of motion because F_{GL}, etc. appear purely in

form of Eqs. (A3-16) through (A3-19). However, in the case of equations of energy, F_{GL}, etc. appear in more complicated form. Therefore, the excess one degree of freedom shall be proven below.

In the equations of energy (Eqs. (80) and (81) in the text of Part I), frictional energy dissipation terms based on Definition I are, for gas and liquid phases:

$$-[\zeta_I\{\alpha u_g f_{GL}+(1-\alpha)u_l f_{LG}\}+\alpha u_g f_{GW}] \tag{A3-20}$$

$$-[(1-\zeta_I)\{\alpha u_g f_{GL}+(1-\alpha)u_l f_{LG}\}+(1-\alpha)u_l f_{LW}] \tag{A3-21}$$

On the other hand, in Definition II they are:

$$-[\zeta_I\{\alpha u_g F_{GL}+(1-\alpha)u_l F_{LG}\}+\alpha u_g F_{GW}] \tag{A3-22}$$

$$-[(1-\zeta_I)\{\alpha u_g F_{GL}+(1-\alpha)u_l F_{LG}\}+(1-\alpha)u_l F_{LW}] \tag{A3-23}$$

Equations (A3-22) and (A3-23) can be transformed, by using Eqs. (A3-11) through (A3-14), into:

$$-[\zeta_I\{\alpha u_g f_{GL}+(1-\alpha)u_l f_{LG}\}-\zeta_I\{\alpha u_g f_{GL}'+(1-\alpha)u_l f_{LG}'\}] -(\alpha u_g f_{GW}+\alpha u_g f_{GL}') \tag{A3-24}$$

$$-[(1-\zeta_I)\{\alpha u_g f_{GL}+(1-\alpha)u_l f_{LG}\}-(1-\zeta_I)\{\alpha u_g f_{GL}'+(1-\alpha)u_l f_{LG}'\}] -\{(1-\alpha)u_l f_{LW}+(1-\alpha)u_l f_{LG}'\} \tag{A3-25}$$

By adding together the latter terms of the first terms of Eqs. (A3-24) and (A3-25), one can obtain:

$$\zeta_I\{\alpha u_g f_{GL}'+(1-\alpha)u_l f_{LG}'\}+(1-\zeta_I)\{\alpha u_g f_{GL}'+(1-\alpha)u_l f_{LG}'\} =\alpha u_g f_{GL}'+(1-\alpha)u_l f_{LG}' \tag{A3-26}$$

By adding together the latter terms of the second terms of Eqs. (A3-24) and (A3-25),

$$-\{\alpha u_g f_{GL}'+(1-\alpha)u_l f_{LG}'\} \tag{A3-27}$$

As known from Eqs. (A3-26) and (A3-27), total energy dissipation is the same between Definitions I and II although the ratio of interfacial frictional energy dissipation and wall frictional energy dissipation is different. Therefore, if one selects ζ_I so as to make Eq. (A3-22) equal to Eq. (A3-20), then Eq. (A3-23) automatically becomes equal to Eq. (A3-21). This fact is valid for any given combination of f_{GL}' and f_{LG}' which are connected together by Eq. (A3-15). Therefore, one can determine ζ_I and complete the set of F_{GL}, F_{LG}, F_{GW} and F_{LW} for any given combination of f_{GL}' and f_{LG}'. This means that there is one excess degree of freedom about the set of F_{GL}, F_{LG}, F_{GW} and F_{LW}. The fact is the reason why the additional condition described by Eq. (105) can be applied to the perfectly settled two-phase flow in the text of Part I.

1. Introduction

In Part I of the present report, hydrodynamical basic equation set was completed for one-dimensional separated two-phase flow (two-fluid model) by strictly describing balance of mass, force (momentum) and energy without introducing any physical models on microscopic mechanism of phase change acceleration. In Part II, analytical results on high speed two-pase flows including two-phase critical flow shall be introduced as an application.

The author's basic equation set is characterized with handling of phase change inertial force terms. Since very large phase change occurs in a high speed two-phase flow within a short channel length, in other words within a short elapsed time, flow characteristics is essentially governed by phase change acceleration. On the other hand, frictional forces may be less important than the case of low speed two-phase flow. Therefore, high speed two-phase flow is one of the most suitable analytical object to verify the author's basic equation set. From such point of view, axial change of high speed two-phase flow from subcritical flow via critical flow to supercritical flow is analyzed in Chapter 2 of Part II for the most simple case without interfacial and wall frictions and without thermal non-equilibrium. And the results shall be compared with experimental knowledges in the literature.

When there is no wall friction, axial change of flow is caused by change of flow area and critical flow occurs at the throat of a converging-diverging nozzle where no axial change of flow area exists. In this case, axial pressure gradient is generally infinite. On the other hand, in a constant-flow-area channel axial change of flow is primarily caused by wall friction and acceleration pressure drop follows it. Critical flow occurs at the point where the ratio of frictional pressure drop to the total or accelerational pressure drop becomes zero. Actually, it realizes at the exit of constant-flow-area channel and pressure gradient becomes minus infinity. In such way, effect of wall friction on change of flow is different between converging-diverging nozzle and constant-flow-area channel, resulting in large difference in approaching process to the critical flow. Critical discharge flow through a constant-flow-area channel will be analized in Chapter 3 taking wall friction into account to demonstrate that the author's basic equation set can correctly predict such difference in approaching process to the critical flow.

Next, the author's basic equation set should be possible to describe two-component two-phase flow without phase change such as air-water two-phase flow if only phase change rate is fixed at zero. To confirm the predictability of such flow is very useful to judge validity of the form of the author's basic equation set. From such point of view, analytical result on two-component two-phase critical flow is introduced in Chapter 4.

Establishment of perfect set of balance equations gives us a general rule for analyzing two-phase flow. Since balance relationship is correctly described, disagreement between analysis and experiment directly indicates invalid assumptions or errors of constitutive equations. In Chapter 5, the effect of thermal non-equilibrium on two-phase critical discharge flow through a converging-diverging nozzle is studied by comparing theoretical and experimental results as such an example.

Futhermore, in Chapter 6, two-phase critical discharge characteristics of large sharp-edged orifice will be discussed from similar point of view. This study was performed as a part of ROSA-I Program[1] at Japan Atomic Energy Research Institute (JAERI) and gave us very useful information for thermal-hydraulic analysis on loss-of-coolant accident (LOCA) of

light water reactor (LWR).

Finally, in Chapter 7, an experimental analysis on wall frictional and interfacial frictional energy dissipations in a vertical air-water two-phase flow will be introduced. This study is not on two-phase critical flow but is very interesting because usefulness of perfectly settled assumption for one-dimensional two-phase flow is demonstrated.

These results indicate respectively the validity and wide applicability of the author's hydrodynamic basic equations for one-dimensional separated two-phase flow (two-fluid model). Rightness of the basic concept of the author's basic equations is proven and the large potential usability is demonstrated through these studies.

2. Saturated Two-Phase Critical Flow without Friction[2]

2.1 Introduction

Correct prediction of the discharge flow rate of reactor coolant from the breaks during postulated loss-of-coolant accident (LOCA) of a light water reactor (LWR) gives very important base for right prediction of thermal-hydraulic behaviors in the primary coolant system including core and those in reactor containment and for correct estimation of release of radioactive fission products to the environment.

It is well known that discharge flow rate from the breaks is governed by two-phase critical flow. Many theoretical analyses[3]-[12] were already published on two-phase critical flow and the agreement with experimental results seems not so poor. However, most of them are applied one or two critical flow conditions without proof, which are expected to hold good at the critical flow point only, to determine the local flow situation at the point. Therefore, it is impossible to understand the entire process of change of flow from subcritical flow via critical flow to supercritical flow by using such kinds of critical flow theories.

Basic equations used in those critical flow theories are supposed not always perfect. Perfectness of basic equation set can be judged by applying to various approaching process to the critical flow.

In the present report, axial change of two-phase flow is analyzed for various type approachings to the critical flow. Especially, in this chapter, saturated critical two-phase flow without friction will be analyzed as the most basic case.

Fundamental assumptions used in this chapter are the following seven:

(1) one-dimensional two-phase flow (two-fluid model)
(2) steady two-phase flow
(3) adiabatic two-phase flow
(4) gravitational force negligible
(5) interfacial frictional force negligible
(6) wall frictional force negligible
(7) saturated two-phase flow

2.2 Basic Equations

Basic equation set introduced in Part I of the present report is the most general one for one-dimensional separate two-phase flow. Let us simplify the basic equations by using the above assumptions (2) through (7) for convenience to critical flow analysis. In the simplification, typical combination of each equation introduced in Part I will be replaced with the equivalent set of more convenient equations for calculation.

2.2.1 Equations of motion

Equations of motion for one-dimensional two-phase flow are Eqs. (45) and (46) of Part I for unit mass of existing two-phase fluid and unit mass of flowing two-phase fluid, respectively, i.e.,

$$\left\{\beta\left(\frac{\partial u_g}{\partial t}+u_g\frac{\partial u_g}{\partial z}\right)+(1-\beta)\left(\frac{\partial u_l}{\partial t}+u_l\frac{\partial u_l}{\partial z}\right)\right\}+(u_g-u_l)\frac{\partial \beta}{\partial t}$$
$$+\frac{1}{2}(u_g{}^2-u_l{}^2)\frac{\partial \beta}{\partial z}+\left(\frac{\beta}{\rho_g}+\frac{1-\beta}{\rho_l}\right)\frac{\partial P}{\partial z}+g\cos\theta$$
$$-\left(\frac{\beta}{\rho_g}F_{GL}+\frac{1-\beta}{\rho_l}F_{LG}\right)-\left(\frac{\beta}{\rho_g}F_{GW}+\frac{1-\beta}{\rho_l}F_{LW}\right)=0 \tag{1}$$

$$\left\{x\left(\frac{\partial u_g}{\partial t}+u_g\frac{\partial u_g}{\partial z}\right)+(1-x)\left(\frac{\partial u_l}{\partial t}+u_l\frac{\partial u_l}{\partial z}\right)\right\}+(u_g-u_l)\frac{\partial x}{\partial t}$$
$$+\frac{1}{2}(u_g{}^2-u_l{}^2)\frac{\partial x}{\partial z}+\left(\frac{x}{\rho_g}+\frac{1-x}{\rho_l}\right)\frac{\partial P}{\partial z}+g\cos\theta$$
$$-\left(\frac{x}{\rho_g}F_{GL}+\frac{1-x}{\rho_l}F_{LG}\right)-\left(\frac{x}{\rho_g}F_{GW}+\frac{1-x}{\rho_l}F_{LW}\right)=0 \tag{2}$$

By the assumption (2), Eq. (1) can be transformed into an ordinary differential equation without transient terms. And by the assumptions (4), the gravitational force term is eliminated. Then,

$$\beta u_g\frac{du_g}{dz}+(1-\beta)u_l\frac{du_l}{dz}+\frac{1}{2}(u_g{}^2-u_l{}^2)\frac{d\beta}{dz}+\left(\frac{\beta}{\rho_g}+\frac{1-\beta}{\rho_l}\right)\frac{dP}{dz}$$
$$-\left(\frac{\beta}{\rho_g}F_{GL}+\frac{1-\beta}{\rho_l}F_{LG}\right)-\left(\frac{\beta}{\rho_g}F_{GW}+\frac{1-\beta}{\rho_l}F_{LW}\right)$$
$$=\frac{1}{2}\frac{d\{\beta u_g{}^2+(1-\beta)u_l{}^2\}}{dz}+\left(\frac{\beta}{\rho_g}+\frac{1-\beta}{\rho_l}\right)\frac{dP}{dz}-\left(\frac{\beta}{\rho_g}-\frac{1-\beta}{\rho_l}\right)F_W=0 \tag{3}$$

Here, in transformation from the first expression of Eq. (3) to the second expression, Newton's third law:

$$\frac{\beta}{\rho_g}F_{GL}+\frac{1-\beta}{\rho_l}F_{LG}=0 \tag{4}$$

and definition of wall frictional force:

$$\frac{\beta}{\rho_g}F_{GW}+\frac{1-\beta}{\rho_l}F_{LW}=\frac{F_W}{\alpha\rho_g+(1-\alpha)\rho_l}=\left(\frac{\beta}{\rho_g}+\frac{1-\beta}{\rho_l}\right)F_W \tag{5}$$

are used. The first expression of this equation is simple sum of the wall frictional forces for each phase but the third expression can be applied to the total two-phase flow only. In the case of Eq. (105) of Part I holds good, the third expression can be divided into the terms for each phase.

Similarly, from Eq. (2),

$$\frac{1}{2}\frac{d\{xu_g{}^2+(1-x)u_l{}^2\}}{dz}+\left(\frac{x}{\rho_g}+\frac{1-x}{\rho_l}\right)\frac{dP}{dz}-\left(\frac{x}{\rho_g}F_{GL}+\frac{1-x}{\rho_l}F_{LG}\right)$$
$$-\left(\frac{x}{\rho_g}F_{GW}+\frac{1-x}{\rho_l}F_{LW}\right)=0 \tag{6}$$

Here, Eq. (6) cannot be simplified by using Eqs. (4) and (5).

Equations (3) and (6) are the two independent equations of motion in this analysis. Let us transform these equations for convenience as follows. At first, pressure gradient in the second term of Eq. (3) shall be divided into two terms: one corresponds to the first term

expressing inertial forces and the other corresponds to the third term representing wall frictional forces. Then, Eq. (3) can be rewitten by using the fraction ξ_W of wall frictional pressure drop to the total pressure drop as follows:

$$\frac{1}{2}\frac{d\{\beta u_g^2+(1-\beta)u_l^2\}}{dz}+(1-\xi_W)\left(\frac{\beta}{\rho_g}+\frac{1-\beta}{\rho_l}\right)\frac{dP}{dz}=0 \tag{7}$$

By integrating Eq. (7) with respect to z,

$$\frac{1}{2}\{\beta u_g^2+(1-\beta)u_l^2\}+\int_{P_0}(1-\xi_W)\left(\frac{\beta}{\rho_g}+\frac{1-\beta}{\rho_l}\right)dP=0 \tag{8}$$

When $\xi_W=0$ because of the assumtion (6),

$$\frac{1}{2}\{\beta u_g^2+(1-\beta)u_l^2\}+\int_{P_0}\left(\frac{\beta}{\rho_g}+\frac{1-\beta}{\rho_l}\right)dP=0 \tag{9}$$

Similarly, let us divide the pressure gradient in the second term of Eq. (6) into two terms: one corresponds to the first term expressing inertial forces and the other corresponds to the third and fourth terms representing inerfacial and wall frictional forces, respectively. Then, Eq. (6) can be rewritten by using the fractionn ξ_T of total frictional pressure drop to the total pressure drop as follows:

$$\frac{1}{2}\frac{d\{xu_g^2+(1-x)u_l^2\}}{dz}+(1-\xi_T)\left(\frac{x}{\rho_g}+\frac{1-x}{\rho_l}\right)\frac{dP}{dz}=0 \tag{10}$$

By integrating Eq. (10) with respect to z,

$$\frac{1}{2}\{xu_g^2+(1-x)u_l^2\}+\int_{P_0}(1-\xi_T)\left(\frac{x}{\rho_g}+\frac{1-x}{\rho_l}\right)dP=0 \tag{11}$$

When $\xi_T=0$ because of the assumptions (5) and (6),

$$\frac{1}{2}\{xu_g^2+(1-x)u_l^2\}+\int_{P_0}\left(\frac{x}{\rho_g}+\frac{1-x}{\rho_l}\right)dP=0 \tag{12}$$

Equations (10) through (12) correspond to Eqs. (7) through (9) for unit mass of existing two phase fluid, respectively. In the present analysis, however, these equations will be transformed into the form of total energy conservation equation instead of direct use of them. In the case, independence from the equations of energy will be important problem. Therefore, this transformation will be performed after describing equations of energy and equations of continuity.

2.2.2 Equations of energy

Equations of energy for one-dimensional separate two-phase flow are Eqs. (80) and (81) of Part I, i.e.,

$$-\alpha\rho_g\frac{Dq_g}{Dt}-[\zeta_I\{\alpha u_g F_{GL}+(1-\alpha)u_l F_{LG}\}+\alpha u_g F_{GW}]+\xi_e Q_e$$

$$-Q_{IG}=0 \tag{13}$$

$$-(1-\alpha)\rho_l\frac{Dq_l}{Dt}-[(1-\zeta_I)\{\alpha u_g F_{GL}-(1-\alpha)u_l F_{LG}\}+(1-\alpha)u_l F_{LW}]$$

$$+(1-\zeta_e)Q_e-Q_{IL}=0 \tag{14}$$

Here,

$$\frac{Dq_g}{Dt}=\left(\frac{dh_g}{dP}-\frac{1}{\rho_g}\right)\left(\frac{\partial P}{\partial t}+u_g\frac{\partial P}{\partial z}\right) \tag{15}$$

$$\frac{Dq_l}{Dt}=\left(\frac{dh_l}{dP}-\frac{1}{\rho_l}\right)\left(\frac{\partial P}{\partial t}+u_l\frac{\partial P}{\partial z}\right) \tag{16}$$

By assumption (2), Eqs. (13) and (14) can be transformed into ordinary differential equations without transient terms, for $Q_e=0$ because of the assumption (3), as follows:

$$-\left(\frac{dh_g}{dP}-\frac{1}{\rho_g}\right)\alpha\rho_g u_g\frac{dP}{dz}-[\zeta_i\{\alpha u_g F_{GL}+(1-\alpha)u_g F_{LG}\}+\alpha u_g F_{GW}]$$
$$=Q_{IG} \tag{17}$$

$$-\left(\frac{dh_l}{dP}-\frac{1}{\rho_l}\right)(1-\alpha)\rho_l u_l\frac{dP}{dz}-[(1-\zeta_i)\{\alpha u_g F_{GL}+(1-\alpha)u_l F_{LG}\}$$
$$+(1-\alpha)u_l F_{LW}]=Q_{IL} \tag{18}$$

Since equations of energy are essentially for describing change of state for each phase, if the following equations are used based on the assumption (7), Eqs. (17) and (18) become not necessary for describing change of state, i.e.,

$$T_g=T_{sat}(P) \tag{19}$$

$$T_l=T_{sat}(P) \tag{20}$$

This situation corresponds to infinite interfacial heat transfer coefficient for each phase.

Although Eqs. (17) and (18) lose the meaning as equations of energy by using Eqs. (19) and (20), they are still necessary to determine Q_{IG} and Q_{IL} and calculate w by using Eq. (17) of Part I, i.e.,

$$w=\frac{Q_{IG}+Q_{IL}}{h_g-h_l} \tag{21}$$

Therefore, let us use Eqs. (19) and (20) as equations of energy and Eqs. (17) and (18) shall be used with including in equations of continuity.

2.2.3 Equations of continuity

Let us pick up the mass conservation equation (8) of Part I for total two-phase flow as one of the two independent equations of motion, i.e.,

$$A\frac{\partial}{\partial t}\{\alpha\rho_g+(1-\alpha)\rho_l\}+\frac{\partial}{\partial z}[A\{\alpha\rho_g u_g+(1-\alpha)\rho_l u_l\}]=0 \tag{22}$$

This equation becomes an ordinary differential equation by removing the transient term based on the assumption (2). And it is simplified by using the definition of mass velocity

$$G=\alpha\rho_g u_g+(1-\alpha)\rho_l u_l \tag{23}$$

The result is:

$$d(AG)=0 \tag{24}$$

or

$$AG=A_C G_C=\text{const.} \tag{25}$$

Here, A_C and G_C are flow area and mass velocity at the critical flow point, respectively.

Another one of the two independent equations of continuity is selected as follows:

$$A\frac{\partial}{\partial t}\{\alpha\rho_g-(1-\alpha)\rho_l\}+\frac{\partial}{\partial z}[A\{\alpha\rho_g u_g-(1-\alpha)\rho_l u_l\}]=2Aw \tag{26}$$

This equation is Eq. (9) of Part I.

Eliminating the transient term based on the assumption (2) and using the definition equation of quality

$$x=\frac{\alpha\rho_g u_g}{\alpha\rho_g u_g+(1-\alpha)\rho_l u_l} \tag{27}$$

one can get the following ordinary differentiation equation:

$$\frac{d}{dz}[AG\{x-(1-x)\}]=\frac{d}{dz}\{AG(2x-1)\}=2Aw \tag{28}$$

By applyign Eq. (24),

$$G\frac{dx}{dz}=w \tag{29}$$

On the other hand, by summing up Eqs. (17) and (18),

$$\begin{aligned}&-\left\{\left(\frac{dh_g}{dP}-\frac{1}{\rho_g}\right)\alpha\rho_g u_g+\left(\frac{dh_l}{dP}-\frac{1}{\rho_l}\right)(1-\alpha)\rho_l u_l\right\}\frac{dP}{dz}\\&-[\{\alpha u_g F_{GL}+(1-\alpha)u_l F_{LG}\}+\{\alpha u_g F_{GW}+(1-\alpha)u_l F_{LW}\}]\\&=Q_{IG}+Q_{IL}\end{aligned} \tag{30}$$

Equation (30) can be transformed, by using Eqs. (21) and (29), into

$$\begin{aligned}&-\frac{1}{(h_g-h_l)G}\left\{\left(\frac{dh_g}{dP}-\frac{1}{\rho_g}\right)\alpha\rho_g u_g+\left(\frac{dh_l}{dP}-\frac{1}{\rho_l}\right)(1-\alpha)\rho_l u_l\right\}\frac{dP}{dz}\\&-\frac{1}{(h_g-h_l)G}[\{\alpha u_g F_{GL}+(1-\alpha)u_l F_{LG}\}+\{\alpha u_g F_{GW}+(1-\alpha)u_l F_{LW}\}]\\&=-\frac{1}{h_g-h_l}\left\{\left(\frac{dh_g}{dP}-\frac{1}{\rho_g}\right)x+\left(\frac{dh_l}{dP}-\frac{1}{\rho_l}\right)(1-x)\right\}\frac{dP}{dz}\\&-\frac{1}{h_g-h_l}\left\{\left(\frac{x}{\rho_g}F_{GL}+\frac{1-x}{\rho_l}F_{LG}\right)+\left(\frac{x}{\rho_g}F_{GW}+\frac{1-x}{\rho_l}F_{LW}\right)\right\}\\&=\frac{dx}{dz}\end{aligned} \tag{31}$$

As known from Eq. (10), pressure drop $\xi_T(dP/dz)$ is due to interfacial and wall frictions and pressure drop $(1-\xi_T)(dP/dz)$ is due to acceleration. Therefore, let us transform Eq. (31) into

$$\begin{aligned}&-\frac{1-\xi_T}{h_g-h_l}\left\{\left(\frac{dh_g}{dP}-\frac{1}{\rho_g}\right)x+\left(\frac{dh_l}{dP}-\frac{1}{\rho_l}\right)(1-x)\right\}\frac{dP}{dz}\\&-\frac{\xi_T}{h_g-h_l}\left\{\left(\frac{dh_g}{dP}-\frac{1}{\rho_g}\right)x+\left(\frac{dh_l}{dP}-\frac{1}{\rho_l}\right)(1-x)\right\}\frac{dP}{dz}\\&-\frac{1}{h_g-h_l}\left\{\left(\frac{x}{\rho_g}F_{GL}+\frac{1-x}{\rho_l}F_{LG}\right)+\left(\frac{x}{\rho_g}F_{GW}+\frac{1-x}{\rho_l}F_{LW}\right)\right\}\\&=\frac{dx}{dz}\end{aligned} \tag{32}$$

Then, the first term of the left hand side gives quality change due to accelerational pressure drop and the sum of second and third terms gives quality change due to interfacial and wall frictional pressure drops. So, let us divide dx into $(dx)_a$ and $(dx)_f$ corresponding to the above two parts of pressure drop, then

$$\begin{aligned}(dx)_a &= -\frac{1-\xi_T}{h_g-h_l}\left\{\left(\frac{dh_g}{dP}-\frac{1}{\rho_g}\right)x+\left(\frac{dh_l}{dP}-\frac{1}{\rho_l}\right)(1-x)\right\}dP \\ &= -\frac{T_{sat}}{T_{sat}}\frac{1-\xi_T}{h_g-h_l}\left\{\left(\frac{dh_g}{dP}-\frac{1}{\rho_g}\right)x+\left(\frac{dh_l}{dP}-\frac{1}{\rho_l}\right)(1-x)\right\}dP \\ &= -\frac{T_{sat}}{h_g-h_l}(1-\xi_T)\{x\,ds_g-(1-x)ds_l\} \\ &= -\frac{1}{s_g-s_l}(1-\xi_T)\{x\,ds_g-(1-x)ds_l\} \qquad (33)\end{aligned}$$

$$\begin{aligned}(dx)_f &= -\frac{\xi_T}{h_g-h_l}\left\{\left(\frac{dh_g}{dP}-\frac{1}{\rho_g}\right)x+\left(\frac{dh_l}{dP}-\frac{1}{\rho_l}\right)(1-x)\right\}dP \\ &\quad -\frac{1}{h_g-h_l}\left\{\left(\frac{x}{\rho_g}F_{GL}+\frac{1-x}{\rho_l}F_{LG}\right)+\left(\frac{x}{\rho_g}F_{GW}+\frac{1-x}{\rho_l}F_{LW}\right)\right\}dz \\ &= -\frac{1}{h_g-h_l}\xi_T\{x\,dh_g+(1-x)dh_l\} \qquad (34)\end{aligned}$$

Here, in the transformations from the second expression to the third expression of Eq. (33) and also from the third expression to the fourth expression, Eqs. (19) and (20) are used. And the frictional force terms and the terms $\xi_T(x/\rho_g)\,dP$ and $\xi_T\{(1-x)/\rho_l\}dP$ are canceled to each other, resulting the last expression of Eq. (34).

Equations (33) and (34) indicate that pressure changes $(1-\xi_T)dP$ and $\xi_T\,dP$ are isentropic and isenthalpic, respectively.

Total change in x is expressed as:

$$\begin{aligned}dx &= (dx)_a+(dx)_f \\ &= \frac{x\,ds_g+(1-x)ds_l}{s_g-s_l}(1-\xi_T)-\frac{x\,dh_g+(1-x)dh_l}{h_g-h_l}\xi_T \qquad (35)\end{aligned}$$

In integral form,

$$\begin{aligned}x &= x_0-\int_{P_0}\frac{x\,ds_g+(1-x)ds_l}{s_g-s_l}(1-\xi_T) \\ &\quad -\int_{P_0}\frac{x\,dh_g+(1-x)dh_l}{h_g-h_l}\xi_T \qquad (36)\end{aligned}$$

Especially, when $\xi_T=0$,

$$x=\frac{\{x_0\,s_{g0}+(1-x_0)s_{l0}\}-s_l}{s_g-s_l} \qquad (37)$$

In this report, Eq. (36) or (37) will be used as an equation of continuity, as well as Eq. (25).

2.2.4 Transformation of equation of motion based on flowing mass

Equation of motion (6) for unit mass of flowing two-phase fluid shall be used after transformation to energy equation type instead of applying directly in the form of Eq. (11).

Since the third and fourth terms of Eq. (6) give frictional heat generation, the equation can be written as:

$$\frac{1}{2}d\{xu_g^2+(1-x)u_l^2\}+\left(\frac{x}{\rho_g}+\frac{1-x}{\rho_l}\right)dP$$
$$+T_{sat}d\{xs_g+(1-x)s_l\}=0 \tag{38}$$

From the general relation in thermodynamics,

$$\left(\frac{x}{\rho_g}+\frac{1-x}{\rho_l}\right)dP+T_{sat}d\{xs_g+(1-x)s_l\}$$
$$=d\{xh_g+(1-x)h_l\} \tag{39}$$

Therefore, Eq. (38) can be rewritten as:

$$\frac{1}{2}d\{xu_g^2+(1-x)u_l^2\}+d\{xh_g+(1-x)h_l\}=0 \tag{40}$$

In integral form,

$$\frac{1}{2}\{xu_g^2+(1-x)u_l^2\}+\{xh_g+(1-x)h_l\}=\{x_0h_{g0}+(1-x_0)h_{l0}\} \tag{41}$$

Equation (41) holds good regardless of energy dissipation.

Equation (40) is Eq. (95) in Part I excluded the transient terms, gravitational terms and external heating term and is essentially the conservation equation of the sum of kinetic energy and thermal energy. However, in this analysis, Eqs. (19) and (20) are already established. These equations describe the thermal energy changes of each phase for the case of infinite interfacial heat transfer coefficients but do not give any restrictions about the kinetic energy changes. Thereforce, Eq. (40) is independent from Eqs. (19) and (20). Information due to Eq. (40) in addition to Eqs. (19) and (20) is on kinetic energy change, and therefore, Eq. (40) actually acts in the basic equation set as an equation of motion. So that the integral form (41) shall be used in this analysis as the equation of motion for unit mass of flowing two-phase fluid.

2.3 Critical Discharge from High Pressure Reservoir

Let us analyze the critical discharge two-phase flow from the infinite high pressure reservoir through a frictionless channel with axially variable cross section to the infinite low pressure space as illustrated in **Fig. 1**, by using Eqs. (9), (41), (19), (20), (25) and (37). As described in the section 2.1, the most simple case without interfacial and wall frictions and also without thermal non-equilibrium shall be discussed. This critical discharge flow is quite simple but gives a firm basis to analize more complicated two-phase critical discharge phenomena. In addition, many practical problems related to two-phase critical flow can be solved under such simple assumptions as described later with the result of numerical calculation.

The high pressure reservoir conditions are assumed to be kept as

$$P=P_0,\quad x=x_0,\quad u_g=u_l=0 \tag{42}$$

By introducing $R=u_g/u_l$, u_g can be obtained from Eq. (41) as

$$u_g=\sqrt{\frac{2R^2[\{x_0h_{g0}+(1-x_0)h_{l0}\}-\{xh_g+(1-x)h_l\}]}{R^2x+(1-x)}} \tag{43}$$

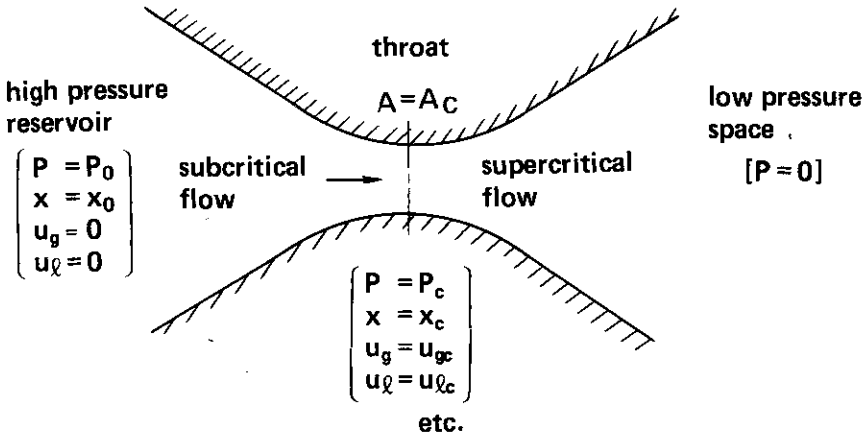

Fig. 1 Change of two-phase flow in a converging-diverging channel.

On the other hand,

$$u_l = \frac{u_g}{R} \tag{44}$$

β is expressed with x and R, as:

$$\beta = \frac{x}{x+(1-x)R} \tag{45}$$

Therefore,

$$R = \left(\frac{x}{1-x}\right)\left(\frac{1-\beta}{\beta}\right) \tag{46}$$

On the other hand, from Eq. (9),

$$\frac{1}{2}\{-(1-\beta)(u_g{}^2-u_l{}^2)+u_g{}^2\}+\int_{P_0}\left(\frac{\beta}{\rho_g}+\frac{1-\beta}{\rho_l}\right)dP=0 \tag{47}$$

So that,

$$1-\beta = \frac{\frac{1}{2}u_g{}^2+\int_{P_0}\left(\frac{\beta}{\rho_g}+\frac{1-\beta}{\rho_l}\right)dP}{\frac{1}{2}(u_g{}^2-u_l{}^2)} \tag{48}$$

Similarly, from Eq. (9),

$$\frac{1}{2}\{\beta(u_g{}^2-u_l{}^2)+u_l{}^2\}+\int_{P_0}\left(\frac{\beta}{\rho_g}+\frac{1-\beta}{\rho_l}\right)dP=0 \tag{49}$$

So that,

$$\beta = -\frac{\frac{1}{2}u_l{}^2+\int_{P_0}\left(\frac{\beta}{\rho_g}+\frac{1-\beta}{\rho_l}\right)dP}{\frac{1}{2}(u_g{}^2-u_l{}^2)} \tag{50}$$

By substituting Eqs. (48) and (50), Eq. (46) is rewritten as:

$$R=-\frac{x}{1-x}\frac{\frac{1}{2}u_g^2-\int_{P_0}\left(\frac{\beta}{\rho_g}+\frac{1-\beta}{\rho_l}\right)dP}{\frac{1}{2}u_l^2+\int_{P_0}\left(\frac{\beta}{\rho_g}+\frac{1-\beta}{\rho_l}\right)dP} \tag{51}$$

Two-phase critical discharge flow from the high pressure reservoir can be analyzed by using these equations as follows. At first, quality x after small pressure drop from the reservoir pressure is calculated for the given reservoir conditions (42) with Eq. (37). Next, u_g, u_l and β are calculated for the guessed value of R with Eqs. (43), (44) and (45), respectively. Corrected value of R is calculated with Eq. (51) by substituting these values. The calculation with Eqs. (43), (44) and (51) is iterated until R is converged. By using the resultant values of x and R, α is calculated with

$$\alpha=\frac{x\rho_l}{x\rho_l+(1-x)\rho_g/R} \tag{52}$$

Furthermore, G is calculated with Eq. (23). In these calculations, ρ_g, ρ_l, h_g and h_l are determined as functions of pressure in the channel with Eqs. (19) and (20). Flow diagram of these calculations are shown in **Fig. 2**.

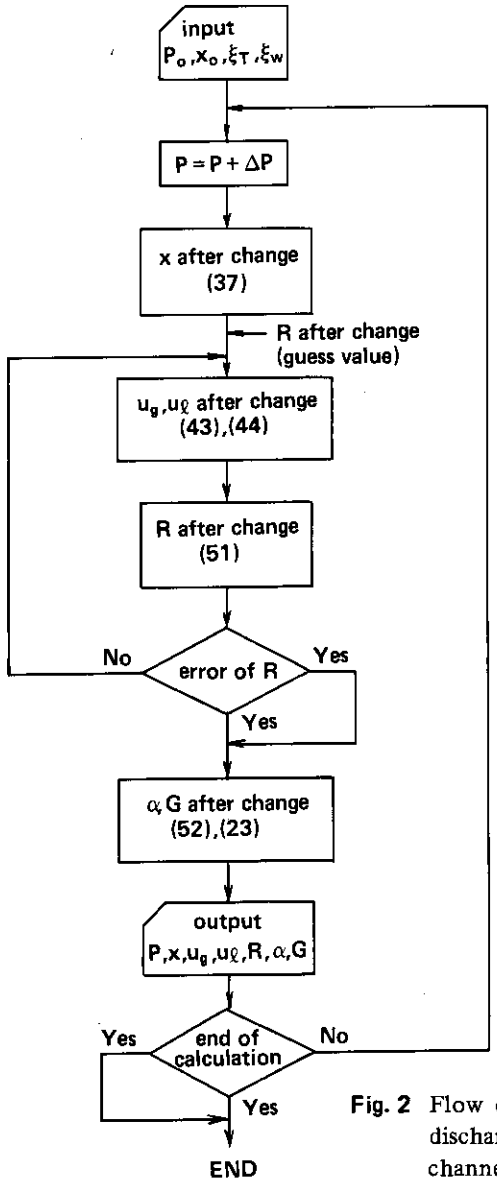

Fig. 2 Flow chart for calculation of two-phase critical discharge flow through a converging-diverging channel.

After determination of x, α, u_g, u_l, R, G etc. as functions of P by repeating the similar calculations, the critical pressure P_c and critical mass velocity G_c are determined with

$$\left.\frac{dG}{dP}\right|_{P_0,\ x_0}=0 \tag{53}$$

which represents the critical flow condition: G becomes the maximum with respect to P. The reason why Eq. (53) is used as the critical flow condition is that the critical flow is realized at the minimum flow area position (throat of the nozzle) under frictionless condition as explained in Appendix 1, where mass velocity is the maximum. Mass velocity at any cross section can be determined with Eq. (25). Since relationships between G and P and between P and any other variables are already uniquely determined for the given P_0 and x_0, all variables can be uniquely determined with respect to A.

G shows a convex characteristic with respect to P as illustrated in **Fig. 3**. The maximum point gives the critical flow. In the right side region with negative gradient, the smaller flow area the lower pressure, representing subcritical flow. In the left side region with positive gradient, on the other hand, the larger flow area the lower pressure, representing supercritical flow. Therefore, two-phase flow from subcritical via the critical to supercritical can be consistently analyzed with the method described previously.

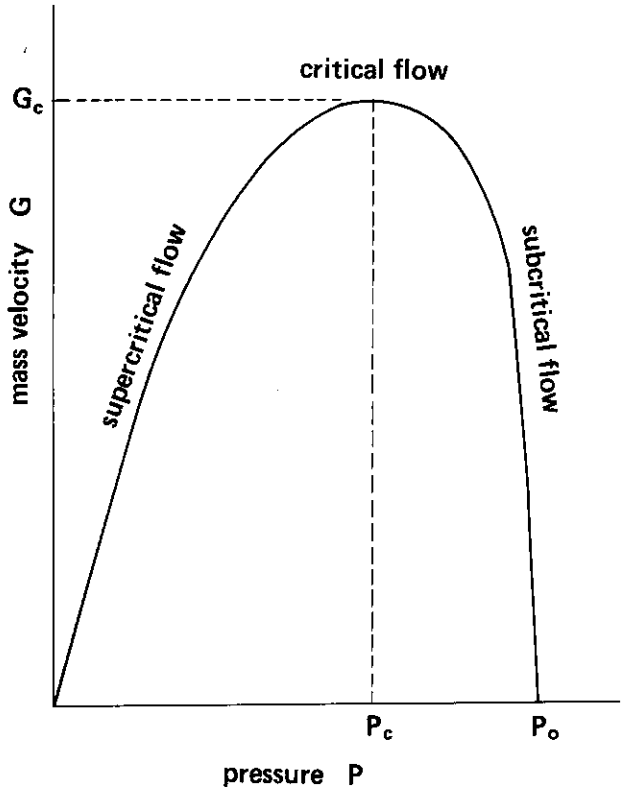

Fig. 3 G–P curve for two-phase critical discharge flow.

2.4 Calculation Results

Some numerical calculations were made on steam-water two-phase critical discharge by using the analytical method introduced in the previous section. The results are described below.

Shown in **Fig. 4** are gas phase velocity, liquid phase velocity and total mass velocity with respect to pressure in the channel, for reservoir pressure of 60 kg-f/cm² abs. and reservoir quality of 0.10. Quality, void fraction and slip ratio for the same calculation are also shown with respect to pressure in **Fig. 5**. As known from these figures, although gas and liquid phase velocities monotonously increase with decrease of pressure, mass velocity has the maximum point, indicating the critical flow phenomenon. Quality increases monotonously with decrease of pressure in this calculation but conversely decreases when reservoir quality is higher than about 0.5. Void fraction decreases in the initial acceleration process due to significantly large increase in slip ratio but increases after that because of increase in gas volume flow rate, indicating the concave characteristic resultantly. Such characteristic of void fraction can be seen in all reservoir conditions except for the case of which reservoir pressure is higher than 30 kg-f/cm² abs. and the reservoir quality is very close to zero.

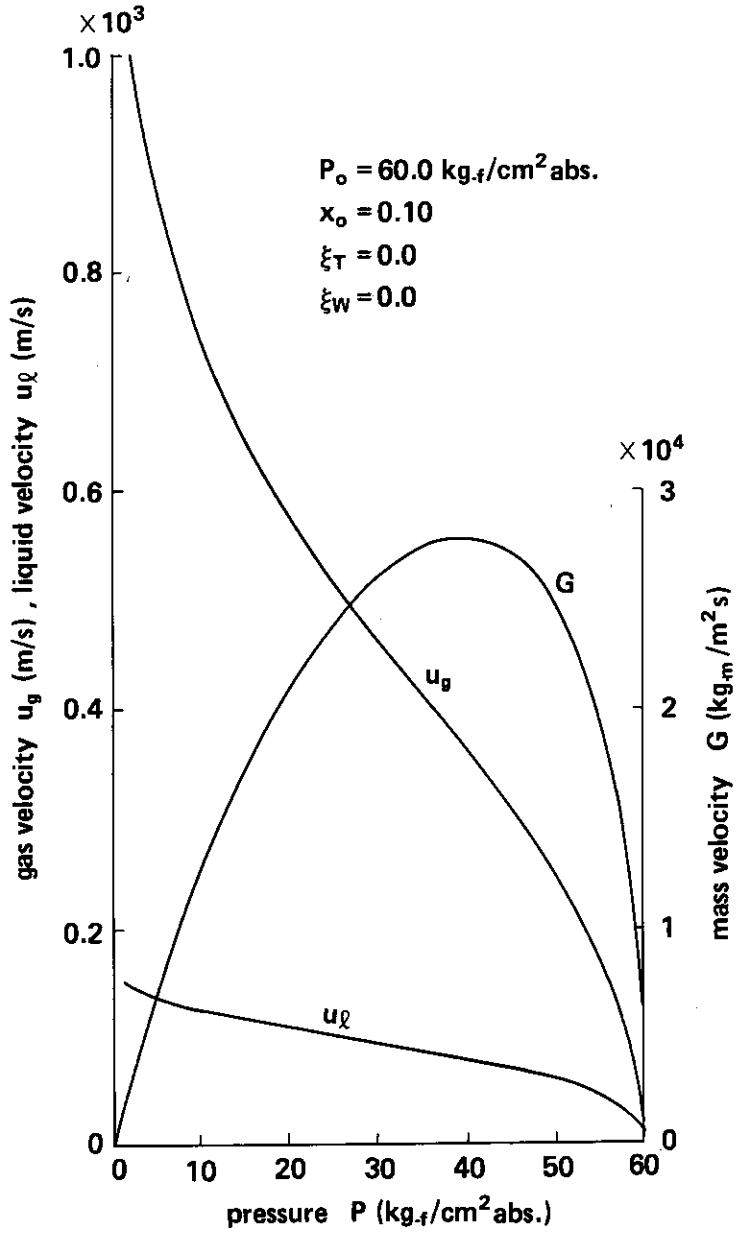

Fig. 4 Change of flow variables in two-phase critical discharge flow through a converging-diverging channel (1).

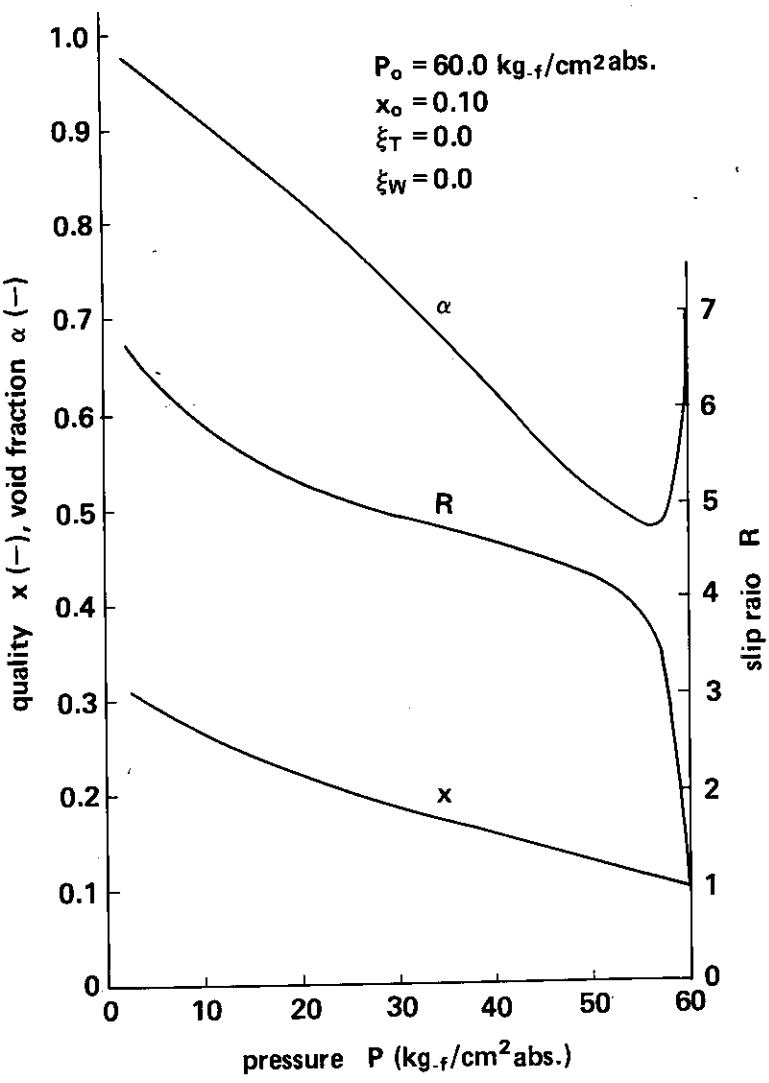

Fig. 5 Change of flow variables in two-phase critical discharge flow through a converging-diverging channel (2).

Figure 6 shows the relationship between pressure and mass velocity (G–P curve) along channel axis at various reservoir quality for reservoir pressure of 60 kg-f/cm² abs. The maximum points of each curve correspond to the two-phase critical flow. The critical pressure slightly decreases and the critical mass velocity decreases remarkably with increase in reservoir quality. The critical pressure is generally 0.5 ~ 0.8 times reservoir pressure as seen in this figure and it is almost consistent with Moody's theory[4]. Since the critical pressure for regular single-phase gas critical flow is about 0.5 times reservoir pressure, the two-phase critical pressure is generally higher than the single-phase critical pressure. This means hydrodynamic effect of compressibility is larger in two-phase flow than in single-phase flow.

Shown in **Fig. 7** is relationship between the critical pressure and the critical mass velocity with the critical quality as a parameter. This result is not so much different from the results by Fauske[3], Moody[4], Ogasawara[5]-[7] and Katto[8],[9]. Prediction of the critical mass velocity is not so much different generally among two-phase critical flow theories except very spacial theories such as the homogeneous two-phase flow model.

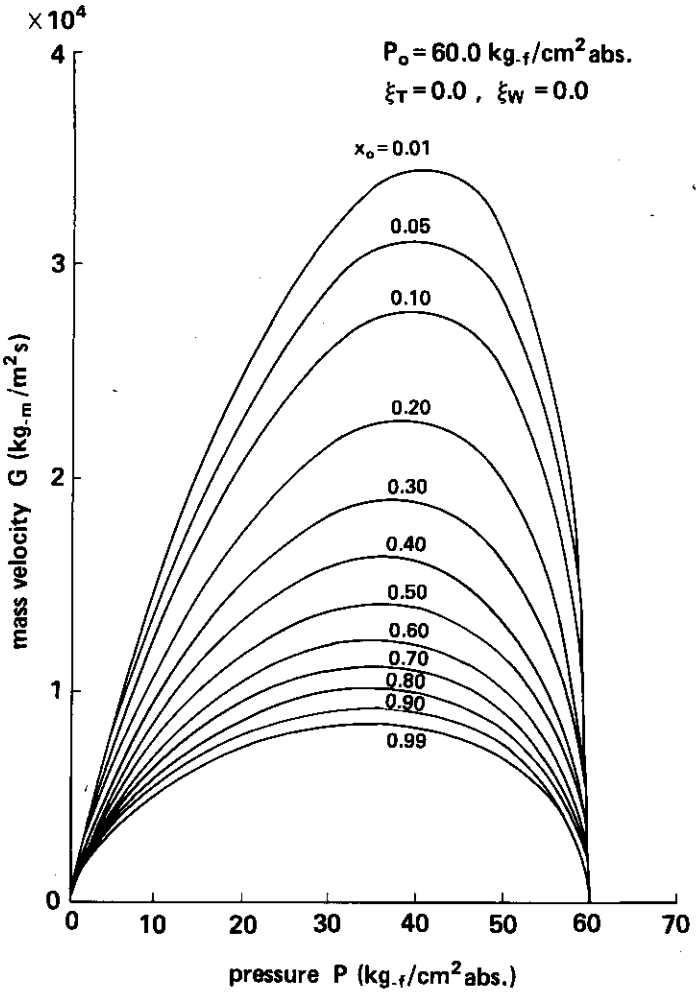

Fig. 6 Relationship between pressure and mass velocity changes in a converging-diverging channel.

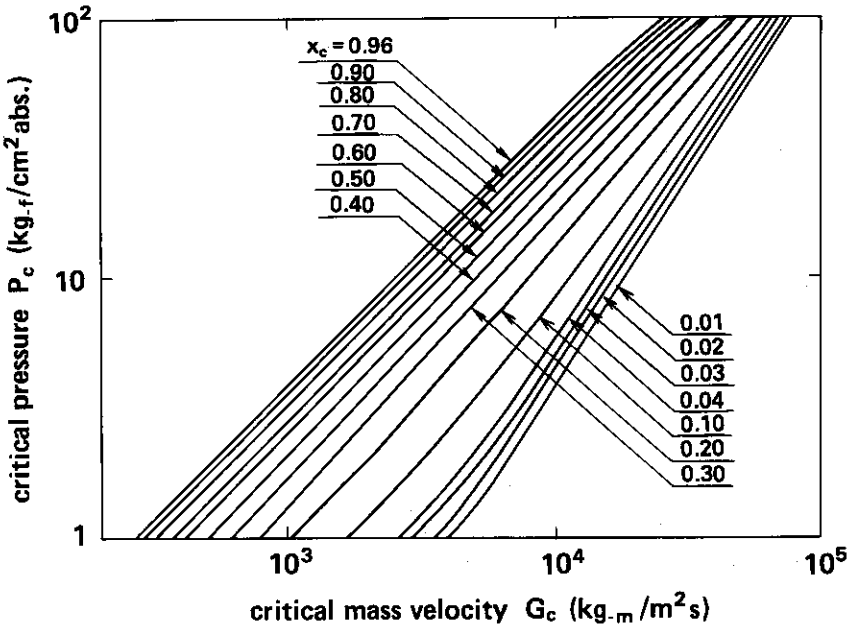

Fig. 7 Relationship among critical pressure, critical quality and critical mass velocity.

The critical mass velocity is shown in **Fig. 8** with respect to reservoir pressure and quality. Since reservoir conditions are given usually instead of the local conditions at the critical flow point, this figure is practically very useful. However, **Fig. 8** gives only the maximum critical mass velocity for the given reservoir conditions, neglecting the effect of acceleration process such as friction and thermal non-equilibrium. Therefore, physical generality is lower than **Fig. 7**.

Figure 9 shows the relationship between pressure and slip ratio along channel axis for varous reservoir quality for reservoir pressure of 60 kg-f/cm^2 abs. The chain line indicates the critical flow. The critical slip ratio is affected not only by the critical pressure but also by the critical quality in the author's theory as described later.

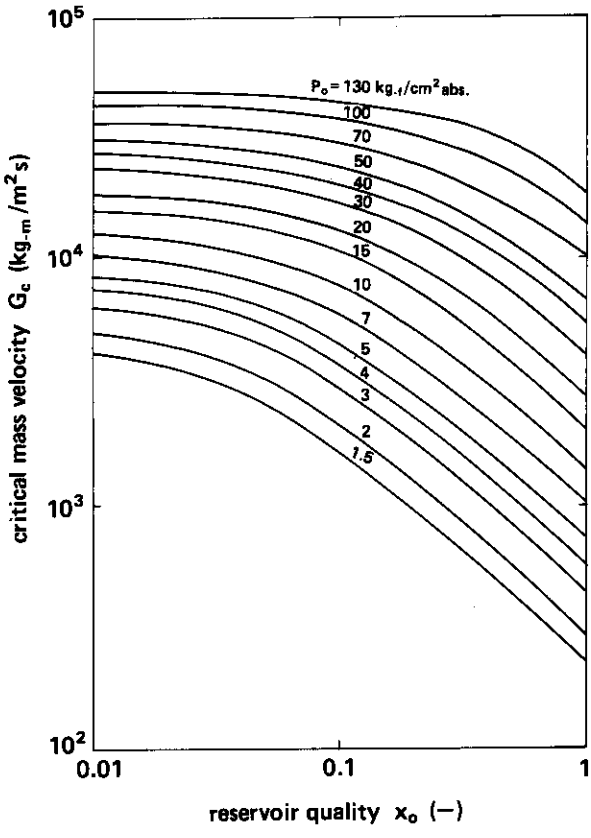

Fig. 8 Relationship between reservoir conditions and critical mass velocity.

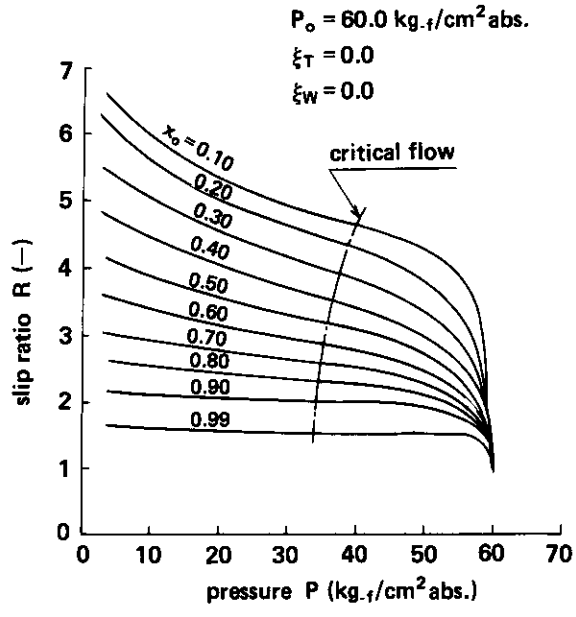

Fig. 9 Relationship between pressure and slip ratio changes in a converging-diverging channel.

2.5 Discussions

Validity of the calculation results introduced in the previous section will be discussed below.

Compared in **Fig. 10** are the calculated critical mass velocities with the author's theory and the measured critical mass velocities by Fauske[13], Falletti[14], Moy[15], and Cruz[16]. Data range compared is 0.7 ~ 25 kg-f/cm^2 abs. in the critical pressure and 0.01 ~ 0.91 in the critical quality. Agreement between the analysis and the experiments is very good.

However, theoretical prediction in the literature of the critical mass velocity is generally not so poor. Important are possibility of consistent analysis from subcritical flow via the critical flow to supercritical flow with physically clear method and the resultant possibility to validly predict the effect of acceleration process on the critical flow.

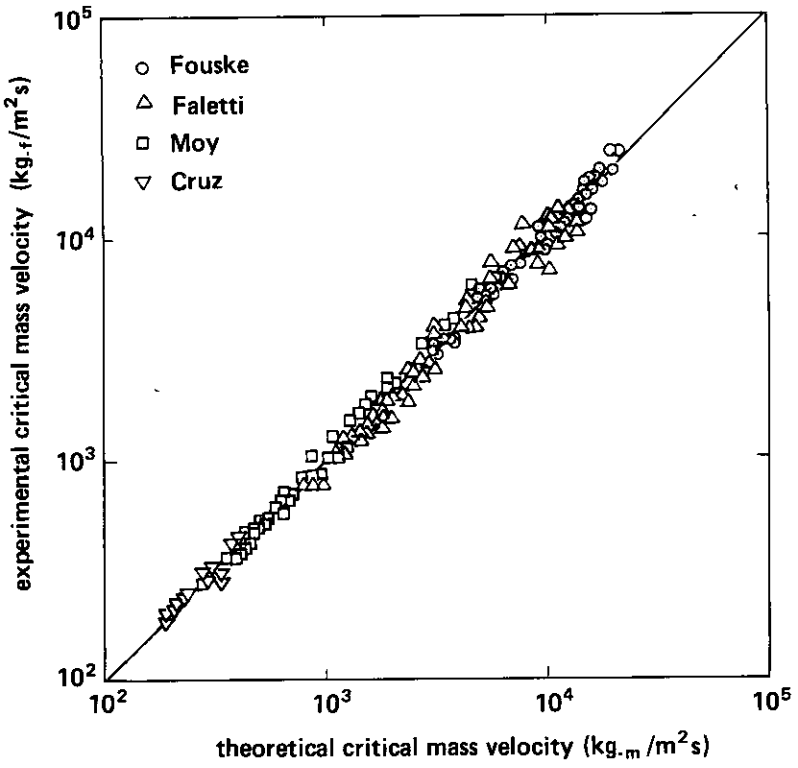

Fig. 10 Comparison between analytical and experimental critical mass velocities.

In the author's theory described in this chapter, pressure gradient at the critical flow point is not the maximum finite (in Fauske's theory) or negative infinite (in Ogasawara's theory) but undeterminate, i.e.,

$$\frac{dP}{dz}=\frac{dG/dz}{dG/dP}=\frac{0}{0}=\text{undeterminate} \tag{54}$$

This is due to the approaching processes to the critical flow, i.e., the flow is accelerated in this calculation by axial change of flow area and approaches to the critical flow. In such approaching, pressure gradient at the critical flow point is undeterminate even in single-phase flow as described in detail in Appendix 1.

Critical flow itself has no any restrictions about the pressure gradient at the critical flow point. It becomes negative infinite or finite depending only on difference in the approaching process. Since frictionless approach due to axial change of flow area was discussed in this chapter, the pressure gradient became undeterminate. If different type approach is examined, the different conclusion will be led because the author's theory has very wide applicability. An example of such cases shall be introduced in the next chapter.

Another feature of the author's critical flow theory is the critical slip ratio. Shown in **Fig. 11** is the relationship between the critical quality and the critical slip ratio for reservoir pressure of 60 kg-f/cm² abs. Here, the critical pressure is given by the author's theory and slightly decreases with the critical quality. Therefore, a small slope can be seen with respect to the critical quality even in the theories of Fauske and Moody in which the critical slip ratio is function of the critical pressure only.

As clearly seen in this figure, all theories except the author's one show the monotonously increasing characteristics. Only in the author's theory the critical slip ratio decreases with the critical quality. In the author's theory, phase change inertial forces act on each phase so

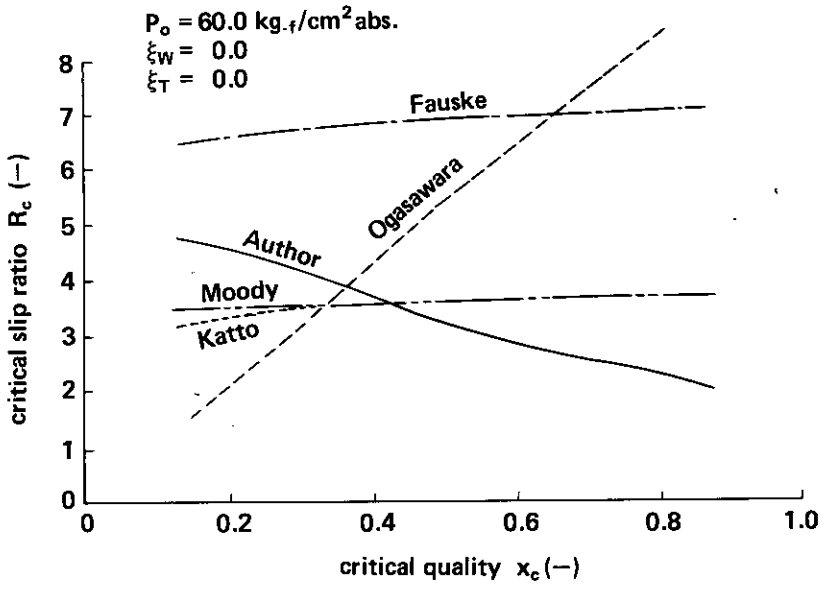

Fig. 11 Comparison among various theoretical critical slip ratios.

as to prevent from tremendous increase in slip ratio as described in Appendix 2. However, such effect is limited in a short initial stage of acceleration in a low quality case. On the other hand, in a high quality case, the effect can be seen until after the critical flow occurrence. This seems the reason why the author's theory shows the monotonously decreasing characteristic. This different characteristic of the author's theory from the others' is considered due to the different form of equations of motion.

2.6 Conclusions

Hydroydnamical basic equations for one-dimensional separated two-phase flow established in Part I of the present report were applied, in this chapter, to the saturated two-phase critical discharge phenomenon without friction. The results were compared with the experimental data and analytical results reported in the literature and the validity was evaluated. Major conclusions obtained are as follows:

(1) General basic equations are simplified and transformed into the critical flow analysis method to calculate the change of flow from subcritical flow via the critical flow to supercritical flow based on the seven fundamental assumptions introduced in the section 2.1.

(2) This analytical method gives good prediction about the critical mass velocity, the critical pressure, etc.

(3) The maximum critical mass velocity is given as function of reservoir pressure and quality by applying the analytical method and the seven fundamental assumptions.

(4) In this analysis, pressure gradient at the critical flow point is undeterminate. This is due to the approaching manner to the critical flow, i.e., the frictionless two-phase critical discharge flow accelerated by axial change of flow area has undeterminate pressure gradient at the critical flow point.

(5) The critical slip ratio monotonously decreases with the critical quality for the given reservoir pressure.

(6) Void fraction once decreases along flow axis and then increases except the case of which reservoir pressure is higher than 30 kg-f/cm² abs. and the reservoir pressure is very close to zero.

3. Saturated Two-Phase Critical Flow in a Constant-Flow-Area Channel[17]

3.1 Introduction

In this chapter, saturated two-phase critical discharge flow in a constant-flow-area channel is examined, which is considered the most popular case practically. In a variable-flow-area channel, change of frictionless flow can be thought, but in a constant-flow-area channel discussion ignoring friction is meaningless because the flow changes essentially due to wall friction. Consequently, the approaching to the critical flow is different from the case without friction. Therefore, to clarify two-phase critical flow in a constant-flow-area channel is no other than to clarify the effect of wall friction on two-phase critical flow phenomenon. The major discussion item in this chapter is whether or not the author's basic equations on one-dimensional two-phase flow introduced in Part I can reasonably predict such critical flow phenomenon with friction.

3.2 Calculation Method

In this chapter, the assumption (6) out of the seven fundamental assumptions introduced in Section 2.1 is eliminated. For the assumption (5), detailed discussion will be made later.

By this elimination, basic equations used in this chapter become Eqs. (8), (41), (19), (20), (25) and (36). Difference from the analysis in the previous chapter is that Eqs. (8) and (36) are used instead of Eqs. (9) and (37), respectively.

From this change, only Eq. (51) is changed as

$$R=-\frac{x}{1-x}\frac{\frac{1}{2}u_g{}^2+\int_{P_0}(1-\xi_w)\left(\frac{\beta}{\rho_g}+\frac{1-\beta}{\rho_l}\right)dP}{\frac{1}{2}u_l{}^2+\int_{P_0}(1-\xi_w)\left(\frac{\beta}{\rho_g}+\frac{1-\beta}{\rho_l}\right)dP} \tag{55}$$

because of change of integrated functions in Eqs. (47)~(50).

By making iteration calculations of Eqs. (36), (43), (44), (45) and (55) with using Eqs. (19) and (20), change of frictional two-phase flow with respect to pressure change along the flow axis can be analyzed.

Here, for simplicity, the flow is assumed to be perfectly settled. Then, from Eq. (105) in Part I,

$$F_{GW}=F_{LW}=F_W \tag{56}$$

And, for horizontal channel without gravitational effect,

$$F_{GL}=F_{LG}=0 \tag{57}$$

because of Eqs. (107) and (108) in Part I*.

As known from the comparison between Eqs. (3) and (7),

* Equation (57) does not mean no interfacial frictional forces but means no more interfacial frictional forces than the wall frictional forces transmitted to the interface.

$$\xi_W \frac{dP}{dz} = F_W \tag{58}$$

On the other hand, from the comparison between Eqs. (6) and (10) under the condition of Eqs. (56) and (57),

$$\xi_T \frac{dP}{dz} = F_W \tag{59}$$

Thus, in the perfectly settled one-dimensional two-phase flow,

$$\xi_W = \xi_T \equiv \xi \tag{60}$$

That is, in the perfectly settled horizontal two-phase flow, interfacial frictional forces can be expressed with Eq. (57) and, in such case, Eq. (60) holds good, if only wall frictional force is defined with Definition II in Appendix 3 of Part I.

3.3 Flow change with Respect to Pressure

Flow change in a constant-flow-area channel, of which upstream end is connected to infinitely large high pressure reservoir and the downstream end to infinitely large low pressure space as shown in **Fig. 12**, is investigated below. Here, pressure and quality in the high pressure reservoir are assumed to be kept at constants, respectively.

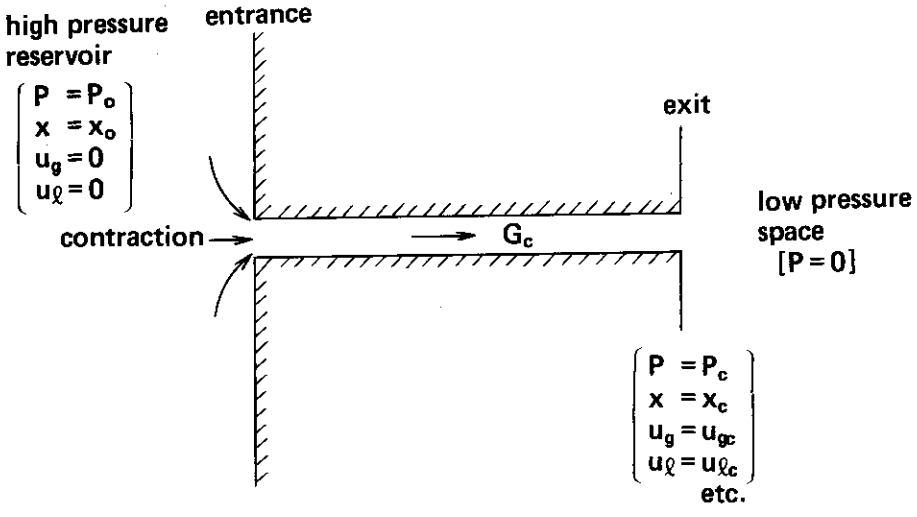

Fig. 12 Two-phase critical discharge through a constant-flow-area channel.

Before introducing the condition of constant flow area, G–P curve calculations similar to those in the previous chapter are made with ξ as a parameter. The result is shown in **Fig. 13**. Here, the reservoir pressure and quality are 60 kg-f/cm² abs. and 0.10, respectively, and ξ is parameterically changed from 0 to 0.9.

In a constant-flow-area channel, flow is characterized by

$$G = G_c = \text{const.} \tag{61}$$

That is, the trace should be a horizontal straight line on **Fig. 13**, e.g., straight line c(or b)-d for $G = 2.0 \times 10^4$ kg-m/m²s. In the contraction region toward the channel inlet, the flow changes along the line a-b of $\xi = 0$ and the point b corresponds to the channel inlet if friction in the contraction region is negligible. If the friction is not negligible, the flow changes along

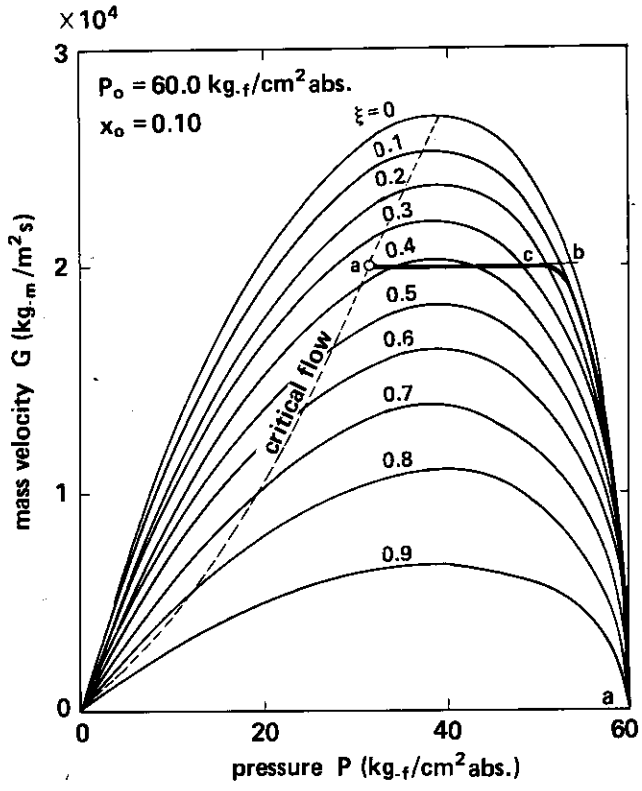

Fig. 13 Effect of ξ on G–P curve.

the thick line a-c and the point c corresponds to the channel inlet. The point d represents the critical flow and flow left side of this point is impossible in the constant-flow-area channel (Detailed discussion will be made later.). The straight line c(or b)-d crosses over many constant ξ lines, suggesting change of local value of ξ in the channel.

Based on the results shown in **Fig. 13**, relationship between integrated total pressure drop

$$\Gamma = -\int_{P_0} dP = P_0 - P \tag{62}$$

and integrated frictional pressure drop

$$\Gamma_{TPF} = -\int_{P_0} dP_{TPF} = (P_0 - P)\xi \tag{63}$$

is determined as shown in **Fig. 14**. The thick line a-c-d and point b in this figure correspond to those in **Fig. 13**.

The right side of the maximum point of each line indicate the negative friction characteristics which cannot be realized. Therefore, flow cannot go across the maximum point from left to right and the maximum point can be realized only at the channel exit.

The maximum point of each line corresponds to the two-phase critical flow. This is explained in more detail below.

Subcritical discharge flow is expressed by, e.g., the line 1-2 (channel exit) on the $\Gamma - \Gamma_{TPF}$ plane as shown in **Fig. 15**. If back pressure is decreased with holding the reservoir conditions, mass velocity increases and the flow situation moves to the lower curves such as the line 1'-2' (channel exit). Trace of the change of channel exit flow 2-2'-2" meets to the maximum Γ_{TPF} line 3-4 at the point 2". Since the line 3-4 has monotonously increasing characteristic, it is impossible to move to the lower curve by decreasing of channel exit pressure*. Therefore,

* If the line 3-4 has monotonously decreasing characteristic, channel exit flow can move to lower curve along the line.

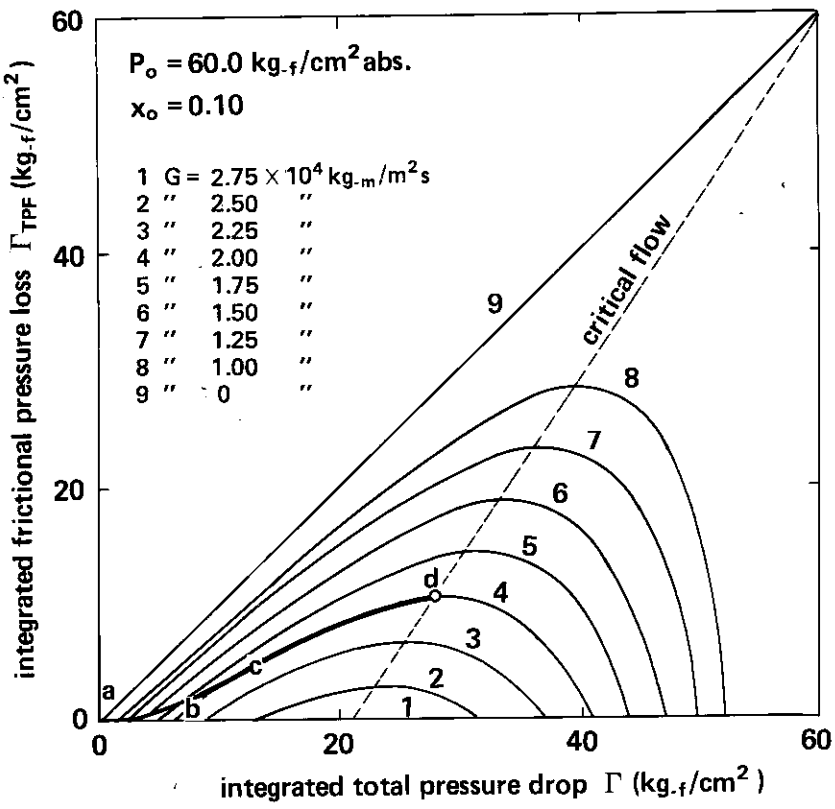

Fig. 14 Characteristics of frictional pressure drop in a constant-flow-area channel.

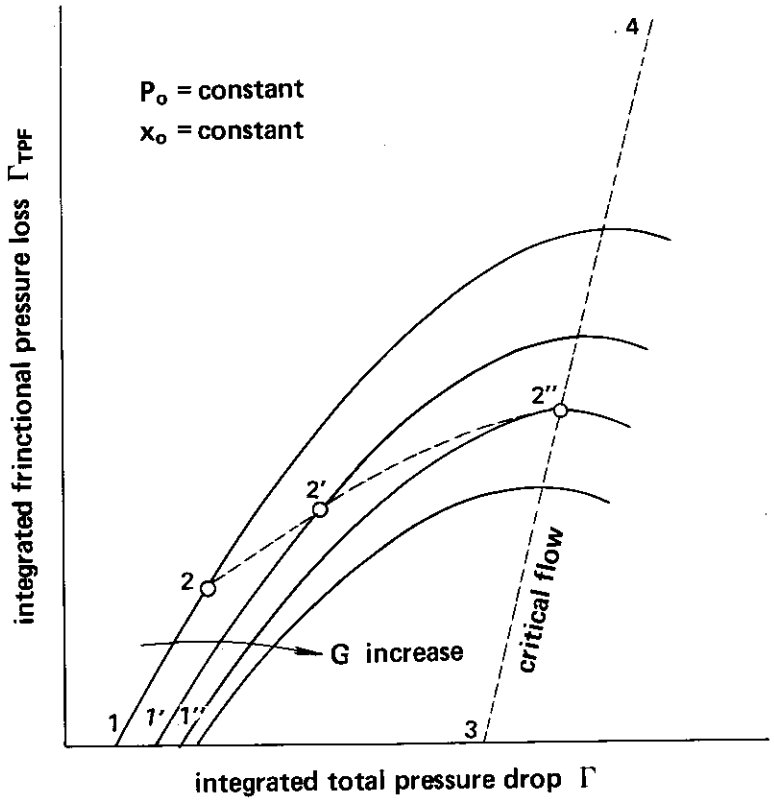

Fig. 15 Occurrence of critical flow at the exit of constant-flow-area channel.

mass velocity of the line 1"-2" gives the maximum mass velocity for the given reservoir conditions, i.e., it is no other than the critical mass velocity. Horizontal axis of the point 2" gives the critical pressure.

Through these discussions, the maximum Γ_{TPF} line of **Fig. 14** is considered the critical flow line. The corresponding curve shown in **Fig. 13** with dashed line gives the relationship between the critical pressure and the critical mass velocity for the given reservoir conditions. The maximum critical mass velocity corresponds to the frictionless case described in the previous chapter and the minimum critical velocity of zero (the origin of **Fig. 13**) corresponds to the discharge flow through a capillary. **Figure 16** shows the relationship between the critical pressure and the critical mass velocity for 60 kg-f/cm² abs. reservoir pressure with reservoir quality as a parameter.

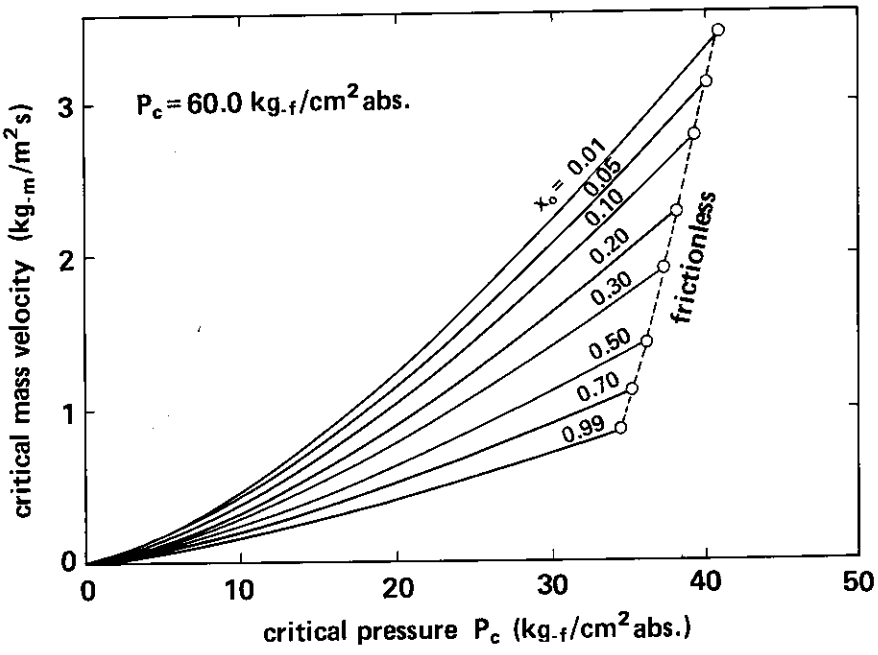

Fig. 16 Relationship between critical pressure and critical mass velocity for various reservoir conditions.

The relationships between pressure and the other variables in the channel have been already determined generally for given constant ξ by using the calculation method described in the previous section. Therefore, one can determine the relationships for constant-flow-area channel by selecting the solutions satisfying Eq. (61). On the other hand, local $\bar{\xi}$, ξ_P, can be determined with respect to P by using

$$\xi_P \equiv \frac{dP_{TPF}}{dP} = \frac{d\Gamma_{TPF}}{d\Gamma}\bigg|_{P_0,\ x_0,\ G} \tag{64}$$

Figs. 17 and **18** were obtaind with such method for reservoir pressure of 60 kg-f/cm² abs., reservoir quality of 0.1 and the critical mass velocity G_c of 0.7 times critical mass velocity G_{c_0} without wall friction. Frictional loss in the flow contraction region was neglected.

Mass velocity is constant along the flow axis because of constant flow area channel. Gas and liquid velocities monotonously increase with decreasing pressure and the critical flow realizes.

When reservoir quality x_0 is small, quality x increases monotonously with decreasing pressure as seen in this example but in large x_0, x decreases monotonously (x_0 at the boundary

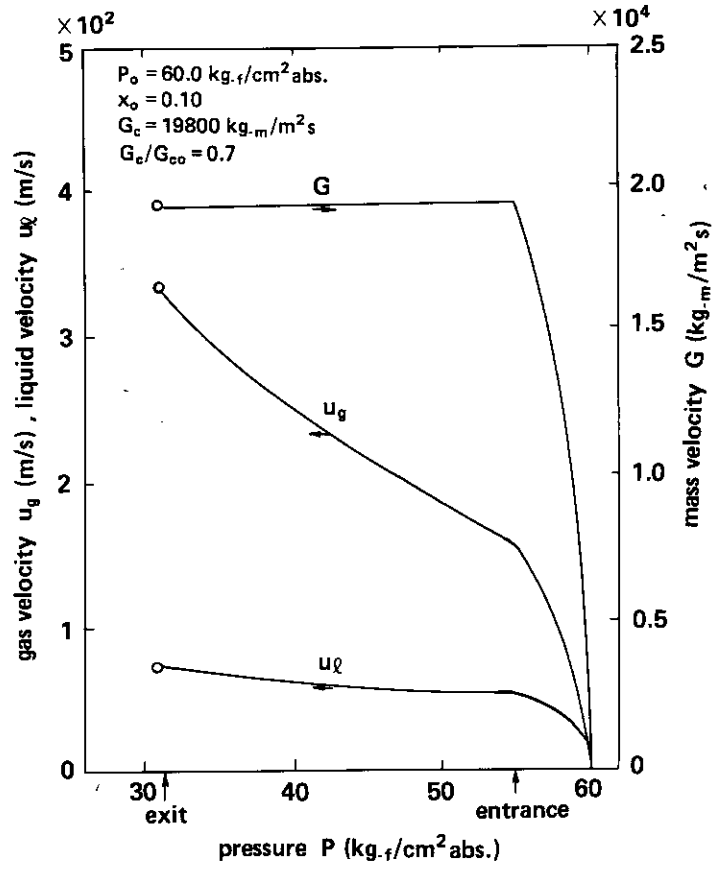

Fig. 17 Change of flow variables in two-phase critical discharge flow through a constant-flow-area channel (1).

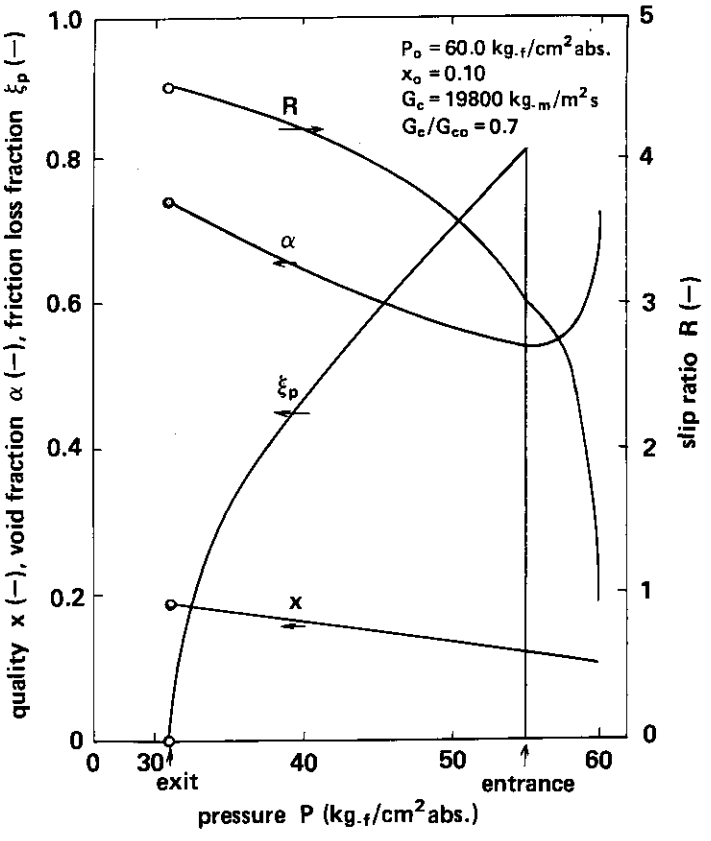

Fig. 18 Change of flow variables in two-phase critical discharge flow through a constant-flow-area channel (2).

between the increasing region and the decreasing region is affected by mass velocity G_C.). Although slip ratio increases significantly with decreasing pressure, void fraction in this example increases monotonously in the constant-flow-area channel. However, when G_C/G_0 is small, α once decreases and then increases in the channel, showing the minimum α point. This characteristic is remarkable when reservoir pressure is low. In such case, liquid velocity u_l also once decreases and increases after that. This phenomenon is due to movement of the minimum α point from the flow contraction region to the channel.

Local frictional pressure drop fraction ξ_P is zero in the high pressure reservoir in this calculation because of neglecting frictional pressure loss in the flow contraction region. However, in the constant-flow-area channel, ξ_P decreases with decreasing pressure within $0<\xi_P<1$. As already described in the explanation of **Fig. 14**, the maximum Γ_{TPF} point, i.e., $\xi_P=0$, gives the critical flow. That is, frictional effect locally disappears in the critical flow at the channel exit. This corresponds to the limiting situation without forced change of flow which was pointed out by Katto[18]. Appendix 1 will describe this point in more detail.

3.4 Axial Change of Each Variable

In this section, general method to correlate pressure change with axial location is described. If this is possible, axial distribution of all variables of flow can be predicted.

Two-phase frictional pressure drop is expressed, from the classic Martinelli-Lockhart's[19] research, in the form of

$$\frac{\Delta P_{TPF}}{\Delta P_0}=f(P, x) \tag{65}$$

Here, two-phase multiplier $\Delta P_{TPF}/P_0$ in Eq. (65) is defined as, e.g., the ratio of the two-phase frictional pressure drop to the pressure drop for single-phase water flow with the same mass velocity. ΔP_0 is expressed by

$$\Delta P_0=-\lambda\frac{L}{D}\frac{\rho_l u_{l0}^2}{2} \tag{66}$$

and single-phase pressure loss coefficient λ can be estimated by, e.g., Blasius' equation[20].

Therefore, by using ξ_P from Eq. (64), pressure drop dP corresponding to distance dz is given as

$$dz=-\frac{2D\xi_P}{\lambda\rho_l u_{l0}^2 f(P, x)}dP \tag{67}$$

Each variable in Eq. (67) can be expressed, by using the result of the previous section, as function of pressure only for the given combination of P_0, x_0 and G_C. Therefore, numerical integration of Eq. (67) can give the relationship between z and P.

This method can be applied even if correlation of two-phase frictional pressure loss is different from Eq. (65). In addition, it must be noted that the result of analysis in this section is directly affected by the two-phase frictional pressure loss correlation used, on the other hand, the discussion until the previous section is more general because only the basic equations are used.

Shown in **Fig. 19** is an example of the results obtained with Martinelli-Nelson's[21] two-phase multiplier. Frictional pressure loss in the flow contraction region is neglected in this calculation (If it is not negligible, the curves should be shifted to left by some distance.). From this figure, it is known that the length of a 100 mm diameter circular pipe in which

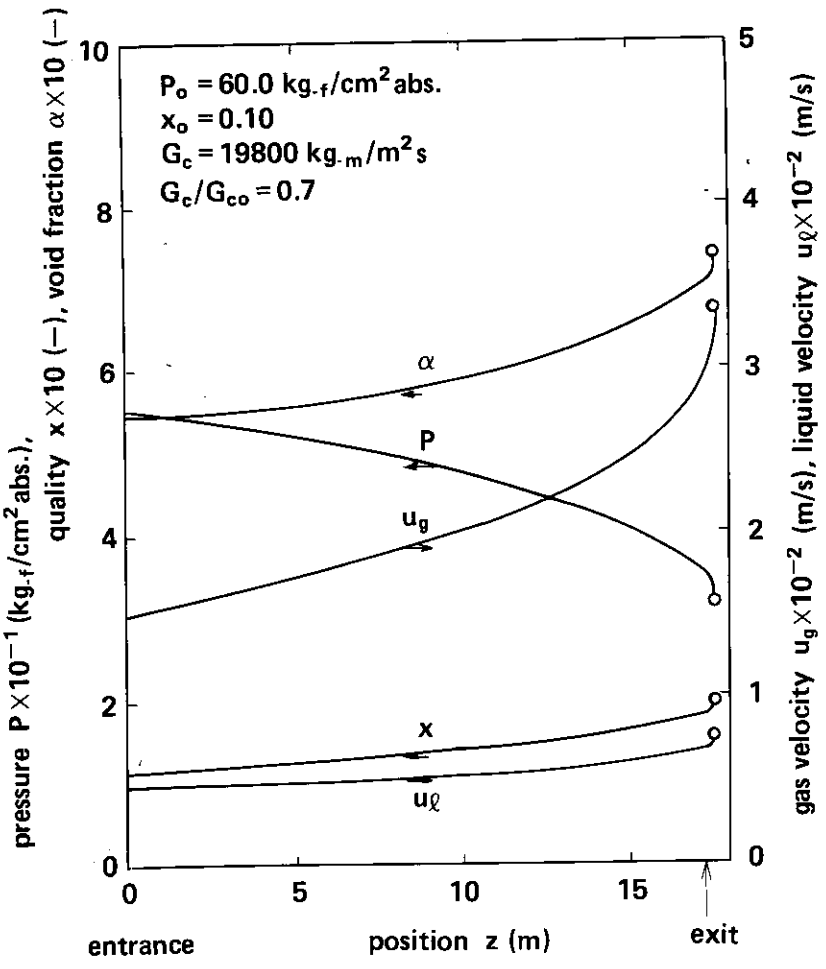

Fig. 19 Example calculation of axial changes of flow variables for two-phase critical discharge through a constant-flow-area channel.

the critical mass velocity is 19,800 kg-m/m²s (0.7 times that for without friction case) for reservoir pressure of 60 kg-f/cm² abs. and reservoir quality of 0.1 is 17.66 m. In this figure, pressure P decreases monotonously and quality x, void fraction α, gas phase velocity u_g and liquid phase velocity u_l increase monotonously and each valiable has an infinite gradient at the channel exit, i.e., the critical flow point. In fact, the infinite gradients of each variable can be theoretically derived as described in the next section.

As already pointed out in the previous section, when reservoir quality is sufficiently high, quality x decreases monotonously. And when reservoir pressure is low, void fraction once decreases and increases after that, showing the minimum point. Even if in high P_0, such behavior is seen in small G_c/G_{c0}. In such case, liquid phase velocity u_l also shows the minimum point.

3.5 Discussions

To verify the validity of the author's theory on two-phase critical discharge flow in a constant flow area channel, comparison of the analysis results with Ogasawara's[22] saturated water discharging experimental results was made.

9.0 mmϕ×1,300 mmL circular pipe was used in the Ogasawara's experiment. The reservoir pressure was lower than 30 kg-f/cm² abs. and the reservoir quality was assumed to be zero although no data were available.

Compared in **Fig. 20** is the calculated and the measured critical pressures. Satisfactory agreement is obtained although the calculated critical pressure is about 8% lower in the maximum than the measured one. Since the experimental value was determined with linear extrapolation from upstream side, the critical pressure should be overestimated. Taking this fact into account, the critical pressure should be overestimated. Taking this fact into account, the author's theory can be considered to more accurately agree with the experimental data than **Fig. 20.**

Calculated axial pressure distribution with Martinelli–Nelson's two-phase multiplier is compared with the measured one in **Fig. 21**. Since frictional pressure loss in the flow contraction region was unknown, the calculation was made at first neglecting the pressure loss and then the resultant curve was shifted to left so as to meet the upstream most data point.

The calculated channel length for realizing the critical flow agrees well with the experimental pipe length (= 1,300 mm) but the pressure distributions are evidently different to each other. That is, calculated pressure is lower in most length of the channel but it becomes opposite near the exit because of very steep pressure drop in the experiment.

According to Baroczy[23] Martinelli-Nelson's two-phase multiplier overestimates the frictional pressure loss of high mass velocity two-phase flow. However, Baroczy's two-phase multiplier seems to have inconsistency in the mass velocity effect. Therefore, Yamazaki's[24] correlation

$$\frac{dP_{TPF}}{dz} = -\lambda \frac{1}{D} \frac{\rho_l u_l^2}{2} \tag{68}$$

is applied, i.e., frictional pressure loss for single-phase water flow with the same liquid velocity is considered to be the two-phase frictional pressure loss. The result of comparison between the calculated and measured pressure distributions is shown in **Fig. 22**. The characteristic of the inlet side of the channel is much improved but very steep pressure drop near the channel exit still cannot be reproduced.

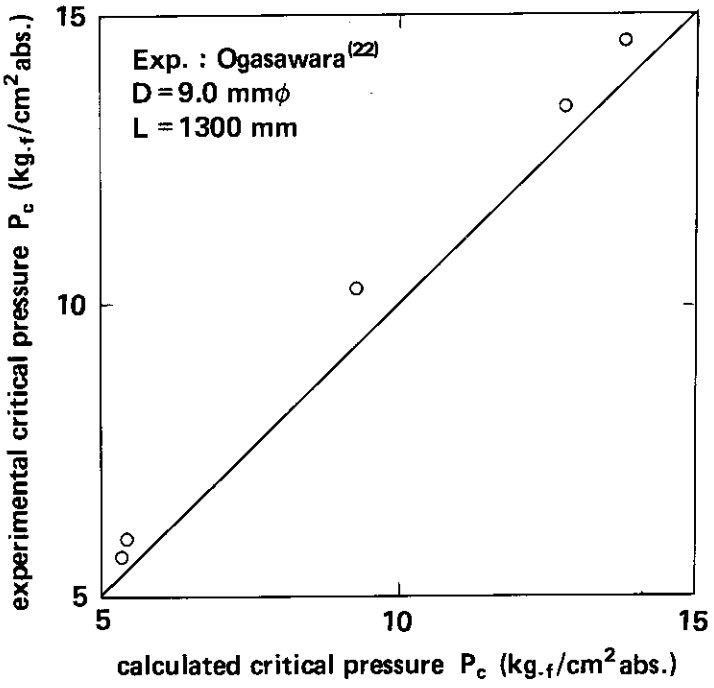

Fig. 20 Comparison between analytical and experimental critical pressures for a constant-flow-area channel.

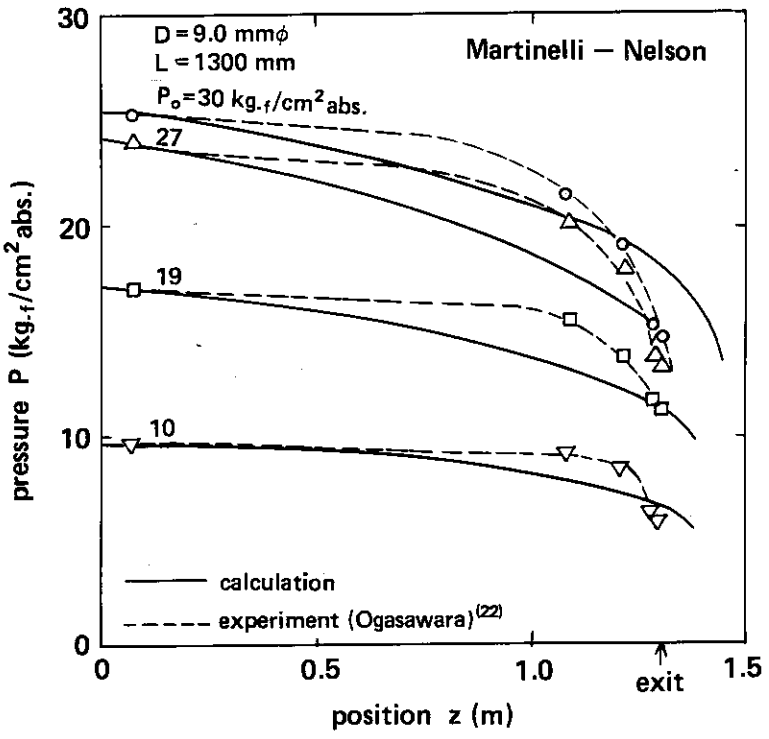

Fig. 21 Comparison between analytical and experimental axial pressure changes for a constant-flow-area channel (1).

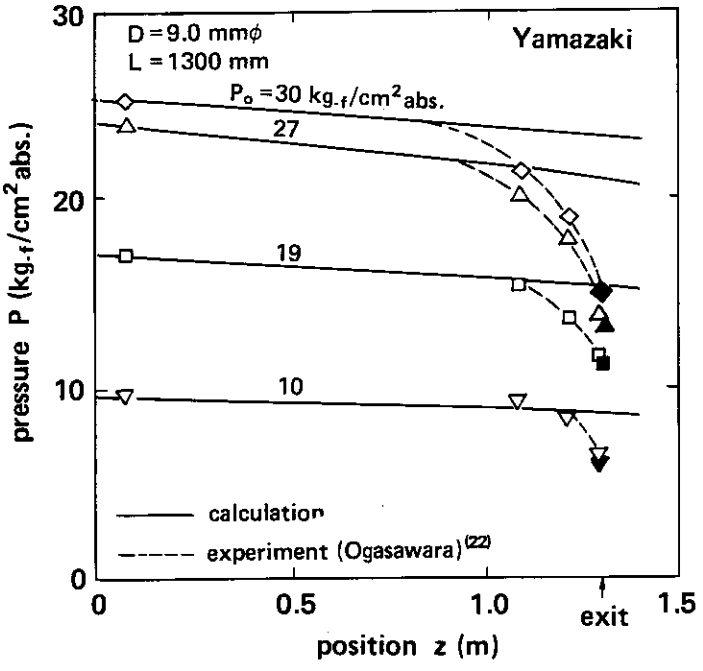

Fig. 22 Comparison between analytical and experimental axial pressure changes for a constant-flow-area channel (2).

The discrepancy between the analysis and the experiment near the channel exit is considered to be caused by the significantly large depressurization rate of the fluid. Shown in **Fig. 23** are estimated depressurization rates of gas and liquid phases, respectively, with respect to axial location in the test pipe for reservoir pressure of 30 kg-f/cm^2 abs. Here, these values were calculated with the experimental pressure distribution in the pipe and analytical phase velocities corresponding to each pressure. Liquid and gas phases already have more than 100 kg-f/cm^2/s and 1,000 kg-f/cm^2/s depressurization rates, respectively, at 900 mm downstream from the channel inlet. Under such very rapid depressurization, the following three situations are expected.

(1) Change of frictional pressure loss characteristic
(2) Thermal non-equilibrium between two phases
(3) Non-settled two-phase flow

All of them are very important study items in the future but the item (1) should be investigated at first. Because the part of the study in this chapter irrelative to the pressure loss correlation gives reasonable agreement with experimental data as shown in **Fig. 20**.

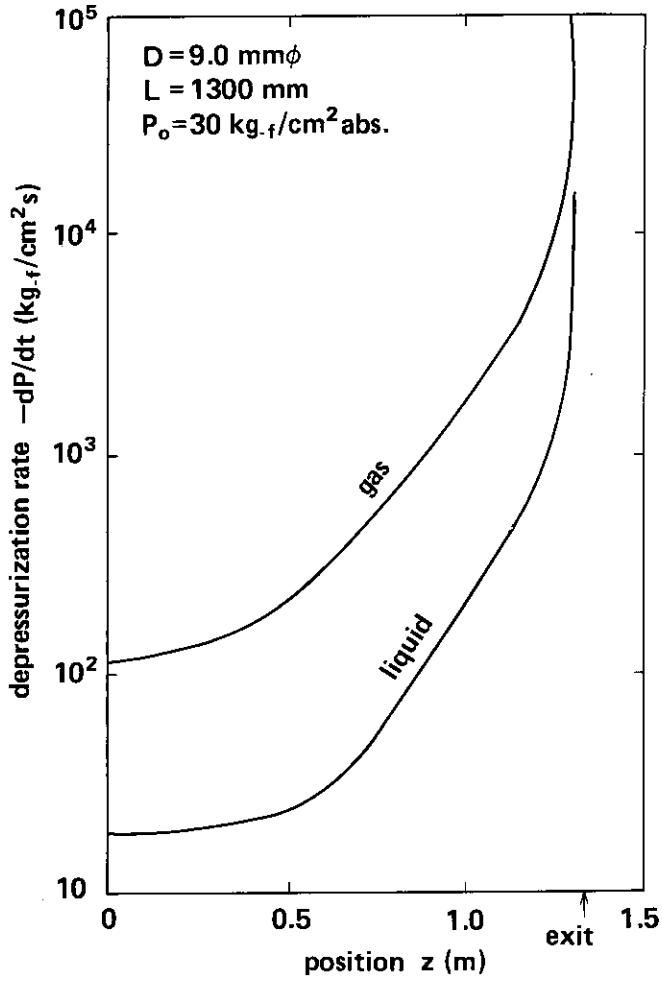

Fig. 23 Estimated axial change of depressurization rates in a two-phase critical discharge experiment with constant-flow-area channel.

Next, the negative infinite pressure gradient at the channel exit can be seen also in single-phase critical discharge flow as described in Appendix 1. For the two-phase critical flow, local relationship at the exit of constant-flow-area channel is considered as follows.

$$\frac{dP_{TPF}}{dz} \to -\text{finite} \tag{69}$$

and from **Fig. 14**,

$$\frac{dP_{TPF}}{dP} \to +0 \tag{70}$$

Therefore,

$$\frac{dP}{dz} = \frac{dP_{TPF}/dz}{dP_{TPF}/dP} \to \frac{-\text{finite}}{+0} = -\infty \tag{71}$$

Since dx/dP, du_g/dP, du_l/dP, $d\alpha/dP$, etc. are negative or positive finite, respectively, dx/dz, du_g/dz, du_l/dz, $d\alpha/dz$, etc. are positive or negative infinite.

The reason why $(dP/dz)_{C0}=-\infty$, etc. hold good in constant flow area channel is that the flow changes essentially due to wall friction. The critical flow occurrence at the channel exit is due to the same reason. Difference from the result of the previous chapter is caused by different approaching manner to the critical flow.

Finally, when G_C/G_{C0} is small (This occurs when L/D of channel is large.), void fraction α and liquid phase velocity u_l once decrease and then increase, showing the minimum points of α and u_l, respectively, as described in the sections 3.3 and 3.4. Sudo[25], et al. pointed out the similar void fraction distribution based on the low pressure air-water two-phase critical flow experiment. They explained this phenomenon as that since boundary between air and water acts like a converging-diverging nozzle, the critical flow of air occurs at the minimum void fraction point. Therefore, the air flow at the channel exit should be supersonic. However, from the author's point of view, the initial decrease in void fraction is only the result of more significant effect of phase slip increasing than the effect of gas phase volume flow rate increasing. The minimum void fraction point does not correspond to any hydrodynamic singular point such like the throat of converging-diverging nozzle. In fact, calculated gas phase velocity at the minimum void fraction point is irrelative to the acoustic velocity and no special phenomena suggesting the chocked flow of gas phase can be seen at the point. Boundary between the two phases is considered quite different from solid wall surface.

3.6 Conclusions

In this chapter, the calculation method of two-phase critical flow established in the previous chapter was applied to the critical discharge flow through a constant-flow-area channel and the effect of wall friction on critical flow phenomena was made clear. The analytical result was compared with the Ogasawara's experimental data to verify the validity of the analysis. Conclusions through the studies are as follows:

(1) The effect of wall friction is reasonably treated in the analytical method to consistently predict change of two-phase flow from subcritical flow via the critical flow to supercritical flow, which has been established in the previous chapter. Calculation method to analyze two-phase discharge flow through a constant-flow-area channel was completed as an application.

(2) It was demonstrated that relationship between the critical pressure and the critical mass velocity in a constant-flow-area channel can be predicted reasonably with this method for the given reservoir conditions.

(3) In a constant-flow-area channel, the critical flow realizes at the channel exit and the gradients of P, x, u_g, u_l, α, etc. become infinite at the critical flow point. This is not always the general features of the two-phase critical flow but due to the approaching manner to the critical flow, i.e., the flow is, in this case, changed essentially by the wall friction.

(4) In a large L/D constant-flow-area channel with signficant effect of wall friction, void fraction once decreases and then increases. This characteristic is more remarkable when reservoir pressure is low.

(5) Axial distribution of pressure was not always predicted perfectly. The possible reason is the large depressurization rate of fluid near the critical flow point. Especially, wall frictional pressure loss correlation should be improved.

4. Two-Phase Critical Flow without Phase Change[26]

4.1 Introduction

Hydrydynamic basic equations for one-dimensional separated two-phase flow established in Part I of this report have the remarkable uniquencess with treatment of the phase change inertial force. The uniquencess can be seen especially in the steady phase change inertial force terms.

The validity of the author's basic equations was demonstrated in Chapters 2 and 3 of Part II by applying them to the two-phase critical flow phenomenon which is governed strongly by the terms. If air-water (two-components) two-phase critical flow without phase change is analyzed and the difference in characteristics from the steam-water (one-component) two-phase critical flow is reasonably explained, validity of the author's basic equations will be confirmed more firmly.

Even in two-components two-phase flow, the fundamental structures of the author's basic equations, such as simultaneously using the two equations of motion for total two-phase flow based on existing mass and based on flowing mass and applying the kinetic energy law to the steady inertial force terms are preserved. Therefore, analysis of two-components two-phase critical flow is quite useful and interesting procedure to prove the validity of the basic equations.

In this chapter, analysis of two-components two-phase critical flow is tried by eliminating phase change terms from the analytical method for two-phase critical flow established in Chapter 2.

4.2 Calculation Method

In the critical discharge of two-phase fluid with negligible phase change such as air-water mixure at the room temperature, Eq. (37) in Chapter 2 becomes

$$dx=0 \quad \text{or} \quad x=\text{const.} \tag{72}$$

The effect of constant quality appears directly in Eq. (43) and indirectly in Eq. (41) through existing mass fraction of gas phase β. Therefore, characteristics of two-companents two-phase critical flow are quite different from those of regular one-component two-phase critical flow.

In this analysis, change of state of each phase is predicted by replacing the assumption (7) out of seven fundamental assumptions introduced in Chapter 2 with:

(7') thermally equiliblium between two phases and totally isentropic two-phase flow

This assumption is equivalent to assume no thermal resistance between two phases. The opposite limiting case of the infinite thermal resistance was also tried:

(7") adiabatic change of each phase

It gaves slightly larger critical mass velocity and very slightly lower critical pressure than in the case of assumption (7') but the characteristics were almost the same. Therefore, the results from the assumption (7') only will be described.

From the assumption (7'), the following two equations are used instead of Eqs. (19) and (20), i.e.,

$$T_g = T_l \tag{73}$$

$$x\left(\frac{\partial s_g}{\partial P}+\frac{\partial s_g}{\partial T}\frac{dT_g}{dP}\right)dP+(1-x)\left(\frac{\partial s_l}{\partial P}+\frac{\partial s_l}{\partial T}\frac{dT_l}{dP}\right)dP=0 \tag{74}$$

Total calculation scheme is the same as described in Chapter 2. That is, at first the state values for each phase after small change in pressure are determined by using Eqs. (73) and (74). Since x is given as the boundary condition, Eq. (72), u_g, u_l and β can be calculated for the guess value of R with using Eqs. (43), (44) and (45), respectively. By substituting them to Eq. (51), one can obtain the corrected value of R. Similar calculation is repeated until guess value and corrected value of R agree to each other.

4.3 Calculation Results and Discussions

Shown in **Fig. 24** is an example of calculated relationship between pressure and mass velocity of air-water mixture which discharges from high pressure reservoir via an axially variable cross-section channel to low pressure space. Reservoir pressure and temperature are 3 kg-f/cm² abs. and 20°C, respectively, and quality is parameterically changed from 0.0 to 0.99. **Figure 25** shows similar result for steam-water mixture for reference. Reservoir pressure is also 3 kg-f/cm² abs. and reservoir temperature is the saturated value, 132.9°C. Parameter x_0 is steam quality in the reservoir and, therefore, quality is different at each section of the channel in this case.

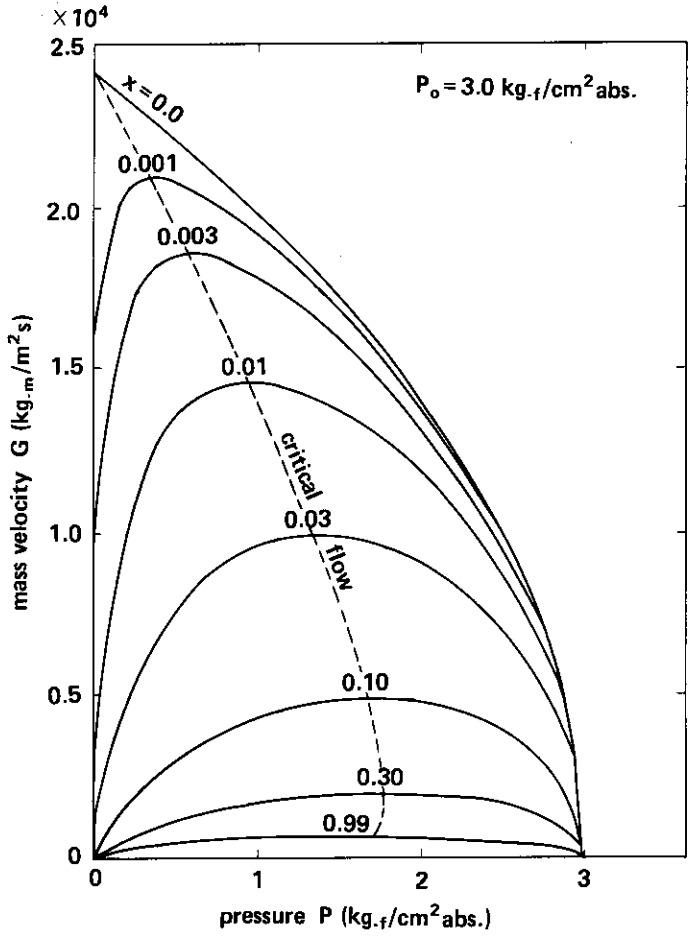

Fig. 24 G–P curves in two-component two-phase critical discharge.

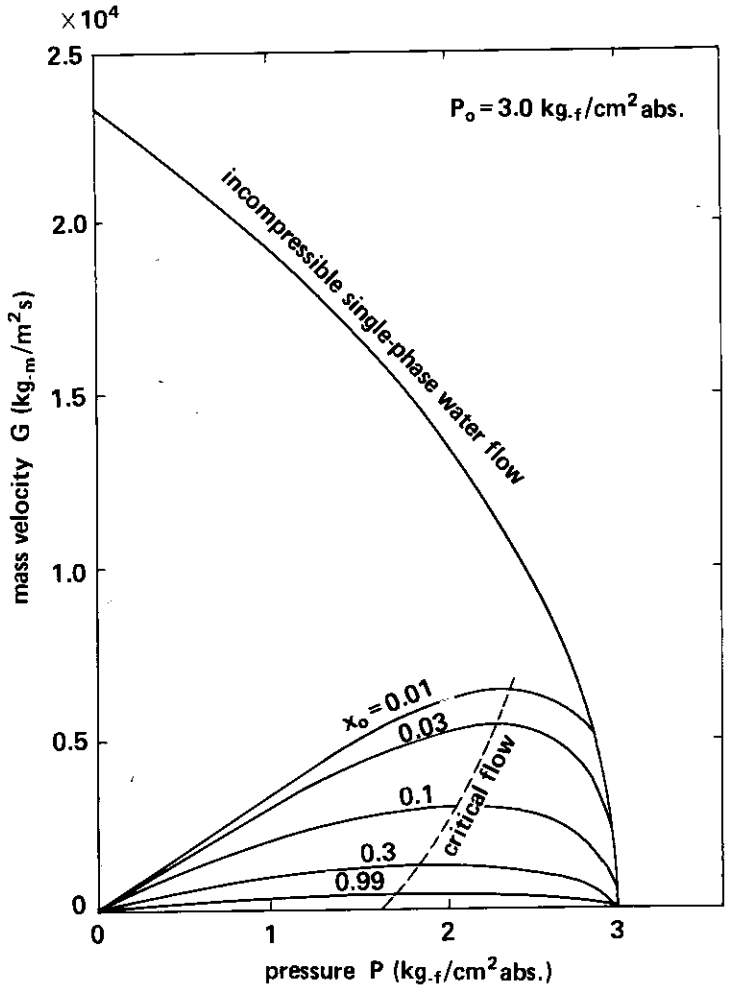

Fig. 25 G–P curves in one-component two-phase critical discharge.

By comparison between the two figures, difference in two-phase critical discharge characteristics caused by with or without phase change becomes very clear. In one-component two-phase flow with phase change, G–P curve becomes distant more and more from the curve for single-phase steam flow but never approaches to the curve for single-phase water flow even if x_0 approaches to 0.0. Because, even if $x_0 = 0.0$, the fluid has a very large compressibility due to flashing in this calculation with assuming thermal equilibrium (Actual critical discharge steam-water two-phase flow does not always show the very compressible characteristics because of possible thermal non-equilibrium. Such example will be introduced in Chapter 6.).

On the other hand, in two-components two-phase flow without phase change, G–P curve continuously changes from that for single-phase air flow to that for single-phase water flow with decreasing x from 1.0 to 0.0. The reason is that since there is no increase in compressibility due to phase change the equivalent compressibility of two-phase fluid is the simple average of compressibilities of each phase. Thus, the same author's basic equations can describe both one-component and two-component two-phase critical flows correctly, if only phase change rate and the consequent state changes of each phase are reasonably estimated. This fact suggests the validity and wide applicability of the author's basic equation set.

Let us examine the two-phase critical flow characteristics in more detail. The ratio

P_c/P_0 of the critical pressure to the reservoir pressure is considered to indicate generally the degree of compressibility effect on flow*. In the case of **Fig. 25** with phase change, P_c/P_0 of two-phase critical flow is much larger than the case of air single-phase critical flow ($P_c/P_0 = 0.528$[27] when $\kappa = 1.40$) and P_c/P_0 increases with decreasing of x_0. In this example, $P_c/P_0 \approx 1.66/3.0 = 0.553$ at $x_0 = 0.99$ and $P_c/P_0 \approx 2.4/3.0 = 0.8$ at $x_0 = 0.01$. These values are not affected so much by reservoir pressure P_0. Thus, two-phase critical discharge phenomenon with phase change is affected by compressibility most strongly when $x_0 = 0.0$.

On the other hand, in the case of **Fig. 24** without phase change, P_c/P_0 becomes the maximum at $x_0 \approx 0.5$ and the value is only $1.73/3.0 = 0.593$. When x decreases from 0.5, P_c/P_0 decreases and approaches to the case of single-phase water flow. At $x = 0.0$, the flow becomes incompressible, i.e., $P_c/P_0 = 0.0$. When x increases from 0.5, P_c/P_0 also decreases and approaches to the case of single-phase air flow. At $x = 0.99$, $P_c/P_0 \approx 1.59/3.0 = 0.53$ in this example.

The critical mass velocity G_c is also quite different depending on with or without phase change, corresponding to the P_c/P_0 characteristics described above. That is, G_c for without phase change case is much larger than that for with phase change case and the value increases significantly toward the mass velocity of single-phase water discharge flow when x approaches 0.0. G_c for with phase change case is, on the other hand, supressed by the large compressibility and the value is limited at about 0.3 times that for single-phase water discharge flow even x_0 approaches 0.0.

This difference in two-phase critical flow characteristics between the with and without phase change cases is physically very reasonable. And the author's basic equation set can predict both cases, indicating the perfectness as the balance equations. The difference is well predicted by correctly describing the phase slip with equation of motion (4) based on existing mass and equation of motion (6) based on flowing mass. For example, **Fig. 26** compares the critical pressure ratios obtained by Akagawa's[28] theory** and author's theory. In Akagawa's theory, the critical pressure ratio does not approach smoothly to the value (0.0) for single-phase water discharge flow when quality approaches zero, although the same total energy conservation equation as Eq. (41) is used. The reason is that phase slip is ignored in the theory.

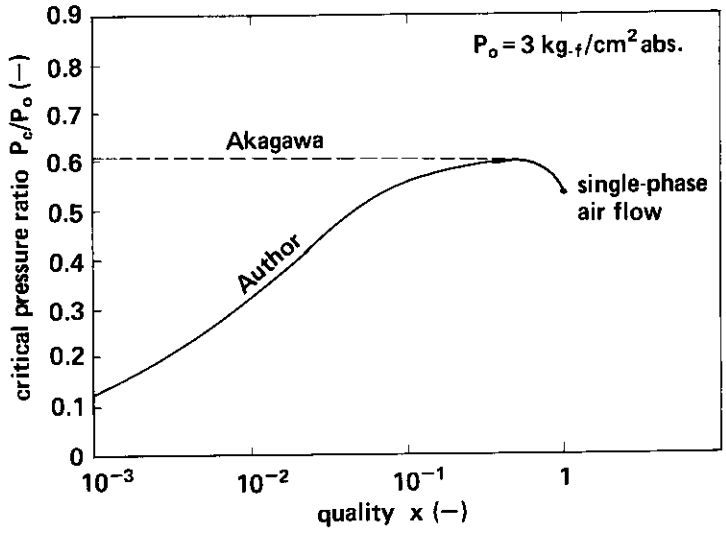

Fig. 26 Comparison in critical pressure ratio between Akagawa's and the author's theories.

* P_c/P_0 is also affected much by wall friction. In this chapter, however, wall friction is ignored.

** The Akagawa's line in **Fig. 26** is calculated by the author with the first equation of Eq. (8.32) and Eq. (8.39) of Ref. (28).

Next, the author's theory shall be compared with the experimental data reported by Smith, et al.[29]. In the air-water upward two-phase critical flow experiment, converging-diverging test channels with annulus cross section are used. The test channel consists of a pipe with 32.39 mm (1.275") diameter and the double conical insertion. The minimum gap between the pipe and the insertion is 1.59 mm (0.0625") or 3.18 mm (0.125"). Axial flow area distribution for the former is shown with solid line in **Fig. 27**.

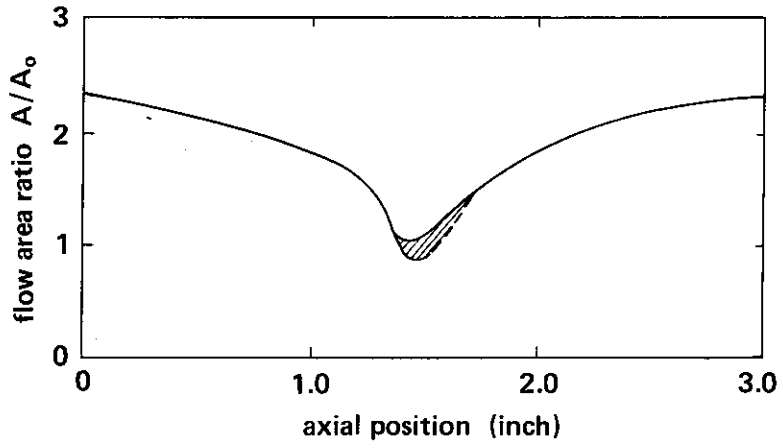

Fig. 27 Axial change of test section flow area at the experiment by Smith, et al.

Shown in **Fig. 28** is comparison of the critical mass velocity between the author's calculation and the experimental data. Numbers written by the data points indicate the quality and "▲" marks are the data points of which axial pressure distribution is given. According to this figure, the author's prediction agrees well with the experimental data in high quality region of $x > 0.5$. However, the experimental value is about 20% lower than the predicted at $x = 0.28$. In the lower quality region, discrepancy between the theory and the experiment becomes more significant and the experimental data becomes only less than a half of the theoretical value at $x = 0.03$.

To make clear the cause of this discrepancy, the relationship between mass velocity and pressure in the channel is obtained for the data of $x = 0.28$ as shown with dashed line in **Fig. 30** based on the axial pressure distribution give in **Fig. 29**. The analytical curve with the author's theory is shown with solid line. The theoretical critical flow in this calculation is given by the maximum point A of the solid line. On the other hand, Smith, et al. give the critical flow point experimentally with the following three methods.

(1) Point where flow area is geometrically minimum (the point B of **Fig. 30**)
(2) Point where pressur ratio P/P_0 is the same as the theoretical critical pressure ratio for isentropic change of air (the point C)
(3) Point where the minimum pressure ratio appears in subcritical flow (the point D)

The critical pressures corresponding the above three cases are 1.8, 1.4 and 1.22 kg-f/cm^2 abs., respectively. The point of "Throat (experimental)" of **Fig. 30** corresponds to the point C.

The point C is, as explained later, basically based on the idea that the interface between gas and liquid phases is equivalent to the solid wall but this understanding is wrong. On the other hand, the point D seems reasonable as described below.

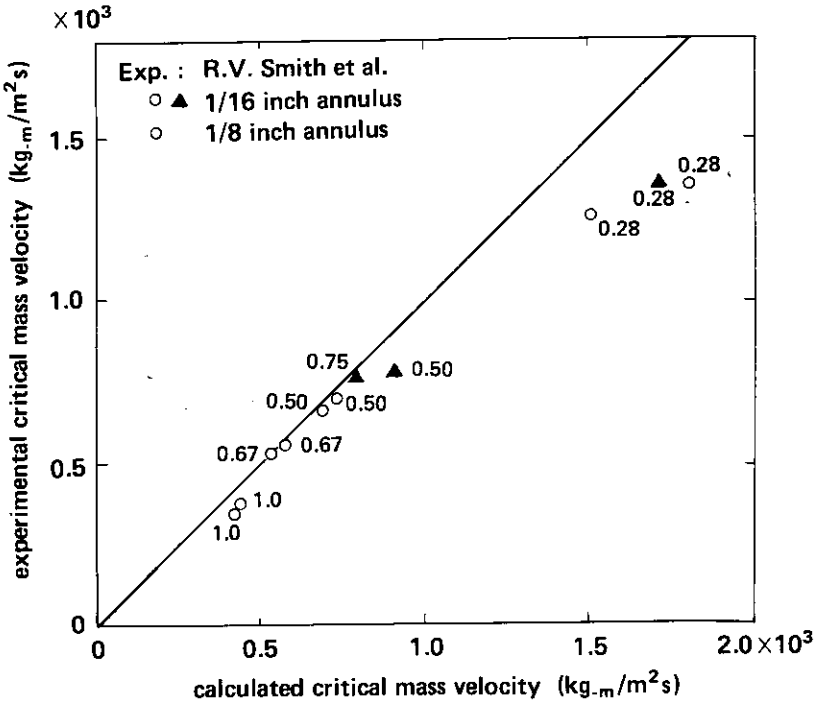

Fig. 28 Comparison between analytical and experimental mass velocities for two-component two-phase critical flow.

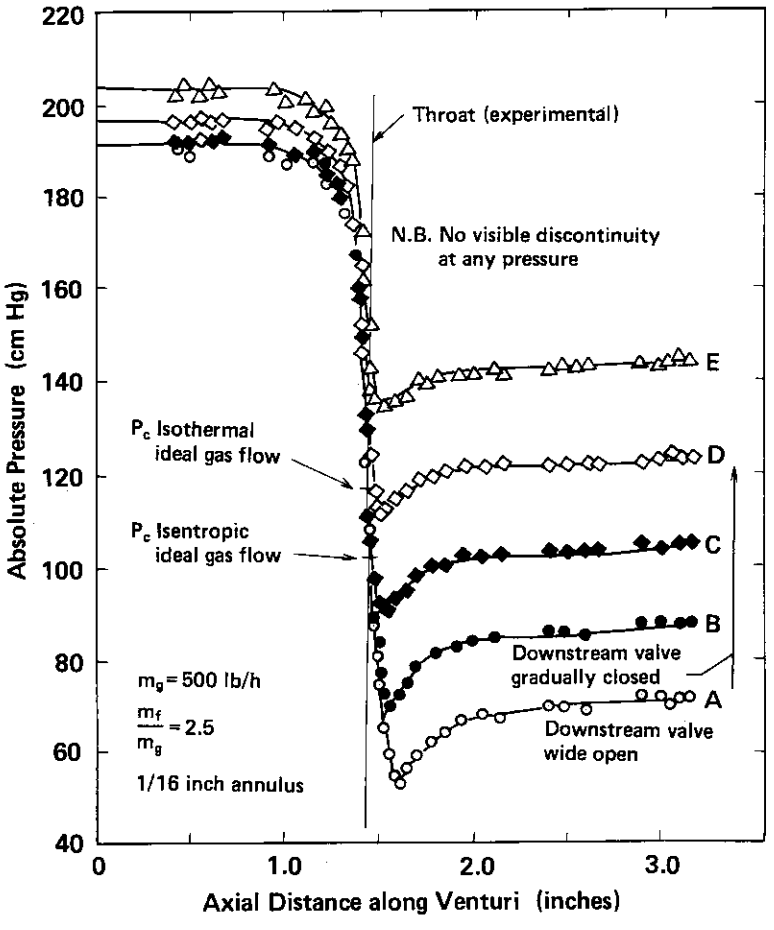

Fig. 29 Measured axial pressure changes (Smith, et al.[29]).

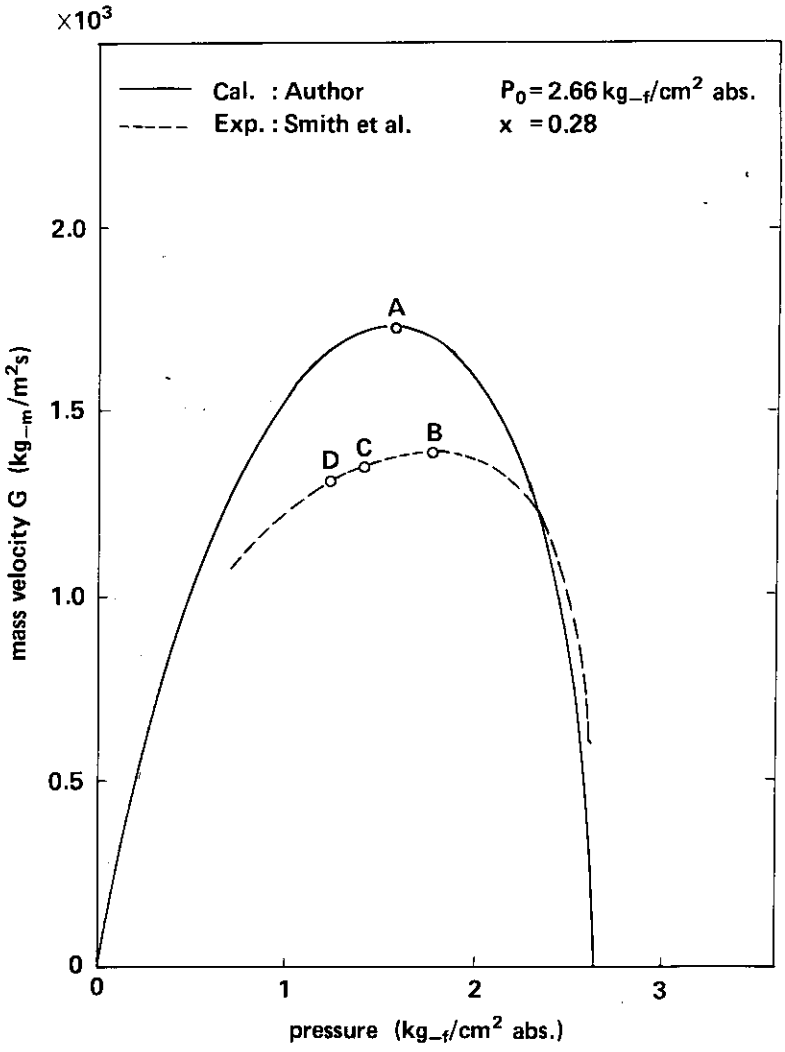

Fig. 30 Gomparison between analytical and experimental G–P curves for two-component two-phase critical flow.

As described in Appendix 1, single-phase subcritical flow in a converging-diverging nozzle with friction has the minimum pressure point in downstream of the geometrical throat. The minimum pressure point moves with decreasing back pressure under constant reservoir pressure and approaches to the critical flow point. If the movement of the minimum pressure point is not so large, the minimum pressure point for subcritical flow gives the location of the critical flow. By applying similar idea to the two-phase flow, the point D is considered to be the most reliable location of the critical flow point.

In fact, the effect of wall friction seems to be not negligible in the experiment of Smith, et al. because of the very small flow channel gap of 1.59 mm. The discrepancies between the analysis and experiment seen in **Figs. 28** and **30**, especially relationship between decreases in the critical mass velocity and the critical pressure of the point D from the point A of **Fig. 30**, can reasonably be understood with taking wall friction into account.

Smith et al. reported, after observation of liquid film pile-up in downstream side of the throat and proposed to interpret their test results by the movement of the effective throat location from the geometrical throat location. This interpretation is quite similar to the explanation of Sudo, et al. of two-phase critical discharge through a constant-flow-area channel. According to this idea, the flow channel gap is supposed to be decreased in the experiment of

$x = 0.28$ by 0.25 mm as shown with hatching in **Fig. 27** due to liquid film pile-up. This value is not so unrealistic for this example but the case of $x = 0.03$ it is very difficult to explain by the same idea. In addition, since water film piled-up in the downstream of the throat is not considered to act like a solid wall as described in the section 3.5, two-phase critical flow characteristics cannot be related directly with the water film pile-up phenomenon.

4.4 Conclusions

In this chapter, analytical method on one component two-phase critical flow established in Chapter 2 was applied to two-components two-phase critical flow without phase change only by equating quality change to zero and the validity and applicability of the method was examined. Validity of estimation of the effect of phase change inertial force on critical flow phenomena of the author's theory can be made clear and fundamental structure of the author's basic equations such as simultaneously using the two equations of motion for total two-phase flow based on existing mass and based on flowing mass can be verified through those examination. Major conclusions are as follows:

(1) Analytical method on one-component two-phase critical flow established in Chapter 2 can be applied to two-components two-phase critical flow without phase change if only quality change is equated to zero.

(2) Characteristics of two-components two-phase critical discharge flow approaches those of incompressible single-phase water discharge flow with approaching of x to zero. That is, the critical pressure approaches zero and the critical mass velocity approaches the mass velocity of single-phase water discharge flow. These facts are quite contrastive to the characteristics of one-component two-phase critical discharge flow with very strong fluid compressibility effect even in low reservoir quality very close to zero.

(3) The author's analysis neglecting the effect of wall friction can predict well the high quality data of the air-water two-phase critical flow experiment of Smith et al. However, it is necessary to take into account the effect of wall friction to predict correctly the critical pressure and mass velocity of the low quality experiments.

5. Two-Phase Critical Discharge Experiment with a Converging-Diverging Nozzle[30]

5.1 Introduction

Through the discussion up to now, validity of basic equations for one-dimensional separated two-phase flow established in Part I of this report is considered to be proven essentially. There are two significances with the establishment of correct basic equation set. The one is that one can perform accurate and reliable two-phase flow analysis. The other is that the basic equation set orientates how to solve two-phase flow problems. Some explanations will be given below about the second point.

To solve two-phase flow problems analytically, not only basic equations but also various constitutive equations (experimental correlations) are necessary. Kinds and number of necessary constitutive equations are determined by the structure of basic equations. Sometimes, various assumptions are introduced to simplify the problems. Validities of such constitutive equations and assumptions are judged by comparing the analytical results with experimental data. However, if the basic equations are not absolutely reliable, such judgement is impossible. Thus, correct basic equations give us the firm start point and the basis for final judgement.

Some examples to use the author's basic equations from such point of view will be introduced in Chapters 5 through 7. In this chapter, at first, the effect of thermal non-equilibrium between two phases on two-phase critical flow is evaluated by comparing the analytical results neglecting the non-equilibrium phenomena with the data from the two-phase critical discharge experiment.

By using a converging-diverging test nozzle with sufficiently gentle axial flow area change, in which no flow separation is anticipated, not only axial distributions of pressure and temperature but also axial change of mass velocity can be measured. Therefore, one can follow experimentally the change of flow in detail from subcritical flow via the critical flow to supercritical flow. In this case, since the major cause of flow change is axial variation of flow area, analysis neglecting the effect of wall friction is considered correct enough. This is quite different situation from the case of constant-flow-area channel.

Many experimental studies on two-phase critical discharge flow were reported in the past for sharp-edged orifice[31]-[37], or similar shape discharge mouth[36],[38],[39] or pipe[3],[7],[13]-[16],[31],[40]. However, only experiment by Brown[41] was reported for converging-diverging nozzle. Most of his experiments are for subcooled water discharge and data for saturated two-phase discharge flow are only few cases.

In two-phase critical discharge flow through a short converging-diverging nozzle, thermally non-equilibrium flow is supposed to realize because of the very rapid expansion and depressurization of the two-phase fluid. In the case of critical discharge of high temperature subcooled water or very low quality two-phase fluid through a sharp-edged orifice or similar shape discharge mouth, thermally non-equilibrium phenomenon appears due to steam generation delay. Similar kind of non-equilibrium was reported also for long pipe[40],[42]. The non-equilibrium realizes in a short converging-diverging nozzle[41], too. In the author's experiment introduced in this chapter, another kind of thermally non-equilibrium phenomenon was found in two-phase critical dhscharge flow except for very low quality cases.

5.2 Experimental Facility and Procedure

5.2.1 Experimental facility

Shown in **Fig. 31** are configuration and major dimensions of the experimental facility used. A stainless steel, vertical cylindrical pressure vessel with inner diameter of 290 mm and axial length of 5,000 mm (max. 40 kg-f/cm²g., 250°C) contains an AC. electric heater (direct heating) of 70 kW in the maximum. The electric heater is placed on the bottom of the pressure vessel in order to heat up the water in the pressure vessel uniformly.

A discharge nozzle with inner diameter of 50 mm is provided at the 950 mm elevation from the pressure vessel bottom and the test nozzle and the discharge system including a quick-opening valve are connected to it. Since the discharge nozzle elevation is 200 mm higher than the top of the electric heater, two-phase discharge flow is not interfered by the heater. A 75 mm long vortex eliminating device with a cross-shaped cross section is set in the discharge nozzle for preventing from natural vortex in the nozzle.

Two chromel-alumel thermo-couples for fluid temperature measurement, one pressure transducer for system pressure measurement, two level glasses for residual water mass caliburation and various instruments for operation are attached to the pressure vessel.

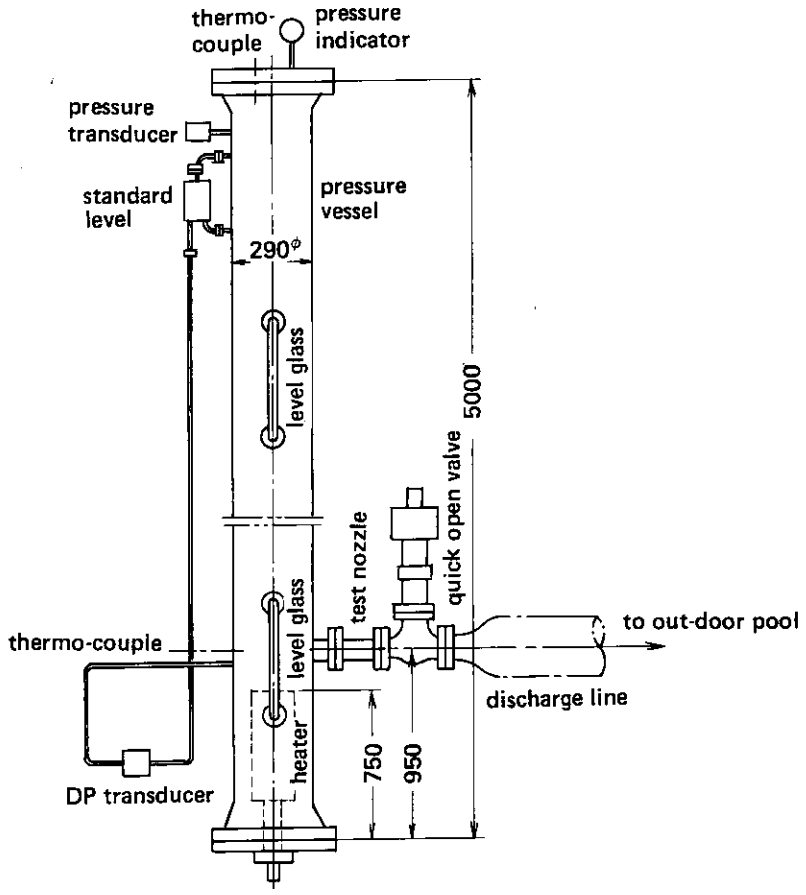

Fig. 31 Experimental facility.

5.2.2 Test nozzle

The converging-diverging nozzle used in this experiment has axial length of 200 mm and the minimum inner diameter of 10 mm (at 75 mm from the entrance). The axial variations in inner diameter and cross sectional area are shown in **Fig. 32**. Pressure measurement holes

(1.0 mmϕ) and thermo-couple penetration holes (2.0 mmϕ) are provided at the axial locations ① through ⑧ shown in the figure. The pressure measurement holes are made perpendicularly to the nozzle inner surface so as to be in right angle to the stream line. On the other hand, thermo-couple penetration holes are made perpendicularly to the nozzle axis to identify the axial location of the sensing parts correctly.

Axial distribution of static pressure in the test nozzle is measured with strain-gauge type pressure transducers. However, static pressures at the measurement locations ① through ③ are measured as differential pressure from the pressure vessel pressure by using strain-gauge type differential pressure transducers because more correct measurement of small pressure drop can be made with this method. On the other hand, axial distribution of fluid temperature is measured with unground type chromel-alumel thermo-couples with diameter of 1.0 mm. The sensing parts are placed at 5 mm inside from the nozzle inner surface. For the thermo-couple at the throat, the location is just at the center of the channel cross section.

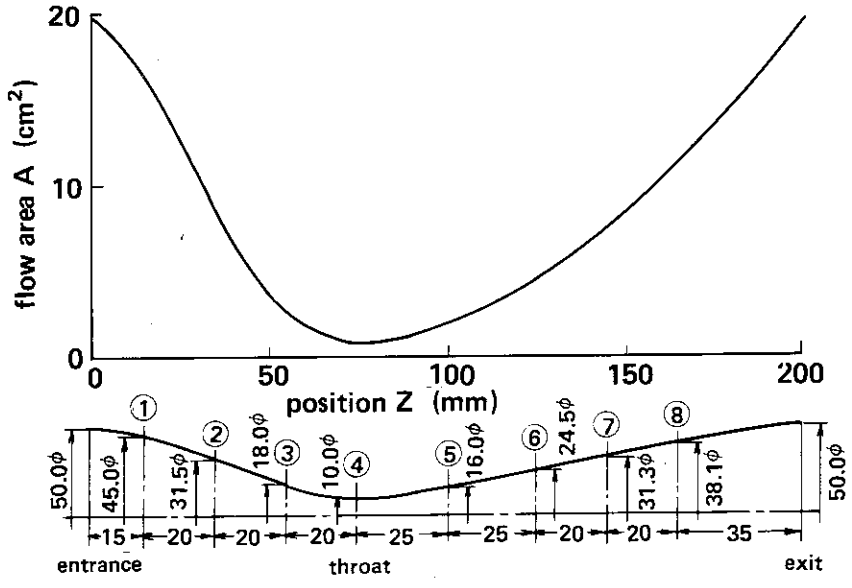

Fig. 32 Axial changes of diameter and flow area of the test nozzle.

5.2.3 Experimental procedure

In advance of initiation of test, the quick opening valve is close and deinoized water (specific electric resistance $>10^6$ Ωcm) is filled upto the set level. On this stage, caliburation of residual water mass measurement system including strain-amplifier and visicorder is performed with the level glasses. After closing the feed water line valve, the pressure vessel is pressurized by heating-up the water with the electric heater. When the pressure vessel conditions become the set values (lower than 30 kg-f/cm^{2}g., 234.6°C), electric heating is terminated and the high temperature, high pressure fluid in the pressure vessel is discharged through the test nozzle to the out-door pool by opening the quick-opening valve. The quick-opening valve is an air-pressure actuation type piston valve and the time from perfect close to full open is 40 ms.

Duration time of discharge is different depending on initial condition but it is in the range of 2 through 5 min. Pressure and residual water mass in the pressure vessel and axial distributions oi static pressure and fluid temperature in the test nozzle are recorded during the duration with the visicorder. Discharge mass flow rate is calculated by differentiating the residual water mass data and mass velocity at each cross section can be obtained by dividing the discharge mass flow rate by the cross-sectional area.

5.2.4 Calculation method of quality

Steam quality of discharge two-phase flow from the pressure vessel toward the test nozzle is difficult to measure. Therefore, it was indirectly evaluated based on the data of pressure and residual water mass transients in the pressure vessel by using the following calculation method. Let us call the indirect measurement method of discharge two-phase flow quality as "depressurization rate method".

Fundamental assumptions for this method are:

(1) Thermal equilibrium in the pressure vessel
(2) No heat exchange through the vessel wall
(3) Negligible kinetic energy of fluid in the pressure vessel
(4) Negligible kinetic energy of discharge two-phase flow at the test nozzle entrance

The assumption (1) is proven on data. The assumption (4) is considered reasonable because the flow area at the test nozzle entrance is 25 times that at the throat and almost no depressurization-expansion occurs as far as the test nozzle entrance. By this assumption, quality of discharge two-phase flow is calculated with respect to the high pressure reservoir condition. Since cross sectional area of the pressure vessel is 34 times that at the test nozzle entrance, the assumption (3) holds good more accurately than the assumption (4). Strictly speaking, the assumption (2) does not hold good correctly but rough estimation showed that the effect on quality calculation would be small enough.

From mass balance,

$$\frac{dw_s}{dt}=-W_g+\frac{dw_{PC}}{dt} \tag{75}$$

$$\frac{dw_w}{dt}=-W_l-\frac{dw_{PC}}{dt} \tag{76}$$

From volume balance.

$$w_s\frac{dv_s}{dt}+w_w\frac{dv_w}{dt}+(v_s-v_w)\frac{dw_{PC}}{dt}=v_sW_g+v_wW_l \tag{77}$$

From energy balance,

$$\frac{d(h_sw_s)}{dt}+\frac{d(h_ww_w)}{dt}=-h_sW_g-h_wW_l+V\frac{dP}{dt} \tag{78}$$

From these equations, steam quality x_0 of discharge two-phase flow is obtained as:

$$\begin{aligned}x_0&\equiv\frac{W_g}{W_g+W_l}\equiv\frac{W_g}{W}\\&=-\frac{v_w}{v_s-v_w}+\left\{\frac{1}{v_s-v_w}\left(w_s\frac{dv_s}{dP}+w_w\frac{dv_w}{dP}\right)\right.\\&\quad\left.-\frac{1}{h_s-h_w}\left(w_s\frac{dh_s}{dP}+w_w\frac{dh_w}{dP}-V\right)\right\}\frac{1}{W}\frac{dP_0}{dt}\end{aligned} \tag{79}$$

Here, from the assumption (1), all state values in Eq. (79) are given for the saturated condition.

One can calculate the steam quality x_0 of discharge two-phase flow with Eq. (79) based on the data of pressure vessel pressure and residual water mass in the pressure vessel and their differentiations with respect to time, i.e., depressurization rate and discharge mass flow rate. The depressurization rate method described above has a large advantage especially in low

quality region because of very high sensitivity on quality.

5.3 Experimental Results

5.3.1 Discharge process

In order to make clear how the data introduced in the following subsections were obtained, overall discharge process shall be described briefly in this subsection.

Shown in **Fig. 33** are examples of transients after the discharge initiation in pressure vessel pressure, residual amount of water (collapsed level), and mass flow rate and quality of discharge two-phase flow. Until 82 s after discharge initiation, when collapsed level arrives at 0.5 mm above the center line of the discharge nozzle, quality of discharge two-phase flow is very small. Therefore, discharge mass velocity is large and depressurization rate is small. After that, however, quality increases rapidly, mass velocity decreases significantly and depressurization rate becomes very large. Such behaviors are qualitatively common among every experiment and repeatability of test is sufficiently good.

As known from the above examples, change of thermal-hydraulic situation in the pressure vessel and test nozzle is sufficiently slow. Therefore one can consider the phenomenon is quasi-steady.

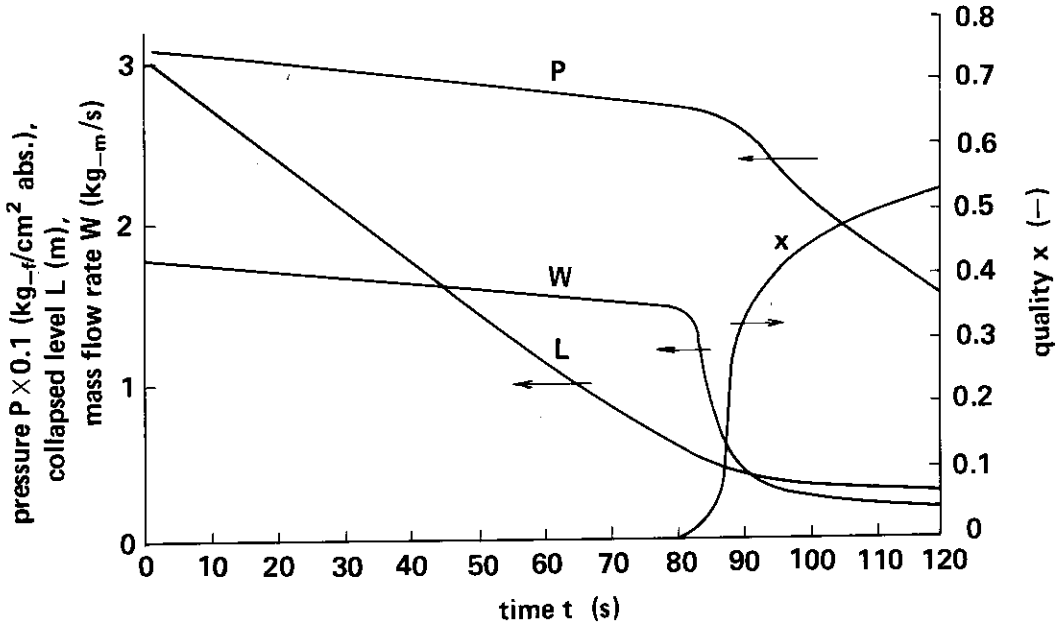

Fig. 33 Example changes of variables during discharge.

5.3.2 Distribution of static pressure

Shown in **Fig. 34** is an example of measured axial static pressure distribution in the test nozzle. According to this figure, only very small pressure drop can be seen until 55 mm from the test nozzle entrance. Almost all pressure drop appears in about 50 mm around the throat, especially in the downstream side. The pressure gradient at around the throat increases once when the collapsed level arrives at near the discharge nozzle elevation and quality of discharge two-phase flow increases rapidly, and then it decreases with reduction of differential pressure across the throat due to depressurization of pressure vessel. On the other hand, pressure recovery is seen in about 50 mm upstream the test nozzle exit, indicating the overexpansion phenomenon.

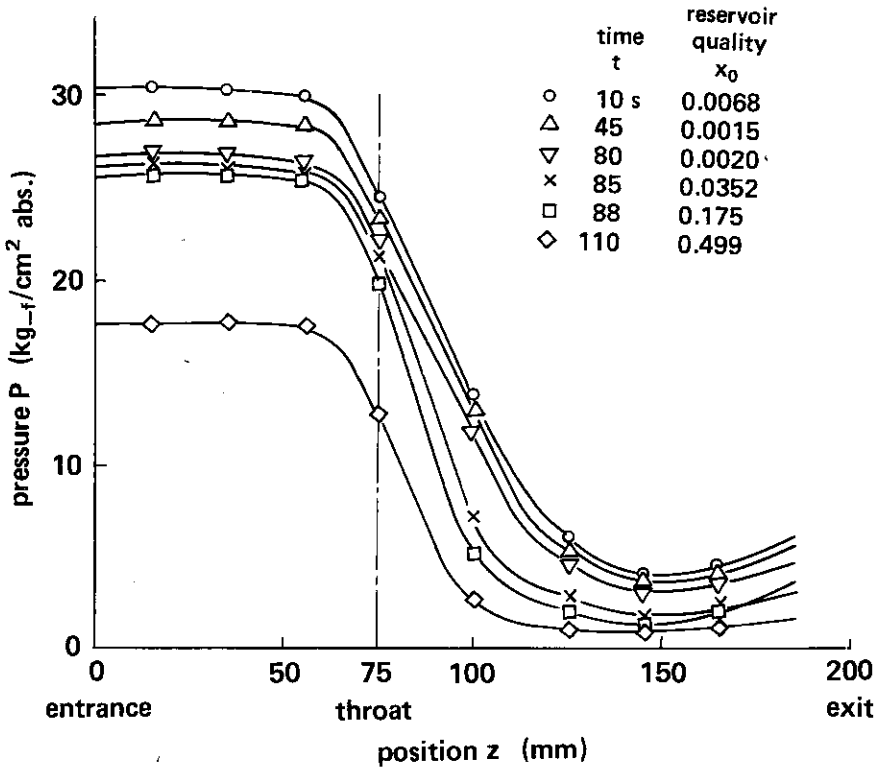

Fig. 34 Examples of axial static pressure change in a converging-diverging nozzle.

5.3.3 G–P curve and critical mass velocity

Figure 35 shows the relationship between pressure and mass velocity in the test nozzle. After the synthetic examination on various similar test results, the following two-phase critical discharge characteristic were made clear for the used converging-diverging nozzle.

When quality of discharge two-phase flow is close to zero, relationship between pressure and mass velocity near the test nozzle entrance is quite similar to that for single-phase water flow. However, the curve turns away rapidly from the single-phase curve with approaching the throat and mass velocity is limited by the relatively small critical value. This fact and the axial static pressure distribution showing remarkable pressure drops from just downstream side of the 55 mm measuring point (see **Fig. 34**.) suggest that the significant effect of sudden vaporization around there.

Mass velocity downstream side of the throat shows concave characteristic with respect to pressure when quality of discharge two-phase flow is less than 0.1. Such characteristic cannot be seen when the qulity is larger than 0.15.

Next, let us examine the value of the critical mass velocity by comparing with the analysis under the assumption of thermal equilibrium, which was introduced in Chapter 2. When quality of discharge two-phase flow is very small (less than 0.01), the measured critical mass velocity can be larger than the analytical value as shown in **Fig. 36**. However, in most case, the former is smaller than the latter as shown in **Fig. 37**. The ratio of measured critical mass velocity to the analytical value for various discharge conditions is plotted with respect to quality of discharge two-phase flow in **Fig. 38**. Brown's data are also plotted in this figure. The ratio of measured and theoretical critical mass velocities is almost independent of reservoir pressure P_0 but is determined mainly be reservoir quality x_0.

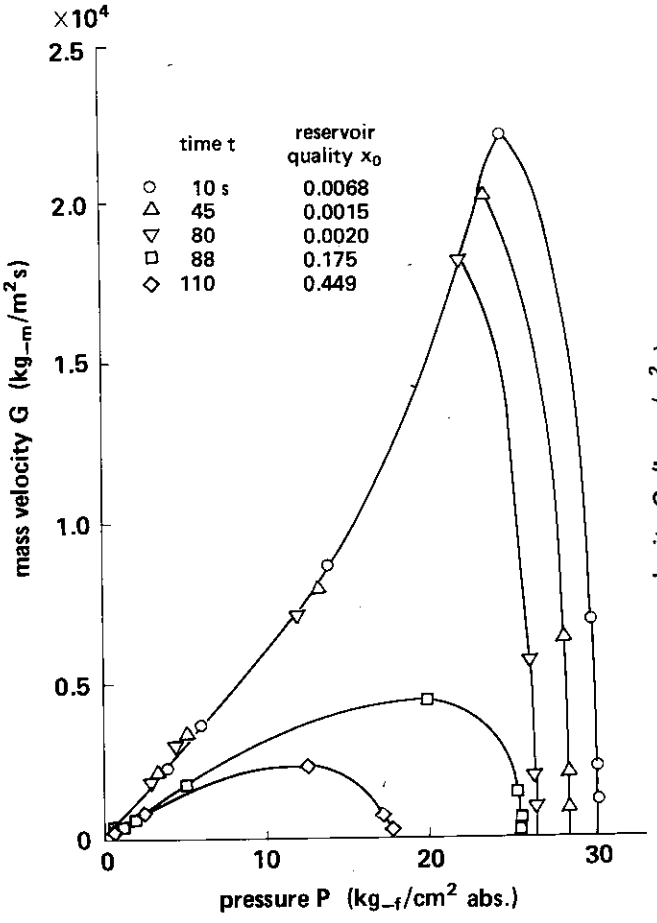

Fig. 35 Examples of G–P curve.

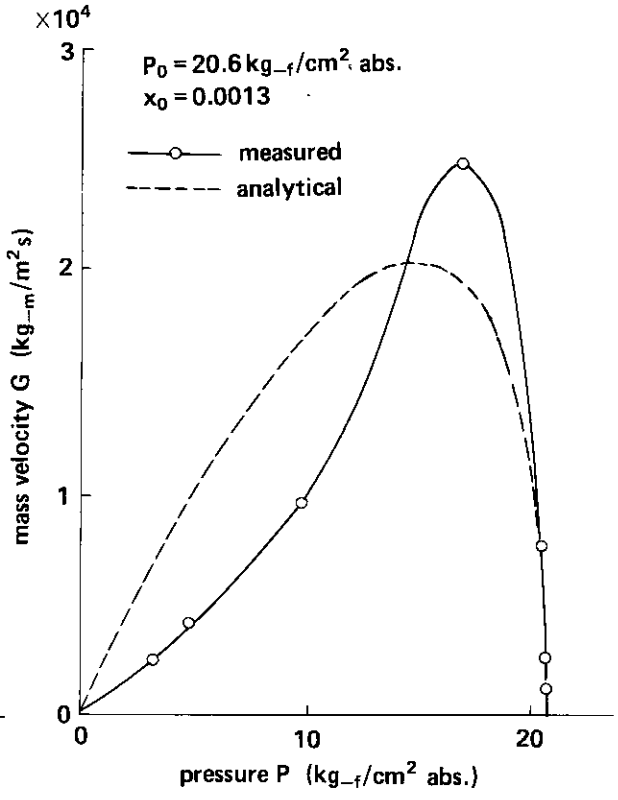

Fig. 36 Comparison between analytical and experimental G–P curves (1).

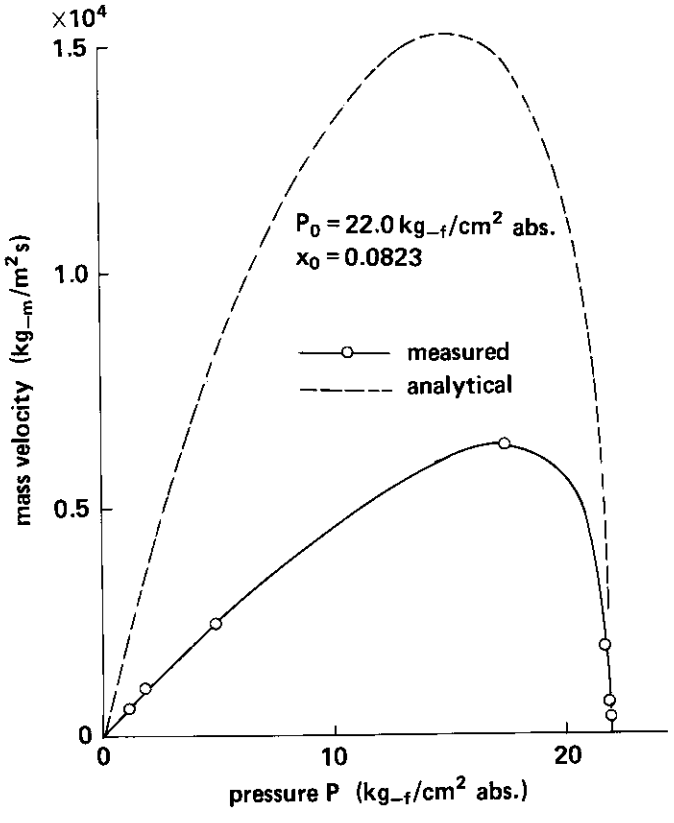

Fig. 37 Comparison between analytical and experimental G–P curves (2).

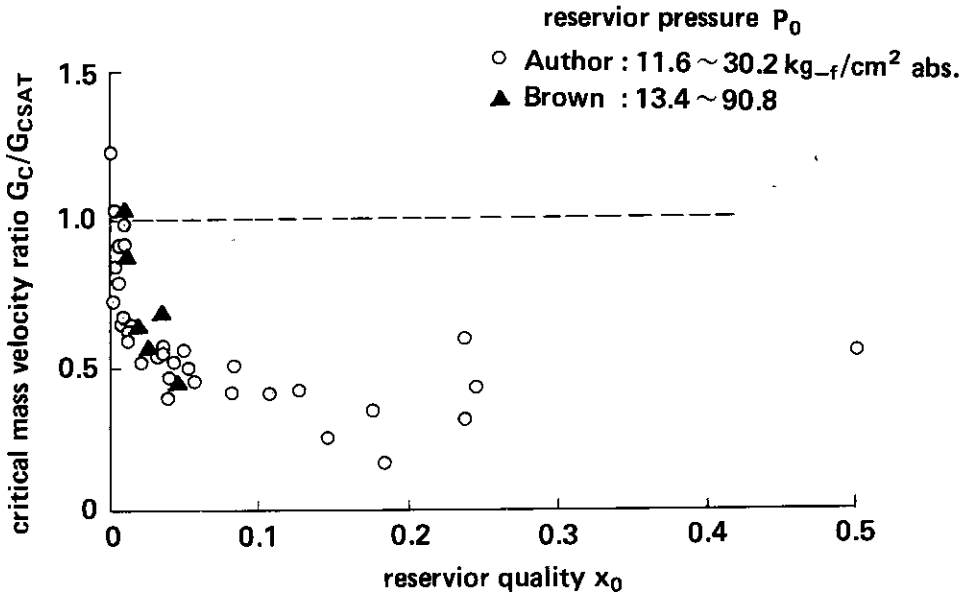

Fig. 38 Comparison between analytical and experimental critical mass velocities.

5.3.4 Distribution of fluid temperature

In order to get information on degree of thermal non-equilibrium of fluid in the test nozzle, fluid temperatures at the points 5 mm from the inner surface of the nozzle were measured by using chromel-alumel thermo-couples with 1.0 mm diameter. Two examples of the result for the different reservoir conditions are shown in **Fig. 39**. Since sensing parts of the thermocouples are placed at 5 mm from inner surface of the nozzle, temperature of liquid film on the wall is never detected even if the flow regime is annular.

The meaning of fluid temperature data measured with such method should be carefully examined. Since heat capacity of the thermocouples is very small and temperature variation at each measuring point is sufficiently slow in comparison with response time of the thermocouple, it is conisdered that thermal equilibrium is established between the sensing part of thermocouple and the surrounding fluid.

As a limiting case, let us assume that the surface temperature of the sensing part goes and backs very quickly between the steam temperature and water temperature, then time-averaged value of steam and water temperatures should be detected as fluid temperature because of heat capacity of the thermo-couple. Since time fractions of contactings with steam and water are α and $1-\alpha$, respectively, the measured fluid temperature should, in this case, be

$$T=\alpha T_g+(1-\alpha)T_l \tag{80}$$

Because, in most cases in this expeirment, α is very large, measured temperature T is considered close to steam temperature T_g.

As the second limiting case, let us assume very thin stagnant water film on the sensing part of thermo-couple. Since subcooled temperature is detected in this experiment, such situation is supposed possible. However, the water film gives only some response delay of temperature measurement due to additional heat capacity and heat conduction time of the stagnent water film and, therefore, no essential difference from the first case is supposed.

As the third case, let us investigate the water film on the sensing part, which is always renewed by evaporation and droplet capturing. In this case, latent heat for evaporation is

provided by sensible heat of water, because there is no heat transmission in time average between thermo-couple and water film as already discussed. Therefore, there must be temperature distribution in the water film and resultant heat flow from inside of the water film to the surface. Since temperature on the surface of water film should be equal to steam temperature and water film is supposed very thin detected temperature by the thermo-couple is considered close to steam temperature, although it may be slightly higher because of water film temperature gradient. Based on the above three examinations, let us assume in the following discussion that the thermo-couples detected the temperature nearly equal to steam temperature in this experiment.

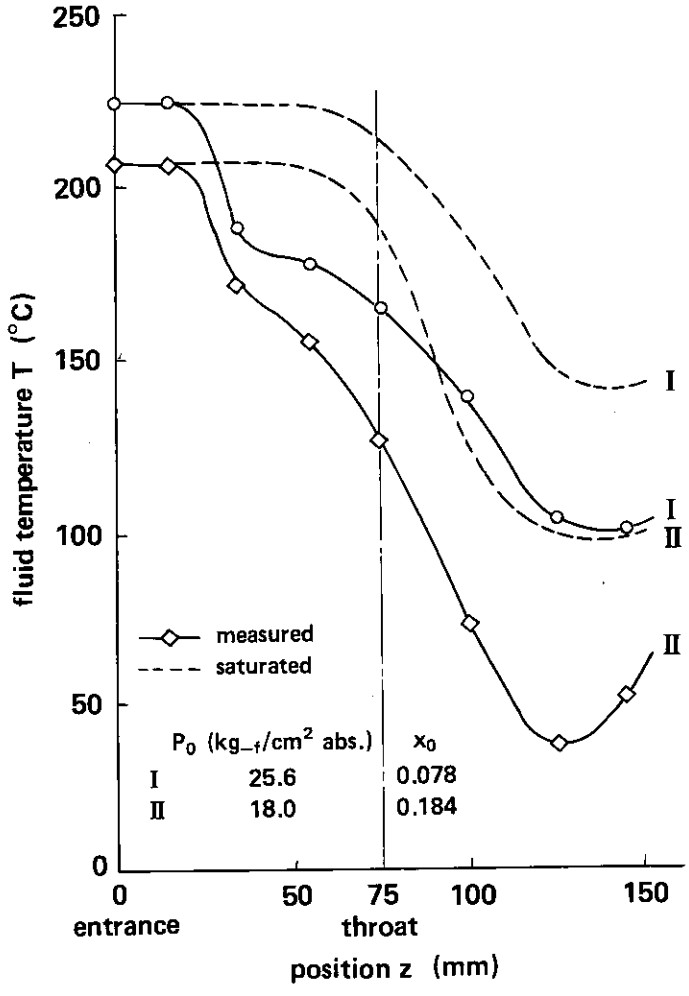

Fig. 39 Examples of axial fluid temperature change in a converging-diverging nozzle.

According to **Fig. 39**, fluid temperature T does not change so much until 15 mm downstream from the test nozzle entrance. And then it significantly decreases into the very strong supercooled state about 50°C lower than the local saturation temperature until 55 mm. After that, it continuously decreases with decrease in the saturation temperature with keeping almost constant supercooling. After arrival at 55 ~ 75 mm upstream form the test nozzle exit, the fluid temperature shows a recovery and supercooling becomes slightly smaller.

Specially interest point of this axial distribution of fluid temperature is the remarkable temperature decrease in the region between 15 and 35 mm. It must be noted that there is

still no significant pressure drop in this region as shown in **Fig. 34**. The ratio of temperature decrease to pressure decrease in this region is much larger than that for adiabatic expansion without phase change of single-phase steam. This fact will be discussed in the next section.

Including the examples shown in **Fig. 39**, difference between fluid temperature and the saturation temperature is almost constant in the region between 55 and 145 mm from the test nozzle entrance. Relationship between measured temperature and pressure in this region for various discharge conditions is shown in **Fig. 40**. It is evident that about 50°C supercooling in average is realized in this region regardless of discharge condition.

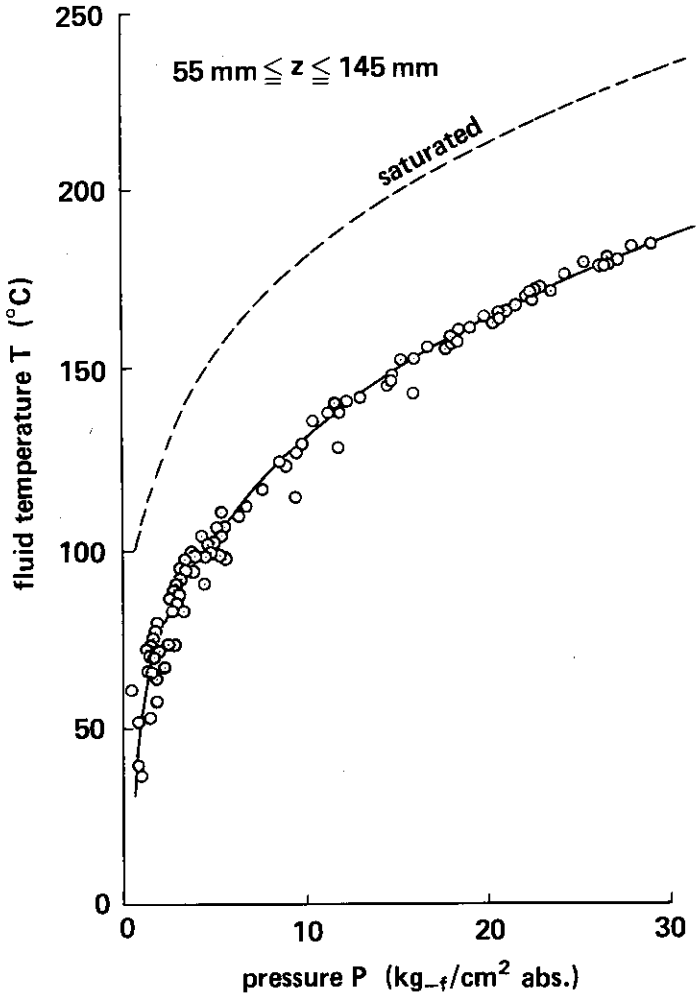

Fig. 40 Relationship between pressure and fluid temperature changes in a converging-diverging nozzle.

5.4 Discussions

Various experimental facts introduced in the previous section indicate the thermal non-equilibrium of two-phase critical discharge flow in a short converging-diverging nozzle. Thermally non-equilibrium phenomenon of two-phase critical discharge flow caused by evaporation delay is well known. That is, when high temperature subcooled water or the saturated water discharges through a sharp-edged orifice, cylindrical mouth (short pipe), diverging mouth, converging-diverging nozzle or long pipe, thermal non-equilibrium is realized because evaporation can not follow the too rapid depressurization of fluid. In such case,

discharge flow rate becomes larger than the equilibrium case and fluid temperature becomes higher than the local saturation temperature. When quality of discharge two-phase flow is almost zero, this kind of thermal non-equilibrium is confirmed in this experiment too, as shown typically in **Fig. 36**.

On the other hand, in this experiment, the other kind thermal non-equilibrium is observed with or without the above described non-equilibrium. The special feature is lower fluid temperature than the local saturation temperature. This kind of thermal non-equilibrium is supposed, as described later, to be caused by lack of interfacial area between two phases when expansion rate is very high. Therefore, let us call it "thermal non-equilibrium due to lack of interfacial area between two phases".

Solid line in **Fig. 41** shows the relationship between pressure and fluid temperature in the test nozzle under thermal non-equilibrium due to lack of interfacial area. Let us call the regions 1-2, 3-4 and 4-5 as Regions A, B and C, respectively. In this example, transition region 2-3 exists between Regions A and B but such transition region is often unclear.

In Region A, corresponding to the region near the test nozzle entrance, remarkable progress of supercooling is seen in spite of relatively small pressure drop. The reason is as follows.

In this example, quality at the test nozzle entrance is 0.082. Therefore, superheating of

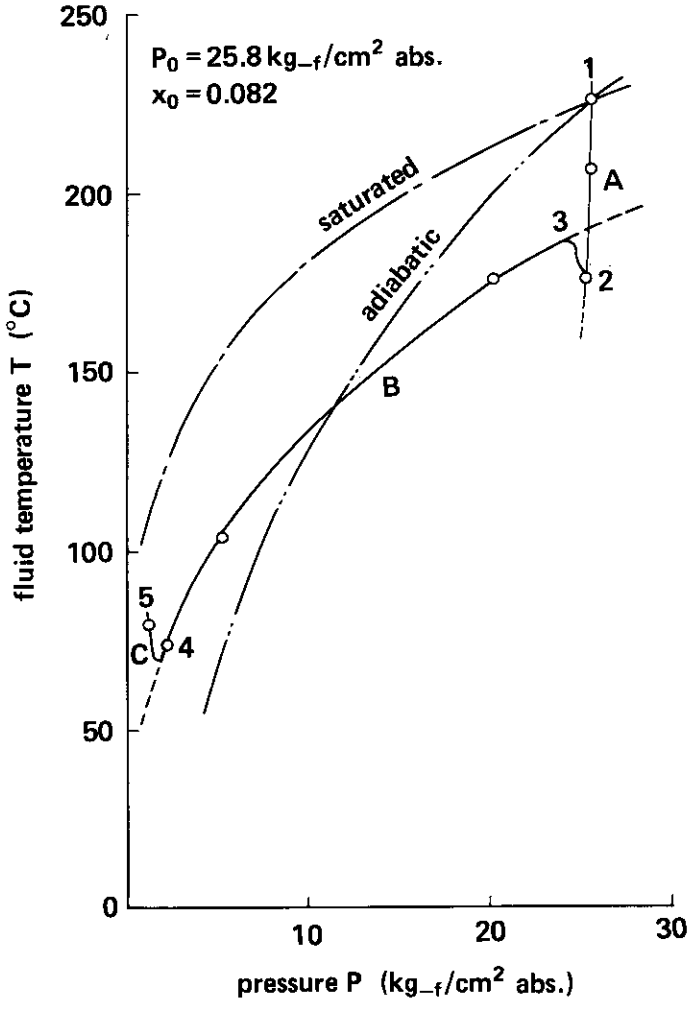

Fig. 41 Example of a temperature decreasing during depressurization in a converging-diverging nozzle.

liquid phase due to lack of boiling nuclei cannot occur. However, mixing of two phase is supposed not so good and resultantly interfacial area is relatively small because flow velocity approaching the test nozzle entrance is very small. Such two-phase fluid is suddenly depressurized after comming into the test nozzle. Axial pressure gradient corresponding to Region A is not so large but the depressurization rate of two-phase fluid is estimated to be larger than at least 500 kg-f/cm^2/s. By this depressurization, evaporation occurs at the interface. And phase change rate per unit interfacial area is supposed very high because of small interfacial area. Since latent heat for the evaporation is provided by heat conduction from inside of liquid phase, conduction limiting would occur. Therefore, very steep temperature gradient would appear in the liquid phase side at the interface.

On the other hand, since there is high speed steam flow from interface toward inside of steam phase, velocity of steam molecules impinging on liquid phase probablistically shifts smaller, i.e., effectivd pressure acts on liquid phase is reduced. Therefore, interfacial temperature can decrease to the saturation temperature corresponding to the reduced pressure. Thus, steam with lower temperature than the saturation temperature corresponding to the measured pressure is possible to be generated.

Steam temperature, in this case, is not limited by the adiabatic expansion curve of steam because temperature of generated steam itself is low. The fact that temperature decreasing rate in Region A of **Fig. 41** is much larger than that for adiabatic expantion of steam without phase change can be explained by the above described idea.

On the other hand, generated steam abides as a gas by the thermodynamical laws. During rapidly decreasing process of interfacial temperature, steam temperature at remote point should be higher than interfacial temperature because steam at the point was generated when interfacial temperature was higher and has been expanded adiabatically. Therefore, temperature distribution near the interface is qualitatively supposed for Region A as illustrated in **Fig. 42(a)**.

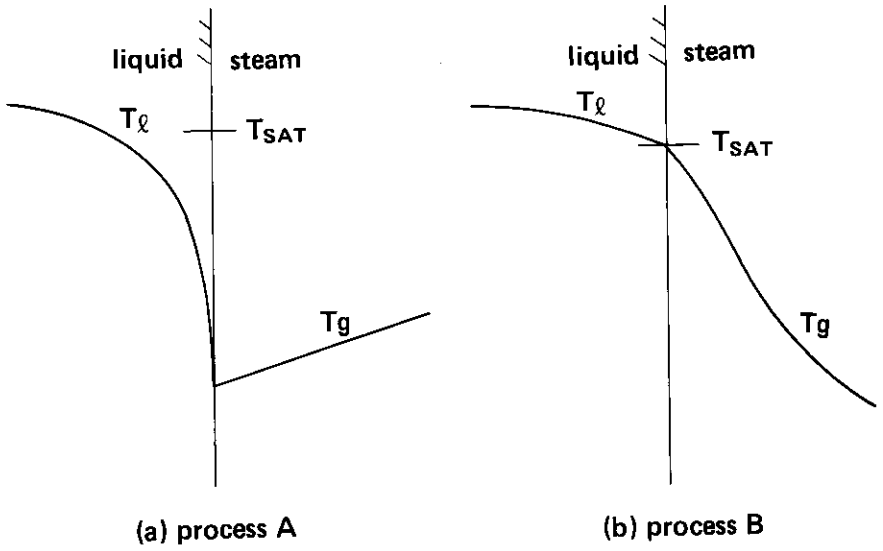

Fig. 42 Supposed temperature distribution near the steam-water interface.

Temperature inside liquid phase is, in such situation, supposed higher than the saturation temperature T_{sat}. Superheat of liquid phase increases with decreasing of T_{sat} due to fluid depressurization. And at last explosive steam generation (sudden boiling) occurs in the liquid phase and flow regime will change into fine droplet flow. Boundary of Regions A and B

(the transition region 2-3) of **Fig. 41** is considered to indicate such sudden boiling. Since interfacial area becomes very large after the sudden boiling, sensible heat of liquid phase is rapidly released and much steam is generated. Resultantly, axial pressure gradient becomes significantly larger and relationship between fluid temperature and pressure drastically changes. These facts were already introduced in the previous section.

After the sudden boiling, since interfacial area is sufficiently large, interfacial temperature will be almost the same as the saturation temperature. However, at remote point, lower temperature steam will exist, which was generated before the sudden boiling. Therefore, temperature distribution near the interface is qualitatively supposed for Region B as illustrated in **Fig. 42(b)**. Indeed but, temperature distribution as shown in **Fig. 42(a)** can continue some axial length because interfacial area is still insufficient.* Concave characteristic of mass velocity shown in **Fig. 35** might be resulted from such kind of lack of interfacial area.

In Region B, steam phase expands not adiabatically but receiving heat from liquid phase. Therefore, gradient of T–P curve is smaller than that for adiabatic expansion of steam without phase change, as seen in **Fig. 41**.

Next, Region C is considered to be the attenuation process of thermal non-equilibrium by termination of depressurization or pressure recovery.

At last, let us investigate the effect of thermal non-equilibrium due to lack of interfacial area between two phases on critical mass velocity.

Firstly, total amount of phase change rate in the test nozzle becomes larger due to the non-equilibrium. Let us assume, for simplicity, that thermal non-equilibrium appears only in the test nozzle and at the entrance and the exit of the test nozzle the fluid state is on the equilibrium. Change of state in the test channel will be not purely isentropic but rather isenthalpic because of the thermal non-equilibrium. Therefore, phase change mass is larger for given pressure drop and increase in kinetic energy is smaller in comparison with the equilibrium case. This is considered to reduce the discharge flow rate.

Secondly, phase change does not occur uniformly throughout the test nozzle but occur mainly in Region B around the throat. The position of critical flow occurrence is the throat or just downstream of the throat evidently included in Region B. Therefore, larger effective compressibility of fluid due to larger phase change per unit pressure drop in Region B in comparison with the equilibrium case will make the critical mass velocity smaller.

Thus, thermal non-equilibrium due to lack of interfacial area is considered to reduce the critical mass velocity and **Fig. 38** evidently indicates the fact. Some reduction of critical mass velocity due to wall friction also should, of course, be seen in this experiment. Therefore, quantitative evaluation of the effect of wall friction is necessary to investigate the effect of thermal non-equilibrium due to lack of interfacial area in more detail.

5.5 Conclusion

The following conclusions were obtained after two-phase critical discharge experiment through a converging-diverging nozzle, which was performed to clarify the effect of thermal non-equilibrium on two-phase critical discharge flow phenomena.

(1) In addition to regular thermal non-equilibrium due to steam generation delay, different kind of thermal non-equilibrium occured, which was supposed to be due to lack of interfacial area between two phases.

* Interfacial area rapidly increases indeed due to the sudden boiling. On the other hand, axial pressure gradient and linear velocity of fluid also increase. Therefore, depressurization rate of fluid drastically increases too. Whether interfacial area is enough or not is the result of these two opposite effects.

(2) Fluid temperature measured were lower than the local saturation temperature under thermal non-equilibrium due to lack of interfacial area and the supercooling attained up to 50°C.

(3) Thermal non-equilibrium due to lack of interfacial area reduced the critical mass velocity. Resultantly, discharge flow rate was smaller than the theoretical value under perfect phase equilibrium assumption except for almost zero reservoir quality case.

(4) Relationship between mass velocity and pressure showed concave characteristic in downstream of throat when reservoir quality was less than 0.10.

6. Two-Phase Critical Discharge Experiment with a Large Sharp-Edged Orifice[43]

6.1 Introduction

Discharge flow rate W from the breaks in loss-of-coolant accident of a light water cooled nuclear reactor can be represented for the saturated blowdown process as:

$$W=C_D A G_C \tag{81}$$

Here, G_C is critical mass velocity of the saturated two-phase flow and can be calculated with respect to given reservoir pressure and quality under the seven fundamental assumptions described in the section 2.1.

On the other hand, discharge coefficient C_D represents the effect of flow contraction, friction and phase non-equilibrium. In the case of sharp-edged orifice directly attached to the pressure vessel it should be expressed generally as function of pressure and quality at the high pressure reservoir and the orifice diameter.

Value of 0.6 through 0.8 is recommended for discharge coefficient C_D through LOFT-Semiscale experimental analysis[44] and also **Table 1** is obtained by Sobajima[1],[45] in ROSA-I Project at JAERI. In these experimental analyses, C_D was determined based on G_C calculated with Moody's theory[4] and, in addition, C_D was selected with a trial-and-error method so as to obtain good prediction of pressure, temperature and residual water mass transients in much smaller scale test facility than actual reactor by using blowdown analysis code such as RELAP-2 or -3.

Table 1 C_D-value determined with RELAP-3 code (ROSA-I)

disch. mode	orifice diameter (mmϕ)	initial pressure (kg-f/cm^2 g)		
		40	70	100
bottom discharge	1 volume			
	25		1.20	
	50		0.80	
	70	0.85	0.73	0.73
	100	0.73	0.63	0.63
	125		0.60	0.60
top discharge	1 volume			
	25	0.60	0.65	
	50		(0.60)	(0.60)
	70	(0.55)	(0.55)	(0.55)
	2 volume			
	25	0.75	0.80	
	50		0.65	0.65
	70	0.60	0.60	0.60
	4 volume			
	25	0.80		
	50	0.65	0.65	

Instant value of C_D cannot be obtained for reservoir pressure and quality at each time point by such method. Therefore, functional relationship among the pressure, quality and C_D cannot be established. In addition, obtained C_D value is directly affected by facility characteristics and imperfectness of blowdown analysis codes used. So that, there is some doubt on applicability of C_D to reactor accident analysis.

In this chapter, G_C will be calculated with the two-phase critical flow theory introduced in Chapter 2 for measured reservoir pressure and estimated reservoir quality with the depressurization rate method established in Chapter 5. C_D of large sharp-edged oriffice will be determined experimentally by directly applying Eq. (81) for various reservoir pressure and quality.

6.2 Test Facility

Detail of ROSA–I Test Facility is given in Ref. (1). The major part is a stainless steel vertical cylindrical vessel with inner diameter of 560 mm and inner axial length of 7080 mm as shown in **Fig. 43**. Volume of the pressure vessel is about 1.9 m^3. It can store high temperature and high pressure water upto 310°C and 100 kg-f/cm^2g. The water is discharged from the top or bottom discharge nozzle with inner diameter of 350 mm by artificially breaking the repture disc attached to the eigher discharge nozzle. Sharp-edged orifice with dimension shown in **Fig. 44**, which is set at just upstream of the rupture disc unit, gives break diameter. Pressure and residual water mass transients in the pressure vessel during blowdown process are detected with strain-gauge type pressure transducers, semi-conductor type pressure

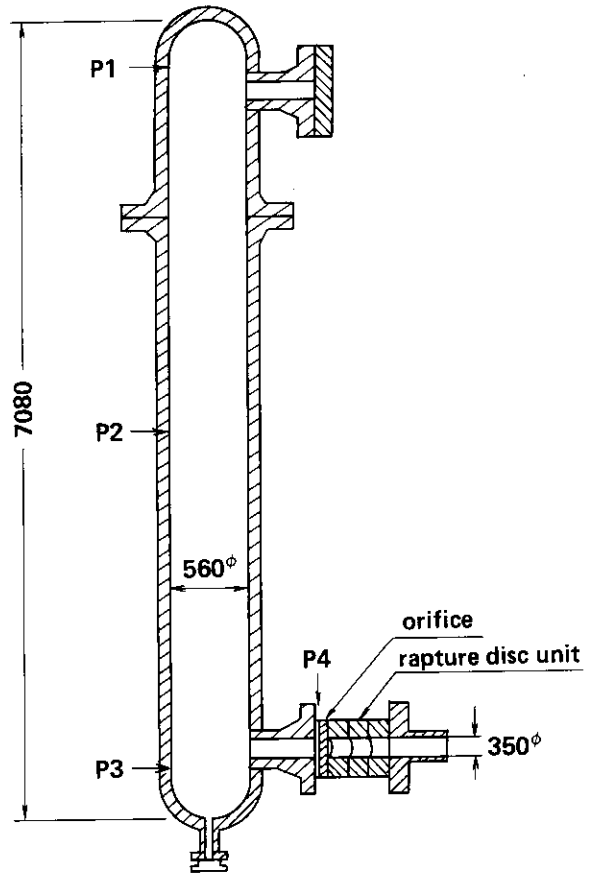

Fig. 43 Pressure vessel of ROSA–I test facility.

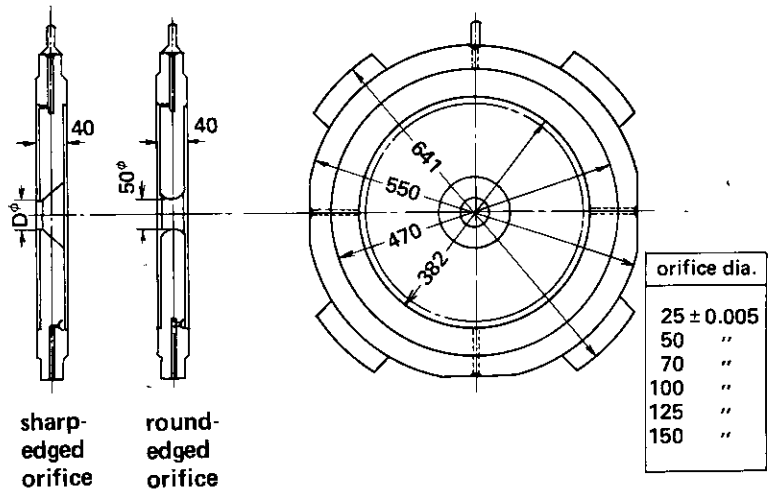

Fig. 44 Test orifices for ROSA–I.

transducers or strain-gauge type differential pressure transducers and are recorded with a data acquisition system.

Many kinds of blowdown tests were performed in ROSA–I Project but only the data from tests without vessel internals are referred in this chapter in order to obtain accurate estimation of flow rate and quality of discharge two-phase flow.

6.3 Analytical Method

Discharge flow rate W from the break was obtained by differentiating residual water mass data with differential pressure method with respect to time.

Reservoir quality was calculated by using depressurization rate method introduced in the subsection 5.2.4. Critical mass velocity G_C was calculated for the reservoir quality and the measured pressure vessel pressure with the theory introduced in Chapter 2 (See **Fig. 8.**) and finally discharge coefficient C_D was calculated by Eq. (81).

To make blowdown behavior clear, normalized steam generation rate B and normalized steam accumulation rate M in the pressure vessel were defined as follows:

$$B \equiv \frac{dw_{PC}/dt}{W}$$

$$= -\frac{1}{h_s - h_w}\left(w_s \frac{dh_s}{dP} + w_w \frac{dh_w}{dP} - V\right)\frac{1}{W}\frac{dP_0}{dt} \tag{82}$$

$$M \equiv \frac{dw_s/dt}{W}$$

$$= \frac{v_w}{v_s - v_w} - \frac{1}{v_s - v_w}\left(w_s \frac{dv_s}{dP} + w_w \frac{dv_w}{dP}\right)\frac{1}{W}\frac{dP_0}{dt} \tag{83}$$

6.4 Experimental Results and Discussions

6.4.1 Discharge process

Shown in **Fig. 45** are typical transients of x_0, B and M for bottom discharge. Here, initial pressure vessel pressure is 70 kg-f/cm²g and orifice diameter is 70 mm. During about 10 s

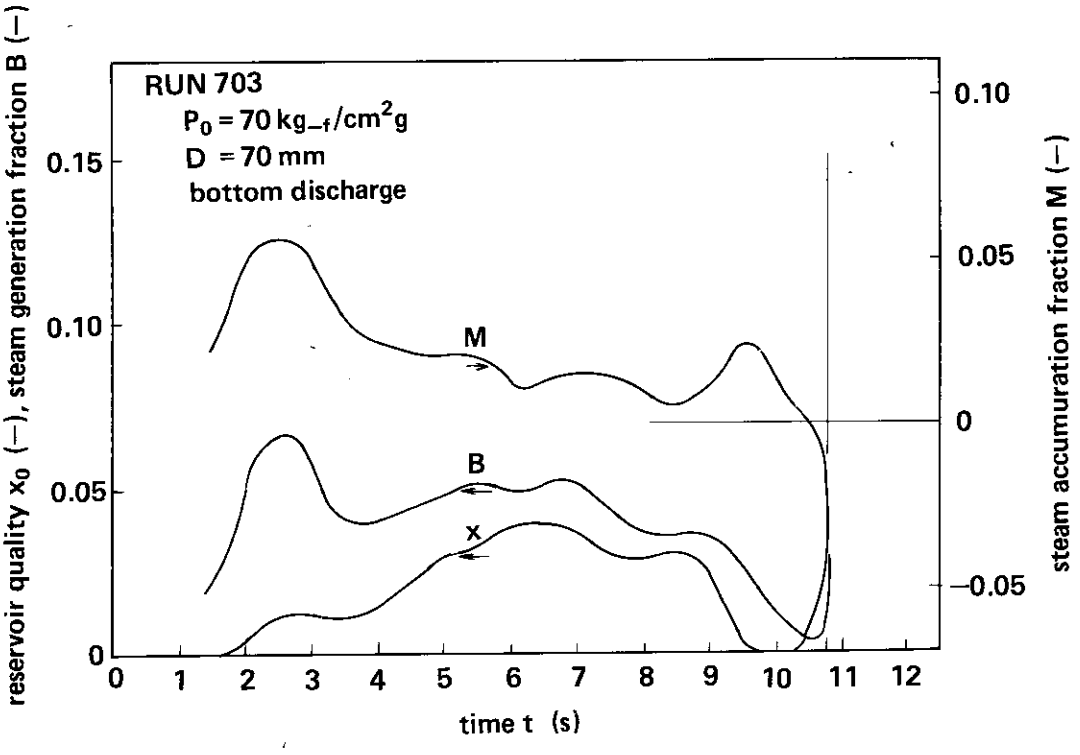

Fig. 45 Examples of variable changes during bottom discharge.

after discharge initiation, normalized steam generation rate B is relatively small and it increases thereafter. Reservoir quality x_0 behaves almost similarly. That is, discharge flow changes, in this example, from water dominant flow to steam dominant one between 10 and 11 s. This transition occured due to pressure vessel water level lowering to around the discharge nozzle elevation. In bottom discharge, water dominant discharge and steam dominant discharge are generally separated clearly.

During water dominant discharge, x_0 increases from about 0.0 at 1.5 s to about 0.05 at 6.5 s and then it decreases and becomes about 0.0 again at 9.7 s.

The reasons of the decrease in x_0 in the latter half of the process are change of state values due to depressurization and reduction of B due to decrease in residual water mass.

Next, normalized steam accumulation rate M is positive and gradually decreases during water dominant discharge and becomes negative large number after entering in steam dominant discharge. That is, flow is maintained by steam expansion more than by steam generation in steam dominant discharge.

Shown in **Fig. 46** are typical transients of x_0, B and M for top discharge. Here, initial pressure vessel pressure is 100 kg-f/cm²g. and orifice diameter is 50 mm. As known from this figure, B and x_0 both increases monotonuously with time and M decreases monotonously from positive to negative in top discharge. Water dominant discharge and steam dominant discharge are not separated clearly in top discharge.

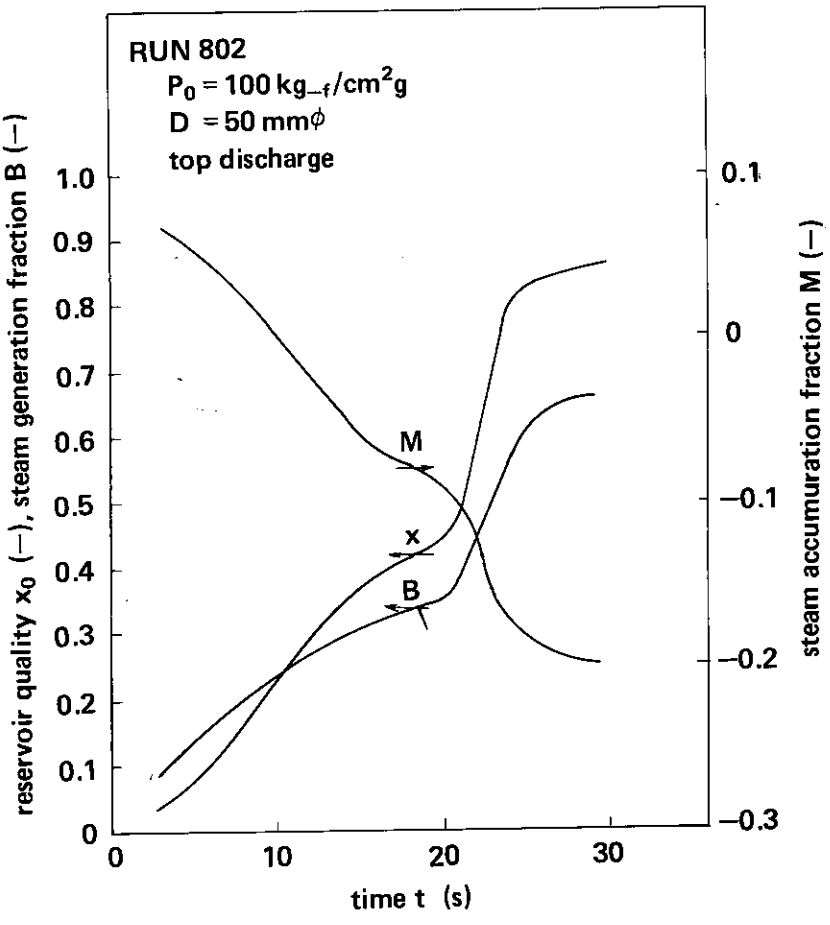

Fig. 46 Examples of variable changes during top discharge.

6.4.2 Discharge coefficient of sharp-edged orifice

Shown in **Figs. 47** and **48** are changes of two-phase discharge coefficient C_D with respect to x_0 for sharp-edged orifices with diameters of 25 mm and 70 mm, respectively. Similar results for varous size sharp-edged orifices are summarized in **Fig. 49**. From these figure, the following knowledges are led.

(1) C_D is almost constant and independent of x_0 except region of x very close to zero. This value is smaller when orifice diameter is larger and effect of pressure is almost negligible between 5 and 100 kg-f/cm^{2}g.

(2) When x_0 is very close to zero, C_D increases drastically with decrease in x and attains 1.5 in the case of 25 mm diameter orifice. Effect of P_0 seems very small but C_D is slightly larger when P_0 is lower.

6.4.2.1 $x_0 \gg 0$

As described previously, C_D is almost constant and independent of x_0 when $x_0 \gg 0$. Some examination will be made below on the value of C_D.

The first possible reason of smaller C_D than 1.0 is the effect of flow contraction just downstream of orifice. In the case of single-phase water flow, orifice coefficient C defined by

$$W = CA\sqrt{2\rho_l(P_0 - P)} \tag{84}$$

is about 0.61 for a sharp-edged orifice. Therefore, if the same order flow contraction occurs in two-phase flow too, $C_D \approx 0.61$ should hold good. Since two-phase fluid has very large

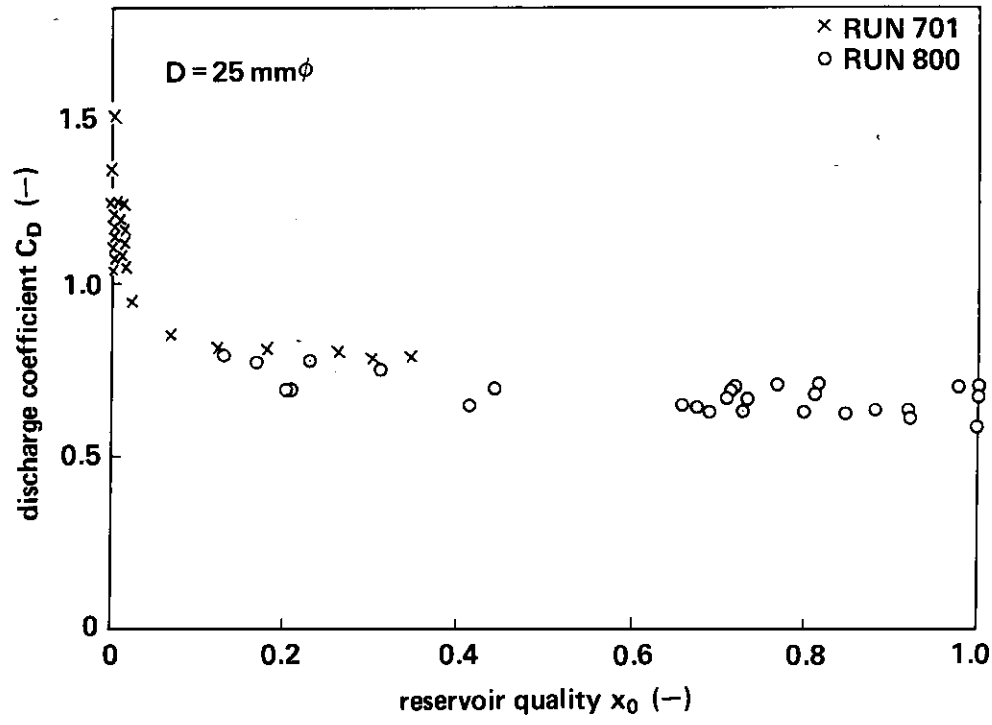

Fig. 47 Two-phase discharge coefficient of sharp edged orifice (1).

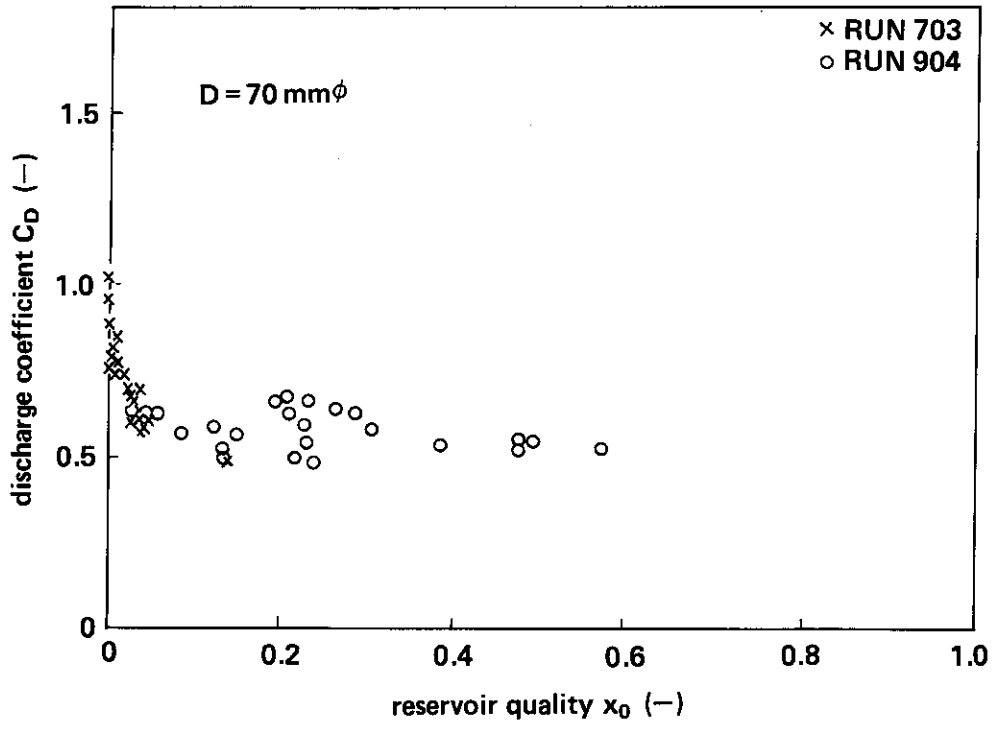

Fig. 48 Two-phase discharge coefficient of sharp edged orifice (2).

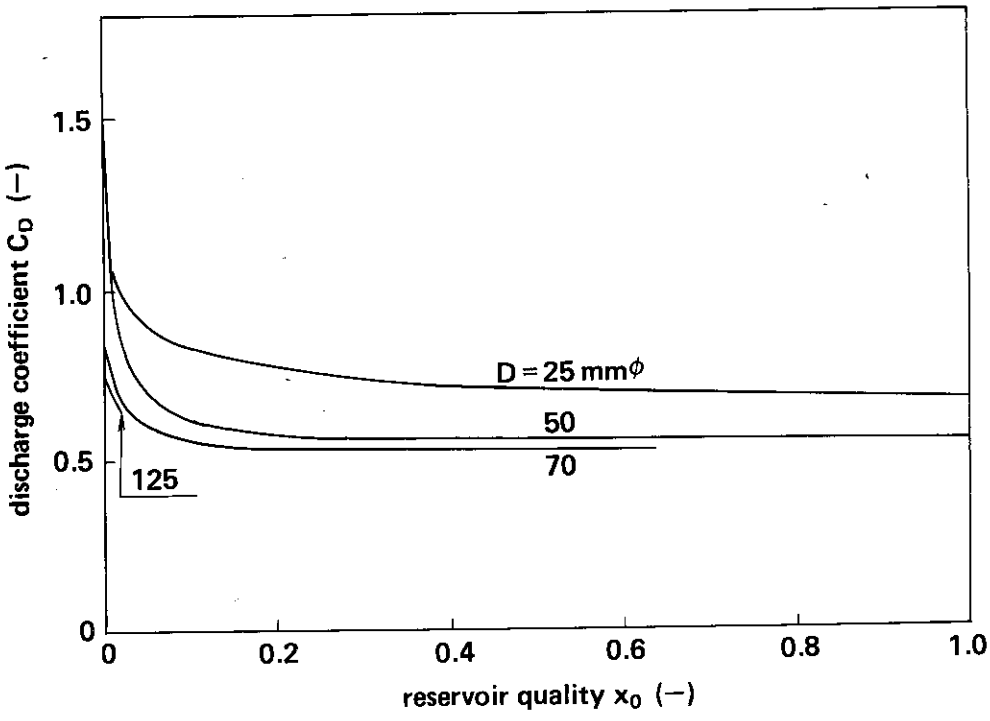

Fig. 49 Summary of two-phase discharge coefficient of sharp-edged orifice.

compressibility, $C_D>0.61$ is supposed rather reasonable. However, measured C_D is, as clearly shown in **Fig. 49**, $C_D<0.61$ except for 25 mm diameter orifice, suggesting the effect of some other phenomenon than flow contraction.

To make clear on this point, C_D data for a round orifice is given in **Fig. 50**, for which almost no flow contraction is expected. Here, initial pressure vessel pressure is 70 kg-f/cm²g. and orifice diameter is 50 mm. The C_D value is only about 0.1 larger than that for sharp-edged orifice, i.e. effect of flow contraction on C_D of sharp-edged orifice is supposed to be in the order of −0.1.

For the other cause of decreased C_D from 1.0 than flow contraction, thermal non-equilibrium due to lack of interfacial area between two phases can be raised, which was pointed out in Chapter 5. That is, when two-phase fluid is very rapidly decompressed, super-cooled steam is generated because of lacking interfacial area and then sudden boiling creates much amount of steam. Due to this series of non-equilibrium phenomena, two-phase critical discharge flow is supposed to be decreased. **Figure 51** shows an example of measured fluid temperature T_b at just downstream of sharp-edged orifice in a bottom discharge experiment. Here, initial pressure vessel pressure is 70 kg-f/cm²g. and orifice diameter is 70 mm. Large supercooling of steam is seen throughout the discharge process in comparison with the saturation temperature T_{sat} obtained from pressure data at just downstream of the orifice. Especially, in initial stage of the steam dominant discharge process with rapid decrease in pressure vessel pressure P, about 50°C supercooling in the maximum is realized. Therefore, it is reasonably supposed that decrease in critical mass velocity due to such remarkable thermal non-equilibrium possibly caused the small C_D.

6.4.2.2 $x_0 \approx 0$

As shown in **Fig. 49**, a large C_D appears when x_0 is very close to zero. The reason is, as well known, lack of boiling nuclei. In such situation, discharge characteristic becomes similar

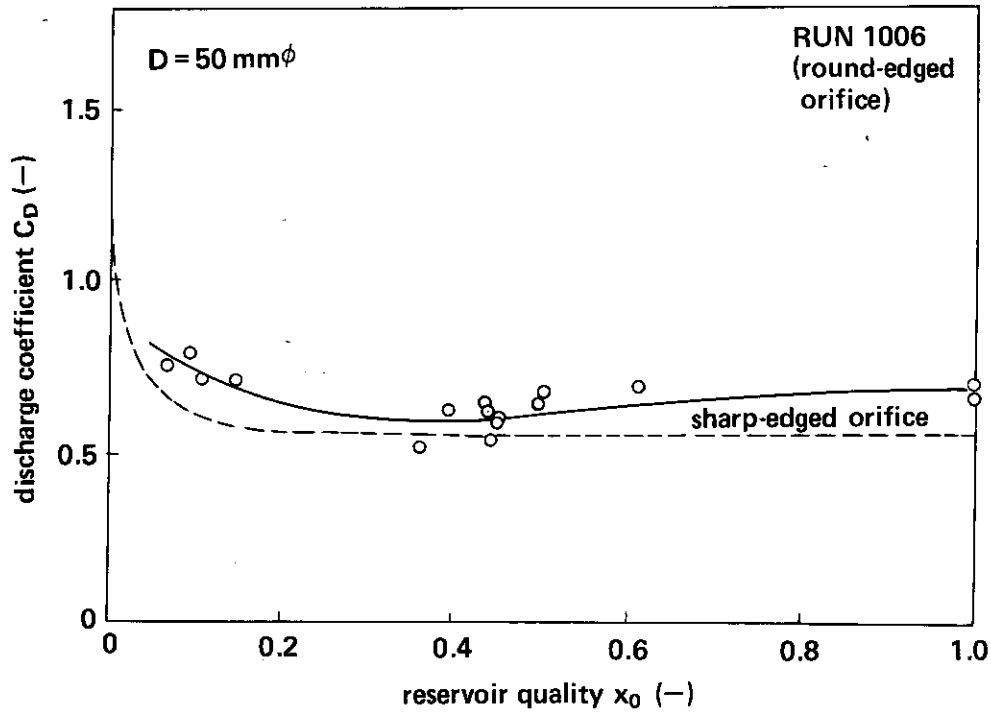

Fig. 50 Two-phase discharge coefficient of round-edged orifice.

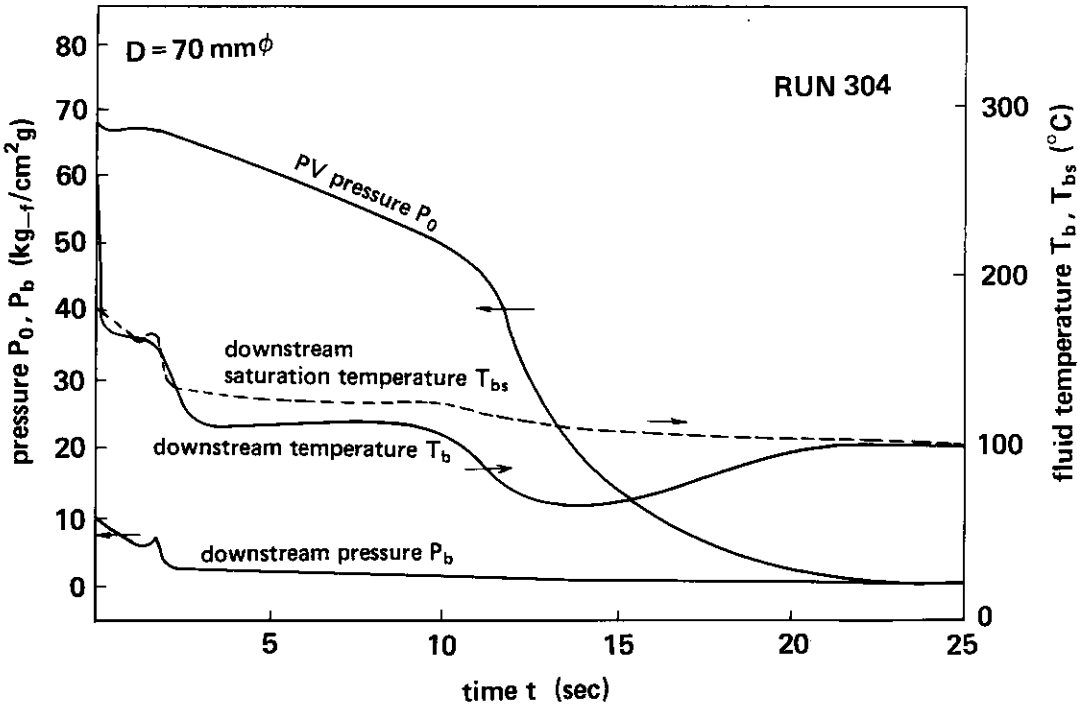

Fig. 51 Thermal non-equilibrium at just downstream of orifice.

to that for single-phase water flow because steam generation cannot follow the too rapid decompression due to flowing through the orifice. Let us estimate C_D for discharge of the single-phase saturation water of $x_0 = 0.0$ without phase change based on Eq. (81). Then

$$C_{D0} = \frac{0.61\sqrt{2\rho_l(P_0 - P_b)}}{G_c(P_0, 0)} \tag{85}$$

When $P_b = 1$ kg-f/cm^2 abs., relationship between P_0 and C_{D0} is calculated as shown in **Fig. 52**. According to this figure, $C_{D0} > 1.0$ holds good except for very low pressure case and C_D of 1.6 ~ 1.7 can be reasonably realized for the range of present experimental condition. $C_D \approx 1.5$ for the 25 mm diameter orifice is, therefore, really reasonable. In addition, C_D monotonously decreases with P_0 for the region of $P_0 > 20$ kg-f/cm^2 abs. in **Fig. 52**. This is considered to have caused a weak negative effect of P_0 on C_D value as previously described.

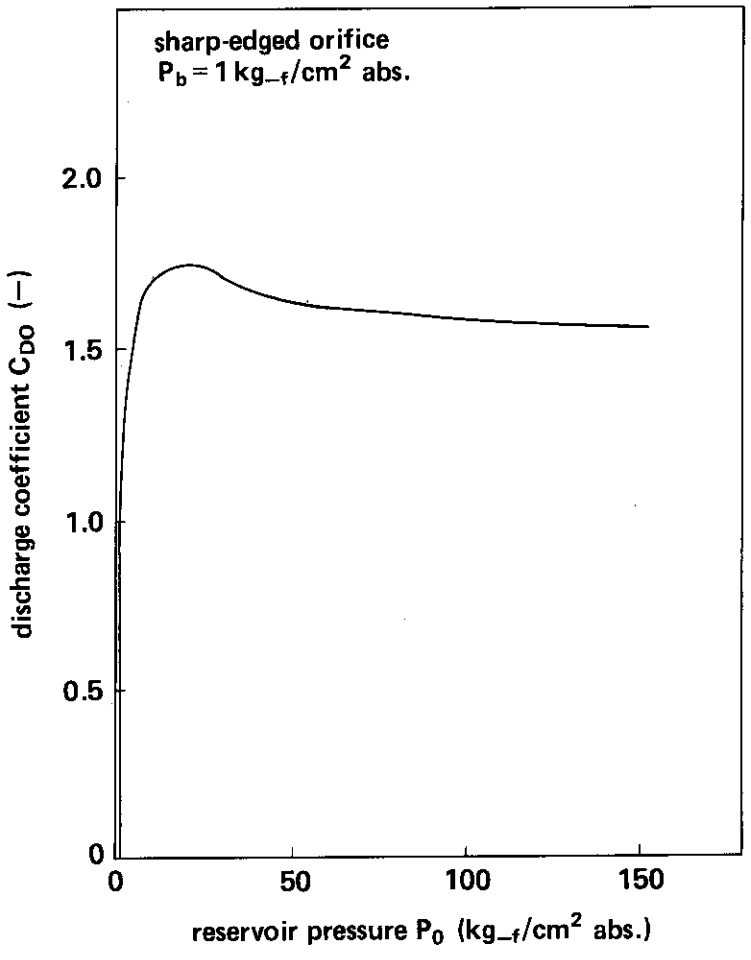

Fig. 52 Predicted two-phase discharge coefficient for the saturation water (non-equilibrium model).

6.4.3 Comparison with RELAP code analysis

C_D value determined by Sobajima based on ROSA–I test data by using a trial-and-error method with RELAP-3 code are given in **Table 1**. Comparison of this table with **Fig. 49** is very interesting.

C_D for bottom discharge listed in **Table 1** was selected so as to predict well the transients of pressure, temperature, etc. mainly during water dominant discharge period. Therefore, the C_D value is corresponding to the average quality in water dominant discharge period, which

is very small. On the other hand, C_D for top discharge is for relatively large quality range.

Taking such facts into account, C_D in **Table 1** is quite reasonable in both effect of orifice diameter and effect of pressure vessel pressure. However, the results listed in **Table 1** is affected not only by prediction ability of RELAP-3 code but also by ROSA–I test itself. For example, average quality in water dominant discharge period can be different depending on facility even if initial pressure vessel and orifice diameter are common. Even for ROSA–I test, the average quality is changeable if vessel internals are inserted. C_D listed in **Table 1** is affected by such various things.

On the other hand, C_D shown in **Fig. 49** is determined for each instant with analytical method introduced in Chapter 2 based on right basic equation set and clear fundamental assumptions and measured values of P_0 and x_0. Therefore, it can be applied to any cases if only the two-phase critical flow is realized at a sharp-edged orifice.

6.5 Conclusions

In this chapter, two-phase discharge coefficient C_D, which is very important parameter to well predict the discharge flow rate from the breakes in LOCA analysis for a light water cooled nuclear reactor, was determined for a large sharp-edged orifice by applying the two-phase critical flow theory introduced in Chapter 2 and the depressurization rate method for measuring quality of discharge two-phase flow introduced in Chapter 5. The results are summarized in **Fig. 49**. The following conclusions are obtained.

(1) The relationship between discharge coefficient C_D and reservoir quality x_0 is devided into two regions: region of $x_0 \gg 0$ without effect of x_0 and region of $x_0 \approx 0$ with strong effect of x_0.

(2) In the region of $x_0 \gg 0$, C_D is almost independent of both x and P_0 and is determined mainly by orifice diameter D. The larger D gives the smaller C_D. C_D is $0.8 \sim 0.52$ when D is $25 \sim 125$ mm, i.e., less than 1.0. Flow contraction effect on C_D is in the order of only 0.1 and thermal non-equilibrium around orifice is supposed to be the major cause of the smaller C_D than 1.0.

(3) In the region of $x_0 \approx 0$, C_D drastically increases with decrease in x_0 and attains up to 1.5 for 25 mm diameter orifice. C_D becomes smaller for larger D and for higher P_0. The larger C_D in the region of $x_0 \approx 0$ is considered to be caused by steam generation delay and the discharge characteristics is rather similar to that for single-phase water flow.

(4) The results shown in **Fig. 49** justifies the C_D values determined with trial-and-error method by using RELAP-3 code.

(5) The results shown in **Fig. 49** have a wide applicability and is applicable if only the break is considered as a sharp-edged orifice, because it is not affected by facility characteristics of ROSA–I.

7. Frictional Energy Dissipation of Vertical Gas-Liquid Two-Phase Flow without Phase Change[46]

7.1 Introduction

In Chapter 6 of Part I, concept of perfectly settled one-dimensional two-phase flow was introduced. The perfectly settled one-dimensional two-phase flow is a special flow from the view point of basic equation set because an additional condition is applied. However, there are actually many one-dimensional two-phase flows which can be considered as perfectly settled. In addition, one can simplify his analysis or can evaluate some quantities which are not measured in his experiment by assuming the perfectly settled situation. Therefore, the perfectly settled assumption is practically very convinient and useful.

In this chapter, as such example, evaluation results on total, interfacial and wall frictional energy dissipations of two-component vertical two-phase flow under the perfectly settled assumption will be introduced.

7.2 Theory

As known from Eqs. (47), (48) or (49), (50) of Part I,

$$\frac{dP}{dz}+\rho_g g-F_{GL}-F_{GW}=0 \tag{86}$$

$$\frac{dP}{dz}+\rho_l g-F_{LG}-F_{LW}=0 \tag{87}$$

hold good for vertical, upward, steady, two-component two-phase flow without acceleration.

By multiplying Eqs. (86) and (87) by Q_g/A and Q_l/A, respectively, and summing up the results, mechanical energy balance equation of two-phase flow per unit volume of channel per unit time can be obtained, i.e.,

$$\frac{Q_g+Q_l}{A}\frac{dP}{dz}+\frac{\rho_g Q_g+\rho_l Q_l}{A}g-\frac{F_{GL}Q_g+F_{LG}Q_l}{A}-\frac{F_{GW}Q_g+F_{LW}Q_l}{A}=0 \tag{88}$$

Here, the third and fourth terms of Eq. (88) are mechanical work done overcoming interfacial and wall frictional forces, respectively, and are the energy dissipations due to these frictions. Representing energy dissipation per unit volume of channel per unit time by E_T

$$E_T=-\frac{F_{GL}Q_g+F_{LG}Q_l}{A}-\frac{F_{GW}Q_g+F_{LW}Q_l}{A} \tag{89}$$

Therefore, from Eqs. (88) and (89)

$$E_T=-\frac{Q_g+Q_l}{A}\frac{dP}{dz}-\frac{\rho_g Q_g+\rho_l Q_l}{A}g \tag{90}$$

On the other hand, in the perfectly settled, vertical upward two-phase flow, interfacial frictional forces F_{GL} and F_{LG} are given, from Eqs. (107) and (108) of Part I, as:

$$F_{GL}=-(1-\alpha)(\rho_l-\rho_g)g \tag{91}$$

$$F_{LG}=\alpha(\rho_l-\rho_l)g \tag{92}$$

Therefore, interfacial frictional energy dissipation E_I per unit volume of channel per unit time is obtained by multiplying Eqs. (91) and (92) by $-\alpha u_g$ and $-(1-\alpha)u_l$, respectively, as:

$$\begin{aligned} E_I&=\alpha(1-\alpha)(\rho_l-\rho_g)(u_g-u_l)g \\ &=\frac{1}{A}\alpha(1-\alpha)(\rho_l-\rho_g)\left(\frac{Q_g}{\alpha}-\frac{Q_l}{1-\alpha}\right)g \end{aligned} \tag{93}$$

Wall frictional energy dissipation E_W per unit volume of channel per unit time is, therefore, derived by subtracting Eq. (93) from Eq. (90), as:

$$\begin{aligned} E_W&=-\frac{Q_g+Q_l}{A}\frac{dP}{dz}-\frac{\rho_g Q_g+\rho_l Q_l}{A}g \\ &\quad-\frac{1}{A}\alpha(1-\alpha)(\rho_l-\rho_g)\left(\frac{Q_g}{\alpha}-\frac{Q_l}{1-\alpha}\right)g \\ &=-\frac{Q_g-Q_l}{A}\frac{dP}{dz}-\frac{Q_g+Q_l}{A}\{\alpha\rho_g+(1-\alpha)\rho_l\}g \end{aligned} \tag{94}$$

With Eqs. (90), (93) and (94), total, interfacial and wall frictional energy dissipations can be evaluated, respectively.

7.3 Application

With using Eqs. (90), (93) and (94), let us examine the frictional energy dissipation characteristics of vertical upward, two components two-phase flow based on the experiment by Shiba, et al.[24),(47)]. The experiment is for air-water two-phase flow at the atmospheric pressure and was performed with a 24.5 mm diameter and 1,350 mm long pipe. The average void fraction in the test section was measured by shutting air in the test section with two linked shut-off valves. Flow regime was also judged by observation.

Since this experiment was performed at tha atmospheric pressure, the effect of expansion of air due to pressure drop cannot be neglected. The increase in specific volume of air is about 14% in the maximum. Estimation error of interfacial frictional energy dissipation due to this is very small but wall and total frictional energy dissipation would be over-estimated because of accelerational pressure drop. This effect may be more significant when both air and water flow rates are large.

Shown in **Fig. 53** is relationship between total frictional energy dissipation E_T and average velocity $\bar{u}=(Q_g+Q_l)/A$. This result is almost same as Sekoguchi's result[48)]. From this figure, it is known that the smaller water velocity the larger total frictional energy dissipation when average velocity is less than 1.5 m/s but the relation is opposite when average velocity is more than 3 m/s. In addition, the curves show convex characteristics when water flow rate is less than 0.166 kg-m/s (355 kg-m/m²s) and average velocity is less than 1.0 m/s.

E_T in **Fig. 53** is divided into E_I and E_W as shown in **Fig. 54**. Symbols B, S, A and T are for flow regime identification and B is bubble flow, S is slug flow, A is annular flow and T is turbulent flow*, respectively. E_I increases with E_W when water flow rate is more than 0.916 kg-m/s (1,905 kg-m/m²s) but shows a concave characteristic with the maximum point when water flow rate is less than 0.166 kg-m/s (355 kg-m/m²s). Flow regime in these two cases changes from bubble flow to turbulent flow in the former and from slug flow to annular

* This naming is by the authors of Ref. (48). Maybe it is corresponding to froth or churn flow.

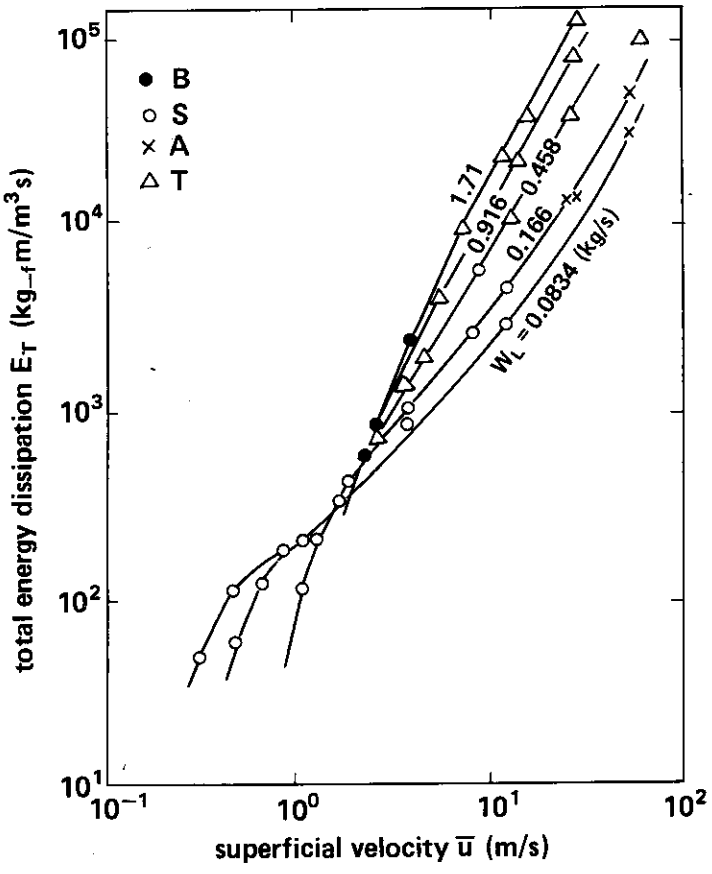

Fig. 53 Relationship between superficial velocity and total frictional energy dissipation in a vertical circular pipe with water flow rate as parameter.

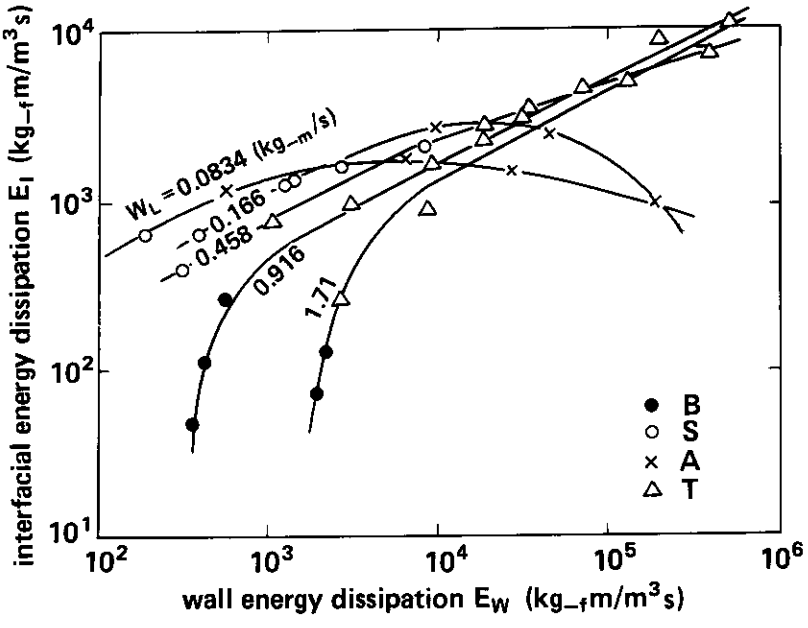

Fig. 54 Relationship between wall and interfacial energy dissipation in a vertical circular pipe with water flow rate as parameter.

flow in the latter. When water flow rate is 0.458 kg-m/s (979 kg-m/m^{2}s), relationship between E_I and E_W shows intermediate of the two and the flow regime changes from slug flow to turbulent flow.

Next, when both air and water flow rates are small in slug flow region, E_I is often larger than E_W. But when air flow rate is large such as in annular flow or turbulent flow, E_I is usually much smaller than E_W. Interfacial friction is basically controled by the gravity force and, therefore, in the higher velocity of two-phase flow the ratio of interfacial friction to wall friction is smaller. This is one of the bases of neglecting the effect of gravity and interfacial frictional forces in the previous chapters of Part II.

Shown in **Fig. 55** with linear coordinate is the similar result for low air flow rate region. There are many negative E_W data (not plotted in **Fig. 54**) in slug flow region, indicating negative wall friction. Since each data point is averaged value of seven raw data, this fact is sufficiently reliable. That is, water flow near the wall is often downward in slug flow.

Shown in **Fig. 56** is E_W with respect to the water linear velocity $u_l=Q_l/(1-\alpha)A$. In this case, also the data for water flow rate less than 0.166 kg-m/s (355 kg-m/m^{2}s) show different characteristics from others.

Dashed line in this figure show the estimated E_W for the same water linear velocity with Blasius'[20] equation. Since work done by steam flow is much larger than that by water flow for the same wall frictional force, wall frictional energy dissipation of about 15 times that for single-phase water flow with the same water linear velocity is realized.

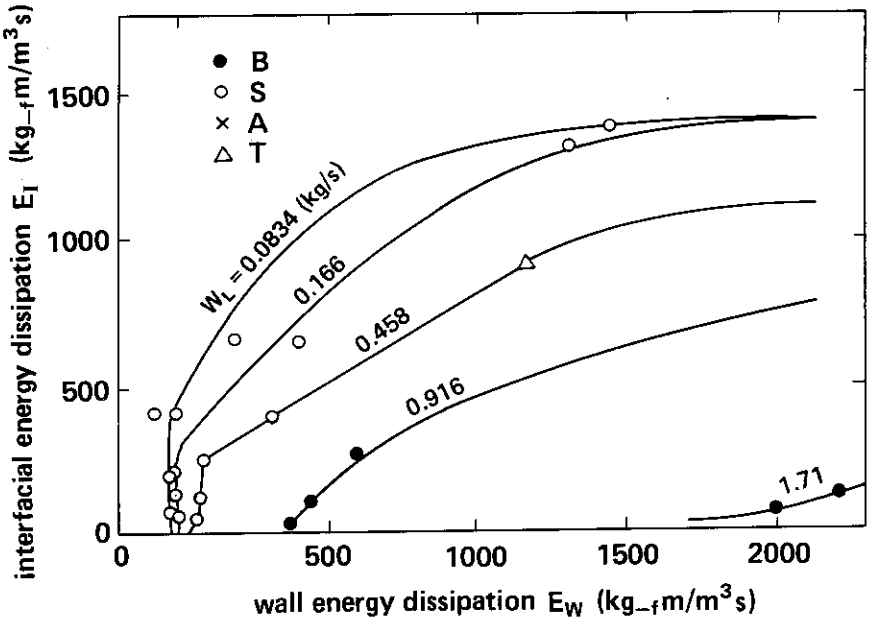

Fig. 55 Energy dissipation characteristics in low air flow rate region for a vertical circular pipe.

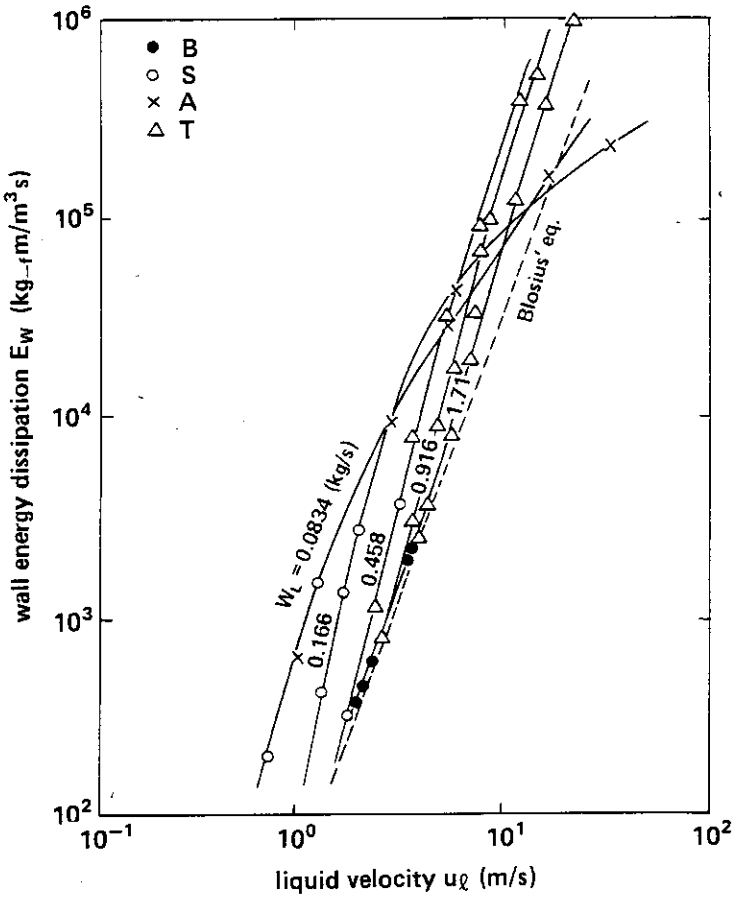

Fig. 56 Relationship between wall frictional energy dissipation and water linear velocity in a vertical circular pipe with water flow rate as parameter.

7.4 Conclusions

Interfacial and wall frictional energy dissipations for vertical upward, air-water two-phase flow were evaluated by applying the concept of perfectly settled two-phase flow proposed in Part I. The major conclusions are as follows.

(1) In the flow (larger than 1,950 kg-m/m^{2}s) of which flow regime changes from bubble flow to turbulent flow with increase of air flow rate at constant water flow rate, interfacial frictional energy dissipation increases with increase of wall frictional energy dissipation. On the other hand, in the flow (less than 355 kg-m/m^{2}s) of which flow regiome changes from slug flow to annular flow, interfacial frictional energy dissipation shows convex characteristics with the maximum point with respect to wall frictional energy dissipation. When flow regime changes from slug flow to turbulent flow (979 kg-m/m^{2}s), the characteristic is intermediate of the two.

(2) When both air and water flow rates are small in slug flow region, interfacial frictional energy dissipation is often larger than wall frictional energy dissipation. However, in annular or turbulent flow with high flow velocity the former is much smaller than the latter. From this fact, interfacial friction is less important in a high speed two-phase flow.

(3) Two-phase flow shows much larger wall frictional energy dissipation than single-phase water flow with the same water linear velocity and the ratio reached up to 15 times. This is because work done overcoming wall frictional force by air with higher linear velocity is larger than that by water with lower linear velocity.

8. Concluding Remarks

In Part II of this report, the validity of the author's hydrodynamic basic equations for one-dimensional separated two-phase flow (two-fluid model) was verified by applying them to various two-phase flows.

Two-phase critical discharge flow was selected as the object of verification because the special uniqueness of the author's basic equations lies on the phase change inertial force terms of equations of motion.

Analytical method of two-phase critical flow based on the author's basic equations can predict well the difference in flow characteristics between two-phase critical discharge flow accelerated by axial change of flow area and that accelerated under wall friction. Furthermore, it can also predict well the difference between one-component two-phase critical flow and two-component two-phase critical flow.

In addition, after performing a two-phase critical discharge flow experiment with a converging-diverging nozzle, new kind of thermal non-equilibrium was pointed out through the comparison of data with the author's analysis. On the other hand, two-phase discharge coefficient for large sharp-edged orifice was experimentally determined based on the author's theory. This discharge coefficient is given for instantaneous pressure and quality in the high pressure reservoir and the latter was estimated by using the depressurization rate method developed by the author. This value of discharge coefficient is considered to be applicable to any sharp-edged orifice regardless of facility characteristics.

Furthermore, concept of the perfectly settled two-phase flow proposed in Part I was applied to vertical upward, air-water two-phase flow and the interfacial and wall frictional energy dissipations were analized. The characteristics were clarified with relation to flow regime.

Through these various analyses, the validity and the consequent wide applicability of the author's basic equations for one-dimensional two-phase flow were demonstraled. This result suggests the large possibility of the anthors basic equations to describe various two-phase flow of wider fields in the future.

9. Nomenclature

Simbols used in Part II of the present report are listed below. The same simbols are commonly used also in Appendices 1 and 2.

A = flow area
B = normalized steam generation rate in pressure vessel
C_D = discharge coefficient
c = acoustic velocity (Appendix 1)
D = channel diameter
E = energy dissipation rate per unit volume of channel
F = frictional force per unit volume of fluid
G = mass velocity
g = gravitational acceleration
h = specific enthalpy
L = channel length; collapsed water level above discharge nozzle
M = normalized steam accumulation rate in pressure vessel
P = pressure
Q = heat transfer rate per unit volume of channel; volumetric flow rate
q = sensible heat per unit mass of fluid
R = slip ratio
s = specific entropy
T = temperature
t = time
u = velocity
V = pressure vessel volume
v = specific volume
W = mass flow rate
w = phase change rate per unit volume of channel; residual fluid mass in pressure vessel
x = gas mass flow rate fraction (quality)
z = position
α = gas volume fraction (void fraction)
β = gas mass fraction
Γ = integrated pressure drop ($=\int_{p0} dP$)
Δ = characteristic matrix (Appendix 1)
η = conversion coefficient of phase change inertial force in momentum equation (Appendix 2)
ζ = distribution fraction to gas phase
λ = frictional loss coefficient of channel
μ = viscosity
ξ = fraction of pressure drop due to energy dissipation to total pressure drop
ρ = density

Subscripts:

g : flowing gas phase
l : flowing liquid phase
PC : phase change part of fluid

s : residual gas phase
w : residual liquid phase
GL : to gas phase from liquid phase
LG : to liquid phase from gas phase
GW : to gas phase from wall
LW : to liquid phase from wall
W : wall
IG : to interface from gas phase
IL : to interface from liquid phase
I : interface
e : external
sat : saturation
T : total energy dissipation
TPF : two-phase friction
0 : high pressure reservoir ($u_g = u_l = 0$); single-phase liquid flow with same mass velocity
c : critical flow
a : acceleration
f : friction
β : variation of β (Appendix 2)
x : variation of x (Appendix 2)
net : total two-phase flow (Appendix 2)
P : local (with respect to P); with respect to P (Appendix 1)

References

(1) H. Shimamune, et al., JAERI−M6318 (1975).
(2) H. Adachi, J. Nucl. Energy Soc. Japan, Vol.15, No.10, pp.693-701 (1973); Heat Transfer Japanese research, Vol.3, No.4, pp.75-88 (1974).
(3) H. Fauske, ANL-6633 (1961).
(4) F.J. Moody, Trans. ASME, Ser.C, Vol.87, No.1, pp.134 (1965).
(5) H. Ogasawara, Trans. JSME, Vol.31, No.225, pp.751 (1965).
(6) H. Ogasawara, Trans. JSME, Vol.32, No.240, pp.1239 (1966).
(7) H. Ogasawara, Trans. JSME, Vol.34, No.267, pp.1985 (1968).
(8) Y. Katto, Trans. JSME, Vol.34, No.260, pp.731 (1968).
(9) Y. Katto, Trans. JSME, Vol.35, No.271, pp.572 (1969).
(10) M. Okazaki, Trans. JSME, Vol.45, No.396, pp.1169 (1979).
(11) M. Okazaki, Trans. JSME, Vol.45, No.409, pp.1797 (1980).
(12) F. D'Auria, P. Vigni, "Two-Phase Critical Flow Models - State of the Art Report -", RP403(80) (1980).
(13) H. Fauske, Dissertation, Univ. of Minnesota (1961).
(14) D.W. Faletti, Dissertation, Univ. of Washington (1959).
(15) J.E. Moy, et al., A.I.Ch.E. J., Vol.13, No.3, pp.361 (1957).
(16) A.J.R. Cruz, Dissertation, Univ. of Minnesota (1953).
(17) H. Adachi, J. Nucl. Energy Soc. Japan, Vol.16, No.5, pp.282-288 (1974); Heat Transfer Japanese Research, Vol.4, No.2, pp.12-21 (1975).
(18) Y. Katto, J. JSME, Vol.72, No.602, pp.355 (1969).
(19) R.W. Lockhart and R.C. Martinelli, Chem. Engg. Progr., Vol.45, No.1, pp.39 (1949).
(20) H. Blasius, Forsch. Arb., Heft 131 (1911).
(21) R.C. Martinelli and D.B. Nelson, Trans. ASME, Vol.70, No.6, pp.695 (1948).
(22) H. Ogasawara, Trans. JSME, Vol.34, No.267, pp.1995 (1968).
(23) C.J. Baroczy, NAA−SA-memo-11858 (1966).
(24) M. Shiba and Y. Yamazaki, Trans. JSME, Vol.32, No.240, pp.1231 (1966).
(25) Y. Sudo and Y. Katto, 8th Japanese Heat Transfer Symposium, I-I-3 (1971).
(26) H. Adachi, J. Nucl. Energy Soc. Japan, Vol.22, No.2, pp.111-120 (1980).
(27) I. Tani, "Kinetics of Flow" (Japanese), Iwanami (1959).
(28) H. Akagawa, "Gas-Liquid Two-Phase Flow" (Japanese), Corona-Sha (1976).
(29) R.V. Smith, et al., Symposium on Two-Phase Flow Dynamics, 4.1 (1967).
(30) H. Adachi and N. Yamamoto, J. Nucl. Energy Soc. Japan, Vol.15, No.12, 847-855 (1973); Heat Transfer Japanese Research, Vol.3, No.4, pp.89-102 (1974).
(31) M.W. Benjamin and J.G. Miller, Trans. ASME, Vol.63, pp.419 (1941).
(32) M.C. Stuart and D.R. Yarnell, Mech. Engg., Vol.58, pp.479 (1936).
(33) M.C. Stuart and D.R. Yarnell, Trans. ASME, Vol.66, pp.387 (1944).
(34) W.J. Kinderman and E.W. Wales, Trans. ASME, Vol.79, pp.183 (1957).
(35) E.S. Monroe and N.Y. Ithaca, Trans. ASME, Vol.78, pp.373 (1956).
(36) J.F. Bailey, Trans. ASME, Vol.73, pp.1109 (1951).
(37) H. Ogasawara, Trans. JSME, Vol.34, No.268, pp.2146 (1968).
(38) P.C. Chen, TID-22145 (1965).
(39) F.R. Zaloudek, HW-77594 (1963).
(40) R.W. Pike and H.C. Ward, A.I.Ch.E. J., Vol.10, No.2, pp.206 (1964).
(41) R.A. Brown, UCRL-6665-T (1961).
(42) H.K. Fauske, JSME 1967 Semi-Int. Symposium, 261 (1967).
(43) H. Adachi, J. Nucl. Energy Soc. Japan, Vol.16, No.6, pp.322-329 (1974); Heat Transfer Japanese Research, Vol.4, No.2, pp.92-103 (1975).
(44) C.E. Slater, IN-1444 (1970).
(45) M. Sobajima, Nucl. Sci. and Engg., Vol.60, pp.10-18 (1976).
(46) H. Adachi and M. Okazaki, J. Nucl. Energy Soc. Japan, Vol.18, No.12, pp.786-795 (1976).
(47) Y. Yamazaki and M. Shiba, Cocurrent Gas-Liquid Flow, Plenum Press. (1969).
(48) K. Sekoguchi, et al. 3rd Japanese Heat Transfer Symposium (1966).

Appendix 1 Local Condition for Single-Phase Critical Flow

It is very useful for analysing two-phase critical flow to examine the basic characteristic of single-phase critical flow.

In a one-dimensional steady single-phase flow, the following three basic equations hold bood on balance of mass, momentum and energy, respectively.

$$\frac{1}{\rho}\frac{d\rho}{dP}\frac{dP}{dz}+\frac{1}{u}\frac{du}{dz}=-\frac{1}{A}\frac{dA}{dz} \tag{A1-1}$$

$$\frac{dP}{dz}+\rho u\frac{du}{dz}=F_W \tag{A1-2}$$

$$\rho\left(\frac{dh}{dP}-\frac{1}{\rho}\right)u\frac{dP}{dz}=Q \tag{A1-3}$$

Out of these three equations, Eq. (A1-3) is necessary to follow the change of state values of the fluid and in this appendix, it is used only for determining $d\rho/dP$ in Eq. (A1-1). Therefore, one can investigate the characteristics of critical flow without any over-looking of the essence by treating $d\rho/dP$ as a known variable.

From Eqs. (A1-1) and (A1-2),

$$\frac{dP}{dz}=\frac{\Delta_p}{\Delta} \tag{A1-4}$$

Here,

$$\Delta=\begin{vmatrix}\frac{1}{\rho}\frac{d\rho}{dP} & \frac{1}{u}\\ 1 & \rho u\end{vmatrix}=u\frac{d\rho}{dP}-\frac{1}{u} \tag{A1-5}$$

$$\Delta_p=\begin{vmatrix}-\frac{1}{A}\frac{dA}{dz} & \frac{1}{u}\\ F_W & \rho u\end{vmatrix}=-\frac{\rho u}{A}\frac{dA}{dz}-\frac{F_W}{u} \tag{A1-6}$$

In subcritical flow, Δ is generally negative and increases with progress of depressurization-acceleration. On the other hand, Δ_p respresents the hydrohynamical characteristics of the channel and can be positive or negative depending on flow situation. Since wall friction acts on fluid in opposite direction to velocity u, the second term of Eq. (A1-6) is always positive. Therefore, Δ_p should be positive if $dA/dz \leqq 0$. However, if dA/dz becomes large enough, the first term of Eq. (A1-6) becomes large negative number exceding the second term and consequently Δ_p becomes negative. When $\Delta_p = 0$,

$$\frac{1}{A}\frac{dA}{dz}=-\frac{F_W}{\rho u^2} \tag{A1-7}$$

That is, $\Delta_p = 0$ is possible in diverging channel only.

In the case of subcritical flow of $\Delta<0$, Eq. (A1-7) is realized on a certain position of, e.g., downstream of the throat of converging-diverging nozzle. In the upstream of the position dP/dz is negative and in the downstream positive. That is, Eq. (A1-7) gives the minimum pressure point for subcritical flow.

Next, let us examine the approaching process of Δ to zero by depressurization-acceleration of a subcritical flow. If Δ_p approaches zero simultaneously, then,

$$\lim_{\Delta \to 0} \frac{dP}{dz} = \frac{+0}{-0} = -(\text{undeterminate}) \tag{A1-8}$$

Here, undeterminate dP/dz means that dP/dz is not determined uniquely with only the local conditions at $\Delta = 0$ but is determined as a limiting value from the upstream side.

Equation (A1-8) represents the critical flow occurred at downstream side of the throat of a converging-diverging nozzle. And if Δ and Δ_p are continuous functions, $\Delta > 0$, $\Delta_p < 0$ and $dP/dz < 0$ hold good in the downstream of the critical flow point. This is no other then supercritical flow. Especially if $F_W = 0$, the critical flow occurs at $dA/dz = 0$, i.e., at the throat.

When the critical flow occurs at the place of $\Delta = \Delta_p = 0$, dP/dz at the critical flow point is a certain negative finite value, although it is very large. In such case, as known from Eq. (A1-3), for $Q \neq 0$

$$dh - \frac{dP}{\rho} = dq = (\text{finite}) \tag{A1-9}$$

That is, state change of fluid is generally not adiabatic.

Next, let us investigate the case of positive Δ_p at $\Delta = 0$. In such case,

$$\lim_{\Delta \to 0} \frac{dP}{dz} = \frac{\pm(\text{finite})}{-0} = -\infty \tag{A1-10}$$

Equation (A1-10) represents the critical flow occurred at, e.g., exit of regular pipe (constant-flow-area channel) or converging nozzle. The reason why this type of critical flow occurs at the channel exit only is that the flow cannot change continuously from the situation of $\Delta = -0$, $\Delta_p > 0$ and $dP/dz = -\infty$ to the situation of $\Delta = +0$, $\Delta_p > 0$ and $dP/dz = +\infty$.

When the critical flow is realized at the place represented by Eq. (A1-10), one can obtain the following equation from Eq. (A1-3), regardless of Q value:

$$dh - \frac{dP}{\rho} = dq = 0 \tag{A1-11}$$

That is, even if there are frictional heating and/or external heating, state change of fluid is adiabatic at the critical flow point.

When $\Delta = 0$, i.e., at the critical flow point, one can obtain from Eq. (A1-5),

$$u = \sqrt{\frac{dP}{d\rho}} \tag{A1-12}$$

On the other hand, $dP/d\rho$ in adiabatic state change gives acoustic velocity c, i.e.,

$$c^2 = \left(\frac{dP}{d\rho}\right)_{\text{adiabatic}} \tag{A1-13}$$

Therefore, critical velocity in a converging-diverging nozzle corresponding to Eq. (A1-8) is generally not equal to acoustic velocity and that at the exit of constant-flow-area channel, etc. corresponding to Eq. (A1-10) is equal to acoustic velocity.

Characteristics of local conditions of single-phase critical flow described above are considered quite similar to those for two-phase critical flow. It was already discussed in detail in Chapters 2 and 3 of this report.

Appendix 2 An Example of ζ_{xz} and Related Parameters

As discussed in detail in Chapter 4 of Part I, fraction of phase change inertial force term to be added to gas phase ζ_β to the total phase change inertial force term for existing two-phase fluid is given, for the steady term (See Section 4.4 of Part I), as:

$$\zeta_\beta = \frac{\beta\left\{(1-\beta)-(1-x)\dfrac{d\beta/dz}{dx/dz}\right\}}{\{x(1-\beta)+\beta(1-x)\}\dfrac{d\beta/dz}{dx/dz}} \tag{A2-1}$$

Similarly, fraction of phase change inertial force term to be added to gas phase ζ_x to the total phase change inertial force term for flowing two-phase fluid is:

$$\zeta_x = -\frac{x\left\{(1-\beta)-(1-x)\dfrac{d\beta/dz}{dx/dz}\right\}}{x(1-\beta)-\beta(1-x)} \tag{A2-2}$$

In momentum equations, steady terms of inertial forces for existing two-phase fluid are evaluated based on momentum balance of flowing two-phase fluid. That is, there is a kind of mixing mode in expression of momentum balance. Resultantly, coefficients of

$$\eta_g = \frac{u_{PC}}{u_g}\zeta_x \tag{A2-3}$$

$$\eta_l = \frac{u_{PC}}{u_l}(1-\zeta_x) \tag{A2-4}$$

should be multiplied to $W(u_g-u_l)(dx/dz)$ to evaluate the steady phase change inertial forces for gas and liquid phases, respectively, for existing two-phase fluid in unit length of channel (See Section 4.5 of Part I.).

For the existing total two-phase fluid, the coefficient to be multiplied is:

$$\eta_{net} = \eta_g + \eta_l = \frac{u_{PC}}{u_g}\zeta_x + \frac{u_{PC}}{u_l}(1-\zeta_x) \tag{A2-5}$$

Here, in Eqs. (A2-3) through (A2-5),

$$u_{PC} = \frac{u_g+u_l}{2} \tag{A2-6}$$

In this appendix, characteristics of ζ_β, ζ_x, η_g, η_l and η_{net} are studied with referring as an example of the analytical results on two-phase critical flow without friction and thermal non-equilibrium between two phases.

Examples of calculated ζ_β, ζ_x, η_g, η_l and η_{net} are shown in **Figs. (A2-1)** through **(A2-6)**, with respect to pressure change in the channel. Reservoir pressure in the examples is fixed at 1.0 MPa and reservoir quality is changed as a parameter.

When reservoir quality is 0.05, ζ_β decreases monotonously, from about -0.3 to $-\infty$ with decrease in pressure except just beginning of acceleration depressurization process. And then it suddenly jumps to $+\infty$ and decreases monotonously again, to about 1.2 except for the last half of acceleration-depressurization process. Here, the negative region of ζ_β is

shown with the reversed axis in this figure.

As the crossing point of ζ_β from $-\infty$ to $+\infty$, $d\beta/dz$ changes from negative via zero to positive. Therefore, phase change inertial force term added to gas phase is always positive and continuously varies along the flow axis.

ζ_β in this example does not get in the range between 0.0 and 1.0. This means that the direction of phase change inertial force added to liquid phase is opposite to that for gas phase. Because, the fraction of phase change inertial force for existing liquid phase is $1-\zeta_\beta$. Therefore, if ζ_β is negative, $1-\zeta_\beta$ should be positive number larger than 1.0 and if ζ_β is possitive number larger than 1.0, $1-\zeta_\beta$ should be negative.

On the other hand, ζ_x monotonously decreases with decrease in pressure from very large positive number to slightly larger than 1.0. Since dx/dz is always positive, this result indicates the positive continuous change in phase change inertial force term added to gas phase and negative continuous change in phase change inertial force term added to liquid phase.

The fact described above is shown more clearly in **Fig. A2-2**. That is, η_g is always positive and η_l is always negative. Since positive η_g decreases the inertial force on main flow gas phase and negative η_l increases the inertial force on main flow liquid phase under given external forces, phase change inertial force decelerates the gas phase and accelerates the liquid phase. That is, phase change affects the flow so as to reduce the increase rate of slip ratio. And, this effect is specially significant in the beginning stage of acceleration-depressurization process with very high increasing rate of slip ratio.

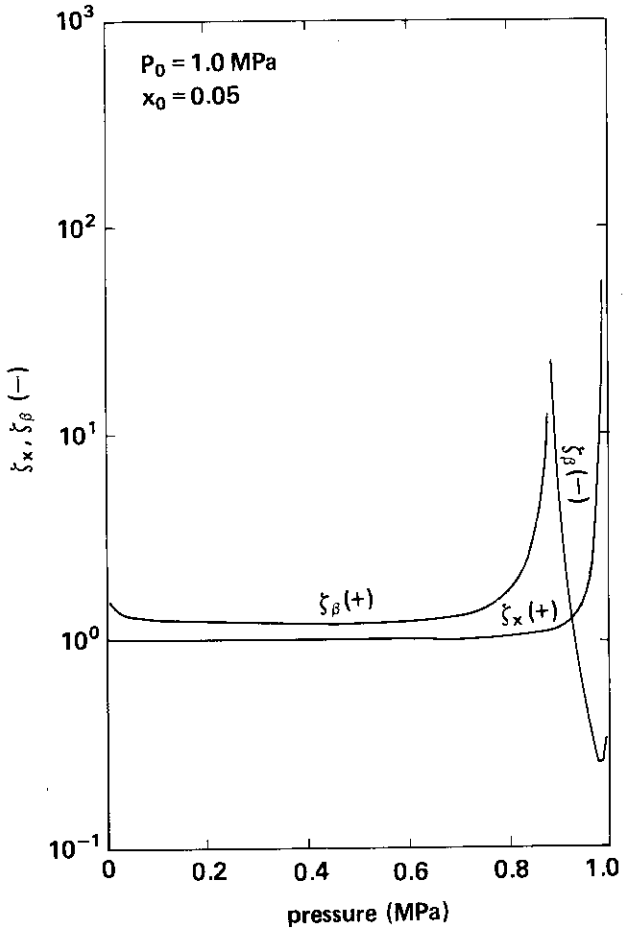

Fig. A2-1 ζ_β and ζ_x at $P_0 = 1.0$ MPa, $x_0 = 0.05$.

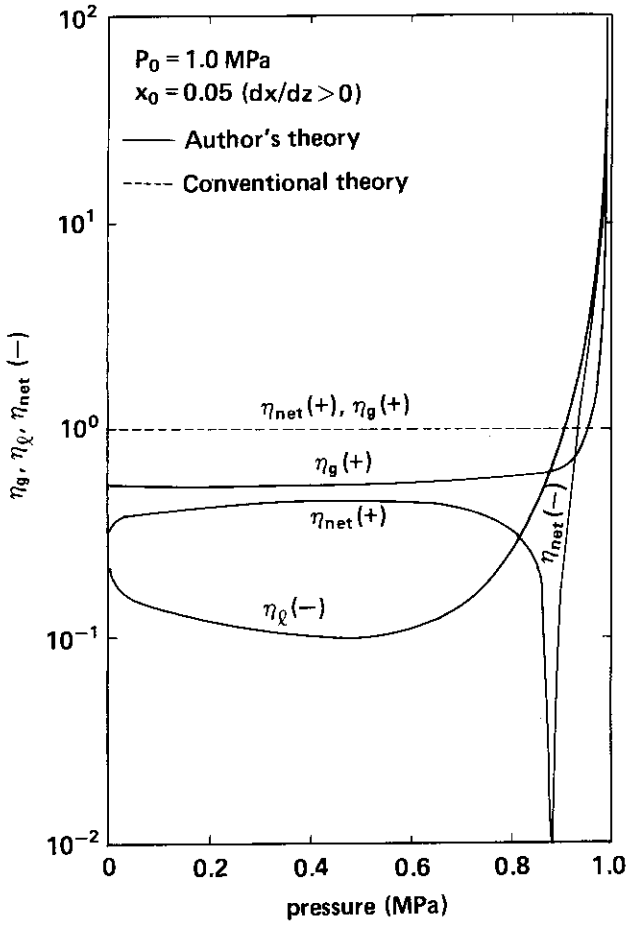

Fig. A2-2 η_g, η_l and η_{net} at $P_0 = 1.0$ MPa, $x_0 = 0.05$.

Net coefficient η_{net} is negative in the beginning stage of acceleration-depressurization process. Since dx/dz is positive in this quality range, this means that the existing two-phase fluid is totally accelerated by phase change inertial force. This fact seems strange but actually very reasonable. Because, gas phase is decelerated and liquid phase is accelerated by phase change inertial force and liquid fraction $1-\beta$ based on existing two-phase fluid is much larger than $1-x$ based on flowing two-phase fluid. In other words, deceleration effect and acceleration effect of phase change inertial forces per unit length of channel are not perfectly but imbalancedly accounted in the equations of motion based on existing two-phase fluid (See the subsection 4.2.3 of Part I.).

In conventional momentum equations, $\eta_g=1$, $\eta_l=0$ and $\eta_{net}=1$ are usually assumed for evaporation process and $\eta_g=0$, $\eta_l=1$ and $\eta_{net}=1$ are for condensation process. As shown with dashed line in **Fig. A2-2**, differences from the author's theory are quite large.

When reservoir quality is 0.3, ζ_β changes complicatedly in the negative range as shown in **Fig. A2-3**. Behavior of ζ_x is not so different qualitatively from the previous case. η_g changes monotonously with deerease in pressure, except for the last stage of acceleration-depressurization process, from very large positive number to about 0.7 as shown in **Fig. A2-4**. η_l increases from very large negative number to about -1 also monotonously, except for the last stage. η_{net} behaves a little bit higher than η_l. Gas phase is always decelerated and liquid phase is always accelerated and resultantly, increase in slip ratio is always supressed also by phase change inertial force in this case. Negative η_{net} also indicates that the existing two-phase fluid is totally accelerated by the phase change inertial forces.

In the case of reservoir quality of 0.7, both ζ_β and ζ_x inclease monotonously with decrease in pressure from negative large number to positive small number less than 1.0 as shown in **Fig. A2-5**. η_g changes monotonously from very large negative number to small positive number less than 1.0 and η_l decreases monotonously from large positive number to small positive number larger than 1.0 as shown in **Fig. A2-6**. Since dx/dz is negative in this case, gas phase is also decelerated and liquid phase is accelerated in most acceleration-depressurization process. After ζ_β and ζ_x become positive, both phases are accelerated. Positive η_{net} under negative dx/dz also indicates the total acceleration of existing two-phase fluid throughout the process.

Based on the above discussions, the following conclusions are obtained.

(1) ζ_β and ζ_x are generally not limited within the range between 0.0 and 1.0.

(2) η_{net} is generally not equal to 1.0.

(3) Except very special cases (such as the region where pressure is lower than about 0.2 MPa in **Figs. A2-5** and **A2-6**), gas phase of two-phase critical discharge flow is decelerated and liquid phase is accelerated and resultantly, increase in slip ratio is supressed by phase change inertial forces, regardless of evaporation or condensation. This effect is specially significant in the beginning stage of acceleration-depressurization process where increase rate of slip ratio is very large.

(4) Except a certain cases (such as the region where pressure is lower than about 0.88 MPa in **Fig. A2-2**), existing two-phase fluid of the critical discharge flow is totally accelerated by phase change inertial forces, regardless of evaporation or condersation.

(5) In the typical conventional momentum equations for two-phase flow, $\eta_g=1.0$, $\eta_l=0.0$ and $\eta_{net}=1.0$ are assumed for evaporation process and $\eta_g=0.0$, $\eta_l=1.0$ and $\eta_{net}=1.0$ for condensation process. Such artificially assumed phase change inertial force terms are kineticly unreasonable and very important characteristics of the terms such as described in the above items (3) and (4) are completely ignored.

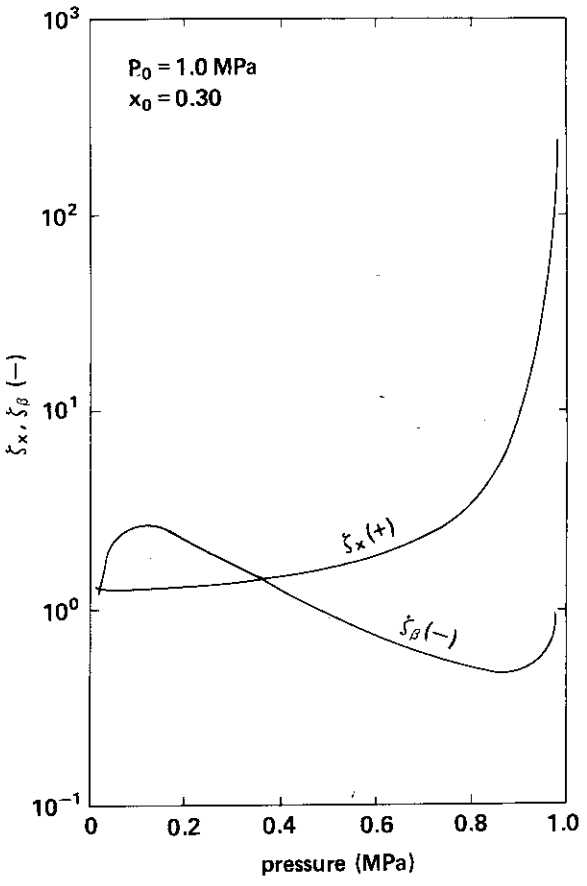

Fig. A2-3 ζ_β and ζ_x at $P_0 = 1.0$ MPa, $x_0 = 0.30$.

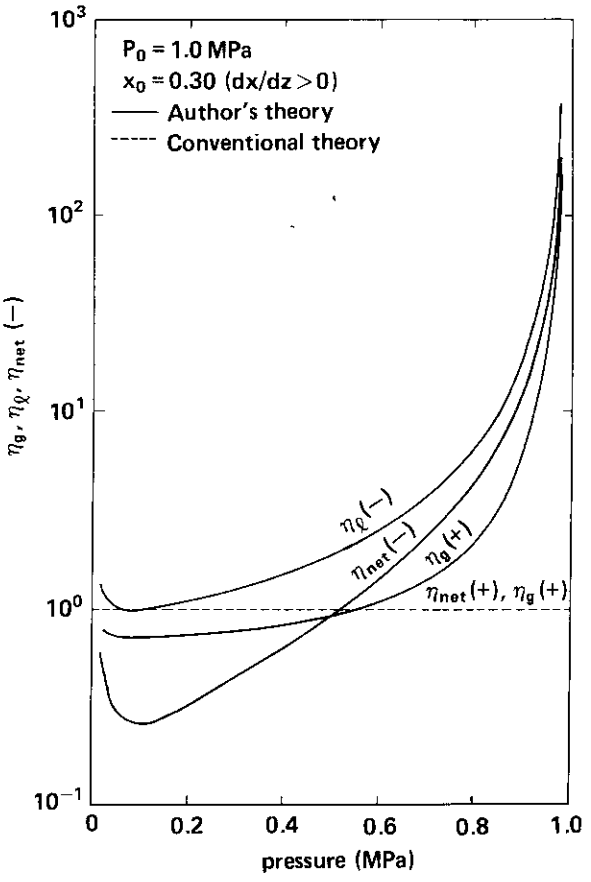

Fig. A2-4 η_g, η_ℓ and η_{net} at $P_0 = 1.0$ MPa, $x_0 = 0.30$.

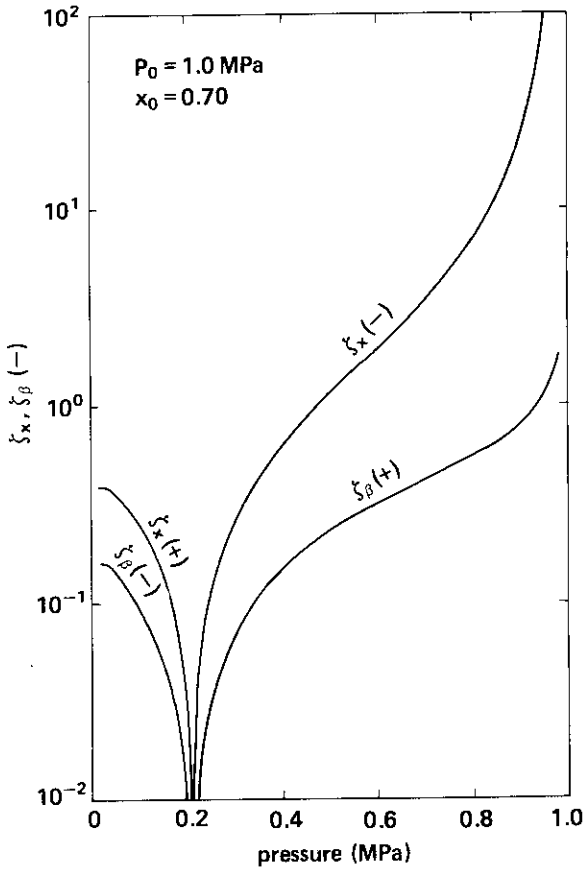

Fig. A2-5 ζ_β and ζ_x at $P_0 = 1.0$ MPa, $x_0 = 0.70$.

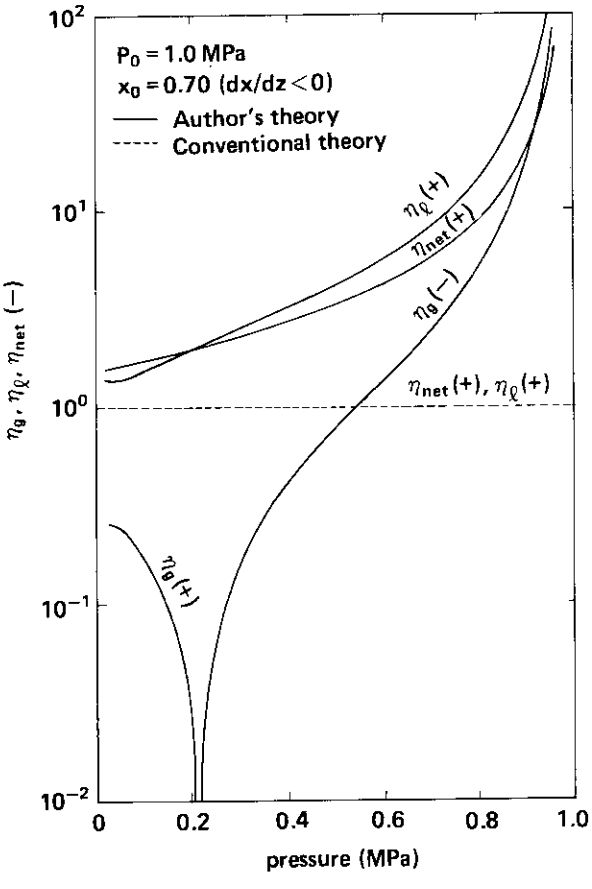

Fig. A2-6 η_g, η_ℓ and η_{net} at $P_0 = 1.0$ MPa, $x_0 = 0.70$.

Concluding Remarks

In Part I of the present report, hydrodynamical basic equations for one-dimensional two-phase flow was discussed generally and several new ideas were given especially on the fundamental form of equations of motion. The author's equations of motion have remarkable uniqueness in features specially in evaluation of phase change inertial force and its distribution to each phase. Therefore, in Part II, the author's basic equation set was applied to high speed two-phase flow (two-phase critical discharge) in which phase change inertial force cannot be ignored and air-water critical discharge flow without phase change to verify the validity of the author's theory. Also the wide applicability was demonstrated through the analyses on various critical discharge flows and regular velocity two-phase flows. Those analyses gave reasonable results and indicated the essential validity of the author's basic equation set.

Of course, reasonable two-phase flow analysis cannot be guaranteed by valid basic equation set only. It depends on the validity of constitutive equations used and also on the numerices. However, correct describing of the balances in mass, force (momentum) and energy is considered the basis for a successful two-phase flow analysis. Especially, importance of the form of basic equations is invaluably large in accident analyses for light water cooled nuclear reactors in which very wide changes in pressure, steam quality, phase velocities and temperatures should be consistently predicted. Furthermore, right basic equations determine necessary number of constitutive equations and their physical contents. Therefore, they will support the development of constitutive equations. The author's basic equations will contribute in such area from now on.

Acknowledgement

The author is much indebted to Drs. M. Akiyama, S. Kondo, K. Miya, G. Yagawa and H. Madarame of Tokyo University and Dr. K. Torikai of Science University of Tokyo for their useful discussions. The author also would like to express great appreciation to Drs. M. Nozawa, K. Sato, M. Shiba, T. Shimooke and Y. Murao for their guidance and encouragement.

Concluding Remarks

In Part I of the present report, hydrodynamical basic equations for one-dimensional two-phase flow was discussed generally and several new ideas were given especially on the fundamental form of equations of motion. The author's equations of motion have remarkable uniqueness in features specially in evaluation of phase change inertial force and its distribution to each phase. Therefore, in Part II, the author's basic equation set was applied to high speed two-phase flow (two-phase critical discharge) in which phase change inertial force cannot be ignored and air-water critical discharge flow without phase change to verify the validity of the author's theory. Also the wide applicability was demonstrated through the analyses on various critical discharge flows and regular velocity two-phase flows. Those analyses gave reasonable results and indicated the essential validity of the author's basic equation set.

Of course, reasonable two-phase flow analysis cannot be guaranteed by valid basic equation set only. It depends on the validity of constitutive equations used and also on the numerices. However, correct describing of the balances in mass, force (momentum) and energy is considered the basis for a successful two-phase flow analysis. Especially, importance of the form of basic equations is invaluably large in accident analyses for light water cooled nuclear reactors in which very wide changes in pressure, steam quality, phase velocities and temperatures should be consistently predicted. Furthermore, right basic equations determine necessary number of constitutive equations and their physical contents. Therefore, they will support the development of constitutive equations. The author's basic equations will contribute in such area from now on.

Acknowledgement

The author is much indebted to Drs. M. Akiyama, S. Kondo, K. Miya, G. Yagawa and H. Madarame of Tokyo University and Dr. K. Torikai of Science University of Tokyo for their useful discussions. The author also would like to express great appreciation to Drs. M. Nozawa, K. Sato, M. Shiba, T. Shimooke and Y. Murao for their guidance and encouragement.